

©2012

Kai Liu

ALL RIGHTS RESERVED

ACCESSING ERYTHRONOLIDE STRUCTURE SPACE:
NEW REACTIONS AND APPLICATIONS

by

KAI LIU

A Dissertation submitted to the
Graduate School-New Brunswick
Rutgers, The State University of New Jersey

in partial fulfillment of the requirements

for the degree of

Doctor of Philosophy

Graduate Program in Chemistry and Chemical Biology

written under the direction of

Professor Lawrence J. Williams, Ph.D

and approved by

New Brunswick, New Jersey

October, 2012

ABSTRACT OF THE DISSERTATION

EXPLORATION OF THE ERYTHRONOLIDE STRUCTURE SPACE: NEW REACTIONS AND APPLICATIONS

By KAI LIU

Dissertation Director:

Professor Lawrence J. Williams, Ph.D

An integrated routing strategy approach towards the synthesis of novel erythronolides is discussed in this dissertation. A macrocyclic bis[allene] compound was made as a synthetic scaffold. To date, more than 30 erythronolide derivatives have been made from this intermediate within 3 steps or less. This approach represents by far the most efficient and economic route for the access of erythronolide structure space.

Many reactions were utilized in the modification of these 14-membered macrolides, including bromination, chelation and non-chelation controlled reductions and benzylic migration, elimination, etc. More importantly, novel allene oxidation conditions such as allene epoxidation, spirodiepoxidation, and osmylation, transformations developed by our group, were applied in the synthesis of diverse erythronolides and were central to our strategy. New reactions, including new procedures of allene dihydroxylation and allene osmylation-electrophile addition, are also discussed.

Acknowledgements

I would like to sincerely appreciate my advisor, Professor Lawrence J. Williams. He has been a wonderful advisor, instructor and mentor for me during the past five years. I can definitely say that I have learned a great deal from him. He not only taught me chemistry, but also showed me how to be an excellent professional scientist. I am deeply affected by his enthusiasm towards research. Every project that I have worked on is challenging, but more importantly, very interesting, exciting, and rewarding. I feel very lucky to have chosen him as my advisor.

I would also like to thank our collaborator, Dr. Novruz G. Akhmedov for his continuous assistance and contribution in the explicit NMR analysis. The assignment of the complex macrocyclic molecules will be much more challenging without his work.

The Williams group has always been like a family for us. I would like give my appreciation to all the current and recent graduate students and postdocs, especially Dr. Hiyun Kim, Libing Yu, Gaojie Hu, Michael Drahl, Rojita Sharma, Da Xu, Dr. Robert V. Kolakowski, Dr. Yue Zhang, Dr. Partha Ghosh, and Dr. Joseph R. Cusick, for the friendship and all useful discussions in the daily research.

I would like to thank the thesis committee members: Prof. Roger Jones, Prof. Daniel Seidel and Prof. Longqin Hu for their participation.

Last but not least, I would like to give my special thanks to my wife, Dr. Tingni Sun, for the continuous support and encouragement during all the hard times in my graduate studies.

Dedication

To my parents,

Daxiang Liu and Jirong Huang

and My Wife, Tingni Sun

Table of Contents

ABSTRACT OF THE DISSERTATION	ii
Acknowledgement	iii
Dedication	iv
List of Tables	ix
List of Schemes.....	x
List of Figures	xiii
Chapter I Erythromycinoid Antibiotics	1
1.1 Introduction	1
1.2 The Development of Erythromycinoid Antibiotics	2
1.3 Previous Approaches to the Total Synthesis of Erythronolides	4
1.4 Limitations of Current Methods of Antibiotic Development	7
1.5 Conclusion	8
1.6 References	9
Chapter II Erythronolide Structure Space	11
2.1 Introduction	11
2.2 An Integrated Routing Strategy for the Exploration of Erythronolide Structure Space.....	12
2.3 Design of the Key Intermediate Structure	14
2.4 Exploration of the Structure Space	16
2.5 References	18
Chapter III Synthesis of the Macrocyclic [Bis]allene.....	20
3.1 Introduction	20

3.2 Synthesis of the Three Key Coupling Units	21
3.3 Coupling of the Three Building Blocks.....	23
3.4 Synthesis of the Macrocyclic [Bis]allene	25
3.5 Flexibility of the Route: Possibilities for Further Modification	28
3.6 Conclusion	29
3.7 References	29
Chapter IV Allene Osmylation: Methods for Improvement of Efficiency	31
4.1 Introduction	31
4.2 Alkene Osmylation: A Brief Overview	32
4.3 Allene Osmylation: An Underexplored Field.....	33
4.4 Mechanistic Insights of Allene Osmylation	35
4.5 Acid-promoted Allene Osmylation	36
4.6 Alternative Procedures for Efficient Allene Osmylation	37
4.7 Conclusion	39
4.8 References	40
Chapter V Synthesis of Erythronolides From a Macrocyclic Bis[allene].....	42
5.1 Introduction	42
5.2 Regioselective Osmylation of the Macrocyclic Bis[allene]	43
5.3 Osmylation of the C10-C12 Allene	45
5.4 Reduction of the 5-Ketone.....	48
5.5 Stereocontrol on the Macrocyclic Ring: Mechanistic Insights.....	51
5.6 Attempts for the Glycosidation on the Macrocyclic Ring.....	53
5.7 Spirodiepoxidation of the Macrocyclic Bis[allene].....	56

5.8 Methods Used in the Structure Determination of the Novel Erythronolides	58
5.9 Conclusion	61
5.10 References	62
Chapter VI Allene Osmylation Promoted by Electrophiles.....	64
6.1 Introduction	64
6.2 The Osmate Enol Ester and Interesting Reactivity Within.....	65
6.3 Halogenation of the Osmate Enol Ester	67
6.4 Catalytic Osmylation-halogenation	68
6.5 Stereoselectivity of Osmylation-halogenation.....	70
6.6 Osmylation of Disubstituted Allene	73
6.6 Osmylation-halogenation on Macrocyclic Bis[allene]	75
6.7 Allene Aminohydroxylation	77
6.8 Addition of Carbon Electrophiles.....	82
6.9 Conclusion	85
6.10 References	85
Chapter VII Experimental Section.....	87
1. General.....	87
2. Chapter III.....	88
3. Chapter IV	98
4. Chapter V	102
5. Chapter VI	151
6. Reference	177
Appendix I	178

Spectra of Compounds.....	178
CURRICULUM VITAE.....	285

List of Tables

Table V.1 Attempts of Glycosilation of 5.2.....	55
Table VI.1 Optimization of Catalytic Allene Osmylation-halogenation	69
Table VI.2 Stereo Outcome of Catalytic Allene Osmylation-halogenation.....	72
Table VI.3 Catalytic osmylation of disubstituted allene.....	73
Table VI.4 Macrocyclic Allene Osmylation-halogenation	76

List of Schemes

Scheme I.1 Acid Induced Degradation of Erythromycin	2
Scheme II.1 Synthesis of Erythromycinoids	16
Scheme II.2 Allene Spirodiepoxidation and Derivitization.....	17
Scheme III.1 Retrosynthetic Analysis of the Macrocyclic Bis[allene]	21
Scheme III.2 Synthesis of the C6-Alkyne	22
Scheme III.3 Synthesis of the C4-Aldehyde	22
Scheme III.4 Synthesis of the C5-Alkyne	23
Scheme III.5 The First Coupling	24
Scheme III.6 The Second Coupling.....	25
Scheme III.7 One-pot Synthesis of the Bis[allene]	26
Scheme III.8 Synthesis of the Seco-Acid and the Macrocyclic Bis[allene]	27
Scheme III.9 Incorporation of Heterofunctionality in the Bis[allene].....	29
Scheme IV.1 The Upjohn Dihydroxylation.....	32
Scheme IV.2 The Sharpless Asymmetric Dihydroxylation.....	33
Scheme IV.3 Crabbe's Stoichiometric Allene Osmylation	34
Scheme IV.4 Fleming's Asymmetric Allene Osmylation	34
Scheme IV.5 Proposed Catalytic Cycle of Allene Osmylation	35
Scheme IV.6 Allene Osmylation Accelerated by Methanesulfonamide	36
Scheme IV.7 Allene Osmylation Accelerated by Acid	37
Scheme IV.8 Allene Osmylation of Protected Allene Alcohols	37
Scheme IV.9 Narasaka's Modification of Upjohn Dihydroxylation	38
Scheme IV.10 Allene Osmylation by Narasaka's Modification	39

Scheme IV.11 Allene Osmylation Using DABCO as Additive	39
Scheme V.1 Regioselective Osmylation of Macrocyclic Bis[allene] 5.1.....	43
Scheme V.2 Effect of Additives to the Osmylation of 5.1	44
Scheme V.3 Steric Difference Between the Two Faces of Allene	45
Scheme V.4 The Osmylation of the C10-C12 Allene	46
Scheme V.5 Mechanistic Framework of the Formation of 5.5	47
Scheme V.6 Osmylation of the 6-Protected Hydroxyl Ketone 5.9	48
Scheme V.7 Paterson's Reduction of C5- Ketone.....	49
Scheme V.8 Reduction of the C5-Ketone	50
Scheme V.9 Bromohydration of the Allene and Reduction of C5-Ketone	51
Scheme V.10 Anti-Felkin-Anh Model of the Chelation Control Reduction.....	52
Scheme V.11 Synthesis of the Desosamine Donor	54
Scheme V.12 Initial Attempts of Bis[allene] Epoxidation.....	56
Scheme V.13 Epoxidation of the Bis[allene] Macrolide 5.1	57
Scheme V.14 Mechanistic Framework of the Epoxidation Cascades	58
Scheme VI.1 Proposed Electrophile Addition of Osmate Enol Ester	66
Scheme VI.2 Stereo Outcome of Allene Epoxidation and Osmylation	66
Scheme VI.3 Allene Osmylation-halogenation.....	68
Scheme VI.4 The Use of Hydrogen Peroxide as Co-oxidant.....	70
Scheme VI.5 Allene Osmylation-halogenation of Chiral Allene	71
Scheme VI.6 Osmylation-fluorination of Disubstituted Allenes.....	74
Scheme VI.7 Osmylation-chlorination mechanism of macrocyclic allene	77
Scheme VI.8 The Sharpless Asymmetric Aminohydroxylation	78

Scheme VI.9 Mechanism of Alkene Aminohydroxylation	78
Scheme VI.10 Proposed Allene Aminohydroxylation	79
Scheme VI.11 Aminohydroxylation of Alkyl Allene 6.4.....	79
Scheme VI.12 Mechanistic Framework of Allene Aminohydroxylation.....	80
Scheme VI.13 Aminohydroxylation of Chiral Allene in Different Solvents	81
Scheme VI.14 Aminohydroxylation of Aryl Allene 6.27	82
Scheme VI.15 Allene Osmylation-iminium Addition.....	83
Scheme VI.16 Iminium Addition on Macrocyclic Bis[allene] 3.1	84

List of Figures

Figure I.1 Erythromycin A	1
Figure I.2 Examples of 2 nd Generation Macrolide Antibiotics.....	3
Figure I.3 Examples of 3rd Generation Macrolide Antibiotics	4
Figure I.4 Key Steps in Woodward's Total Synthesis of Erythromycin.....	4
Figure I.5 Key Steps in Carreira's Synthesis of Erythronolide A	5
Figure I.6 Key Steps in the Hoffmann and Woerpel Syntheses of (9S)-Dihydroerythronolide	6
Figure I.7 Key Steps in Andrade's Synthesis of 4,8,10-Tridesmethylnelithromycin	7
Figure II.1 Structure-activity Space.....	11
Figure II.2 Erythromycin A	13
Figure II.3 Integrated Routing Strategy.....	13
Figure II.4 Previous SAR Studies of Erythromycinoids	15
Figure III.1 The Dimerized Byproduct of Lactonization	28
Figure V.1 The 3D Looking of the Ketone Reduction	53
Figure V.2 Key HMBC Correlations of 5.1 and 5.5.....	59
Figure V.3 ORTEP Diagram of Compound 5.5	60
Figure V.4 Key NOESY Correlations of 5.2.....	61

Chapter I

Erythromycinoid Antibiotics

1.1 Introduction

Macrolide antibiotics are very important drugs used widely against infections. Erythromycin (**1.1**) is an archetypal macrolide antibiotic. It is a secondary metabolite produced by soil inhibiting actinomycete family of bacteria *Saccharopolyspora erythraea* (formerly known as *Streptomyces erythraea*) and was first isolated in 1952 by the group of J. M. McGuire at Eli Lilly¹ and was quickly launched commercially later that year under the brand name of Ilosone[®]. It is a broad spectrum antibiotic and is often used by people who are allergic to penicillin.

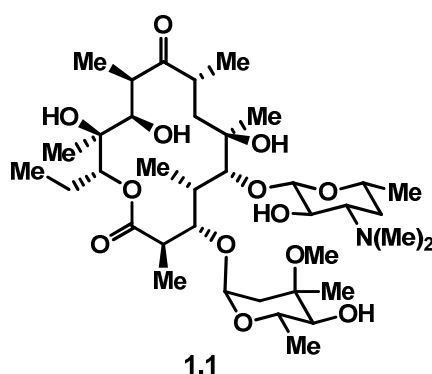


Figure I.1 Erythromycin A

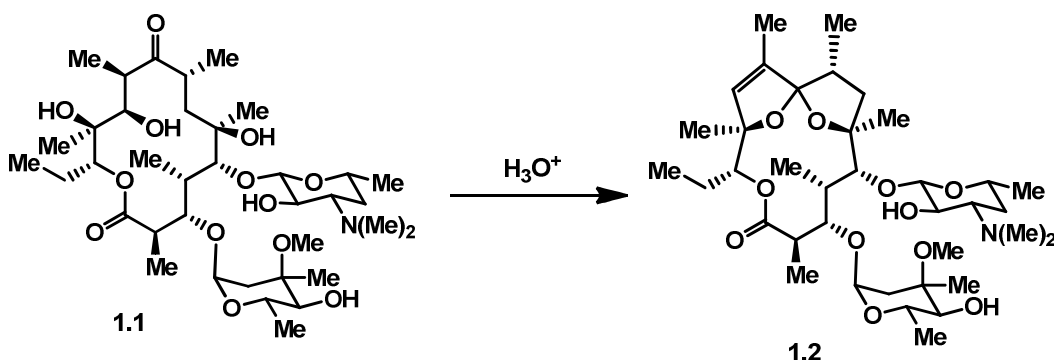
The mechanism of erythromycin's antibiotic action has been studied extensively. Its superior bioactivity arose from binding to the bacterial ribosome and inhibiting bacterial

protein transferase. In the early 2000s, X-ray crystal structures of erythromycin were reported by Steitz^{2,3} and Yonath^{4,5} and showed that this macrolide binds to the 50S ribosomal subunit, blocking the peptide exit tunnel near the peptide transferase center and thereby shutting down protein synthesis. The presences of the deoxysugars, especially the desosamine, are key to the biological activity. Since ribosomal structure is highly conserved among bacteria, erythromycin can be used as a broad spectrum antibiotic.

Despite its significant clinical use in human medicine, erythromycin suffers certain limitations. For example, it is highly unstable in acid. Also, it has weak activity against gram-negative bacteria, and is ineffective against resistant bacterial mutants. Hence, there is a high demand for novel antibiotics.

1.2 The Development of Erythromycinoid Antibiotics

It has long been recognized that acid induces the degradation of erythromycin **1.1** to an intramolecular hemiketal **1.2** forming between the C-6 alcohol and the C-9 ketone⁶ (Scheme I.1). Such degradation is responsible for the low stability of erythromycin in the stomach and causes stomach cramps⁷.



Scheme I.1 Acid Induced Degradation of Erythromycin

Modifications have been made in order to overcome this problem. For example, the 2nd generation of macrolide antibiotics, which were developed in the 1980s and commercialized in the 1990s, are significantly more stable to acid. Modifications included the alkylation of the C-6 tertiary alcohol in Clarithromycin **1.3** and altering the C-9 ketone to an amine in Azithromycin **1.4** (Figure I.2).

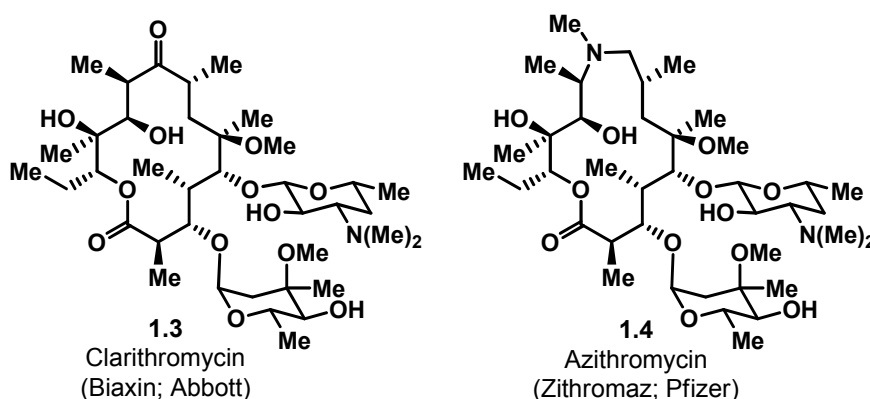


Figure I.2 Examples of 2nd Generation Macrolide Antibiotics

Despite their improvements, the 2nd generation macrolide antibiotics were inactive against certain types of bacteria, e.g. *Streptococcus pneumoniae*⁸ and *Haemophilus influenzae*⁹. Hence, there was still a demand for a new generation of antibiotics. Many new drug candidates were developed, and Telithromycin **1.5** (marketed by Sanofi-Aventis under the brand name Ketek[®]) and Cethromycin **1.6** were the best among them. This 3rd generation of macrolides was commercialized during the past decade (Figure I.3).⁹ While they have a C-6 alkylated alcohol similar to the 2nd generation compounds, the cladinose conjugate at the C-3 position was replaced with a ketone. Consequently, these macrolides are referred to as ketolides. Another interesting common structural motif is the carbamate group across the C-11 and C-12 positions in place of the diol.

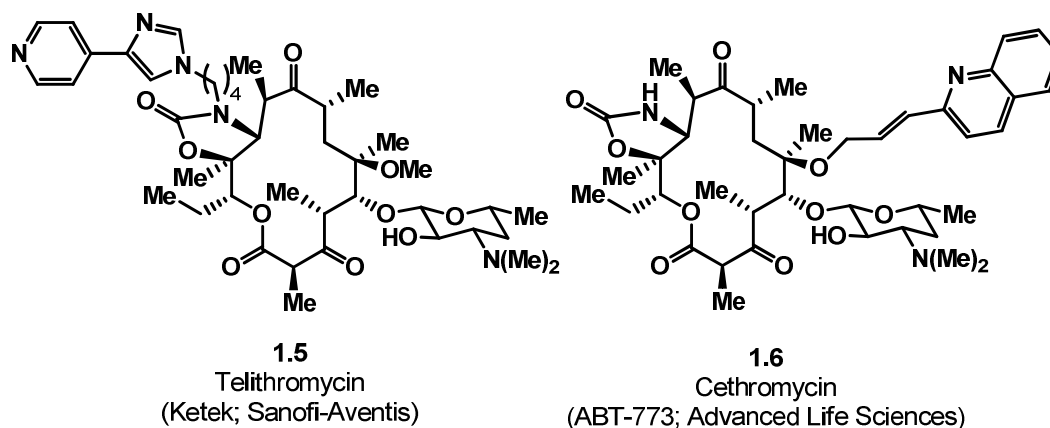


Figure I.3 Examples of 3rd Generation Macrolide Antibiotics

1.3 Previous Approaches to the Total Synthesis of Erythronolides

Natural substances of high structural complexity have always drawn the interest of leading synthetic organic chemists. The complex structure of erythromycin posed unprecedented challenges, especially the stereocontrol. In 1956 R. B. Woodward wrote: “Erythromycin, with all our advantages, looks at present quite hopelessly complex, particularly in view of its plethora of asymmetric centers.”¹⁰

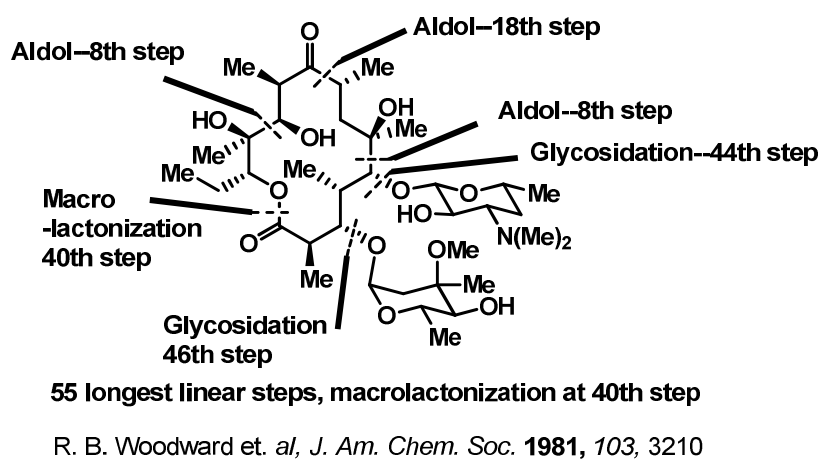
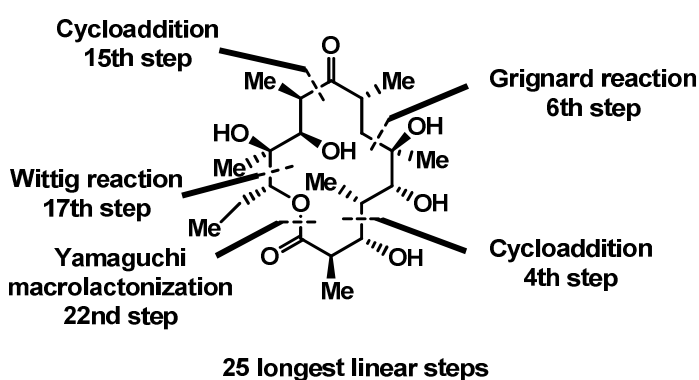


Figure I.4 Key Steps in Woodward's Total Synthesis of Erythromycin

In 1981, the Woodward group reported the first and only total synthesis of erythromycin (Figure I.4).¹¹ Despite a longest linear sequence of 55 steps, it is a milestone in the study of erythromycin compounds. One of the key findings in their synthetic study was that the macrolactonization step was important and extremely challenging. Woodward found that in order to close the fully functionalized seco-acid, it was important to modify the precursor so that the chain is folded into a favorable configuration. Many subsequent syntheses of erythronolides were guided by this finding.

Erythronolide A, the aglycone of erythromycin A, is also an interesting target for synthetic organic chemists. Many efforts were made towards this molecule. Among them, the most recent as well as the shortest route was reported by the Carreira group¹² in 2009 (Figure I.5). In their synthesis, a 23 longest linear step sequence was employed, and Mg (II) mediated cycloadditions of nitrile oxides were used as the key steps for setting many of the stereocenters.



E. M. Carreira et. al, *J. Org. Chem* **2009**, 74, 8695

Figure I.5 Key Steps in Carreira's Synthesis of Erythronolide A

Studies have shown that (9*S*)-dihydroerythronolide, the reduced form of erythronolide at the 9-keto position, was an important intermediate in the synthesis of erythromycin¹³.

According to Woodward, the 9*S* configuration was critical in the cyclization of the seco-acid. The synthesis of (9*S*)-dihydroerythronolide itself represents a formal synthesis of erythromycin. As a consequence, this molecule became another target of synthetic chemists despite its lack of biological activity. The shortest synthetic route was reported by the Hoffman group¹⁴ in 1993, while the most recent route was published by the Woerpel group¹⁵ in 2003 (Figure I.6).

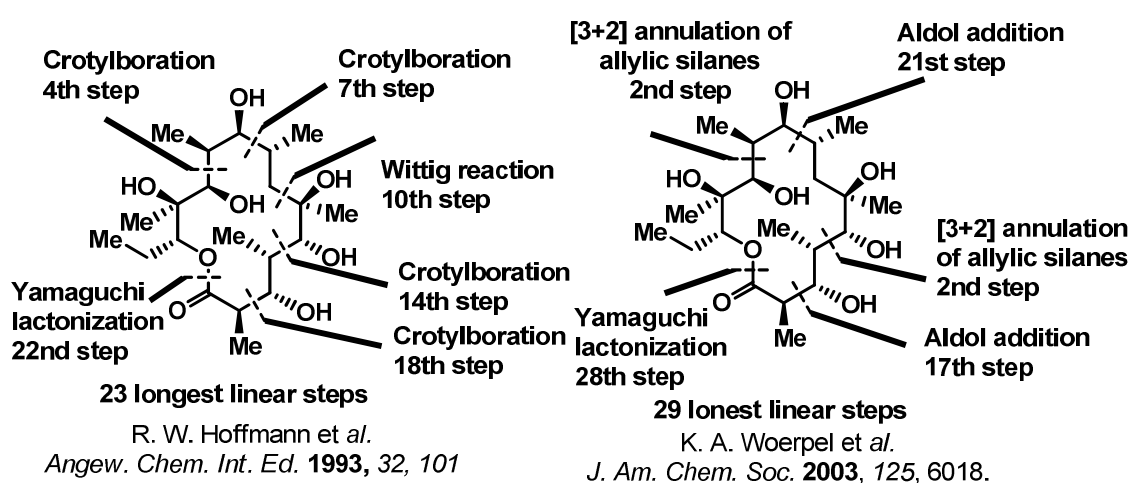
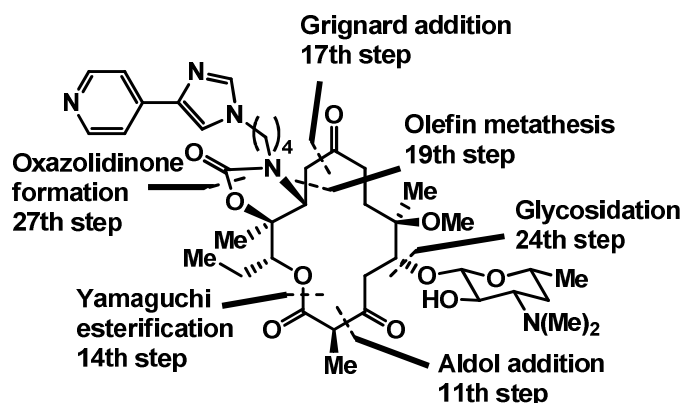


Figure I.6 Key Steps in the Hoffmann and Woerpel Syntheses of (9*S*)-Dihydroerythronolide

Total syntheses of erythromycin analogues are very rare. No such effort was reported until 2011, when the total synthesis of 4,8,10-tridesmethyl telithromycin was reported by the Andrade group¹⁶ with thirty-one longest linear step sequence. They designed this desmethyl structure based in part on the structural data from Steitz and his co-workers. Bacterial strains resistant to ketolide (MLSBK) antibiotics commonly possess either an N-methyl transferase that methylates the exocyclic N6 amine in A2058Ec in 23S rRNA or a mutated 23S rRNA, often A2058G.¹⁷ Steitz and coworkers postulated the cause of

resistance might due to a steric clash of the amino group of guanine 2058 with the C4 methyl of the drug.¹⁸



**Figure I.7 Key Steps in Andrade's Synthesis of
4,8,10-Tridesmethylnelithromycin**

1.4 Limitations of Current Methods of Antibiotic Development

The antibiotics were widely used in the treatment of infections, and as a consequence of their abuse, resistance from the bacterial mutants developed rapidly. There are three major mechanisms of resistance: 1) enzymatic modification of the drug molecule, 2) modification of the bacterial ribosome, and 3) efflux of the drug from the cell. To address the problem of resistance due to bacterial mutation, novel antibiotics must be developed. Before Andrade's studies, all the commercial erythromycin antibiotics were developed by semi-synthesis. Erythromycin was produced on large scale by fermentation and was then modified to the designed candidate. The most obvious advantage of this strategy is that it provides a short and efficient way to make complex natural product-like structures. However, a major drawback of this semi-synthetic strategy is the severe limitations placed on target choice. The fully functionalized macrolide core is very sensitive and thus requires

excessive and redundant protection-deprotection sequences for nearly any modification. More importantly, it is extremely challenging to make modifications to the macrolide core such as the removal of methyl groups. Although the study by Steiz indicates the potential benefits of removing methyl groups¹⁸, such a molecule is unlikely to be obtained by semi-synthesis. As a result, few SAR studies have focused on modifications of the main carbon skeleton of macrolides.

In contrast, modern methods enable chemists to make almost any designed structure by total synthesis. Andrade's synthesis of 4,8,10-tridesmethyl telithromycin is one such example: a target that cannot be made from erythromycin but can be made by total synthesis. However, we found that it is far from trivial to make many macrolides. Traditional syntheses target one molecule, not the diverse collection of structures that is demanded by medicinal chemists. Developing a specific route for one drug candidate does not allow for the preparation of a large sample pool for drug discovery.

1.5 Conclusion

The structural complexity of erythromycin macrolides is one of the major obstacles in the related drug discovery process, and it is widely accepted that the development of erythromycin antibiotics requires a complete understanding of their structure-activity relationships. Therefore, an urgent need exists to develop a method to gain rapid access to erythromycin structure space. As we have reviewed above, both semi-synthesis and total synthesis have had some, though quite limited, success in the development of novel antibiotics.

Herein we will discuss a novel integrated routing strategy to address this problem. The details of the integrated routing strategy will be discussed in chapter II; the synthesis of the macrocyclic bis[allene] will be discussed in chapter III; a new method for allene oxidation and derivitization will be discussed in chapters IV and VI; The synthesis of erythronolide derivatives will be discussed in chapter V.

1.6 References

1. McGuire, J. M.; Bunch, R. L.; Anderson, R. C.; Boaz, H. E.; Flynn, E. H.; Powell, H. M.; Smith, J. W. *Antibiot. Chemother.* **1952**, 2, 281.
2. Nenad Ban; Poul Nissen; Jeffrey Hansen; Peter B. Moore; Steitz, T. A. *Science* **2000**, 289, 905.
3. Hansen, J. L.; Ippolito, J. A.; Ban, N.; Nissen, P.; Moore, P. B.; Steitz, T. A. *Molecular cell* **2002**, 10, 117.
4. Harms, J.; Schlunzen, F.; Zarivach, R.; Bashan, A.; Gat, S.; Agmon, I.; Bartels, H.; Franceschi, F.; Yonath, A. *Cell* **2001**, 107, 679.
5. Schlunzen, F.; Zarivach, R.; Harms, J.; Bashan, A.; Tocilj, A.; Albrecht, R.; Yonath, A.; Franceschi, F. *Nature* **2001**, 413, 814.
6. Kurath, P.; Jones, P.; Egan, R.; Perun, T. *Cellular and Molecular Life Sciences* **1971**, 27, 362
7. Itoh, Z.; Nakaya, M.; Suzuki, T.; Arai, H.; Wakabayashi, K. *Am. J. Physiol.* **1984**, 247, G688.
8. Doern, G. V.; Richter, S. S.; Miller, A.; Miller, N.; Rice, C.; Heilmann, K.; Beekmann, S. *Clinical Infectious Diseases* **2005**, 41, 139.
9. Katz, L.; Ashley, G. W. *Chem. Rev.* **2005**, 105, 499.
10. Woodward, R. B. *Perspective in organic synthesis*, Interscience, London **1956**, p.160.
11. Woodward, R. B. et al. *J. Am. Chem. Soc.* **1981**, 103, 3215.
12. Muri, D.; Carreira, E. M. *J. Org. Chem.* **2009**, 74, 8695

13. Toshima, K.; Nozaki, Y.; Mukaiyama, S.; Tamai, T.; Nakata, M.; Tatsuta, K.; Kinoshita, M. *J. Am. Chem. Soc.* **1995**, *117*, 3717.
14. Sturmer, Rainer.; Kerstin, R.; Hoffmann, R. W. *Angew. Chem. Int. Ed. Engl.* **1993**, *32*, 101.
15. Peng, Z.; Woerpel, K. A. *J. Am. Chem. Soc.* **2003**, *125*, 6018.
16. Velvadapu, V.; Paul, T.; Wagh, B.; Klepacki, D.; Guvench, O.; MacKerell, A.; Andrade, R. B. *ACS Med. Chem. Lett.* **2011**, *2*, 68.
17. Weisblum, B. *Antimicrob. Agents Chemother.* **1995**, *39*, 577.
18. Tu, D.; Blaha, G.; Moore, P. B.; Steitz, T. A. *Cell* **2005**, *121*, 257.

Chapter II

Erythronolide Structure Space

2.1 Introduction

The beauty of complex small molecule natural products lies not only in their structure, but also in their promising biological activity. Synthetic organic chemists have traditionally focused on the construction of these complicated structures. Exploration of structure-activity relationships (SARs) was not a general priority until two decades ago.

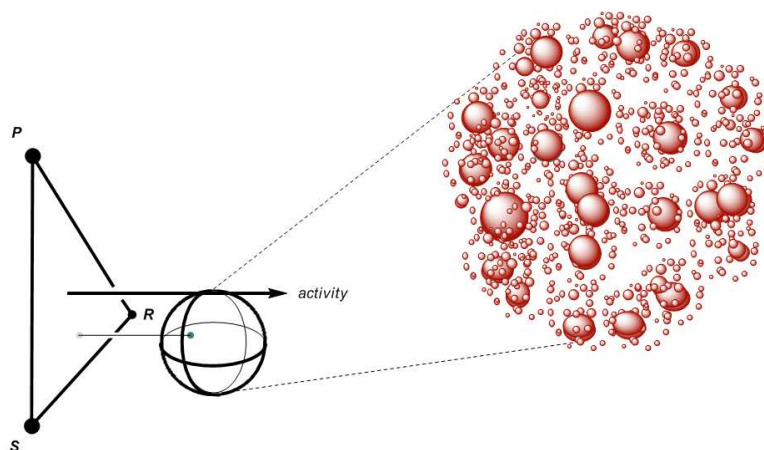


Figure II.1 Structure-activity Space

The triangle plane represents the structural similarity of molecules
(P=planar, R=rod-like, S=sphere-like)

Consider a family of complex molecules that have the similar core structures and exhibit similar activity. If the molecules are plotted in structure-activity space, those with similar functionality, shape, and activity will be close to each other (Figure II.1).

Our efforts to access natural product structure space focus on synthesizing molecules that have similar or superior biological activities. In the modern pharmaceutical industry, one of the main goals of the synthetic organic chemist is to gain access to one or more sectors of the targeted structure space. Many methods and strategies have been developed to achieve this goal.

2.2 An Integrated Routing Strategy for the Exploration of Erythronolide Structure Space

The exploration of unknown structure space is quite valuable. One major reason is that a natural product, although being the result of evolution, may not meet the needs of human health. Erythromycin (Figure II.2) is one such example. Having been widely used for several decades, it is one of the most efficient broad spectrum antibiotics. However, as described in Chapter I, its usefulness is compromised due of its instability in the human body and the resistance developed by certain types of bacterial mutants. Thus, it has become important to explore the structure space of erythromycin, targeting molecules that have similar activity but without the drawbacks.

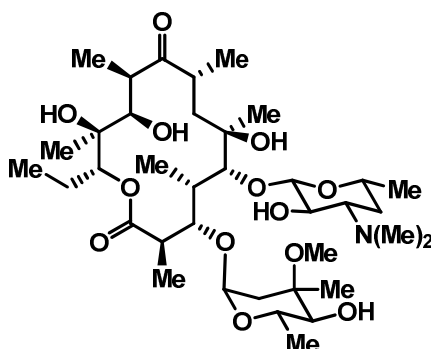


Figure II.2 Erythromycin A

Pharmaceutical scientists have been working in this area for over twenty years, and some progress has been made. However, their methods and results can be further optimized to address deficiencies in efficient methods to gain unlimited access to erythromycin structure space. Described herein is an integrated routing strategy for the exploration of erythronolide structure space.

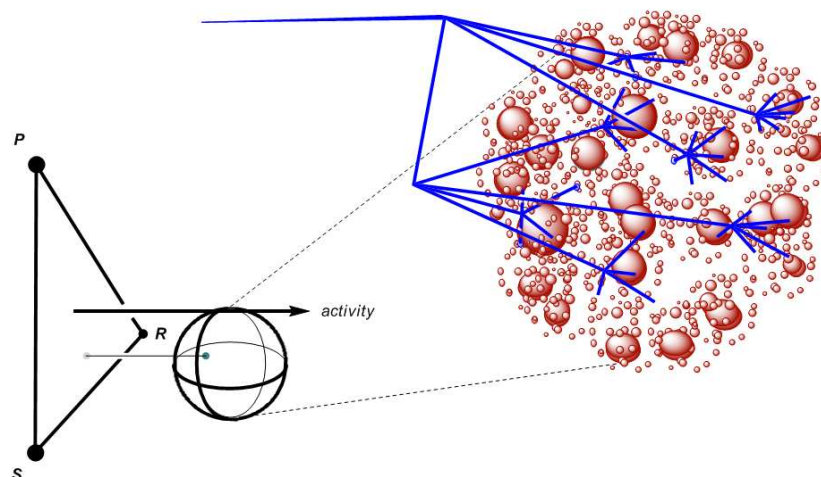


Figure II.3 Integrated Routing Strategy

Our group has been working on the integrated routing strategy towards the synthesis of some natural product families.^{1,2} The most important feature of the integrated routing strategy is that a common intermediate is synthesized as the precursor of many targeted

products (Figure II.3). This intermediate is designed to be structurally very similar to the target molecules in the structure space, therefore making the conversions easier. Ideally, one would design such an intermediate that can be modified as divergently and extensively as possible. Hence, the design of this intermediate is one of the most important facets of the strategy.

2.3 Design of the Key Intermediate Structure

The design of the key intermediate structure is highly dependent on the target structure space that one would like to access. In order to achieve maximum efficiency, the best choice of molecule would be one with a high degree of complexity while remaining modifiable at the important sites which are likely involved in biological interactions.

Guided by this principle, the data from previous SAR studies was taken as reference for the design of the key intermediate.³⁻⁵ As shown in Figure II.4, prior studies indicates the following: (a) portions of the glycans, especially the amino sugar, are critical, and both the hydrophilic character of the β -face and the hydrophobic character of the α -face of the macrolide contribute to binding (center structure);⁶ (b) C9 amine or oxime functionality suppresses unwanted side effects (V);^{3,5} (c) C9_C11 or C11_C12 heteroannulation can improve binding and appears to represent opportunities to overcome resistance (VI, VII);^{7,8} (d) C6_C9 heterocyclization leads to interesting (albeit nonantibiotic) activity (VIII);⁹ and (e) retention of the C6 and C12 heteroatom connectivity is desirable, and ether formation at C6 may improve the antibiotic activity and suppress other activity (V, IX).^{10,11} (f) C3 ketone derivatives (X) and alterations to the hydrophobic face of the macrocycle (e.g., at C4, C8, and C10; XI and XII) may overcome resistance.^{12,13} Hence, modification

of the C3_C6 and C9_C12 regions offers opportunities to improve drug properties and avoid bacterial resistance.

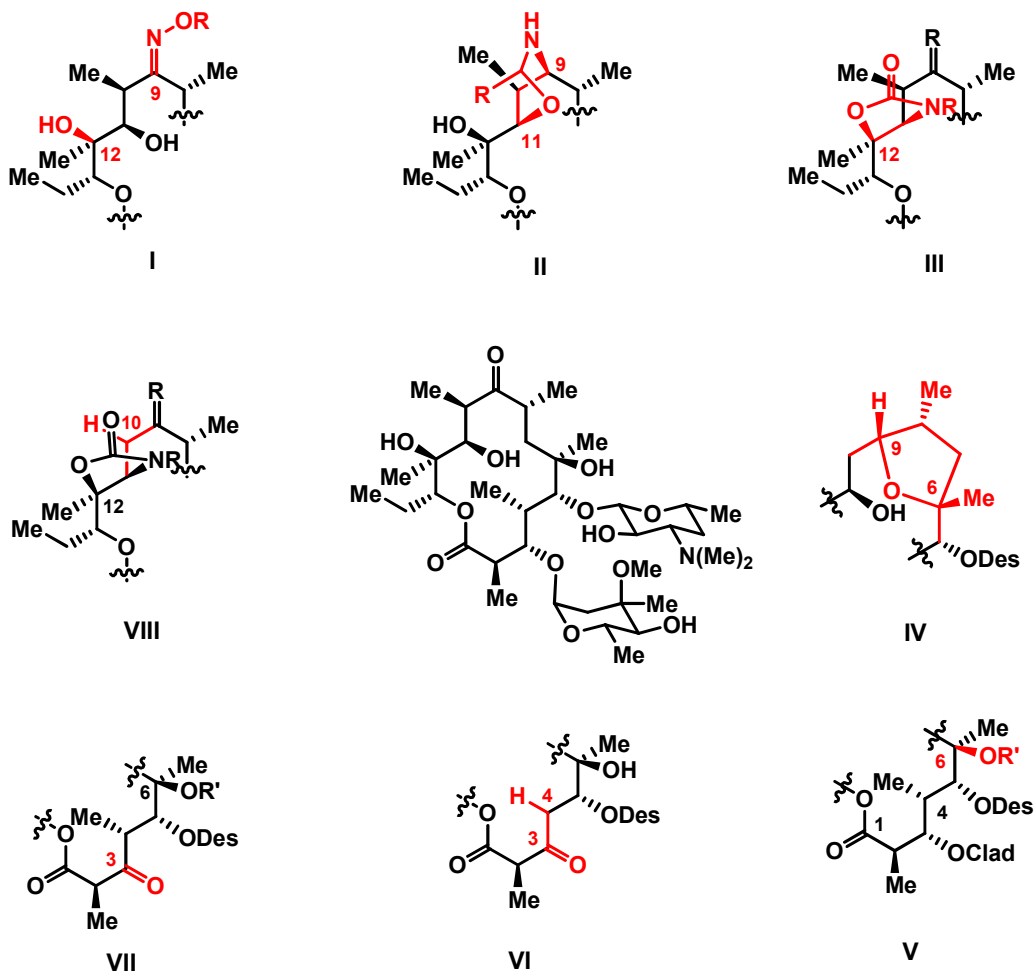
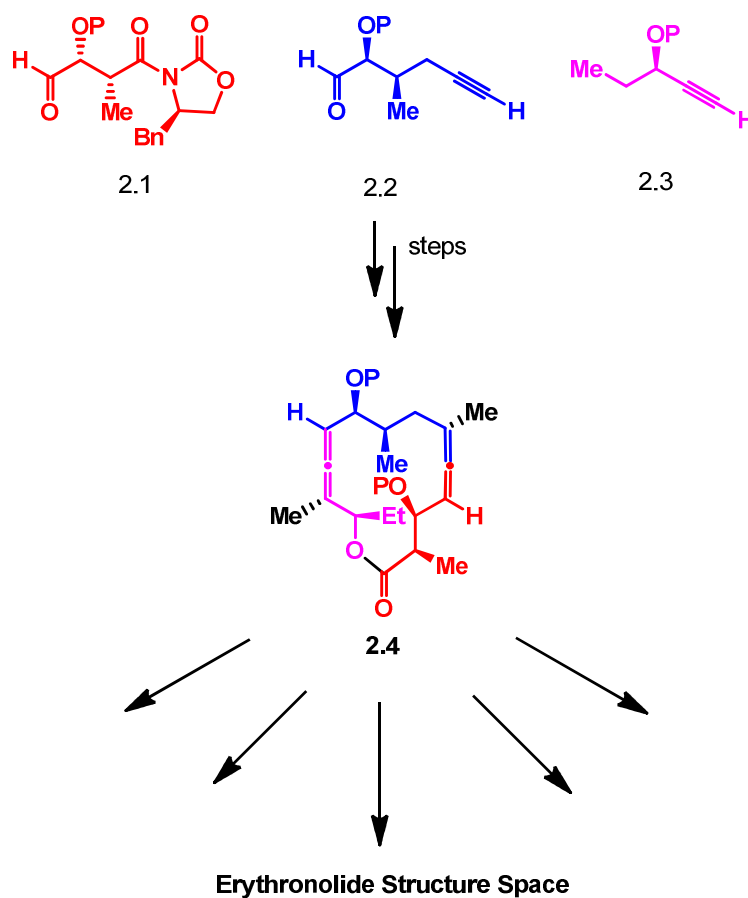


Figure II.4 Previous SAR Studies of Erythromycinoids

We decided to use a bis-allenic structure to replace these active binding areas in order to enable diverse modifications. The macrocyclic bis[allene] was planned to be synthesized from the coupling between a C4 aldehyde **2.1**, a C6 alkyne **2.2** and a C5 alkyne **2.3** (Scheme II.1). The synthesis is convergent, and the routes are short.

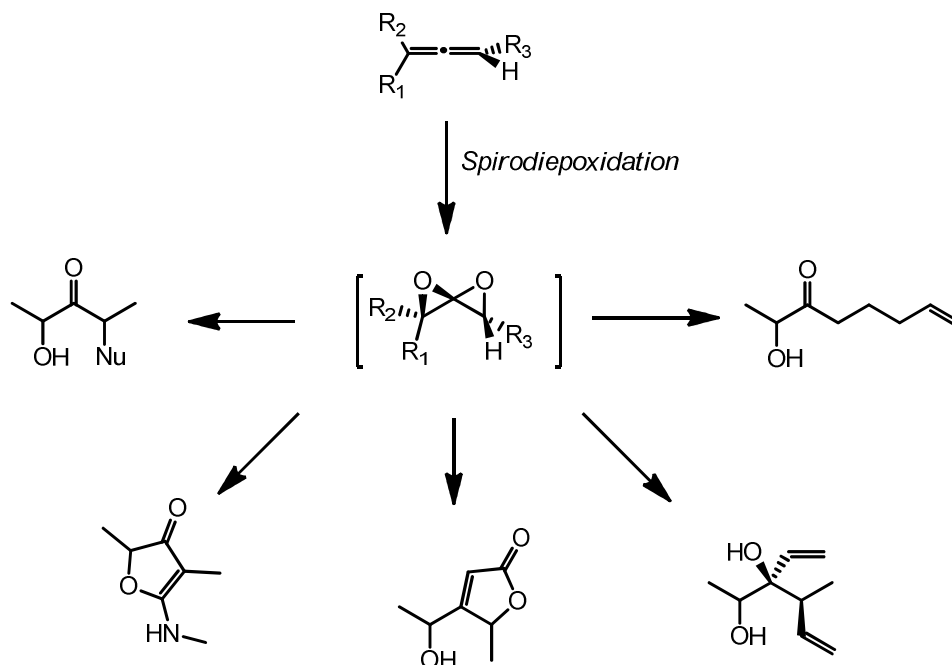


Scheme II.1 Synthesis of Erythromycinoids

2.4 Exploration of the Structure Space

The modification of allenes is central to the execution of this synthetic strategy. The properties of allenes are relatively underexplored compared with other unsaturated groups such as alkenes and alkynes. One of the main focuses of our research group is the oxidation and derivatization of allene-containing compounds. The use of dimethyldioxirane (DMDO) enables oxidation of the allene to a spirodiepoxide (SDE) intermediate (Scheme II.2). There has been little precedent on the chemistry of spirodiepoxides, primarily because they have very low stability towards acids, bases, and heat.^{14,15} Our group has demonstrated that

by employing proper reaction conditions, the reactive spirodiepoxides can be efficiently converted into various types of structural motifs.¹⁶⁻¹⁸



Scheme II.2 Allene Spirodiepoxidation and Derivatization

However, there are still several concerns regarding the application of SDE chemistry. First, the properties of SDEs in a macrolide system are unexplored, except by our group, and we have little insight as to how they may react. My colleague Dr. Partha Ghosh and Dr. Yue Zhang conducted a model study using an unfunctionalized macrocyclic bis[allene].¹⁹ The results showed that the resulting SDEs are not as well behaved as they are on linear systems; however, desired products were still observed. Another concern was that despite the richness of SDE chemistry, this chemistry will not grant us unlimited access to erythromycinoid structure space. In order to solve this problem, new methods for allene derivatization would need to be developed.

2.5 References

1. Drahl, M. A.; Akhmedov, N. G.; Williams, L. J. *Tetrahedron Lett.* **2011**, 52, 325.
2. Xu, D.; Drahl, M. A.; Williams, L. J. *Beilstein J. Org. Chem.* **2011**, 7, 937.
3. Chantot, J.-F.; Bryskier, A.; Gasc, J.-C. *J. Antibiot.* **1986**, 39, 660.
4. Gouin d'Ambrieres, Solange; Lutz, Andre; Gasc, Jean Claude. (Demande, Fr.).
Erythromycin oxime derivatives and their use as drugs. FR Patent 2473525 A1 19810717.
Language: French. 1981.
5. Gasc, J.-C.; D'Ambrieres, S. G.; Lutz, A.; Chantot, J.-F. *J. Antibiot.* **1991**, 44, 313.
6. Mao, J. C. H.; Putterman, M. *J. Mol. Bio.* **1969**, 44, 347.
7. Counter, F. T.; Ensminger, P. W.; Preston, D. A.; Wu, C. Y.; Greene, J. M.; Felty-Duckworth, A. M.; Paschal, J. W.; Kirst, H. A. *Antimicrob. Agents Chemother.* **1991**, 35, 1116.
8. Agouridas, C.; Denis, A.; Auger, J.-M.; Benedetti, Y.; Bonnefoy, A.; Bretin, F. o.; Chantot, J.-F. o.; Dussarat, A.; Fromentin, C.; D'AmbriÃ`res, S. G.; Lachaud, S.; Laurin, P.; Le Martret, O.; Loyau, V. r.; Tessot, N. *J. Med. Chem.* **1998**, 41, 4080.
9. Omura, S.; Tsuzuki, K.; Sunazuka, T.; Marui, S.; Toyoda, H.; Inatomi, N.; Itoh, Z. *J. Med. Chem.* **1987**, 30, 1941.
10. Morimoto, S.; Takahashi, Y.; Watanabe, Y.; Omura, S. *J. Antibiot.* **1984**, 37, 187.
11. Morimoto, S.; Adachi, T.; MisawaI, Y.; Nagate, T.; Watanabe, Y.; Omura, S. *J. Antibiot.* **1990**, 43, 544.
12. Velvadapu, V.; Paul, T.; Wagh, B.; Klepacki, D.; Guvench, O.; MacKerell, A.; Andrade, R. B. *ACS Med. Chem. Lett.* **2011**, 2, 68.
13. Dunkle, J. A.; Xiong, L.; Mankin, A. S.; Cate, J. H. D. *P. Natl. Acad. Sci. USA* **2010**, 107, 17152.
14. Crandall, J. K.; Machleder, W. H. *J. Am. Chem. Soc.* **1968**, 90, 7292.
15. Crandall, J. K.; Conover, W. W.; Komin, J. B.; Machleder, W. H. *J. Org. Chem.* **1974**, 39, 1723.
16. Ghosh, P.; Lotesta, S. D.; Williams, L. J. *J. Am. Chem. Soc.* **2007**, 129, 2438.

17. Lotesta, S. D.; Kiren, S.; Sauers, R. R.; Williams, L. J. *Angew. Chem., Int. Ed.* **2007**, *46*, 7108.
18. Sharma, R.; Manpadi, M.; Zhang, Y.; Kim, H.; Akhmedov, N. G.; Williams, L. J. *Org. Lett.* **2011**, *13*, 3352.
19. Ghosh, P.; Zhang, Y.; Emge, T. J.; Williams, L. J. *Org. Lett.* **2009**, *11*, 4402.

Chapter III

Synthesis of the Macrocyclic [Bis]allene

3.1 Introduction

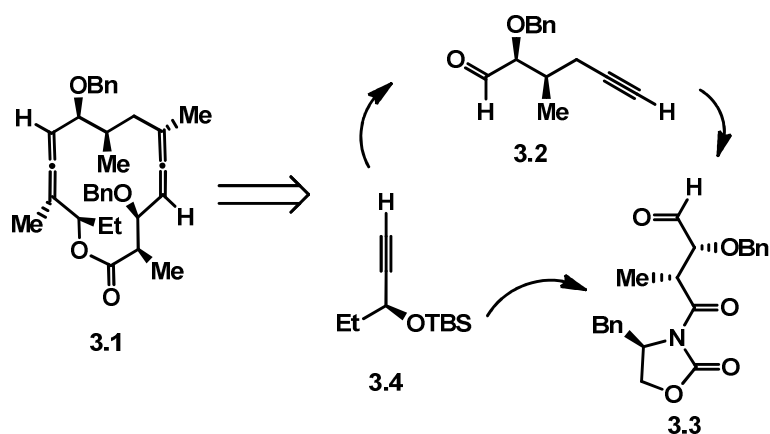
One of the key molecules in this integrated routing strategy is the macrocyclic [bis]allene. Up until now, there was only one report of a similar cyclic [bis]allene by our group.¹ Therefore, the synthesis of such a structure was unprecedented.

There are a few concerns regarding the synthesis. First of all, the macrocyclization could be challenging. According to Woodward, the cyclization of a 14-membered ring is not easy and requires a specific placement of atoms. However, even small modifications could possibly change the conformation of the seco-acid considerably, hence making the lactonization step problematic. Another unknown factor is the stability and reactivity of such a bis[allene] in somewhat strained cyclic system. Although we do have a handful of data regarding allene oxidation, allenes on 14-membered rings have rarely been examined. Despite all of these concerns, we still believed that allenes are rich in interesting reactivity, and that this would be a promising way to solve the existing problem of accessing erythromycin structure space. We will focus on the synthesis of the macrocyclic [bis]allene. The route was first developed by my colleague, Dr. Partha Ghosh.² Since then, Dr. Hiyun

Kim and I have made improvements to the initial route in terms of efficiency and reproducibility. Our implements are presented below.

3.2 Synthesis of the Three Key Coupling Units

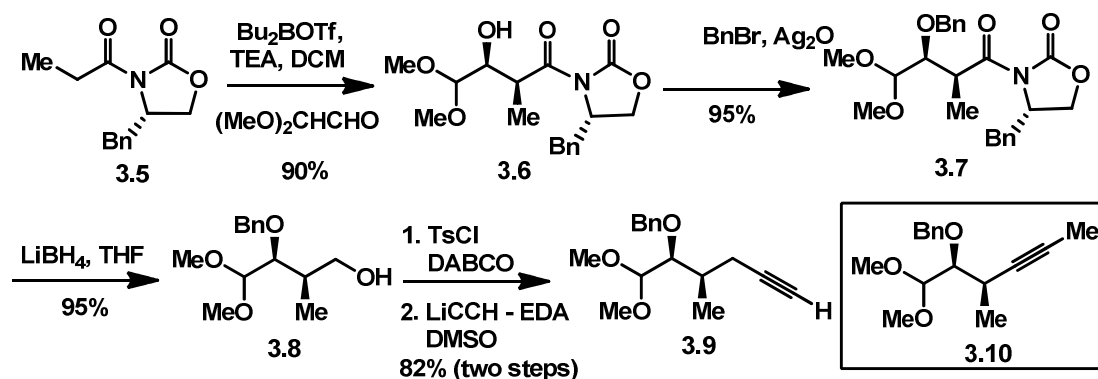
The macrocyclic bis[allene] structure was designed to be **3.1** (Scheme III.1). The route was planned to be convergent. Three fragments were designed as shown, including a C6-terminal alkyne **3.2**, a C4-aldehyde **3.3**, and a C5-terminal alkyne **3.4**. They would be coupled to each other by metal-mediated alkynylation then converted to allenes. Yamaguchi lactonization was planned to be the last step.



Scheme III.1 Retrosynthetic Analysis of the Macrocyclic Bis[allene]

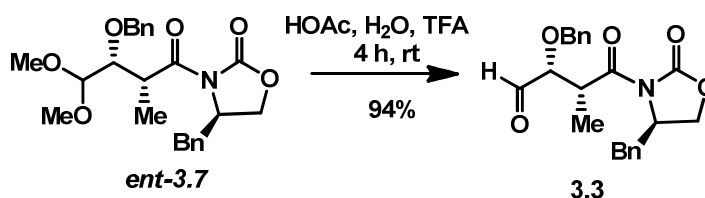
The synthesis of the C6-alkyne began with an aldol reaction using the Evans chiral auxiliary **3.5** (Scheme III.2).³ The desired *syn*-aldol adduct **3.6** was obtained in desirable yield and d.r. It is remarkable in that it is the first example of a dimethoxyacetaldehyde being used in the Evans aldol reaction. The benzylation attempts of **3.6** using NaH and BnBr were not successful, presumably due to the retro-aldol reaction. However, an alternative condition using silver (I) oxide and BnBr was successful.⁴ Although it was

sensitive to water and slow (usually taking about two days for completion), we were still able to isolate the product in excellent 95% yield.



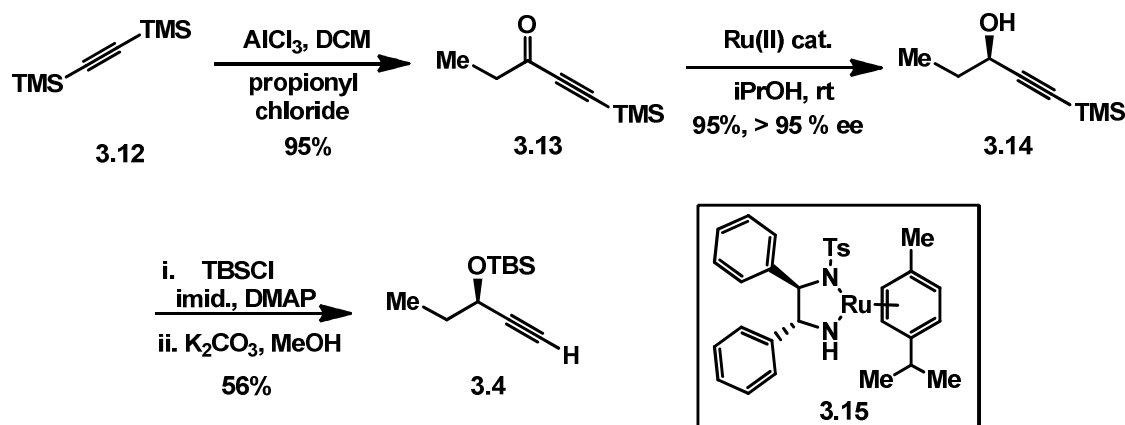
Scheme III.2 Synthesis of the C6-Alkyne

The benzylated compound **3.7** was then reduced with LiBH_4 to afford the primary alcohol **3.8** via cleavage of the chiral auxiliary (Scheme III.2). Dr. Partha Ghosh reported that the tosylation of **3.8** using pyridine takes twelve hours to complete. The reaction time was reduced to one hour by using DABCO instead of pyridine.⁵ The crude tosylate product was then added to a solution of lithium acetylide ethylenediamine complex to give the terminal alkyne **3.9**. A significant amount of byproduct **3.10**, which is very difficult to separate from the desired product, was observed if this reaction was quenched with NH_4Cl at room temperature. The formation of this byproduct could be suppressed by adding NH_4Cl solution dropwise over twenty minutes at 15°C instead of adding it in a single portion.



Scheme III.3 Synthesis of the C4-Aldehyde

The C4-aldehyde was synthesized in one step from the enantiomer of **3.7**, which was made using the same two-step sequence (Scheme III.3). Mild acid hydrolysis of the acetal group over four hours afforded the desired C4-aldehyde **3.3** in 94% yield.

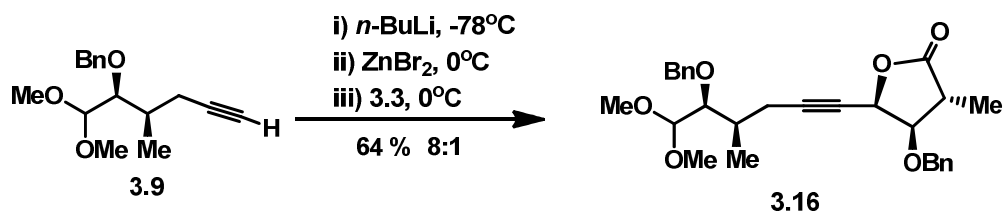


Scheme III.4 Synthesis of the C5-Alkyne

The synthesis of the C5-alkyne starts with the simple bis-TMS acetylene **3.12** (Scheme III.4). Friedel-Crafts type acylation afforded the C5-ynone, which was reduced with excellent enantioselectivity using the (*R,R*)-Noyori catalyst **3.15**.⁶ A simple protection-deprotection sequence of the product **3.14** gave the desired known C5-alkyne **3.4** in 56% yield. The low yield is presumably due to the loss of volatile product under reduced pressure.

3.3 Coupling of the Three Building Blocks

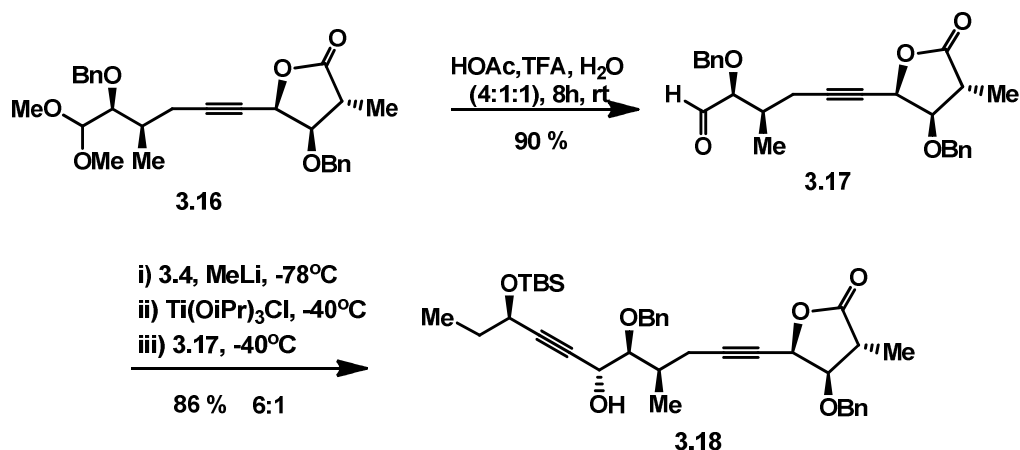
The C6-alkyne **3.2**, C4-aldehyde **3.3**, and C5-alkyne **3.4** were brought together sequentially by metal-mediated alkynylation. The first coupling was done between **3.2** and **3.3** (Scheme III.5).



Scheme III.5 The First Coupling

This reaction was first done by Dr. Partha Ghosh using zinc bromide mediated chelation-controlled alkynylation. Dr. Hiyun Kim and I found that some details are not fully understood, hence the reaction was capricious. After extensive modifications, we found that an carefully and fully dried solution of zinc bromide in diethyl ether was the key to reaction success. Moreover, the reaction temperature was also important, requiring careful monitoring and control at 0°C at the coupling stage.

One major drawback of the reaction is that to ensure good yield and selectivity, excess (often >2 equivalents) of alkyne **3.9**, is needed. This limits the efficiency, especially since this fragment requires more effort to prepare. Still, the unreacted alkyne can be recovered, and the yield based on recovered material is an excellent 90%. Further attempts to optimize this reaction with Carreira's asymmetric alkynylation conditions using Jiang's chiral ligand⁷ were found to be inferior. These experiments helped determine the *syn* configuration of the product formed, which is also the expected configuration from chelation-controlled alkynylation.⁸



Scheme III.6 The Second Coupling

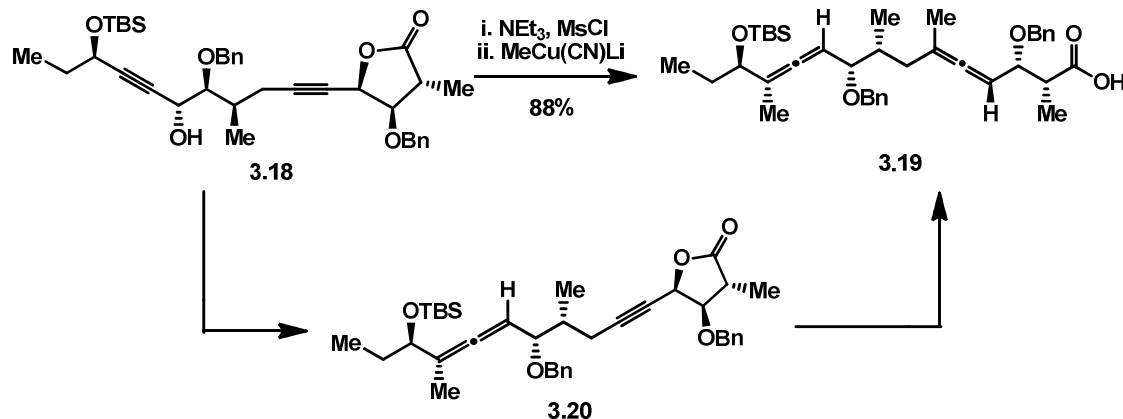
The second coupling between **3.17** and C5-alkyne **3.4**, however, was much smoother, presumably because of the higher stability of aldehyde **3.17**. Acid hydrolysis of the first coupling product **3.16** gives the desired aldehyde, though it takes longer to go to completion.

In order to obtain the *anti*-adduct, non-chelation controlled alkynylation conditions were employed.⁹ Thus, **3.4** was treated with methyl lithium followed by addition of chloritriisopropoxyl titanium (IV) solution. Aldehyde **3.17** was then added to afford **3.18** with the desired stereochemical configuration. Variation of experimental conditions showed that it is very important to maintain the temperature at -40°C during the addition of the titanium reagent, failure to do so resulted in low yield and diastereoselectivity.

3.4 Synthesis of the Macrocyclic [Bis]allene

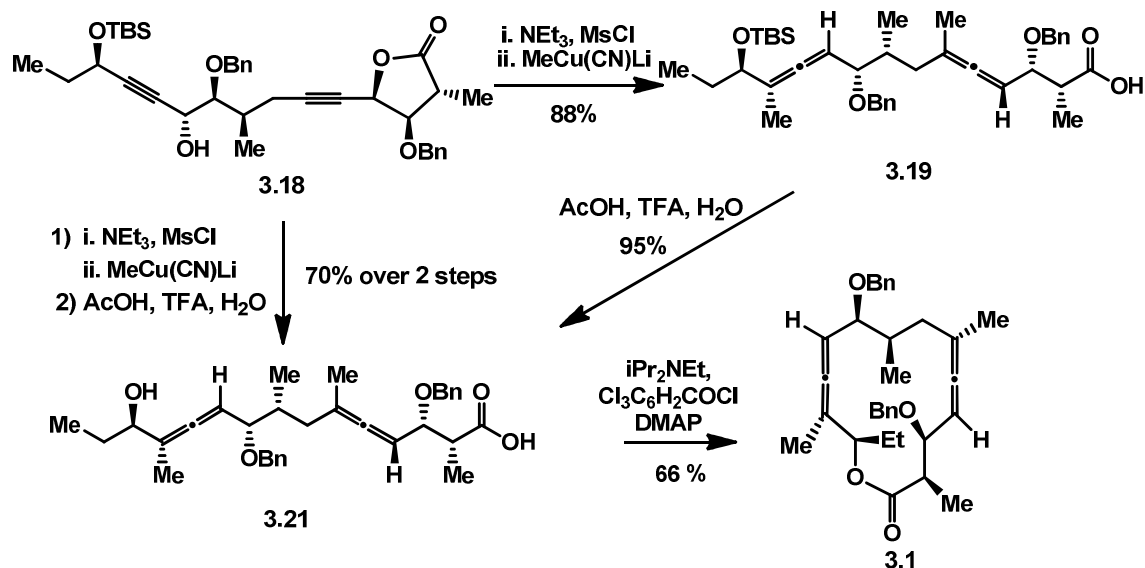
The coupling product **3.18**, which can be made on multi-gram scale, was then taken forward. It was first activated as the methanesulfonyl ester, then a single flask allene

synthesis with excess methyl cyano cuprate afforded the desired bis-allene **3.19** (Scheme III.7).



Scheme III.7 One-pot Synthesis of the Bis[allene]

An interesting feature of this reaction is that although it can give the desired product in one step, we found that we were able to stop the reaction at the mono-allene **3.20** stage by using a stoichiometric amount of cuprate. This is reflective of the increased reactivity of the mesylated relative to the lactone. The mono-allene can be converted to the bis[allene] **3.19** by further treatment with fresh cuprate. Although this seems redundant at this stage, we thought we could further utilize this differentiated reactivity. Details concerning this will be discussed in later sections.



Scheme III.8 Synthesis of the Seco-Acid and the Macrocyclic Bis[allene]

The TBS ether on **3.19** was removed with acid to afford seco-acid **3.21** in 95% yield (Scheme III.8). The overall process time can be shortened by skipping the purification of **3.19** and instead pushing the crude material through the deprotection step. In this way, **3.21** can be obtained with a satisfying 70% yield.

Yamaguchi lactonization of **3.21** affords the desired bis[allene] macrolide **3.1**.¹⁰ One major byproduct was found to be the dimerized macrolide **3.22** (Figure III.1). After optimization, we were able to obtain the desired product in good yield (64%) by using dilute solution and slow addition of the active ester into a hot DMAP solution over the course of two hours.

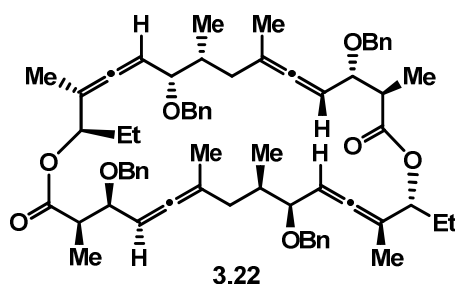
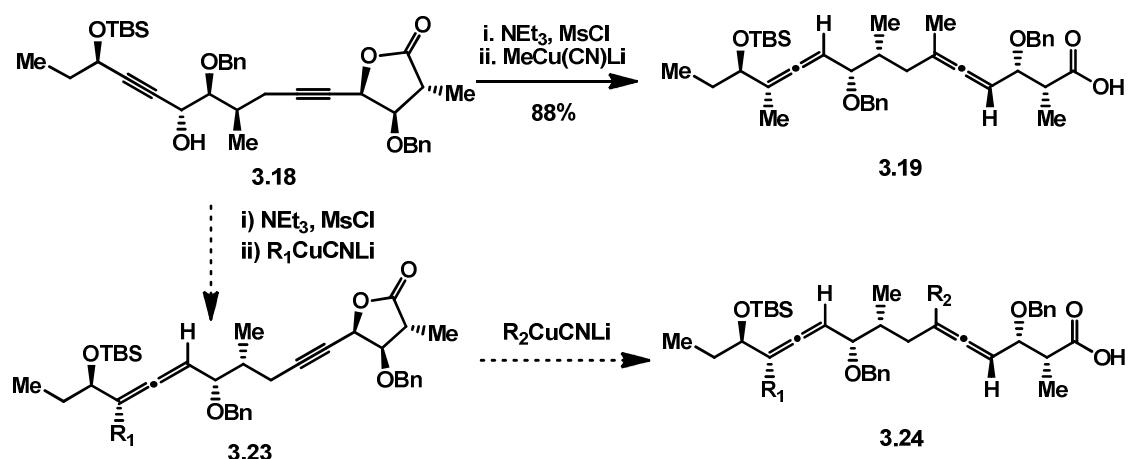


Figure III.1 The Dimerized Byproduct of Lactonization

3.5 Flexibility of the Route: Possibilities for Further Modification

As we discussed in chapter 2, one of the major drawbacks of the total synthesis approach to erythromycin antibiotics is the lack of flexibility in the synthetic route. One has to start over from an early stage of the route to make any new target molecule. However, by using the convergent synthetic strategy described above, this problem can possibly be addressed. For example, we could imagine the possibility of modifying one of the three building blocks without changing the other two. This way the route itself is not significantly different, and changes will not be made until after the 6-8th step. Another possibility for modification is enabled by the stepwise bis[allene] formation (Scheme III.9). Since we were able to differentiate the rate of formation of the two allenes, the incorporation of heterofunctionality was possible.



Scheme III.9 Incorporation of Heterofunctionality in the Bis[allene]

3.6 Conclusion

The macrocyclic bis[allene] was made in eleven longest linear steps, only nine of which require purification. The overall yield is 10% from commercially available material. We were able to make the seco-acid **3.21** on gram scale and macrolide **3.1** in 500 mg scale. Although it is also interesting to explore the possibility of assembling new macrolide scaffolds with different building blocks, we decided to start working on the bis[allene] in hand. The oxidation and derivatization of allenes is our next focus.

3.7 References

1. Ghosh, P.; Zhang, Y.; Emge, T. J.; Williams, L. J. *Org. Lett.* **2009**, *11*, 4402.
2. Ghosh, P. New methods and strategies towards total synthesis of (9S)-dihydroerythronolide A. Ph.D. Thesis, Rutgers, The State University of New Jersey, New Brunswick, 2008.
3. Evans, D. A.; Ratz, A. M.; Huff, B. E.; Sheppard, G. S. *J. Am. Chem. Soc.* **1995**, *117*, 3448.
4. Vlahov, I. R.; Vlahova, P. I.; Schmidt, R. R. *Tetrahedron Lett.* **1991**, *32*, 7025.

- 5.Hartung, J.; Hunig, S.; Kneuer, R.; Schwarz, M.; Wenner, H. *Synthesis* **1997**, 1433.
- 6.Matsumura, K.; Hashiguchi, S.; Ikariya, T.; Noyori, R. *J. Am. Chem. Soc.* **1997**, *119*, 8738.
- 7.Jiang, B.; Chen, Z.; Xiong, W. *Chem. Comm.* **2002**, *14*, 1524.
- 8.Mead, K. T. *Tetrahedron Lett.* **1987**, *28*, 1019.
- 9.Shimizu, M.; Kawamoto, M.; Niwa, Y. *Chem. Comm.* **1999**, *12*, 1151.
- 10.Inanaga, J.; Hirata, K.; Saeki, H.; Katsuki, T.; Yamaguchi, M. *Bull. Chem. Soc. Jpn.* **1979**, *52*, 1989.

Chapter IV

Allene Osmylation: Methods for Improvement of Efficiency

4.1 Introduction

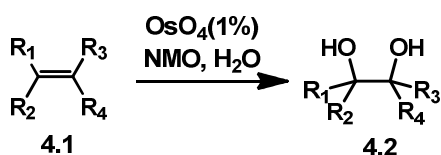
Synthetic organic chemists have been studying the reactivity of all types of unsaturated systems including alkenes, allenes and alkynes for many decades. Among these, allenes have received the least attention. For example, unlike the well developed methods for alkene epoxidations, allene epoxidations were rarely reported. The initial research on the allene epoxides and spirodiepoxides (SDEs), which were the mono- and bis- epoxidation product of an allene, respectively, was reported many years ago.^{1, 2} It was thought that the allene epoxides were highly unstable and would easily undergo rearrangement under many reaction conditions. Our group has extensively studied SDEs and has shown that the SDEs can be used in structure motif building studies.³⁻⁶ Routes toward synthesis of complex natural products via allene spirodiepoxidation as the key reaction have also been also reported.⁷⁻¹¹

However the application of SDE chemistry in the macrocyclic bis[allene] derivitization was still a concern. The reactivity of a SDE on a strained system is not well preceded

and the stability is not guaranteed. Dr. Partha Ghosh showed that methyl cuprate can be successfully added to the SDE in a single macrocyclic bis[allene], however the yield is low.¹⁰ More importantly, the same reaction conditions failed to deliver methyl group to the fully functionalized macrocyclic bis[allene], which is designed to be the key step of the synthesis of (9*S*)-dihydroerythronolide. Hence, a new method for allene oxidation and modification is needed.

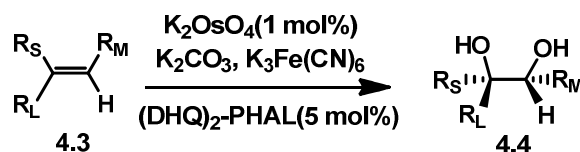
4.2 Alkene Osmylation: A Brief Overview

The osmium tetroxide catalyzed dihydroxylation is one of the most important methods for the oxidation of alkenes. It has been studied for almost a century. It is a powerful tool to make vicinal diols, a common structure motif in the polyketide natural product. At first, catalytic osmium tetroxide was employed along with stoichiometric amount of a strong co-oxidant such as hydroperoxides. However, significant amount of over oxidation byproduct such as the vicinal diketone was usually observed.



Scheme IV.1 The Upjohn Dihydroxylation

A modification of this procedure was made by V. VanRheenen et al of the Upjohn Company in USA in 1976.¹² *N*-methylmorpholine *N*-oxide (NMO) was employed as the co-oxidant instead of hydroperoxides. This reagent is very mild and significantly suppressed the formation of over oxidation byproducts and increased the yield of the desired vicinal diol (Scheme IV.1).



Scheme IV.2 The Sharpless Asymmetric Dihydroxylation

The most widely used asymmetric dihydroxylation method was developed by K. B. Sharpless.¹³ Using the K_2OsO_4 dihydrate powder as osmium source, $\text{K}_3\text{Fe(CN)}_6$ with the combination of K_2CO_3 as the co-oxidant, and the use of chiral quinine ligand $(\text{DHQ})_2\text{-PHAL}$ or $(\text{DHQD})_2\text{-PHAL}$ can afford the vicinal diol in high yield and *ee*. This method is well known as the Sharpless Asymmetric Dihydroxylation (SAD).

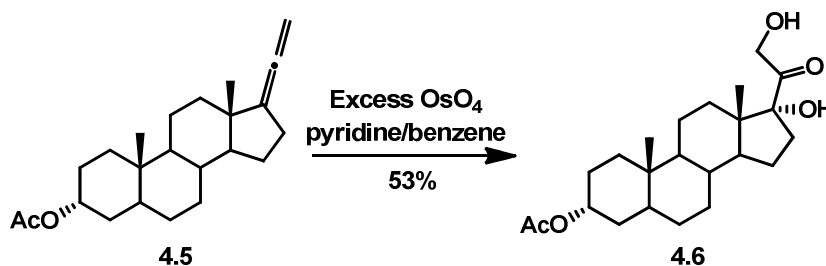
There are several major advantages of this method, not only because of its high yield and stereoselectivity. For example, it is one of the easiest reactions to perform: water is used as solvent and atmosphere oxygen is not a concern. Also this reaction is mild and chemo-selective, few other functional groups are affected, and it is also very selective between alkenes with different electron density and steric accessibility.

The development of the SAD reaction greatly enhanced the practicality of the alkene osmylation, and it has been widely used in the total synthesis of natural products. Numerous reports of successful applications have appeared since the original Sharpless publications.

4.3 Allene Osmylation: An Underexplored Field

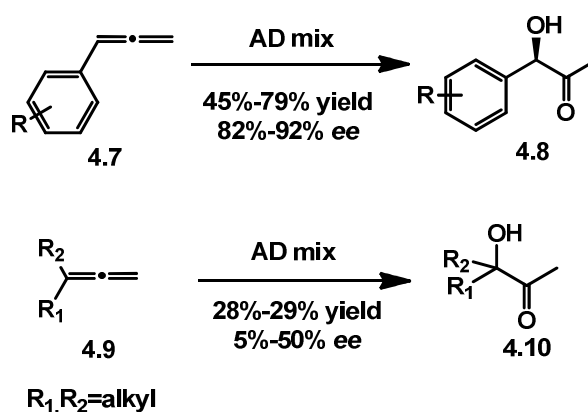
Compared with alkene osmylation, allene osmylation received much less attention. Up to now, there are only 7 reports regarding the osmium tetroxide oxidation of allenes. The first stoichiometric allene osmylation was reported by Crabbe¹⁴ in 1971 when they used OsO_4

to oxidize a steroidal exo-allene **4.5** into a hydroxyl ketone **4.6** (Scheme IV.2). According to Crabbe, some over oxidation byproduct was observed, and as a result the yield of this reaction was not impressive.



Scheme IV.3 Crabbe's Stoichiometric Allene Osmylation

The only catalytic asymmetric allene osmylation work was done by the Fleming group.^{15, 16} They showed that AD-mix could catalyze the dihydroxylation of mono- or di-substituted allenes that had an aromatic substituent directly attached to the allene. The product, a hydroxyl ketone, was formed in moderate yield.



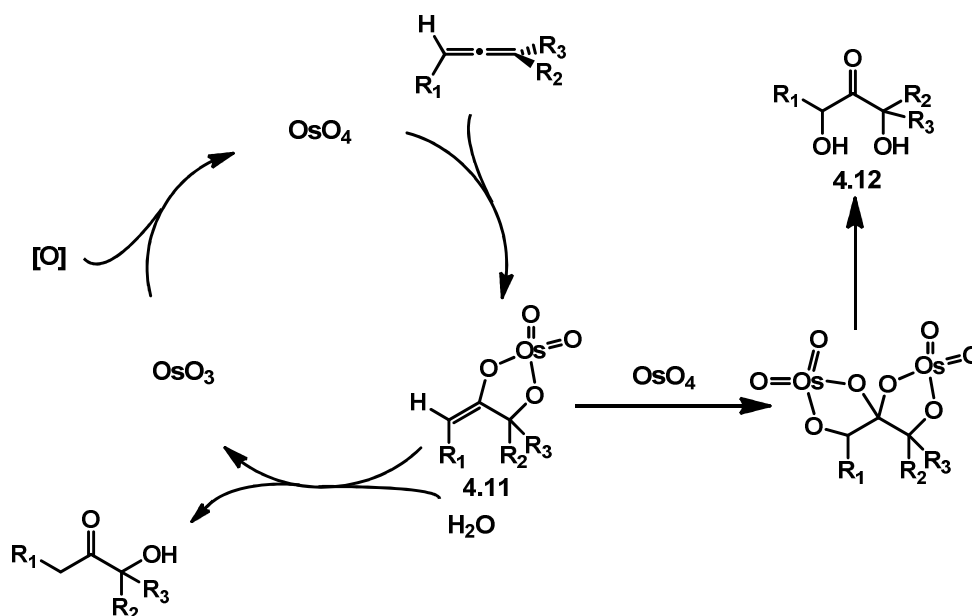
Scheme IV.4 Fleming's Asymmetric Allene Osmylation

Despite the fact that desired hydroxyl ketone product could be obtained, this reaction still has significant drawbacks: the yield and *ee* is very low for allenes with only alkyl

substituent, and the catalyst turnover is significantly lower than the alkene osmylation (Scheme IV.4).

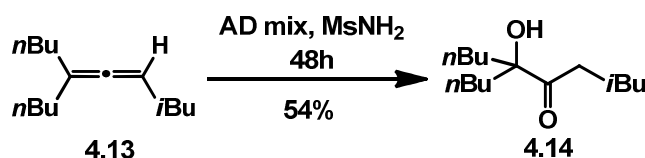
4.4 Mechanistic Insights of Allene Osmylation

The detailed mechanistic rationale for the low yield and catalyst turn over of an allene osmylation is not clear yet. One possible reason is that the osmium tetroxide adduct **4.12**, which is an osmate enol ester (Figure IV.1), was more stable than the osmate ester formed from reaction of osmium tetroxide with an alkene. As a result, the hydrolysis of an allene-derived osmate ester may be much slower. Moreover, the enol ester may also be reactive towards excess osmium tetroxide, and hence a second molecule of OsO_4 would add, giving over oxidation product **4.12** as side products. If this hypothesis were true, then an additive that accelerates the hydrolysis of the osmate ester would solve this problem.



Scheme IV.5 Proposed Catalytic Cycle of Allene Osmylation

We started our exploration with the use of methanesulfonamide. This reagent is known to be a phase-transfer catalyst, and can accelerate the SAD reaction.¹⁷ As we expected, for the simple tri-substituted alkyl allene **4.13**, the combination of AD-mix and methanesulfonamide gives the desired hydroxyl ketone **4.14** in 56% yield after 48 hours (Scheme IV.6). Note that this substrate lacks the phenyl substituent that was required by Flemming's report (Scheme IV.4). When only AD-mix was used (without methanesulfonyl amide), only trace product and the majority of the starting material was recovered (not shown).

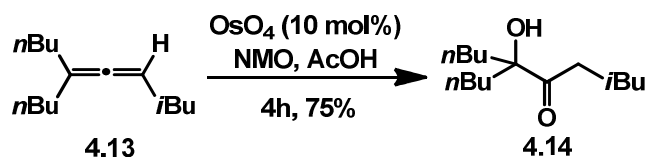


Scheme IV.6 Allene Osmylation Accelerated by Methanesulfonamide

This result supports the hypothesis that hydrolysis is the rate determining step of allene osmylation. Although the yield and catalyst turn over is greatly enhanced, there is room for further improvement. Accordingly, we turned to seek for alternative solutions.

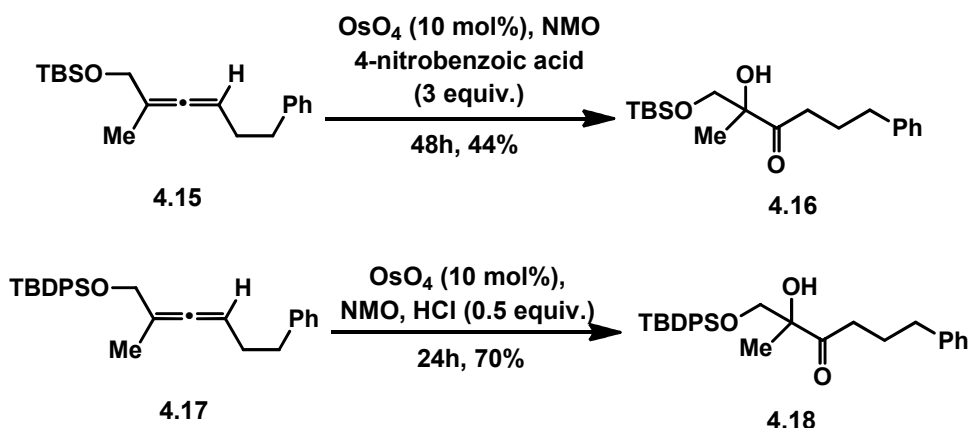
4.5 Acid-promoted Allene Osmylation

The presence of acid is known to accelerate the hydrolysis of osmate ester in alkene dihydroxylation.¹⁸ In the case of allene-derived osmate ester, the enol moiety should be nucleophilic and react with acid. Initial experiments were performed with alkyl allene **4.13**. The use of 3 equiv. of acetic acid in the presence of catalytic (10 mol%) OsO₄ and NMO gave the desired hydroxyl ketone **4.14** in 75% yield (Scheme IV.7). Stoichiometric amount of acetic acid was found to be less effective, whereas using too much (>10 equiv.) of acetic acid slows down the reaction dramatically.



Scheme IV.7 Allene Osmylation Accelerated by Acid

When these reaction conditions were applied to a more complex silyl protected allene alcohol **4.15**, similar outcomes were observed, however the reaction rates and yields were inferior. The use of a stronger 4-nitrobenzoic acid instead of acetic acid improved the overall efficiency. Stability of the substrate to acid is important. For example, similarly, allene **4.17** which bears the more acid stable TBDPS group, was efficiently reacted with OsO_4 in the presence of HCl. (Scheme IV.8). As with the other reactions, the presence of acid has a beneficial effect on reaction rate and yield.

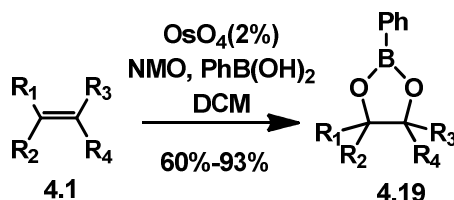


Scheme IV.8 Allene Osmylation of Protected Allene Alcohols

4.6 Alternative Procedures for Efficient Allene Osmylation

Several other procedures have been developed to improve the allene osmylation significantly. In 1988, Narasaka reported a modified Upjohn's procedure for alkene dihydroxylation.¹⁹ Phenyl boronic acid was employed as the water equivalent. This

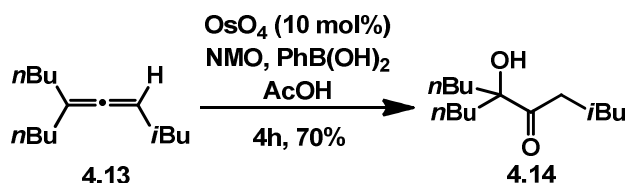
reaction can be conducted under anhydrous conditions using DCM as solvent. The resulting boronic ester can be further oxidized and cleaved to release the desired diol (Scheme IV.9).



Scheme IV.9 Narasaka's Modification of Upjohn Dihydroxylation

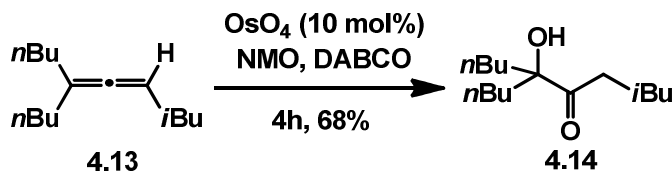
This procedure can significantly increase the rate of the Upjohn dihydroxylation. We were intrigued by possibility that this procedure might be applicable to improving allene osmylation. According to our mechanistic proposal, the hydrolysis is the rate determining step of allene dihydroxylation, and since a very different mechanism of hydrolysis is involved in the Narasaka's procedure, it seemed plausible that it would also be beneficial.

Initial attempts were performed on simple alkyl allene **4.13**. In the event, 10 mol% of OsO_4 and 2 equiv. of NMO as co-oxidant effected consumption of the allene starting material within 4 hours. However the product was isolated as a mixture of the boronic enol ester (40%) and the free hydroxy ketone (35%). The addition of molecular sieves to the reaction mixture significantly suppressed the formation of the hydroxyl ketone. On the other hand, adding AcOH instead of molecular sieves will accelerate the decomposition of boronic ester and forms the hydroxyl ketone in 70% yield.



Scheme IV.10 Allene Osmylation by Narasaka's Modification

Another interesting observation regarding allene osmylation is that tertiary amines accelerate the overall reaction rate as well. When 10 mol% of OsO_4 and 2 equiv of NMO as co-oxidant was employed, adding catalytic to substoichiometric (10 mol% to 50 mol%) amount of diazabicyclo(2,2,2)octane (DABCO)²⁰ significantly enhanced the reaction rate. The desired hydroxy ketone could be formed in 68% yield within 2 hours, down from over 4 hours when AcOH was used. However this procedure has a major drawback that a small portion of overoxidation product is always observed. This side reaction is rare in other procedures.



Scheme IV.11 Allene Osmylation Using DABCO as Additive

4.7 Conclusion

Significant progress towards the allene osmylation has been made. The limit in the oxidation of alkyl allenes now can be overcome by using acid, phenylboronic acid or DABCO. The result was still not optimal: the yield is moderate and although catalyst loading is low (5%-10%), we would prefer significantly lower catalyst loading. However, the current procedure seems suitable for the modification of the bis[allene] macrolide, a

late-stage intermediate which do not require a large scale method. Therefore we decided to return to the modification of the bis[allene] macrolide intermediate, our main goal.

4.8 References

1. Crandall, J. K.; Machleder, W. H. *J. Am. Chem. Soc.* **1968**, *90*, 7292.
2. Crandall, J. K.; Conover, W. W.; Komin, J. B.; Machleder, W. H. *J. Org. Chem.* **1974**, *39*, 1723.
3. Ghosh, P.; Lotesta, S. D.; Williams, L. J. *J. Am. Chem. Soc.* **2007**, *129*, 2438.
4. Lotesta, S.D.; Kiren, S.; Sauers, R. R.; and Williams, L. J. *Angew. Chem. Int. Ed.* **2007**, *46*, 15.
5. Sharma, R.; Manpadi, M.; Zhang, Y.; Kim, H.; Ahmedov, N. G.; and Williams, L. J. *Org. Lett.* **2011**, *13*, 3352.
6. Ghosh, P.; Cusick, J. R.; Inghrim, J.; Williams, L. J. *Org. Lett.* **2009**, *11*, 4672.
7. Katukojvala, S.; Barlett, K. N.; Lotesta, S. D.; Williams, L. J. *J. Am. Chem. Soc.* **2004**, *126*, 15348.
8. Lotesta, S. .D.; Hou, Y.; Williams, L. J. *Org. Lett.* **2007**, *9*, 869.
9. Shangguan, N.; Kiren S.; Williams, L. J. *Org. Lett.* **2007**, *9*, 1093.
10. Ghosh, P.; Zhang, Y.; Emge, T. J.; Williams, L. J. *Org. Lett.* **2009**, *11*, 4402.
11. Joyasawal, S.; Lotesta, S. D.; Akhmedov, N. G.; Williams, L. J. *Org. Lett.* **2010**, *12*, 988.
12. V. VanRheenen, R. C. Kelly and D. Y. Cha *Tetrahedron Lett.* **1976**, 1973.
13. Kolb, Hartmuth C.; VanNieuwenhze, Michael S.; Sharpless, K. Barry *Chemical Reviews*, **1994**, *94*, 2483.
14. Biollaz, M.; Haefliger, W.; Velarde, E.; Crabbe, P.; Fried, J. H. *J. Chem. Soc. D: Chem. Comm.* **1971**, *21*, 1322.
15. Fleming, S. A.; Carroll, S. M.; Hirschi, J.; Liu, R.; Lee Pace, J.; Ty Redd, J. *Tetrahedron Lett.* **2004**, *45*, 3341.
16. Fleming, S. A.; Liu, R.; Redd, J. T. *Tetrahedron Lett.* **2005**, *46*, 8095.

- 17.M. H. Junttila, O. O. E. Hormi, *J. Org. Chem.* **2009**, 74, 3038-3047.
- 18.Dupau, P.; Epple, R.; Thomas, A. A.; Fokin, V. V.; Sharpless, K. B. *Adv. Synth. Catal.* **2002**, 344, 421.
- 19.Iwasawa, N.; Kato, T.; Narasaka, K. *Chem. Lett.* **1988**, 1721.
- 20.Minato, Makoto; Yamamoto, Keiji; Tsuji, Jiro *Journal of Organic Chemistry* **1990**, 55, 766.

Chapter V

Synthesis of Erythronolides From a

Macrocyclic Bis[allene]

5.1 Introduction

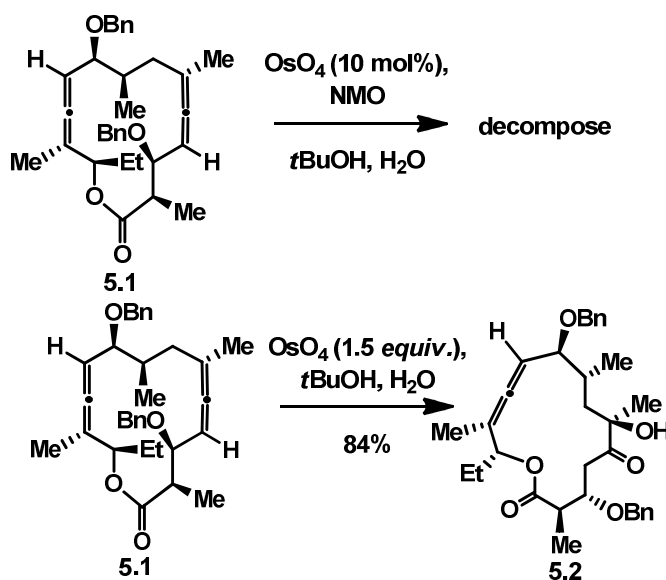
As described in the preceding chapters, the macrocyclic bis[allene] **3.1** is central to our integrated strategy towards the entry of erythronolide structure space. Reactions on the two allenic groups are particularly important. We planned to use our mild osmium tetroxide catalyzed allene oxidation as described in chapter IV. We were also interested in the spirodiepoxidation by DMDO and the consequential derivitization of the formed spirodiepoxide (SDE).

There are several major challenges. First of all, the oxidation of a macrocyclic bis[allene] is unprecedented. Would the desired reaction proceed at any of four possible π -bonds? Would the regioselectivity be problematic? Moreover, unlike the total syntheses which have a certain known structure to compare with, the targeted new molecules have never been reported before. We would have to fully determine the absolute structures of each new product.

Despite these concerns, the success in the model study done by Dr. Partha Ghosh and Dr. Yue Zhang was encouraging.¹ We decided to move forward toward our goal, starting with the allene osmylation, which was believed to be mild and selective.

5.2 Regioselective Osmylation of the Macrocyclic Bis[allene]

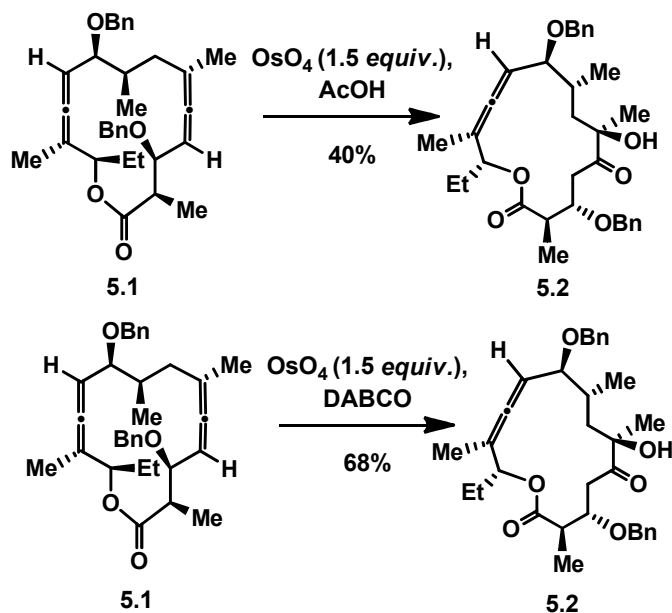
The osmylation of non-cyclic allene was done successfully under catalytic conditions, as stated in chapter IV. However, catalytic oxidation of macrocyclic bis[allene] **5.1** failed. The combination of 10 mol% osmium tetroxide and 2 equiv. of NMO gave a complex mixture of products, and no desired product was isolated. To simplify the relative complex situation, dihydroxylation conditions using stoichiometric amount of osmium tetroxide were used. Fortunately this modification successfully provided the desired hydroxy ketone **5.2** in up to 84% yield (Scheme V.1).



Scheme V.1 Regioselective Osmylation of Macrocyclic Bis[allene] **5.1**

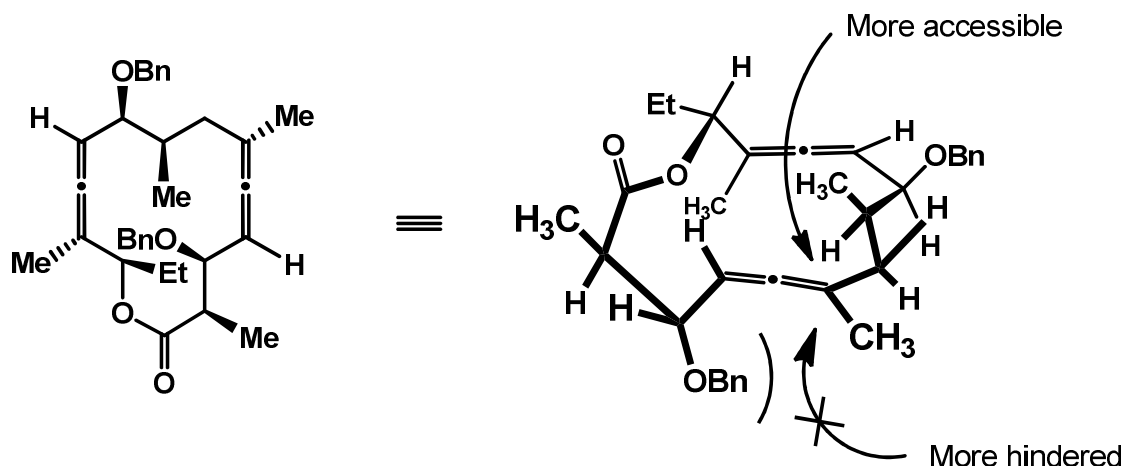
It is remarkable that this reaction is highly regio- and stereoselective. We can only observe a single diastereomer product. This reaction is sensitive to pH: 3 equiv of AcOH

significantly reduced the yield to 40% (Scheme V.2). Neutral or buffered weak basic conditions ensured consistent yields. This reaction could be significantly accelerated by amine ligand: stoichiometric DABCO reduced the reaction time from 1 hour to 15 mins, although the yield dropped to 68%. Also with amine ligand, the reaction mixture became a transparent homogenous brownish solution instead of a heterogeneous solution with significant amounts of black precipitate. Since the heterogeneous reaction was much more difficult to work up, the addition of amine provided help in a procedural level as well.



Scheme V.2 Effect of Additives to the Osmylation of 5.1

The high stereoselectivity of the addition of OsO_4 was expected. As shown in the figure, 3D modeling of the macrocyclic bis[allene] shows that one side of the allene is more hindered than the other side substituted with H. (Scheme V.3)

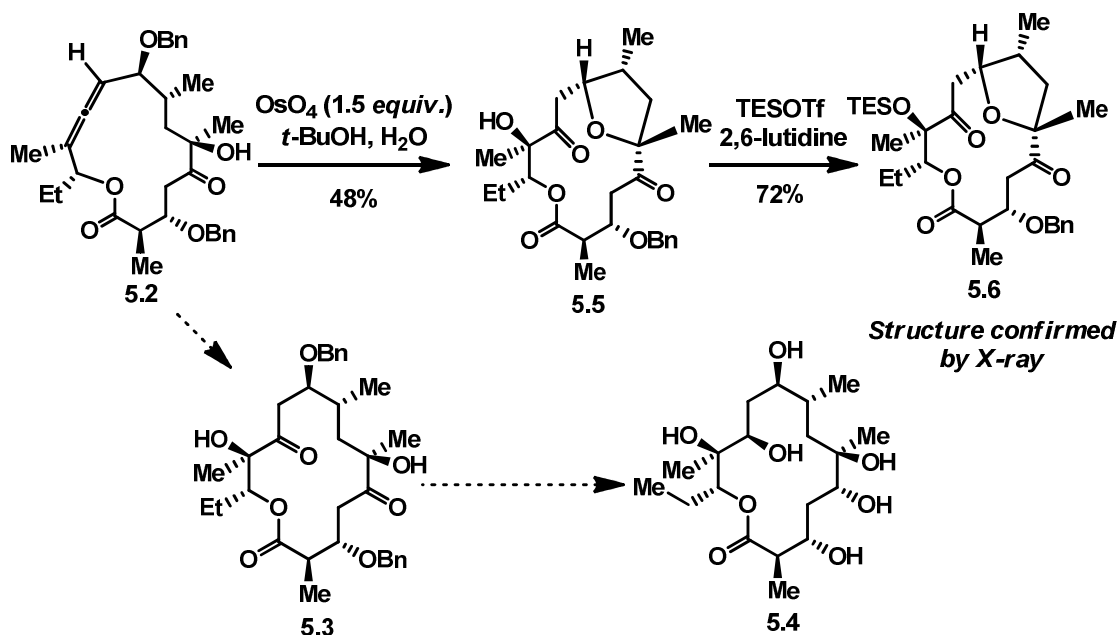


Scheme V.3 Steric Difference Between the Two Faces of Allene

However we do not fully understand the significant rate difference between the oxidation of the two allenes. One possibility is that the C4-C6 allene is more electron rich than the C10-C12 allene, especially on the more substituted site. Due to the high sensitivity of osmylation towards electron density, the rate could be differentiated. Another possibility is that the C10-C12 allene might be more sterically hindered; hence the rate of addition of osmium tetroxide would be attenuated.

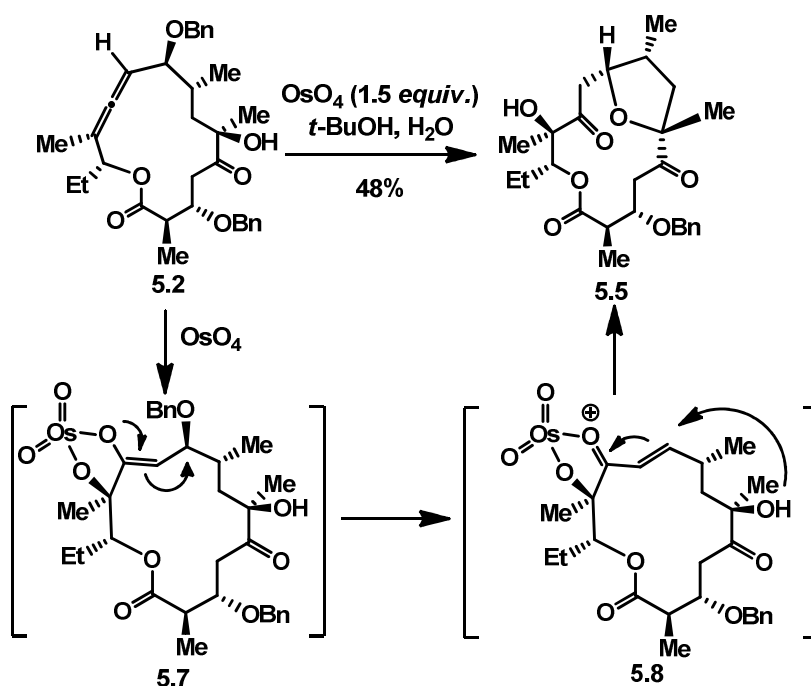
5.3 Osmylation of the C10-C12 Allene

Having the mono- dihydroxylation product **5.2** in hand, we then started to investigate the possibility of the osmylation of the second allene in order to obtain a bis-hydroxyketone **5.3** (Scheme V.4), which is a precursor of 4,10-didesmethyl erythronolide (Scheme V.4).² Ideally we could obtain the 4,10-didesmethyl erythronolide **5.4** after controlled reduction of two ketones and debenzoylation, in less than 15 steps.



Scheme V.4 The Osmylation of the C10-C12 Allene

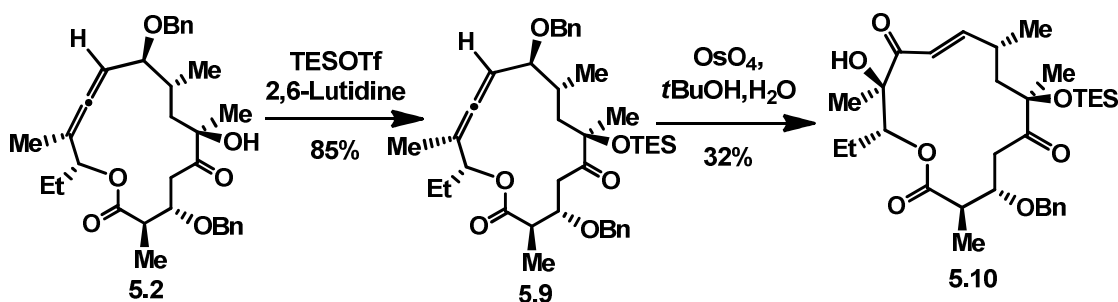
The osmylation of the second allene, however, gave product **5.5** instead of the desired **5.3** in 48% yield (Scheme V.4). In contrast with the first oxidation which was complete within 1 hour, the second oxidation was much slower and required 4 hours for completion. We were not certain about the structure of the product at first. Fortunately, upon silylation of the C12 tertiary alcohol, we were able to isolate the **5.6** as a white crystalline in 72% yield. The X-ray diffraction crystallography confirmed that the compound is a bicyclic lactone, with a tetrahydrofuran moiety from C6-C9 area. This structure also confirmed the assignments of the many precursors of this complex compound. Interestingly, the C9 benzyl group was eliminated during this process. Although this substance was not the immediate desired product, it's still of considerable interest. It has been reported in 1980's that this type of structure, derived from the acid induced cyclization of erythromycin, shows similar activity as motilin, and as a result such macrolides are called "motilids".^{3,4}



Scheme V.5 Mechanistic Framework of the Formation of **5.5**

This transformation was unprecedented. Our mechanistic framework for this transformation is shown in Scheme V.5. The osmate enol ester intermediate **5.7** is electronrich and therefore may readily eliminate the C9 benzyl group. The resulting intermediate **5.8**, with or without osmium, is electrophilic and the C6 tertiary alcohol could attack the C9 position to give the tetrahydrofuran ring.

Based on above rationale, installation of a protection group on C6 tertiary alcohol before the second osmylation would prevent the formation of the tetrahydrofuran ring. In the event, the TES protected mono hydroxyl ketone **5.9** (Scheme V.6) gave the unsaturated ketone **5.10** in 34% yield upon osmylation instead of cyclizing. This result is consistent with our mechanistic hypothesis.



Scheme V.6 Osmylation of the 6-Protected Hydroxyl Ketone **5.9**

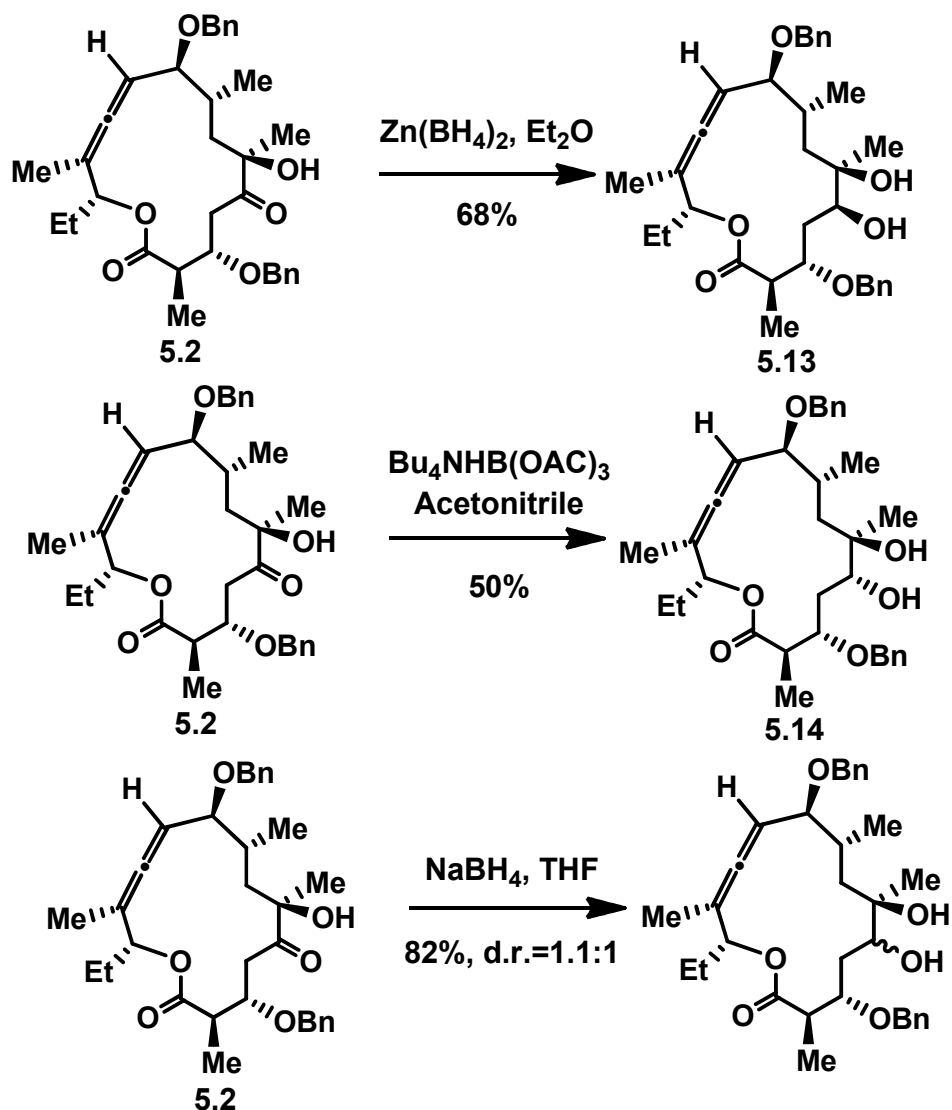
Considering the possibility for derivitization, this unsaturated ketone **5.10** is a promising substrate for further study.

5.4 Reduction of the 5-Ketone

As for the synthesis of bioactive erythromycinoids, it is critical to reduce of all ketones on the macrolide ring to alcohol form in a stereoselective fashion. The C5 alcohol is the site of glycosylation with desosamine, which is found to be important in binding the bacterial ribosome.⁵⁻⁸ Paterson reported a reduction of an analogous C5 ketone in 1989 (Scheme V.7). The chelation-controlled reduction of **5.11** using zinc borohydride was employed. An interesting fact was that the obtained product **5.12** was the diastereomer of the desired product predicted based on acyclic model.¹⁰ Paterson explained this phenomenon to be the result of the intrinsic stereoselectivity lying in the macrolide and called it macrocyclic stereocontrol. We thought we might be able to take advantage of this protocol to reduce the C5 ketone of compound **5.2** (Scheme V.8).



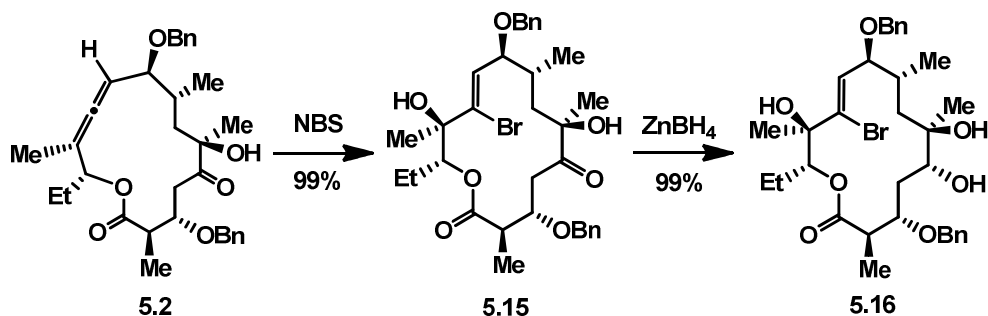
Zinc borohydride reduction of the mono hydroxyketone gave the 5,6-diol **5.13** in 68% yield. Upon extensive 2D-NMR analysis, we found that the obtained product was not the desired diastereomer. In contrast, the non-chelation controlled reduction using tetrabutylammonium triacetoxyborohydride⁹ gave the desired diastereomer **5.14**, whereas the uncontrolled NaBH₄ reduction affords a mixture of two diastereomers in close to 1:1 ratio (Scheme V.9).



Scheme V.8 Reduction of the C5-Ketone

Admittedly, we were surprised that we were not able to get the desired diastereomer following Paterson's procedure. Still, there can be little doubt that this procedure worked as described by Paterson: the product was taken on and the structure was assigned by correlation to the natural product. We later found that this procedure effected Paterson-like selectivity on another substrate (Scheme V.9). By treating the mono hydroxyketone with *N*-bromosuccinimide (NBS) and water in acetonitrile solvent, we were able to isolate the

alkene **5.15**. The bromohydrin was then reduced using zinc borohydride to afford the C5 alcohol with desired stereoconfiguration, which was confirmed by extensive 2D-NMR analysis.



Scheme V.9 Bromohydration of the Allene and Reduction of C5-Ketone

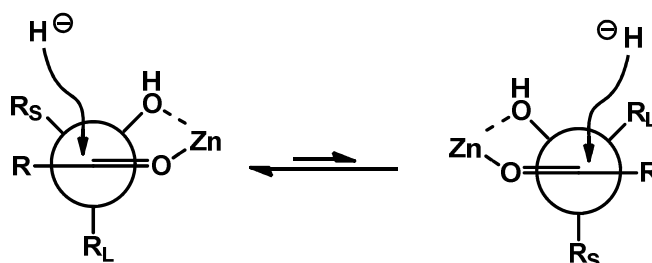
The above result was a good demonstration of macrocyclic stereocontrol: the macrolide, because of its structural topology, is sterically biased. Stereo control methods that work on linear systems sometimes fail on the cyclic system, and the stereo outcome of the reactions on it is a reflection of its 3D structure.

5.5 Stereocontrol on the Macrocyclic Ring: Mechanistic Insights

Zinc borohydride reduction of ketones is well precededented.^{10,11} The *anti*- diol is favored as the major product – at least in the overwhelming number of cases. However, when it was applied in our cyclic system the *syn*- product was formed in our case

As shown in the Scheme V.10, the zinc chelated hydroxyl ketone has two major conformations. According to the anti-Felkin-Anh model (Scheme V.10), the nucleophile will attack the more accessible face as determined by the relative size of the adjacent

substituents. The size difference between the R_S (S=small) and R_L (L=Large) determines the stereoselectivity of the following hydride addition.



Scheme V.10 Anti-Felkin-Anh Model of the Chelation Control Reduction

This model is based on the assumption that the R group, which is on the other side of the ketone does not have any impact with the reaction center. This is typically true under most circumstances. For acyclic hydroxyketones the rotation barrier of the carbonyl- R bond is normally not very high and can rotate easily, thus diminish the steric difference between different substitution groups. However this is not necessarily the case for complex macrolides. In our cyclic systems, few of the bonds on the ring can rotate easily and hence the steric differences imposed by the R group cannot be ignored (see Figure V.1, compound **5.2**), especially when the difference between R_S and R_L is not large. In hydroxyl ketone **5.2**, the difference between the C6- methyl and the C7 methylene is modest; therefore the conformation of the ring system especially the C3-C6 region becomes important. (Figure V.1) Functional groups such as the BnO- group may block one face over the other and interfere with the diastereoselectivity.

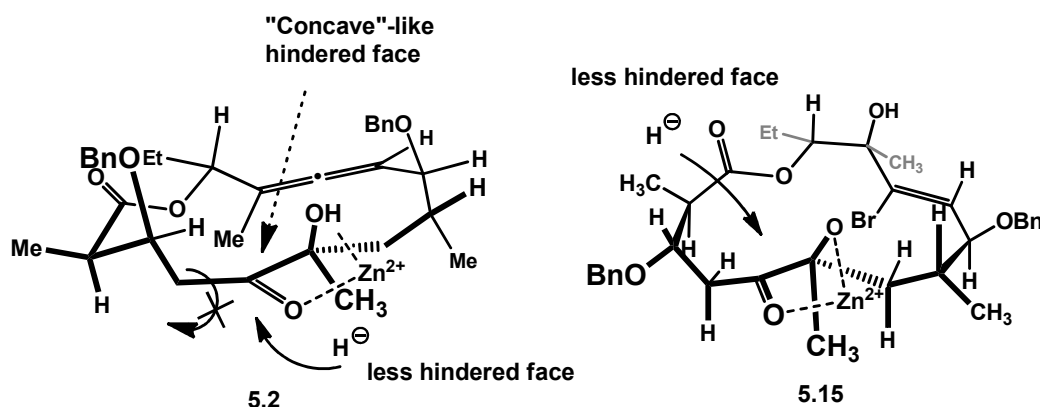


Figure V.1 The 3D Looking of the Ketone Reduction

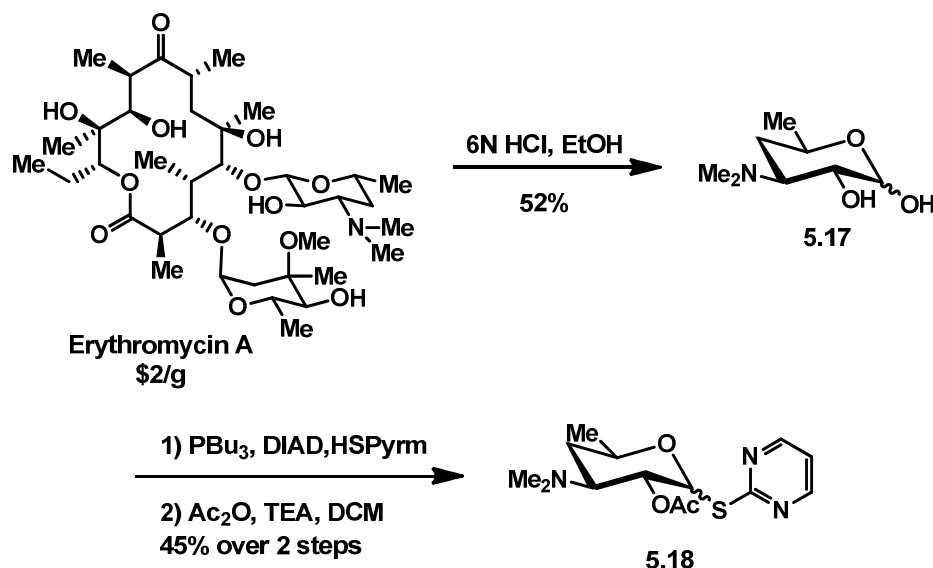
The conformation of the ring changes when the C10-C12 allene is converted into the vinyl bromide, due to the large difference in rigidity and topographical constraints between the allene and alkenes (Figure V.1). The structure of the vinyl bromide macrolide is very similar to the intermediate in Paterson's synthesis of (9*S*)-dihydroerythronolide. Accordingly, these substrates exhibit similar reactivity under the same reaction condition. Although extensive computational studies are needed to understand the mechanistic details, this rationale accounts for all the available data.

5.6 Attempts for the Glycosidation on the Macrocyclic Ring

Although the zinc borohydride reduction gives the undesired diastereomer for substrate **5.13**, we were still interested in adding the desosamine to it since our main goal was not only making the natural product, but also making diversified analogues.

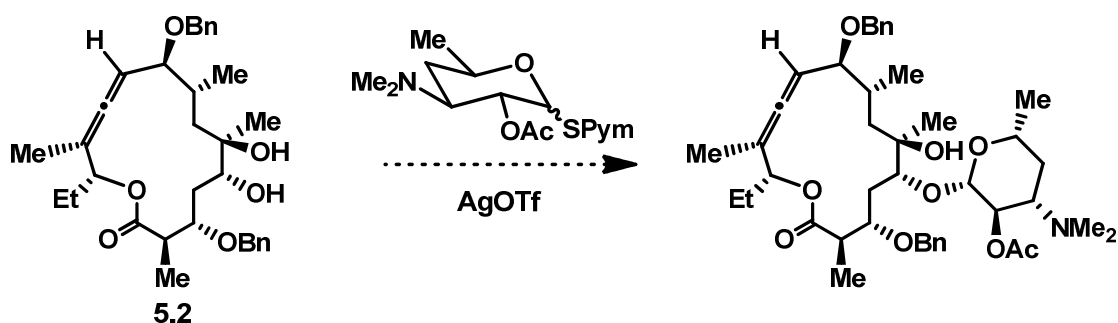
The glycosidations of macrolides have been known and carried out repeatedly over the past several decades. The first attempt appears to have been carried out by Woodward and coworkers in their synthesis of erythromycin A. A 2-mercaptopyrimidine substituent was

used in the desosamine glycosylate.¹² Upon activation by silver (I) triflate, the sugar donor was successfully installed onto the macrolide ring. This method was also used in several other syntheses of macrolide antibiotics.^{2,13-16} Therefore we started with this procedure.



Scheme V.11 Synthesis of the Desosamine Donor

The sugar donor was prepared in three steps as described in the original report. The desosamine was obtained in 52% yield as a mixture of anomers by hydrolysis of erythromycin A under strong acidic conditions.¹⁷ Although it could also be made from a commercial available pyranose, we chose to obtain it from the erythromycin because of time efficiency. Mitsunobu reaction using 2-mercaptopyrimidine as nucleophile replaced the 1-alcohol group of the desosamine with a thiopyrimidine. The product was an inseparable mixture with the Mitsunobu reaction side product, and the mixture was acylated on the 2-alcohol to give the desired glycosyl donor in 45% yield over 2 steps.

Table V.1 Attempts of Glycosilation of 5.2

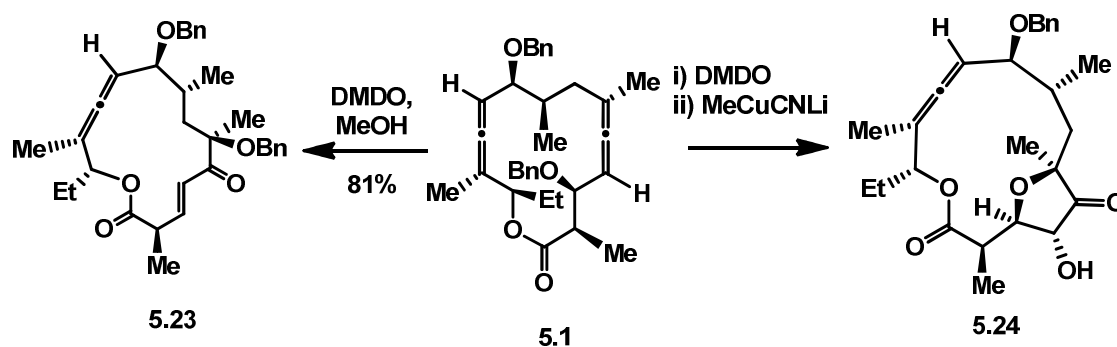
Entry	Eq. of AgOTf	Eq. of glycosyl donor	Temp.	Addition order	Result
1	6	5	rt.	Donor mixture to AgOTf	Recovery of S.M.
2	12	12	rt. to 60°C	Donor mixture to AgOTf	decompose
3	15	30	rt.	AgOTf to donor mixture	decompose
4	30	0	rt.	-	decompose

The glycosidation, however, was not successful. As shown in the Table V.1, no desired product was observed by either changing the order of addition or the equivalence of material used (entries 1-3). In most cases decomposition of starting material occurred. Silver triflate reacts with allenes and effects decomposition of the substrate (entry 4).

On the other hand, the glycosidation is more promising on other macrolide substrates. My colleague Libing Yu successfully glycosylated the bromohydrin **5.16**. The sugar donor was different and work in this area is still ongoing.^{18,19}

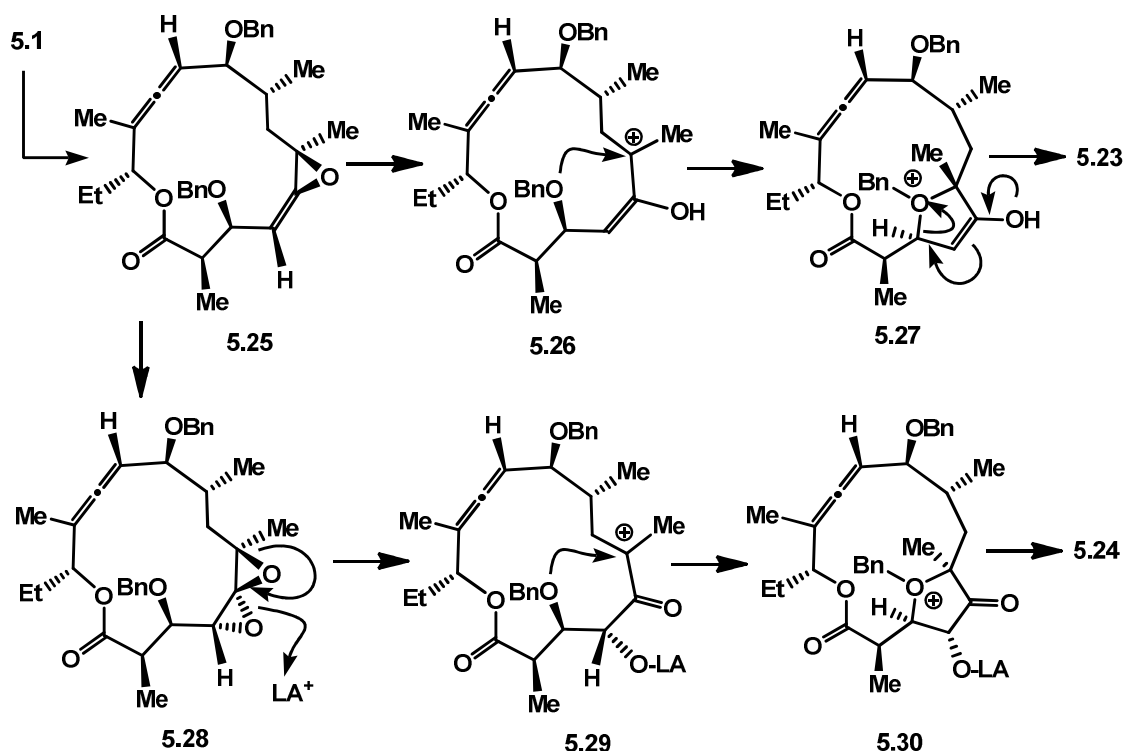
In collaboration with Dr. Hiyun Kim, I extensively studied on the epoxidation of the bis[allene] macrolide. She found that under certain conditions, the allene epoxidation could be conducted in a controlled manner, and gave some very interesting products. For example, when the macrolide **5.1** was treated with DMDO using methanol as solvent, a α,β -unsaturated ketone **5.23** was formed in an excellent 81% yield. What is particularly interesting here is that the benzyl group on C3 migrates to C6 position, and hence formed

C6-ether functionality which is favorable because it could prevent the formation of C6-C9 hemiketal. Moreover, this procedure is very sensitive to the solvent systems. By using chloroform as solvent and using MeCuCNLi as additive after the treatment of DMDO, we were able to isolate a furanone **5.24** in 64% yield, which is different structurally than the previous product.



Scheme V.13 Epoxidation of the Bis[allene] Macrolide **5.1**

These two transformations were unexpected and very interesting to us. Several mechanistic proposals were brought up and the most reasonable ones are shown in Scheme V.16. The first epoxidation occurs rapidly and gives the allene oxide **5.25**. The presence of hydrogen bonding in the polar protic solvents promotes epoxide opening^{21,22} before the second epoxidation and thereby generates a tertiary carbocation **5.26**. The C3-benzyl ether is then trapped intramolecularly by the carbocation. This 5-membered ring intermediate (**5.27**) is not stable and undergoes eliminative opening to form the unsaturated ketone. In the other case when aprotic conditions are used (e.g. chloroform), the allene oxide is longer-lived and the second epoxidation takes place. The resulting spirodiepoxide **5.28** is not stable in the presence of Lewis acid (Li^+), and is then opened to generate a slightly different carbocation (**5.29**). The benzyl ether oxygen then forms the ring of **5.30**. The benzyl group is then attacked by weak nucleophile and thereby forms the observed product.



Scheme V.14 Mechanistic Framework of the Epoxidation Cascades

Interestingly the stereoconfiguration at C6 is different for **5.23** and **5.24**. We suggest that this is due to different carbocations involved in the reaction. These intermediates adopt significantly different 3D structures, which lead to different biases of facial selectivity. Extensive modeling of these intermediates shows that the benzyl group is displaced above the macrocyclic framework in one instance and below it in the other instance. Hence the benzyl ether approaches from different faces.

5.8 Methods Used in the Structure Determination of the Novel Erythronolides

The structure determination of the many macrolide structures was one of the most important processes in this project. Unlike polycyclic compounds that are rigid, the

14-membered macrolide's configuration is often hard to determine because it may adopt multiple conformations. In this section the detailed method used in the structure determination and some examples will be described.

The basic connectivity was confirmed by the combination of several 2D-NMR correlation methods including TOCSY, HMBC and HETCOR. These methods serve different functions: TOCSY identified different types of hydrogen atoms that coupled to each other in the same spin system; HMBC identified the through-bonding interaction of C and H that are 2-3 bonds away from each other, whereas HETCOR identified the interactions of C and H that are directly connected. These methods enabled us to establish the basic connectivity of these complex molecules.

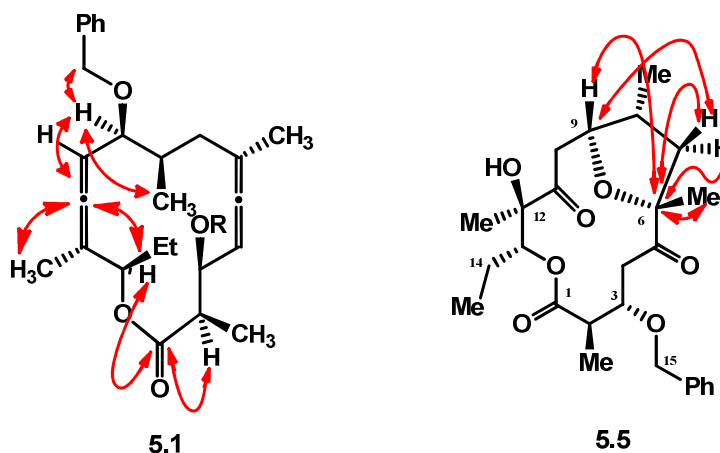


Figure V.2 Key HMBC Correlations of 5.1 and 5.5

For example, the macrolactone functionalities in nearly all macrolides we have made were confirmed by HMBC. The bis[allene] macrolide **5.1** is one example (Figure V.2). We found the HMBC correlation between the allene C11 and H13, also the correlation between H13 and ester C1. Also we were able to find the correlation between C1 and H2, which

confirms the connectivity. Another example was the bis-osmylation product **5.5**. Although we have obtained the X-ray crystallography of this molecule, we already realized that the HMBC correlation between C6 and H9 is characteristic for a 5-membered tetrahydrofuran ring before we obtained the crystal structure. In the benzyl migration molecule (compound **5.23**, Scheme V.15) the HMBC correlation between the C6 and the two benzyl hydrogens is also the key method that identified the position of the benzoxy group.

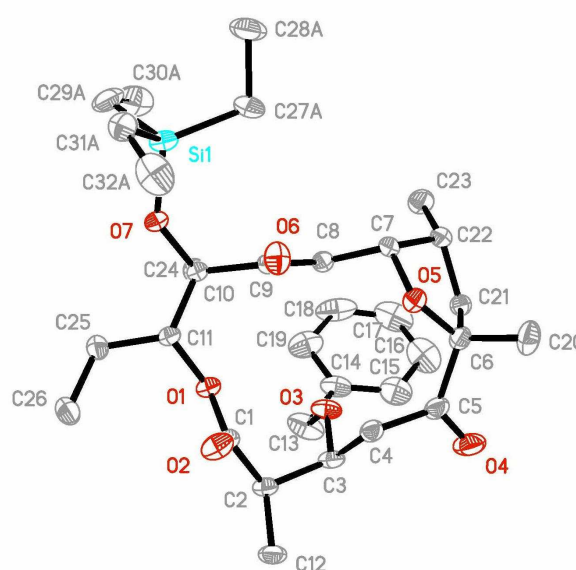


Figure V.3 ORTEP Diagram of Compound 5.5

Determination of stereocenters, however, were sometimes very challenging. The success in obtaining X-ray crystallography of compound **5.5** (Figure V.3) helped us in setting some of the stereocenters such as C2, C3, C8 and C13. These became the starting point for structure determination and used in conjunction with observed NOESYs and coupling constant analysis. Different spin systems could be correlated and eventually the full structure could be unambiguously assigned. For example, the stereoconfiguration of C6 in



5.9 Conclusion

As described in this chapter, allene osmylation and allene epoxidation both gave many valuable derivatives of erythronolides. Up to now, more than 40 novel macrolides have

been made from the bis[allene] macrolide **3.1** within 3 steps or less. The synthesis is easy to execute, and the route is short. This is already a good demonstration that the modification of the macrolide ring can be extensive and selective. Also we have demonstrated the value of cyclic allenes in accessing the erythronolide structure space. Many functional groups have been introduced in the ring, including α -hydroxy ketone, enone, vinyl bromohydrin, tetrahydrofuran ring, etc. More importantly those structures are inaccessible from the natural product.

We are still exploring new reactions and possibilities in applying them in this integrated strategy. These reactions will be described in the following chapter.

5.10 References

1. Ghosh, P.; Zhang, Y.; Emge, T. J.; Williams, L. J. *Org. Lett.* **2009**, *11*, 4402.
2. Velvadapu, V.; Glassford, I.; Lee, M.; Paul, T.; DeBrosse, C.; Klepacki, D.; Small, M. C.; MacKerell, A. D. Jr.; Andrade, R. B. *ACS Med. Chem. Lett.* **2012**, *3*, 211.
3. Tsuzuki, K.; Sunazuka, T.; Marui, S.; Toyoda, H.; Omura, S.; Inatomi, N.; Itoh, Z. *Chem. Pharm. Bull.* **1989**, *37*, 2687.
4. Faghih, R.; Lartey, P. A.; Nellans, H. N.; Seif, L.; Burnell-Curty, C.; Klein, L. L.; Thomas, P.; Petersen, A.; Borre, A.; Pagano, T.; Kim, K. H.; Heindel, M.; Bennani, Y. L.; Plattner, J. J. *J. Med. Chem.* **1998**, *41*, 3402.
5. Ban, N.; Nissen, P.; Hansen, J.; Moore, P. B.; Steitz, T. A. *Science* **2000**, 289, 905.
6. Hansen, J. L.; Ippolito, J. A.; Ban, N.; Nissen, P.; Moore, P. B.; Steitz, T. A. *Molecular cell* **2002**, *10*, 117.
7. Harms, J.; Schlunzen, F.; Zarivach, R.; Bashan, A.; Gat, S.; Agmon, I.; Bartels, H.; Franceschi, F.; Yonath, A. *Cell* **2001**, *107*, 679.
8. Schlunzen, F.; Zarivach, R.; Harms, J.; Bashan, A.; Tocilj, A.; Albrecht, R.; Yonath, A.; Franceschi, F. *Nature* **2001**, *413*, 814.

9. Evans, D. A.; Chapman, K. T.; Carreira, E. M. *J. Am. Chem. Soc.* **1988**, *110*, 3560.
10. Nakata, T.; Tanaka, T.; Oishi, T. *Tetrahedron Lett.* **1983**, *24*, 2653.
11. Nakata, T.; Tani, Y.; Hatozaki, M.; Oishi, T. *Chemical & Pharmaceutical Bulletin* **1984**, *32*, 1411.
12. Woodward, R. B. et al. *J. Am. Chem. Soc.* **1981**, *103*, 3215.
13. Toshima, K.; Nozaki, Y.; Mukaiyama, S.; Tamai, T.; Nakata, M.; Tatsuta, K.; Kinoshita, M. *J. Am. Chem. Soc.* **1995**, *117*, 3717
14. Martin, Stephen F.; Hida, Tsuneaki; Kym, Philip R.; Loft, Michael; Hodgson, Anne J. *Am. Chem. Soc.*, **1997**, *119*, 3193
15. Kim, H. C.; Kang, S. H. *Angew. Chem. Int. Ed.*, **2009**, *48*, 1827
16. Velvadapu, V.; Paul, T.; Wagh, B.; Klepacki, D.; Guvench, O.; MacKerell, A.; Andrade, R. B. *ACS Med. Chem. Lett.* **2011**, *2*, 68
17. Farmer, J. J.; Ashoke, B.; Chen, Y.; Sutcliffe, J. A., Preparation of macrocyclic azithromycin compounds as antibacterial, anti-proliferative, and anti-inflammatory agents, US Patent WO 2005085266 (A2), 2005.
18. Kahne, et al. *J. Am. Chem. Soc.* **1989**, *111*, 6881
19. Yu, L.; Williams, L. J. unpublished results
20. Ghosh, P. New methods and strategies towards total synthesis of (9S)-dihydroerythronolide A. Ph.D. Thesis, Rutgers, The State University of New Jersey, New Brunswick, 2008.
21. Lotesta, S. D.; Hou, Y.; Williams, L. J. *Org. Lett.* **2007**, *9*, 869.
22. Shangguan, N.; Kiren, S.; Williams, L. J. *Org. Lett.* **2007**, *9*, 1093.

Chapter VI

Allene Osmylation Promoted by Electrophiles

6.1 Introduction

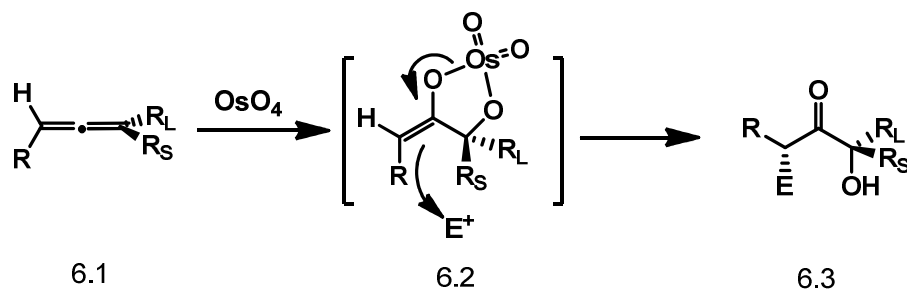
In this chapter we focus on the osmylation of allenes. The reactivity of osmium enolates is unknown. Our studies provide the first look at the functionality and its reactivity.

Osmium catalyzed dihydroxylation reactions are among the most important oxidation reactions due to their high efficiency, excellent chemoselectivity and tolerance to air and moisture. Over the past several decades, numerous studies and reports have been focused on the catalytic asymmetric osmylation of various types of olefins. Many well developed procedures, including the most widely known Sharpless Asymmetric Dihydroxylation (SAD),¹ have been extensively utilized in the synthesis of complex molecules. However, in contrast to the abundant data revealing the reactivity of OsO₄ towards alkenes, the knowledge of allene osmylation is quite limited. Up until now, only eight relevant reports are available. As mentioned in Chapter IV, several drawbacks severely curb the use of allene osmylation: it typically results in low regioselectivity and is often accompanied by significant amount of over-oxidation byproducts. Although the oxidations employing stoichiometric OsO₄, for example the oxidation of the bis[allene] macrolide **3.1** (see chapter 5), are satisfactory,² the toxicity and high expense of OsO₄ dramatically limit its applications. More general methods for allene dihydroxylation need to be developed.

Several procedures for osmium tetroxide catalyzed allene dihydroxylation have been described, including the use of acid or DABCO as additive to increase the reaction rate and catalyst turnover number. Those are all successful applications of known procedures. We began to speculate on the broader potential application of allene osmylation reactions. Our focus was on the osmate ester. This species is an enolate of uncharted reactivity.

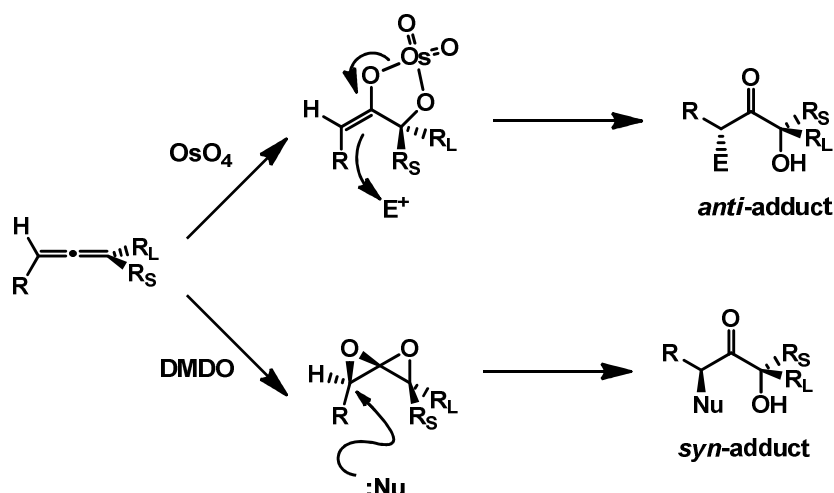
6.2 The Osmate Enol Ester and Interesting Reactivity Within

Taking tri-substituted allene **6.1** as an example, we envisioned that OsO₄ will first add to the more substituted and electron rich double bond. This selectivity is disfavored by sterics and favored by electrons. The osmium tetroxide adduct to the allene, osmate enol ester **6.2**, is an interesting compound that has rarely been mentioned in the literature. Although there is no obvious precedent for its reactivity, one could imagine that a compound with similar structure will have mild to good nucleophilicity, a typical reactivity exhibited in nearly other metal enolates or a silyl enol ether. Being nucleophilic, this adduct should be able to attack some electrophiles and hence install a group at the α' -position of the hydroxy ketone (**6.3**). Importantly, we postulated that the electrophile would accelerate the dissociation of osmium-oxygen bond thus facilitate catalyst turnover. We described in Chapter IV that osmate ester hydrolysis may be rate limiting. Hence addition of an electrophile could well accelerate the overall reaction.



Scheme VI.1 Proposed Electrophile Addition of Osmate Enol Ester

The α -substituted hydroxyl ketones derived from allenes are not without precedent. Our group has been working on the derivitization of spirodiepoxides (SDEs) formed by DMDO oxidation of allenes. If a nucleophile is added to the SDE, it may open the SDE and form a α -substituted α' -hydroxyl ketone (Scheme VI.2).^{3,4} The DMDO oxidation of allenes is stepwise: The first oxidation is at the more electron rich site and is highly selective (>20:1); the second oxidation is at the less substituted double bond, and its selectivity depends on the substitution groups. As a result, the second epoxide is usually formed from the less sterically hindered side. Since the addition of nucleophile is from the back side of the epoxide, this reaction reliably gives a *syn*- adduct.

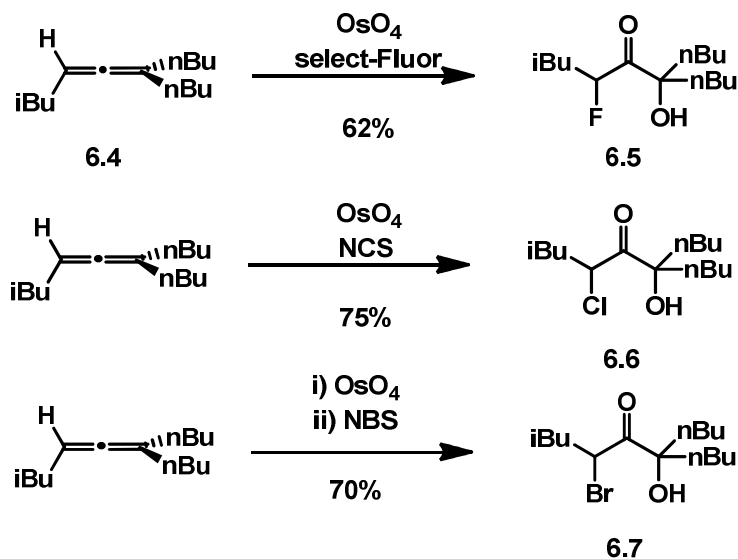


Scheme VI.2 Stereo Outcome of Allene Epoxidation and Osmylation

In contrast, the allene osmylation-electrophilic addition will give different stereo outcome and could potentially be complementary to the SDE method. It was predicted that the osmium enolate would be formed with high selectivity and then the electrophile would approach to the osmate enol ester from the less hindered side. Thus, osmylation/electrophile addition would provide the *anti*- adduct as the major isomer (Scheme VI.2).

6.3 Halogenation of the Osmate Enol Ester

The choice of electrophile is important. The osmium tetroxide catalyzed dihydroxylation reaction often requires water to be a co-solvent to enable the catalytic cycle. Therefore, in order to avoid decomposition in water, the electrophile should not be too reactive. However, it must be reactive enough to consume the osmate enolate. These requirements narrow down the choice of electrophiles significantly. Several carbon electrophiles were tested, including β -nitrostyrene, diisopropylazodicarboxylate (DIAD) and benzaldehyde. However, they either reacted with allene or did not consume the osmium enolate.



Scheme VI.3 Allene Osmylation-halogenation

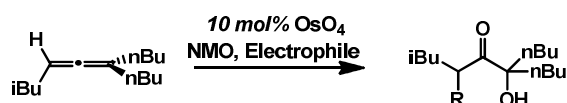
Halogen electrophiles are considered to be reactive toward enolates and stable in water, so they became our choice of electrophiles. Gratifyingly, by using *N*-chlorosuccinimide (NCS) as the electrophile, the stoichiometric osmylation of alkyl allene **6.4** afforded an α -chloro α' -hydroxyl ketone **6.6** (Scheme VI.3). Similarly, *N*-bromosuccinimide (NBS) and select-fluor delivered bromine or fluorine to the α' -position of the hydroxy ketone, respectively. It is remarkable that neither NCS nor Select-Fluor react with this allene, and hence can be pre-mixed with allene before OsO_4 was added. NBS is very reactive and will add to allene spontaneously. So stoichiometric osmium tetroxide needs to be added first followed by the addition of NBS after two minutes.

6.4 Catalytic Osmylation-halogenation

The stoichiometric osmylation has severe drawbacks: the osmium tetroxide is costly and toxic; a large quantity of black precipitate byproduct renders the workup difficult. Therefore, a catalytic procedure becomes the research focus.

The initial attempts at catalytic osmylation-chlorination are shown in Table VI.1. Multiple products were observed when allene was mixed with NCS, NMO and osmium tetroxide in *t*-BuOH and H₂O, and only 10% of the desired product was isolated (entry 1). Changing the solvent system to acetone and water afforded 34% of the desired product together with an unknown byproduct as an inseparable mixture (entry 2). The best result was obtained by using acetone and pH=7.4 phosphate buffer as solvent to give the desired product in 68% yield over 24 hours (entry 4). As a control experiment, the reaction condition using no osmium tetroxide gave no product (not shown). Similarly, the catalytic osmylation-fluorination using Select-Fluor instead of NCS gave the desired fluorination product in 40% yield (entry 7).

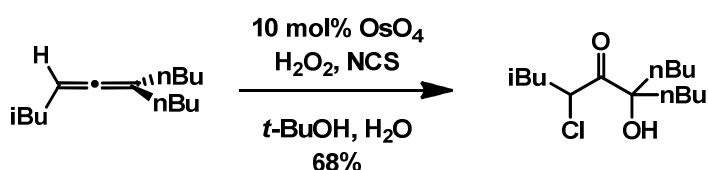
Table VI.1 Optimization of Catalytic Allene Osmylation-halogenation



Entry	Reagent	Solvent	R	Time	Yield (%)
1	NCS	<i>t</i> -BuOH: H ₂ O (1:1)	Cl	12 h	10
2	NCS	Acetone: H ₂ O (1:1)	Cl	3 h	34
3	NCS	<i>t</i> -BuOH: buffer (1:1)	Cl	24 h	47
4	NCS	Acetone: buffer (1:1)	Cl	24 h	68
5	NBS	Acetone: buffer (1:1)	Br	2 d	31
6	NBS	<i>t</i> -BuOH: buffer (1:1)	Br	5 h	68
7	Selectfluor	<i>t</i> -BuOH: buffer (1:1)	F	12 h	40

The effect of pH=7.4 buffer in the catalytic osmylation-chlorination is not clear yet, since a mixed solvent system with *t*-BuOH and pH=7.4 buffer was much inferior (entry 3). However, it was found that even though NCS does not react with allenes under regular conditions, it reacts with allene rapidly in the presence of catalytic amounts of *N*-methylmorpholine (NMM), the by-product of the reaction when NMO is used as

cooxidant. This result explains the relatively lower yield in catalytic osmylation-chlorination, and also encouraged us to explore new co-oxidants. It was shown that when hydrogen peroxide was used in place of NMO, no buffer solution was needed, and this reaction can be done in *t*-BuOH and H₂O to give the desired product in 68% yield (Scheme VI.4).



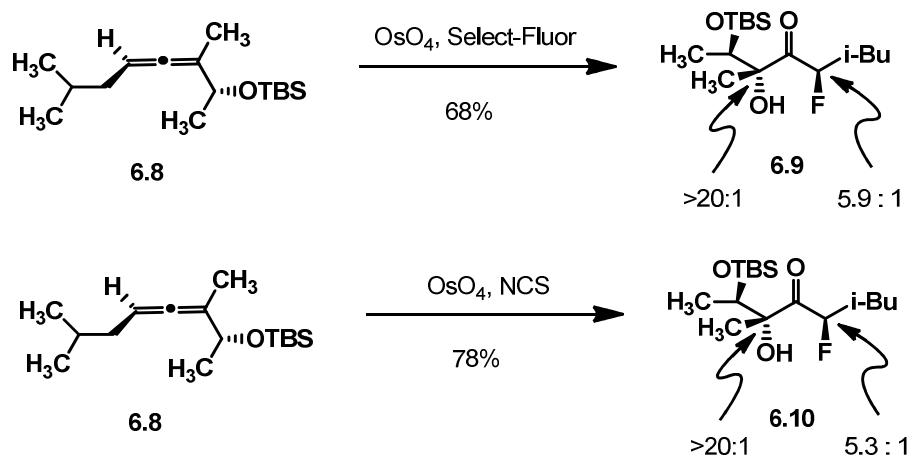
Scheme VI.4 The Use of Hydrogen Peroxide as Co-oxidant

The catalytic osmylation-bromination, however, was very different. None of the reaction conditions above gave the desired bromo-hydroxyketone. Instead, multiple byproducts were formed. Thin layer chromatography (TLC) shows that those byproducts also form without the addition of osmium tetroxide. Therefore this is likely resulting from NBS reacting rapidly with allene. We expected the nucleophilicity of the osmate enol ester to be greater than that of the allene. Accordingly we sought to determine the reaction outcome by controlling the concentration of NBS in solution. After extensive optimization, the best procedure found was to slowly add a solution of NBS in acetone and water to the reaction mixture over five hours. This procedure gave the desired bromination product in 68% yield (Table VI.1, entry 6).

6.5 Stereoselectivity of Osmylation-halogenation

The addition of osmium tetroxide to trisubstituted allenes was found to be highly stereoselective. This mirrors other allene addition reactions and is attributable to the large

steric bias imposed by the hydrogen and the alkyl substituents on non-reacting terminus of the allene. The halogenation step, however, is less selective and depends on fine structural details of the allene and the electrophile.

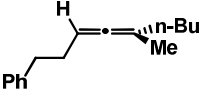
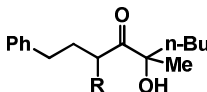
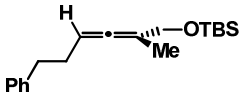
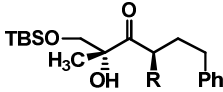


Scheme VI.5 Allene Osmylation-halogenation of Chiral Allene

The initial study focused on biased allene **6.8** and used stoichiometric amount of OsO_4 . It was found that Select-Fluor and NCS could deliver halide to the desired position to give the halo-ketone with satisfying d.r. (**6.9**, d.r. = 5.9:1 and **6.10**, d.r. = 5.3:1, respectively).

The results of catalytic osmylation-halogenation are shown in Table VI.2. Interestingly, stereoselectivity was noted for sterically unbiased allene **6.11**. The catalytic osmylation-fluorination and bromination gave the desired product with 1.8:1 d.r. and 2:1 d.r., respectively (entry 2 and 3).

Table VI.2 Catalytic Allene Osmylation-Halogenation Stereoselectivity

Entry	Allene	Product	d.r.		Yield (%)
			Osmylation	Addition	
	 6.11	 R	>20:1		71
1	6.11	H	>20:1		71
2	6.11	F	>20:1	1.8:1	58
3	6.11	Br	>20:1	2:1	64
	 6.12	 R	>20:1	—	44
4	6.12	H ^e	>20:1		44
5	6.12	F	>20:1	5 : 1	57
6	6.12	Cl	>20:1	2.4 : 1	55
7	6.12	Br	>20:1	1.6 : 1	46

In our previous work, fluorine, chlorine and bromine electrophiles exhibited similar stereoselectivity. However, for the somewhat electron deficient allene **6.12**, the d.r. was much differentiated. Fluorination gave the highest d.r. (5:1, entry 5), and chlorination gave d.r. = 2.4:1 (entry 6), and the d.r. of bromination was only 1.6:1 (entry 7).

The origin of such differences is difficult to know with certainty. Many factors are probably important such as the reactivity of the electrophile. Further research regarding the d.r. is ongoing in our lab.

6.6 Osmylation of Disubstituted Allene

The osmylation of disubstituted allenes was quite different from that of the trisubstituted allenes. We have demonstrated that the catalytic osmylation of the trisubstituted alkyl allene is often slow and fails to go to completion. However, the catalytic osmylation of disubstituted alkyl allene **6.13** was significantly faster and gave significantly more overoxidation product. Indeed, **6.14** was isolated as the major product (Table VI.3, entry 1). Using strong acid as additive suppressed the over-oxidation and give a mixture of the desired hydroxyl ketone and over-oxidation product (entry 2). When NMO was used as the co-oxidant, increasing the amount of HCl resulted in no reaction and the recovery of starting material (entry 3). However, hydrogen peroxide as co-oxidant in place of NMO gave the desired product **6.15** in 51% yield (entry 4).

Table VI.3 Catalytic osmylation of disubstituted allene

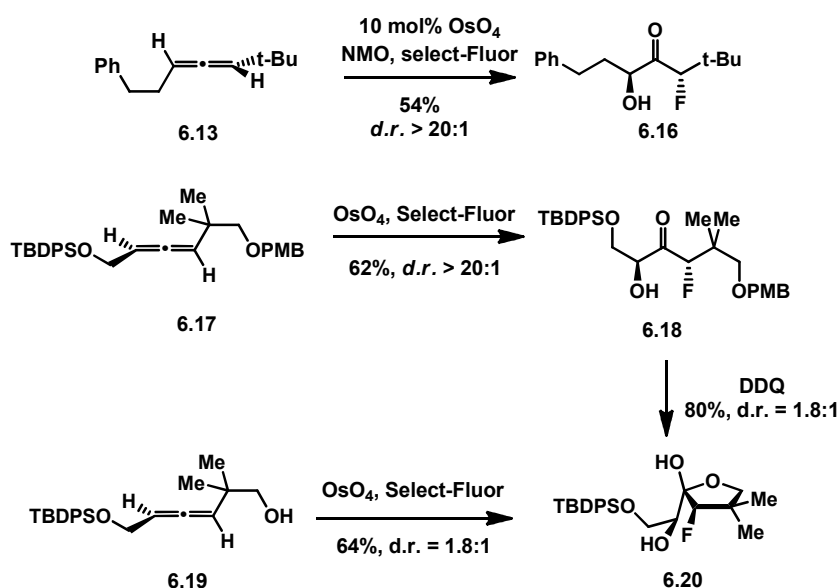
CC(C)(C)C=Cc1ccccc1 (6.13) $\xrightarrow{10\text{ mol\% OsO}_4}$ CC(C)(C)C(=O)C(O)Cc1ccccc1 (6.14) + CC(C)(C)C(=O)C(O)Cc1ccccc1 (6.15)

Entry	Additive	Co-oxidant	Yield (6.14)	Yield (6.15)
1	None	NMO	57%	0
2	HCl (0.5 equiv.)	NMO	34%	26%
3	HCl (10 equiv.)	NMO	N.R	N.R
4	HCl (10 equiv.)	H ₂ O ₂	21%	51%

We note that the overoxidation of disubstituted allenes is consistent with our mechanistic framework (Chapter IV, Scheme IV.5): the trisubstituted allene is bulky, hence the second

osmium tetroxide addition is hard; the disubstituted allene is less bulky, and as a result the addition of second osmium tetroxide is faster.

In theory, the regioselectivity of disubstituted allene should be low due to similar electron density of the two double bonds. However, since osmylation is sensitive to steric hindrance we wondered at the possibility of designed substrates that would react selectively. As shown in Table VI.3, osmylation of a sterically biased allene **6.13** gives the desired hydroxy ketone **6.15**, and no formation of the regio isomer was observed. Similarly, the osmylation-fluorination of **6.13** gave the **6.16** as a single diastereomer in 54% yield (Scheme VI.6). However, a small amount of regio-isomer of **6.16** was observed, and the ratio is found to be 4:1 (**6.16** : undesired).



Scheme VI.6 Osmylation-fluorination of Disubstituted Allenes

Oxidation-fluorination of a more highly functionalized allene **6.17** gave fluoro ketone **6.18** in 62% yield as a single diastereomer. When allene **6.19** with an unprotected alcohol was oxidized under the same reaction condition, an 1.8:1 mixture of 5-membered cyclic hemiacetal **6.20** was formed (Scheme VI.6). When the osmylation product **6.18** was treated

with DDQ, the fluorohydroxyketone was converted to **6.20** spontaneously, giving the same 1.8:1 mixture of diastereomers as obtained in the previous reaction. We conclude that the osmylation/fluorination reaction was fully selective for **6.13**, **6.17** and **6.19**.

6.6 Osmylation-halogenation on Macrocyclic Bis[allene]

As described in Chapter V, one of our main goals was to modify the two allenic groups of the macrocyclic bis[allene] **3.1** in order to access erythronolide derivatives. With the promising osmylation data in hand, it was of great interest to explore the possibility of applying these methods to the oxidation of macrocyclic bis[allene]. More importantly, the resulting α -halo- α' -hydroxyketone product, especially the fluorinated ketone, has drawn broad interest in numerous fields including drug discovery and molecule labeling.^{5,6} The successful osmylation-halogenation reactions would potentially provide an alternative and direct procedure for making such compounds.

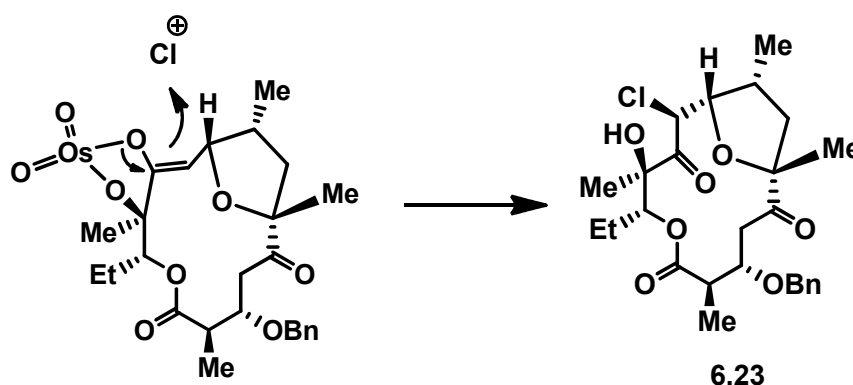
Table VI.4 Macrocyclic Allene Osmylation-halogenation

Entry ^a	Allene	Product (R)	d.r.		Yield%
			1	2	
	 6.21	 6.22			
1	6.21	H	>20:1	-	45
2	6.21	F	>20:1	>20:1	56
3	6.21	Cl	>20:1	>20:1	52
4	 6.22	 6.23	>20:1	>20:1	59

The results are shown in Table VI.4. We started with unfunctionalized model bis[allene] macrolide. Simple osmylation of **6.21** without additive afforded the hydroxyl ketone product in 45% yield (entry 1). This is a significant improvement over other methods, since oxidation of such a system is not trivial.⁷ Also, in the presence of either Select-Fluor or NCS the oxidation-halogenation process successfully gave the desired product in >50% yield (entries 2, 3). The relative configuration of the chloride group and alkyl substitution group were confirmed by X-ray crystallographic analysis of the product in entry 3. The

catalytic osmylation-fluorination employing 10 mol% OsO_4 also gave the difluoro-dihydroxyketone of entry 2 in 26% yield (data not shown).

On the other hand, the osmylation-chlorination using the same procedure were able to convert a more densely functionalized macrocyclic allene **6.22** to the corresponding chloro ketone **6.23**. Similar to the known elimination-cyclization observed in simple osmylation (see Chapter 5, compound **5.5**), a tetrahydrofuran moiety was found in the product. The benzyl eliminates presumably via the same process as described in Scheme V.5, and the cyclization intermediate, which is also an osmium enolate (Scheme VI.7), is nucleophilic and attacks the NCS to give the observed product **6.23**. The unexpected syn- relationship is also the result of macrocyclic stereocontrol.

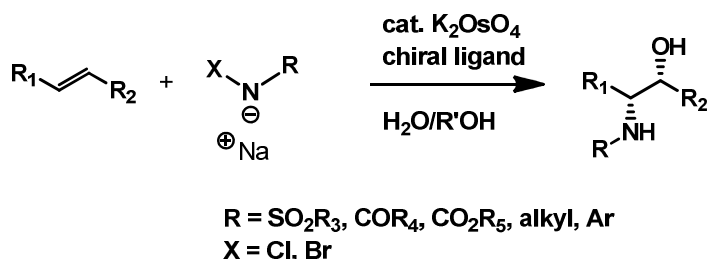


Scheme VI.7 Osmylation-chlorination mechanism of macrocyclic allene

6.7 Allene Aminohydroxylation

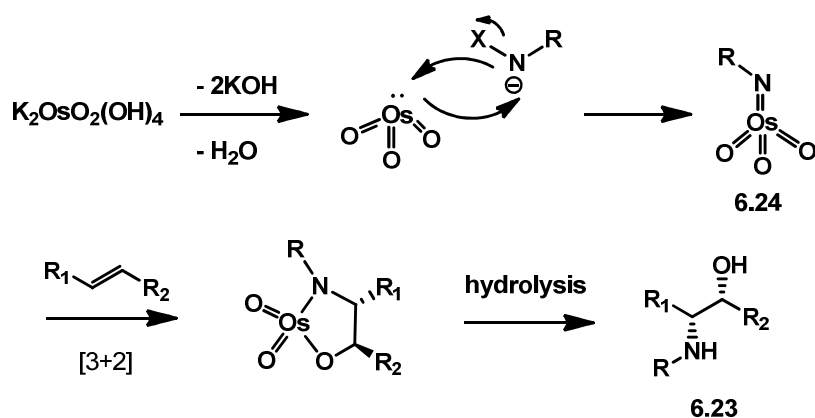
Aminohydroxylation is a known method for alkene oxidation and is similar to alkene dihydroxylation. The method uses a nitrogen-containing co-oxidant, usually *N*-halo amides, carbamates or sulfonamides.^{8,9} The product is typically an amino alcohol of type **6.23** (Scheme VI.7). The best asymmetric approach is developed by Sharpless, and is known as the Sharpless Asymmetric Aminohydroxylation (SAA). Similar to the Sharpless

Asymmetric Dihydroxylation (SAD) reaction, dihydroquinine ligand is used to induce enantioselectivity in the products.



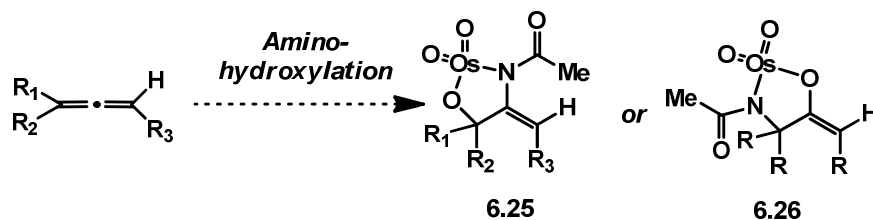
Scheme VI.8 The Sharpless Asymmetric Aminohydroxylation

The accepted mechanism of alkene aminohydroxylation is similar to the dihydroxylation, albeit different in the form of **6.24**, a nitrogen-containing imidotriooxosmium (VIII) intermediate. The nitrogen can be delivered to alkenes by a [3+2] cycloaddition process. Hydrolysis of the 5-membered ring intermediate gives the aminoalcohol product.



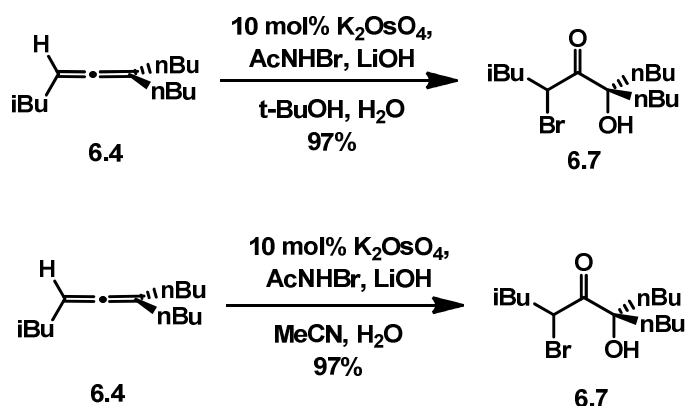
Scheme VI.9 Mechanism of Alkene Aminohydroxylation

The regioselectivity of aminohydroxylation remains difficult to predict yet. Sharpless has shown that the use of dihydroquinine ligand can control the regioselectivity of aryl alkenes efficiently, whereas the regio control of non-aryl alkenes is challenging.^{10,11}



Scheme VI.10 Proposed Allene Aminohydroxylation

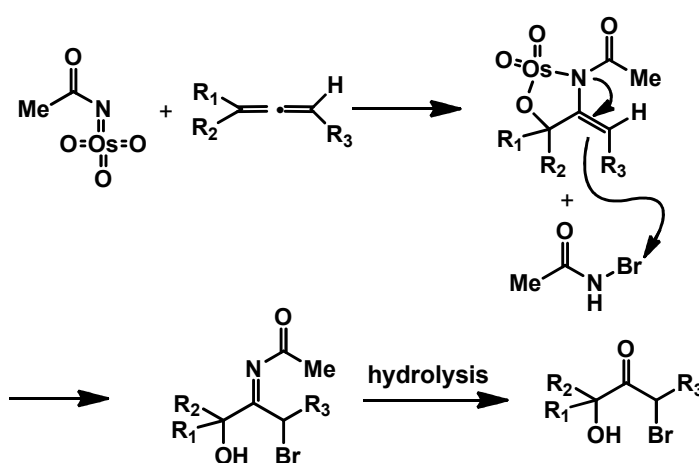
Encouraged by our success with allene dihydroxylation, we wondered about the reactivity of allenes toward aminohydroxylation. We recognized that if the nitrogen is delivered to the center carbon of the allene **6.25**, we could well obtain the hydroxyl N-aclylenamide; whereas if the nitrogen is added to the tertiary carbon of the allene **6.26**, we should be able to obtain a tertiary amine product. Both outcomes represent important functionality.



Scheme VI.11 Aminohydroxylation of Alkyl Allene **6.4**

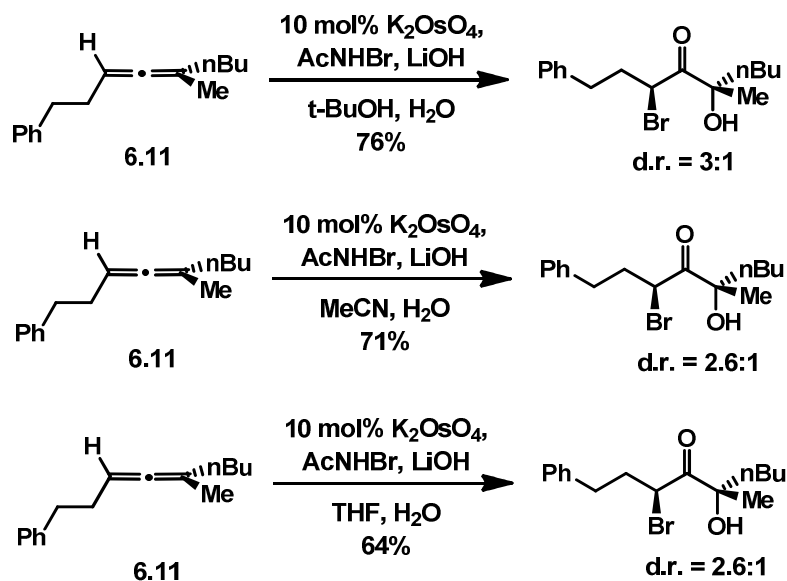
Initial attempts used *tert*-butylhypochlorite as the co-oxidant. However, complex mixtures were observed (data not shown). After screening other mild nitrogen sources, we found that excess *N*-bromoacetamide gave a single product in the presence of catalytic K_2OsO_4 and excess LiOH (Scheme VI.10). This reaction appeared complete within thirty minutes in $t\text{-BuOH}/H_2O$ or $MeCN/H_2O$. The product was a bromohydroxyketone and was shown to be identical to compound **6.7**.

The formation of this product is reasonable. For example, one reasonable pathway includes addition of the imidotrioxoosmium (VIII) intermediate to the allene. The resulting osmium enamide would be nucleophilic and could attack the unreacted *N*-bromoacetamide (Scheme VI.11). This rationale is consistent with the mechanistic framework of allene osmylation-bromination sequence. The resulting bromo imine is then hydrolyzed to release the observed ketone.



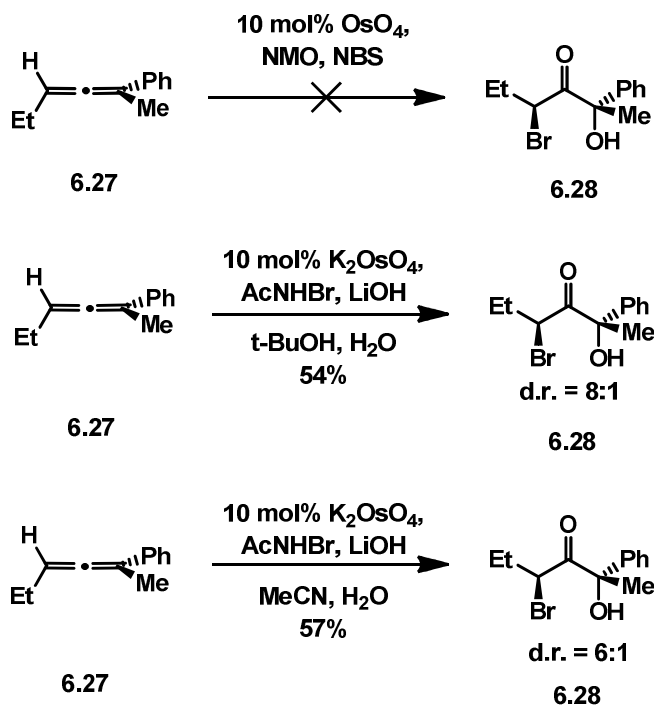
Scheme VI.12 Mechanistic Framework of Allene Aminohydroxylation

This reaction has some advantages: It is much faster than the osmylation-bromination sequence which takes several hours to complete. The yield is excellent and no side products were observed. To secure success of this reaction, at least 5% of K_2OsO_4 as well as excess (3-4 equiv) *N*-bromoacetamide and LiOH proved most reliable. It was also found to be important to add exactly a 1:1 ratio of *N*-bromoacetamide and LiOH . Otherwise, a complex reaction mixture was observed.



Scheme VI.13 Aminohydroxylation of Chiral Allene in Different Solvents

This reaction also shows some tolerance regarding the choice of solvent. Not only *t*-BuOH, but also acetonitrile and THF were found to be suitable for reaction (Scheme VI.12). Another promising observation was that the *n*-butyl and methyl substituents on allene **6.11** were differentiated with some selectivity. Nearly a 3:1 d.r of the corresponding bromo ketone was obtained in contrast to single osmylation-bromination sequence (Table VI.2, entry 3, d.r. = 2:1).



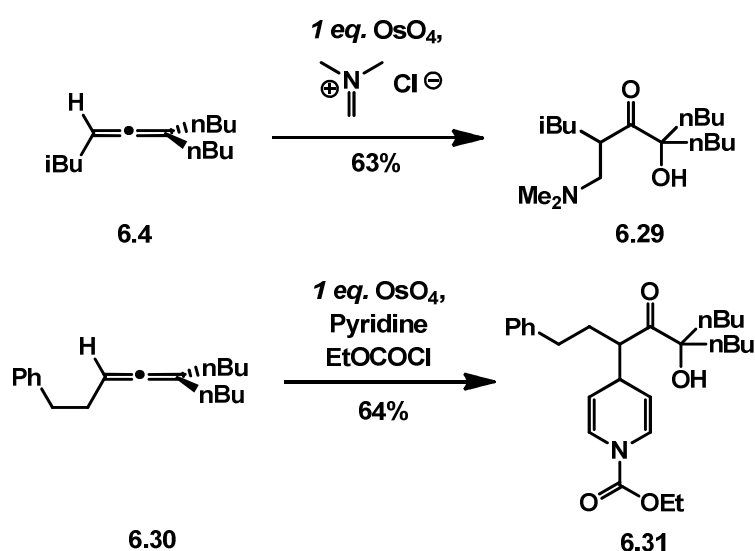
Scheme VI.14 Aminohydroxylation of Aryl Allene 6.27

As mentioned in Chapter V, the allene osmylation promoted by NBS works for alkyl allenes, but it fails to give the desired bromo ketone **6.28** from aryl allene **6.27**. Presumably this is traceable to the high reaction rate of OsO_4 towards the aryl allene.¹² Hence, in this case dihydroxylation and over oxidation occur before addition of Br. This problem can be partially solved by employing our aminohydroxylation procedure. The use of catalytic K_2OsO_4 , *N*-bromoacetamide and excess LiOH was found to successfully install the bromo ketone moiety on the aryl allene in 54% yield and >6:1 d.r.

6.8 Addition of Carbon Electrophiles

One of the most important applications of metal enolates is the construction of C-C bonds. Therefore, it was also of great interest to determine whether this osmate enol ester is nucleophilic enough for the addition to carbon electrophiles. This is proved to be a

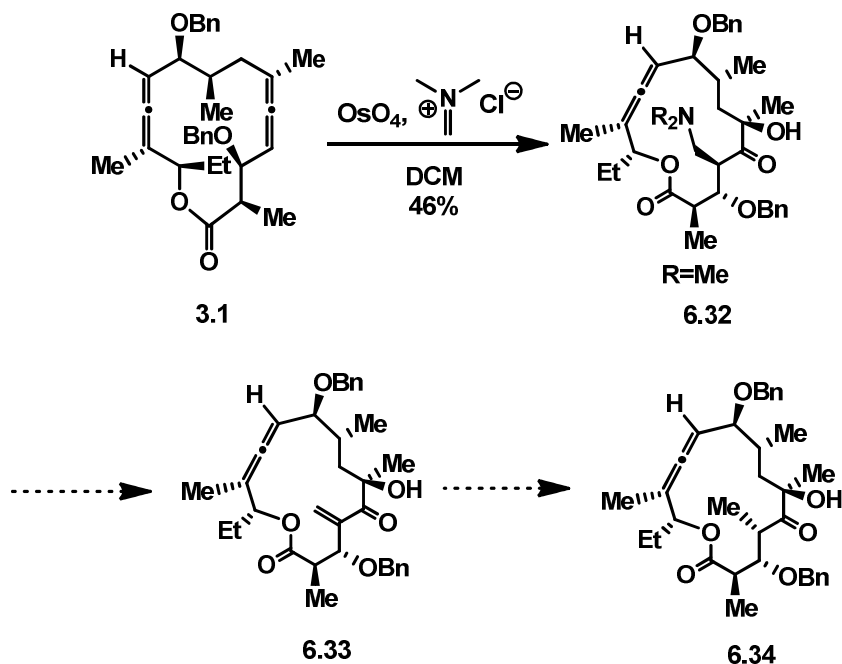
challenging problem. Previous studies using relatively weak carbon electrophiles such as aldehydes, enones and nitro alkenes gave no desired product and mostly recovered starting materials. It was unclear whether the electrophile was reactive enough. Therefore, stronger electrophiles were examined. There were several issues to consider in addressing this challenge. For example, many reactive carbon electrophiles are not stable and need to be generated *in situ*. As a result, water is not a favorable solvent, because it is very likely to react with the electrophiles faster than the osmate enol ester would form and react as desired. Such limitations suggested that the initial attempts should be done with stoichiometric OsO_4 .



Scheme VI.15 Allene Osmylation-iminium Addition

The commercially available dimethylmethyleniminium iodide was chosen as potential electrophile.¹¹ As expected, it successfully added to the osmate enol ester to give the tertiary amine product. The procedure was simple: the allene was dissolved in DCM, mixed with the iminium salt and then OsO_4 solution in DCM was added. This reaction, as predicted, is sensitive to moisture, and the addition of molecular sieves further improved

the yield. Similarly, the *in situ* generated pyridinium salt¹² can also be used as electrophile to form the C-C bond from osmate enol ester. The *para*-adduct **6.31** was observed as the only product.



Scheme VI.16 Iminium Addition on Macrocyclic Bis[allene] 3.1

Successes in iminium ion addition demonstrate that the osmium enolate is suitable at least for some substrates for the formation of new C-C bonds. Since one of our main goals is to make erythronolide derivatives, we wondered whether this reaction would deliver an aminomethyl group to the macrolide ring. Pleasingly, the reaction conditions described above was able to install the desired tertiary amine on the macrolide (Scheme VI.15). In principle, this reaction could be followed eventually by elimination of the amino group (compound **6.33**) and the reduction of the alkene to give the compound **6.34**, a methyl group substituted the macrolide corresponding to erythromycin. This would provide an alternative to the original route based on a spirodiepoxide strategy.

6.9 Conclusion

We have developed the first osmylation of allenes and have further shown that this catalyzed process can be accelerated by using the electrophilic additives. The addition of electrophile to osmate enol ester delivers the α -substituted α' -hydroxyl ketone. This collection of reactions promises great potential in the synthesis of complex molecules. Carbon-halogen bonds, as well as carbon-carbon bonds, are constructed directly by this method.

Also, it has been shown that aminohydroxylation of allenes also give the hydroxyketone. Most of this work had little precedent in the allene literature. Indeed, there have been no relevant studies on osmium enolates. This work demonstrates that this functionality is interesting and useful. Finally, although we have not performed mechanistic studies per se, all of the available data are nicely rationalized with our mechanistic framework. Further studies are needed, but thus far, these methods look very promising.

6.10 References

1. Kolb, Hartmuth C.; VanNieuwenhze, Michael S.; Sharpless, K. Barry *Chemical Reviews*, **1994**, *94*, 2483.
2. Liu, K.; Kim, H.; Ghosh, P.; Akhmedov, N. G.; Williams, L. J. *J. Am. Chem. Soc.* **2011**, *133*, 14968.
3. Ghosh, P.; Lotesta S. D.; Williams, L. J. *J. Am. Chem. Soc.* **2007**, *129*, 2438.
4. Sharma, R.; Manpadi, M.; Zhang, Y.; Kim, H.; Akhmedov, N. G.; Williams, L. J. *Org. Lett.* **2011**, *13*, 3352.
5. Müller, K.; Faeh, C.; Diederich, F. *Science* **2007**, *317*, 1881.

6. Phelps, M. E. *Proc. Natl. Acad. Sci. USA* **2000**, 97, 9226 – 9233.
7. Ghosh, P.; Zhang, Y.; Emge, T. J.; Williams, L. J. *Org. Lett.* **2009**, 11, 4402.
8. Li, G.; Chang, H.-T.; Sharpless, K. B. *Angew. Chem. Int. Ed. Engl.* **1996**, 35, 451.
9. Bodkin, J. A.; McLeod, M. D. *J. Chem. Soc., Perkin Trans. 1*, **2002**, 2733.
10. Tao, B.; Schlingloff, G.; Sharpless, K. B. *Tetrahedron Lett.* **1998**, 39, 2507.
11. Han, H.; Cho, C.-W.; Janda, K. D. *Chem. Eur. J.* **1999**, 5, 1565–1569.
12. Fleming, S. A.; Liu, R.; Redd, J. T. *Tetrahedron Lett.* **2005**, 46, 8095.
13. Schreiber, J.; Maag, H.; Hashimoto, N.; Eschenmoser, A. *Angew. Chem. Intl. Ed.* **1971**, 10, 330.
14. Comins, D.L.; Brown, J. D. *Tetrahedron Lett.* **1984**, 25, 3297.

Chapter VII

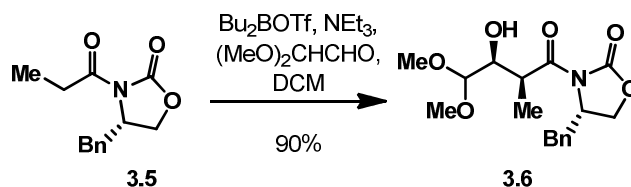
Experimental Section

1. General

Starting materials, reagents and solvents were purchased from commercial suppliers (Aldrich, Strem, TCI America and Ochem.) and used without further purification unless otherwise stated. All reactions were conducted in oven-dried (135 °C) glassware under an inert atmosphere of argon. The progress of reactions was monitored by silica gel thin layer chromatography (TLC) plates (mesh size 250 μm with F-254 indicator, Dynamic Adsorbent), visualized under UV and charred using anisaldehyde or ceric ammonium molybdate (CAM) stain. Products were purified by flash column chromatography (FCC) on 120-400 mesh silica gel (Fisher). Infrared (FTIR) spectra were recorded on an ATI Mattson Genesis Series FTInfrared spectrophotometer. Proton nuclear magnetic resonance spectra (^1H NMR) were recorded on either a Varian-600 instrument (600 MHz) or a Varian-500 instrument (500MHz). Chemical shifts are reported in ppm relative to residual CHCl_3 signal. Data is reported as follows: chemical shift, multiplicity (s=singlet, d=doublet, t=triplet, q=quartet, br=broad, m=multiplet), coupling constant (Hz), and integration. Carbon nuclear magnetic resonance spectra (^{13}C NMR) were recorded on either a Varian-600 instrument (150 MHz) or a Varian-500 instrument (125 MHz). Mass spectra were recorded on a Finnigan LCQ-DUO mass spectrometer. Optical rotations were

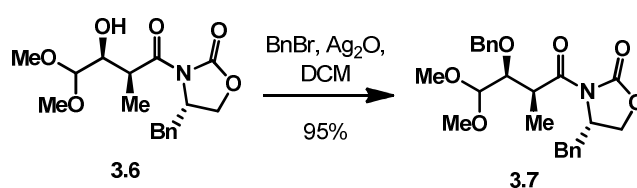
recorded at room temperature using the sodium D line (589 nm), on a Perkin Elmer 343 Polarimeter.

2. Chapter III



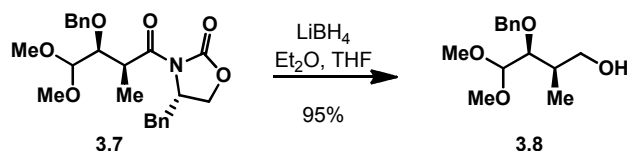
To a solution of 4(*S*)-benzyl N-propionyl oxazolidinone **3.5** (16.0 g, 68.6 mmol) in dichloromethane (DCM) (343 mL) was added dibutylboron triflate (75.0 mL, 75.0 mmol) and triethylamine (TEA) (9.72 g, 96.0 mmol) respectively at $-78\text{ }^\circ\text{C}$. The reaction mixture was then warmed to $0\text{ }^\circ\text{C}$ and stirred for one hour then cooled back to $-78\text{ }^\circ\text{C}$. A DCM solution (1.0 M) of 1,1-dimethoxy acetaldehyde (100 mL, 100 mmol) was added to the reaction mixture slowly at $-78\text{ }^\circ\text{C}$. The mixture was slowly warmed to $0\text{ }^\circ\text{C}$ over one hour and stirred for one hour at that temperature. The reaction was then quenched with 100 mL solution of methanol and pH=7.4 phosphate buffer (1:3 ratio) at $0\text{ }^\circ\text{C}$, followed by addition of 100 mL solution of 30% H_2O_2 and methanol (1:2 ratio). The mixture was then stirred for 10 minutes at $0\text{ }^\circ\text{C}$ then diluted with 200 mL DCM. The organic layer was separated, washed with water (2 x 100 mL), dried over anhydrous Na_2SO_4 , filtered, and then concentrated under reduced pressure to give the crude product, which was purified by FCC using 40% ethyl acetate in hexane to afford aldol product **3.6** as white crystalline (20.9 g, 90% yield). $[\alpha]_{\text{D}}^{25} = +50.0$ ($c = 0.01$, CHCl_3); M.P. $67\text{ }^\circ\text{C}$; IR $\nu_{\text{max}}(\text{neat})/\text{cm}^{-1}$ 3485, 2937, 1778, 1696, 1386; ^1H NMR (500 MHz, CDCl_3) δ 7.35-7.25 (m, 3H), 7.21 (d, $J = 7.0\text{ Hz}$,

2H), 4.72-4.65 (m, 1H), 4.33 (d, $J = 6.0$ Hz, 1H), 4.23- 4.15 (m, 2H), 4.05-3.96 (m, 1H), 3.42 (s, 3H), 3.38 (s, 3H), 3.26 (dd, $J = 13.5, 3.5$ Hz, 1H), 2.78 (dd, $J = 13.5, 10$ Hz, 1H), 2.68-2.60 (bs, 1H), 1.32 (d, $J = 7.0$ Hz, 3H); ^{13}C NMR (125 MHz, CDCl_3) δ 176.1, 153.2, 135.4, 129.6 (2), 129.1 (2), 127.5, 104.9, 71.4, 66.3, 55.4, 54.9, 54.4, 39.2, 38.1, 12.8; MS (ESI⁺) calculated for $[\text{C}_{17}\text{H}_{23}\text{NO}_6+\text{Na}]^+$: 360.2, found: 360.2

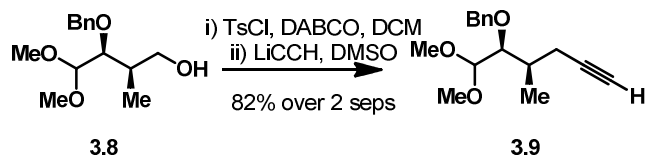


Powdered 4Å molecular sieves (20.0 g) and Ag_2O (35.0 g, 151 mmol) were combined under inert atmosphere (glove bag) and to that was added anhydrous DCM (150 mL) followed by the addition of a solution of aldol product **3.6** (17.0 g, 50.4 mmol) in anhydrous DCM (100 mL). After stirring for 10 minutes at room temperature BnBr (18.5 g, 108 mmol) was added to this heterogeneous mixture. The system was then covered with aluminum foil and stirred for 2 days under inert atmosphere in the dark at room temperature. The mixture was then filtered over celite and the solid residue was rinsed with DCM (3 x 100 mL). The organic filtrate was concentrated under reduced pressure to give crude product, which was purified by FCC using 20% ethyl acetate in hexane to afford **3.7** as colorless oil (20.4 g, 95% yield). $[\alpha]_{\text{D}}^{25} = +21.0$ ($c = 0.01$, CHCl_3); IR $\nu_{\text{max}}(\text{neat})/\text{cm}^{-1}$ 2934, 1778, 1698, 1383, 1107; ^1H NMR (500 MHz, CDCl_3) δ 7.39-7.23 (m, 8H), 7.19 (d, $J = 7.0$ Hz, 2H), 4.81 (d, $J = 11.5$ Hz, 1H), 4.64 ($J = 11.5$ Hz, 1H), 4.59- 4.53 (m, 1H), 4.34 (d, $J = 6.0$ Hz, 1H), 4.14-4.03 (m, 3H), 3.84 (dd, $J = 7.5, 6.5$ Hz, 1H), 3.43 (s, 3H), 3.34 (s, 3H), 3.24 (dd, $J = 13.5, 3.5$ Hz, 1H), 2.75 (dd, $J = 13.5, 9.5$ Hz, 1H), 1.31 (d, $J = 7.0$ Hz,

3H); ^{13}C NMR (125 MHz, CDCl_3) δ 175.2, 153.3, 138.6, 135.5, 129.6 (2), 129.0 (2), 128.4 (2), 128.2 (2), 127.8, 127.4, 107.0, 79.8, 74.4, 66.1, 55.5, 55.4, 55.2, 39.5, 38.1, 13.8; MS (ESI+) calculated for $[\text{C}_{24}\text{H}_{29}\text{NO}_6+\text{Na}]^+$: 450.2, found: 450.2;.



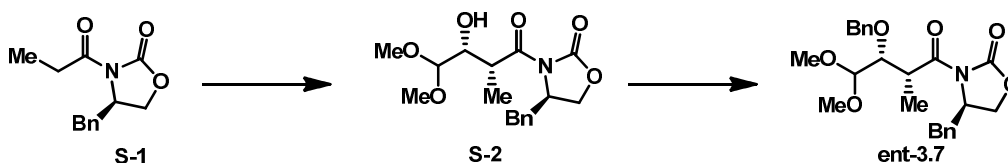
To a solution of **3.7** (17.8 g, 41.6 mmol) in diethyl ether (200 mL) was added 5 mL methanol. The reaction mixture was cooled to 0 °C and then 2.5 M solution of LiBH_4 in tetrahydrofuran (THF) (33.2 mL, 83.0 mmol) was added slowly under argon. The resulting solution was stirred at 0 °C for 2 hours then quenched with aqueous NH_4Cl (50 mL) and extracted with ethyl acetate (3 x 200 mL). The organic layer was separated, dried over anhydrous Na_2SO_4 , filtered and then concentrated under reduced pressure to give crude product, which was purified by FCC using 15% ethyl acetate in hexane to afford **3.8** as colorless oil (10.1 g, 95% yield). $[\alpha]_{\text{D}}^{25} = -33.0$ ($c = 0.01$, CHCl_3); IR $\nu_{\text{max}}(\text{neat})/\text{cm}^{-1}$ 3431, 2934, 1454, 1071; ^1H NMR (500 MHz, CDCl_3) δ 7.38-7.32 (m, 4H), 7.30-7.25 (m, 2H), 4.82(d, $J = 11.5$ Hz, 1H), 4.58 (d, $J = 11.5$ Hz, 1H), 4.39 (d, $J = 6.5$ Hz, 1H), 3.59 (dd, $J = 6.0, 3.5$ Hz, 1H), 3.59-3.46 (m, 2H), 3.49 (s, 3H), 3.41 (s, 3H), 2.02-1.96 (m, 1H), 1.90 (bs, 1H), 0.94 (d, $J = 7.0$ Hz, 3H); ^{13}C NMR (125 MHz, CDCl_3) δ 138.9, 128.5 (2), 128.2 (2), 127.8, 106.5, 79.6, 74.1, 65.8, 56.2, 54.6, 36.9, 11.4; MS (ESI+) calculated for $[\text{C}_{14}\text{H}_{22}\text{O}_4+\text{Na}]^+$: 277.2, found: 277.2.



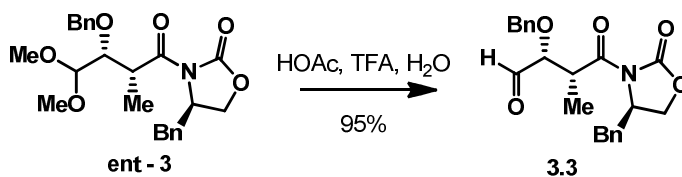
To a stirring solution of **3.8** (7.30 g, 28.7 mmol) in DCM (150 mL) was added DABCO (3.22 g, 28.7 mmol). The reaction mixture was cooled to 0 °C and then tosyl chloride (5.47 g, 28.7 mmol) was added. The resulting solution was then warmed to room temperature and stirred for 1 hour then diluted with 150 mL of DCM, washed with saturated NH_4Cl solution (3 x 50 mL) and water (50 mL). The organic layer was separated, dried over anhydrous Na_2SO_4 , and concentrated under reduced pressure to give crude tosylate, which was taken on without further purification as described below.

The above tosylate was dissolved in anhydrous DMSO (70 mL), and then lithium acetylide-ethylenediamine (4.76 g, 52.9 mmol) solution in 30 mL DMSO was added. The resulting mixture was stirred for 3 hours at room temperature, then cooled to 10 °C then quenched carefully with aqueous NH_4Cl (50 mL) so that the temperature of the solution was controlled below 20 °C. The quenched solution was then diluted with ethyl acetate (300 mL) and washed with water (3 x 100 mL). The organic layer was separated, dried over anhydrous Na_2SO_4 , filtered, and then concentrated under reduced pressure to give crude product, which was purified by FCC using 3% ethyl acetate in hexane to afford **3.9** as colorless oil (5.95 g, 82% yield). $[\alpha]_{\text{D}}^{25} = -39.0$ ($c = 0.01$, CHCl_3); IR $\nu_{\text{max}}(\text{neat})/\text{cm}^{-1}$ 3295, 2935, 2116, 1096; ^1H NMR (500 MHz, CDCl_3) δ 7.38-7.30 (m, 4H), 7.28-7.22 (m, 1H), 4.68 (d, $J = 11.5$ Hz, 1H), 4.56 (d, $J = 11.5$ Hz, 1H), 4.36 (d, $J = 7.0$ Hz, 1H), 3.65 (dd, $J = 7.0, 3.0$ Hz, 1H), 3.47 (s, 3H), 3.38 (s, 3H), 2.23- 2.12 (m, 2H), 2.10- 2.00 (m, 2H), 1.96 (t, $J = 7.5$ Hz, 1H), 0.98 (d, $J = 7.0$ Hz, 3H); ^{13}C NMR (125 MHz, CDCl_3) δ 139.3, 128.4 (2),

127.9 (2), 127.6, 106.4, 83.7, 80.3, 74.8, 69.6, 56.0, 53.8, 34.4, 23.5, 14.0; MS (ESI+) calculated for $[C_{16}H_{22}O_3+Na]^+$: 285.1, found: 285.2.

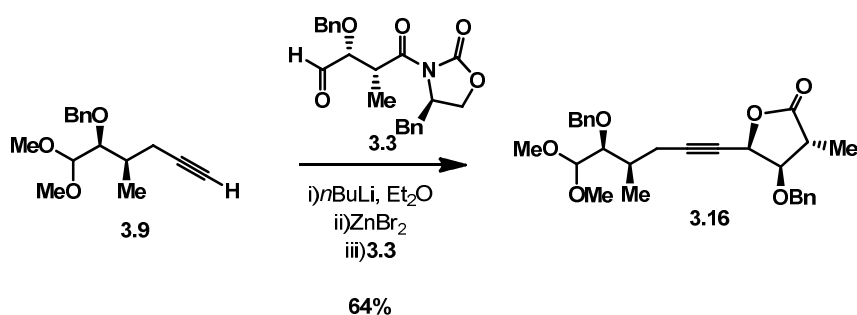


Compound **S-2** and **ent-3.7** were prepared following the same procedure used for the synthesis of their antipods **3.6** and **3.7** respectively. The observed optical rotation ($[\alpha]_D^{25}$) for the compound **S-2** and **ent-3.7** are -50.0 ($c = 0.01$, $CHCl_3$), and -21.0 ($c = 0.01$, $CHCl_3$) respectively.



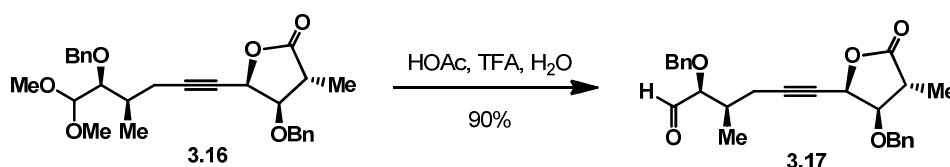
Ent-3.7 (1.00 g, 2.34 mmol) was dissolved in 10ml water: acetic acid : trifluoroacetic acid = 1:4:1 mixed solution at room temperature for 3hours and 30 mins. The acidic solvent was co-removed with toluene (5 x 20 mL) under reduced pressure and the resulting crude product was taken on without further purification as described below. It could also be further purified by FCC using 15% ethyl acetate in hexane to afford **3.3** as colorless viscous oil (847 mg, 95% yield). $[\alpha]_D^{25} = -30.0$ ($c = 0.01$, $CHCl_3$); IR $\nu_{max}(neat)/cm^{-1}$ 1778, 1730, 1693, 1390, 1212; 1H NMR (500 MHz, $CDCl_3$) δ 9.81 (s, 1H), 7.38-7.22 (m, 8H), 7.17 (d, $J = 7.0$ Hz, 2H), 4.75 (d, $J = 12.5$ Hz, 1H), 4.64-4.54 (m, 1H), 4.59 (d, $J = 12.5$ Hz, 1H), 4.32-4.24 (m, 1H), 4.16-4.06 (m, 2H), 3.92 (d, $J = 6.0$ Hz, 1H), 3.20 (dd, $J = 13.5, 3.5$

Hz, 1H), 2.76 (dd, $J = 13.5, 10$ Hz, 1H), 1.33 (d, $J = 7.0$ Hz, 3H); ^{13}C NMR (125 MHz, CDCl_3) δ 202.0, 173.8, 153.1, 137.2, 135.1, 129.6 (2), 129.1 (2), 128.7 (2), 128.4, 128.3 (2), 127.5, 83.3, 73.1, 66.4, 55.4, 41.5, 37.8, 13.4; MS (ESI+) calculated for $[\text{C}_{22}\text{H}_{23}\text{NO}_5 + \text{Na}]^+$: 404.2, found: 404.2.

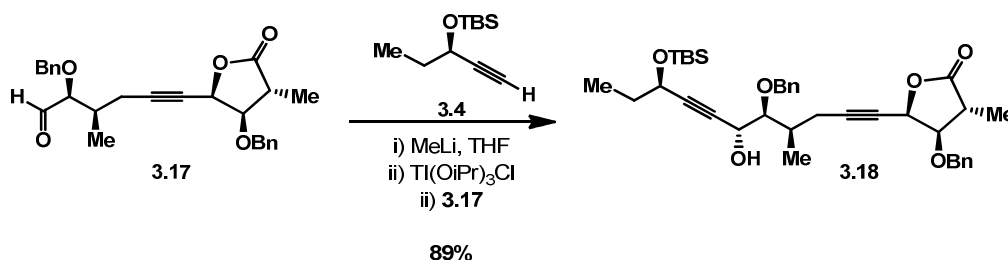


A stirring solution of alkyne **3.9** (2.04 g, 7.76 mmol) in diethyl ether (40 mL) was cooled to -78 °C and then n -BuLi (3.10 mL, 7.76 mmol) was added slowly. The reaction mixture was stirred at -78 °C for 1 hour and then a solution of ZnBr_2 (1.75 g, 7.76 mmol) in diethyl ether (20 mL) was added. The resulting milky white solution was stirred for 10 mins at -78 °C then warmed to 0 °C and then a solution of above aldehyde **3.3** (0.804 g, 2.1 mmol) in diethyl ether (15 mL) was added drop wise using a syringe pump for 2 hours. The solution was then stirred for another 4 hours then quenched with aqueous NH_4Cl (50 mL) at 0 °C, diluted with ethyl acetate (200 mL) and washed with water (2 x 50 mL). The organic layer was separated, dried over anhydrous Na_2SO_4 , and then concentrated under reduced pressure to give the crude product (8:1 ratio by ^1H NMR), which was purified by FCC using 10% ethyl acetate in hexane to afford major isomer of **3.16** as colorless oil (570 mg, 58% yield). $[\alpha]_{\text{D}}^{25} = +18.0$ ($c = 0.01$, CHCl_3); IR $\nu_{\text{max}}(\text{neat})/\text{cm}^{-1}$ 2935, 2238, 1786, 1454; ^1H NMR (500 MHz, CDCl_3) δ 7.38-7.24 (m, 10H), 5.12 (td, $J = 2.0$ Hz, 6.5 Hz, 1H), 4.82

(d, $J = 11.5$ Hz, 1H), 4.72 (d, $J = 12.0$ Hz, 1H), 4.53 (d, $J = 11.5$ Hz, 1H), 4.51 (d, $J = 11.5$ Hz, 1H), 4.35 (d, $J = 6.9$ Hz, 1H), 3.88 (dd, $J = 9.5, 6.5$ Hz, 1H), 3.57 (dd, $J = 10.0, 7.0$ Hz, 1H), 3.47 (s, 3H), 3.37 (s, 3H), 2.86-2.76 (m, 1H), 2.38-2.20 (m, 2H), 2.10-2.00 (m, 1H), 1.25 (d, $J = 7.0$ Hz, 3H), 0.99 (d, $J = 7.0$ Hz, 3H); ^{13}C NMR (125 MHz, CDCl_3) δ 176.0, 139.1, 137.1, 128.8 (2), 128.5 (2), 128.4, 128.1 (2), 127.9 (2), 127.7, 106.4, 90.5, 81.0, 80.5, 74.7, 73.9, 72.4, 70.5, 56.1, 54.1, 39.4, 34.4, 24.0, 14.0, 12.7; MS (ESI+) calculated for $[\text{C}_{28}\text{H}_{34}\text{O}_6 + \text{Na}]^+$: 489.3, found: 489.2.

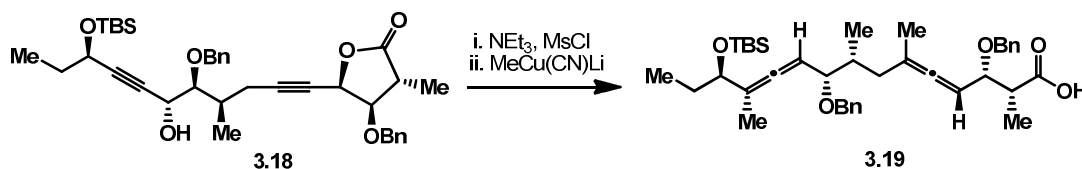


Alkyne **3.16** (280 mg, 0.600 mmol) was dissolved in 20 mL mixed solution of acetic acid, TFA and water (4:1:1) at room temperature and stirred for 14 hours. The acidic solvent was co-removed with toluene (5 x 100 mL) under reduced pressure to afford the crude product, which was taken on without further purification as described below. It could also be further purified by FCC using 12% ethyl acetate in hexane to afford **3.17** as colorless viscous oil (227 mg, 90% yield). $[\alpha]_{\text{D}}^{25} = +22.0$ ($c = 0.01$, CHCl_3); IR ν_{max} (neat)/ cm^{-1} 2935, 2240, 1786, 1730, 1455; ^1H NMR (500 MHz, CDCl_3) δ 9.65 (s, 1H), 7.4-7.25 (m, 10H), 5.11 (d, $J = 6$ Hz, 1H), 4.67 (d, $J = 13$ Hz, 2H), 4.54 (d, $J = 11.5$ Hz, 1H), 4.46 (d, $J = 12$ Hz, 1H), 3.95-3.85 (m, 2H), 2.85-2.75 (m, 1H), 2.48-2.26 (m, 2H), 2.26-2.16 (m, 1H), 1.27 (d, $J = 7.0$ Hz, 3H), 1.01 (d, $J = 6.5$ Hz, 3H); ^{13}C NMR (125 MHz, CDCl_3) δ 204.3, 175.9, 137.6, 137.1, 128.8 (2), 128.7 (2), 128.5, 128.3, 128.2 (2), 128.0 (2), 89.2, 85.1, 81.0, 74.9, 73.4, 72.4, 70.4, 39.4, 35.2, 23.1, 14.5, 12.7; MS (ESI+) calculated for $[\text{C}_{26}\text{H}_{28}\text{O}_5 + \text{Na}]^+$: 443.2, found: 443.2.

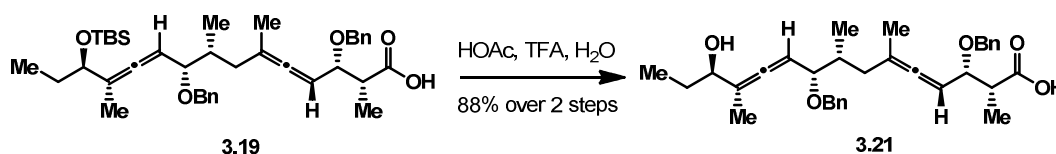


A solution of known alkyne **3.4** (594 mg, 3.00 mmol) (The description of preparation of compound **3.4** could be found in the supporting information of the following publication: Ghosh, P.; Lotesta, S. D.; Williams, L. J. *J. Am. Chem. Soc.* **2007**, *129*, 2438) in THF (25 mL) was cooled to $-78\text{ }^{\circ}\text{C}$ and then MeLi solution in diethyl ether (1.4 mL, 2.25 mmol) was added slowly. The reaction mixture was stirred for 1 hr and then a 1 M hexane solution of chlorotriisopropoxytitanium (IV) (3.00 mL, 3.00 mmol) was added. The solution was slowly warmed to $-40\text{ }^{\circ}\text{C}$ and then a solution of aldehyde **3.17** (315 g, 0.749 mmol) in THF (10 mL) was added slowly at $-40\text{ }^{\circ}\text{C}$. The mixture was warmed slowly to $-20\text{ }^{\circ}\text{C}$ over 2 hours, diluted with ethyl acetate (200 mL) and washed with water (50 mL). The organic layer was separated, dried over anhydrous Na_2SO_4 , and then concentrated under reduced pressure to give the crude product (6:1 ratio by ^1H NMR) which was purified by FCC using 10% ethyl acetate in hexane to afford major isomer of **3.18** as colorless oil (411 mg, 89% combined yield for both diastereomers). ^1H NMR (300 MHz, CDCl_3) δ 7.16 – 7.44 (m, 1H), 5.11 (td, $J = 2.1\text{ Hz}, 6.0\text{ Hz}$, 1H), 4.76 (d, $J = 12.0\text{ Hz}$, 1H), 4.72 (d, $J = 12.0\text{ Hz}$, 1H), 4.58 (d, $J = 12.0\text{ Hz}$, 1H), 4.53 ($J = 12.0\text{ Hz}$, 1H), 4.43–4.54 (m, 1H), 4.32 (t, $J = 6.6\text{ Hz}$, 1H), 3.87 (dd, $J = 9.6, 6.6\text{ Hz}$, 1H), 3.58 (dd, $J = 5.4, 5.4\text{ Hz}$, 1H), 2.88–2.76 (m, 1H), 2.46–2.13 (m, 1H), 1.75–1.60 (m, 1H), 1.24 (d, $J = 7.2\text{ Hz}$, 3H), 1.06 (d, $J = 6.9\text{ Hz}$, 3H), 0.87 (s, 9H), 0.08 (s, 3H), 0.10 (s, 3H); ^{13}C NMR (125 MHz, CDCl_3) δ 175.92, 138.48, 137.09, 128.84, 0.08 (s, 3H), 0.10 (s, 3H).

128.61, 128.50, 128.08, 127.93, 127.90, 89.79, 88.49, 83.51, 82.67, 80.97, 77.49, 77.23, 76.98, 74.60, 74.35, 72.38, 70.47, 64.43, 63.54, 39.40, 34.69, 31.93, 26.00, 23.80, 18.45, 14.99, 12.68, 9.89, 0.22, -4.28, -4.80. MS (ESI+) calculated for $[C_{37}H_{50}O_6Si+Na]^+$: 641.3, found: 641.3

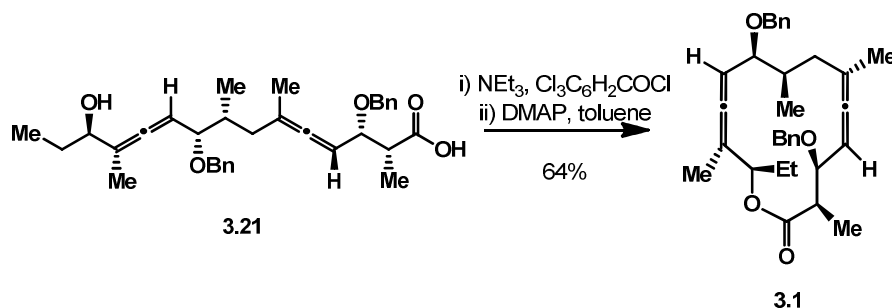


To a solution of **3.18** (1.53 g, 2.47 mmol) in 50 mL anhydrous diethyl ether was added Et₃N (377 mg, 3.71 mmol) and MsCl (424 mg, 3.71 mmol) respectively at 0 °C. The reaction mixture was warmed to room temperature and stirred for 1 hour at room temperature. The solution was then cooled to –20 °C and then a solution of methyl cyanocuprate was added, prepared from CuCN (1.32 g, 14.8 mmol) and MeLi (9.2 mL, 14.7 mmol) in 75 mL Et₂O at –20 °C. The reaction mixture was then warmed to room temperature and stirred for 2 h, quenched with aqueous NH₄Cl (50 mL), extracted in diethyl ether (3 x 100 mL) and washed with water (100 mL). The organic layer was separated, dried over anhydrous Na₂SO₄, and then concentrated under reduced pressure to give crude product **3.19** which was then taken on without further purification as described below.



The above bis-allenic acid **3.19** (1.39 g, 2.20 mmol) was dissolved in 80% acetic acid (50 mL) and stirred for 8 hours at room temperature. The solvent 80% acetic acid was

co-removed with toluene (3 x 50 mL) under reduced pressure and the resulting crude product was purified by FCC using 50% ethyl acetate in hexane to afford **3.21** as colorless oil (1.14 g, 88% yield). $[\alpha]_{\text{D}}^{25} = +45.0$ ($c = 0.01$, CHCl_3); IR $\nu_{\text{max}}(\text{neat})/\text{cm}^{-1}$ 3388, 2933, 1965, 1710, 1454; ^1H NMR (500 MHz, CDCl_3) δ 7.36-7.27 (m, 10H), 5.18-5.10 (m, 1H), 5.08-5.02 (m, 1H), 4.70 (d, $J = 11.5$ Hz, 1H), 4.68 (d, $J = 12.0$ Hz, 1H), 4.45 (d, $J = 11.5$ Hz, 1H), 4.41 (d, $J = 12.0$ Hz, 1H), 4.04 (dd, $J = 7.0, 7.0$ Hz, 1H), 3.99 (t, $J = 6.5$ Hz, 1H), 3.69 (dd, $J = 8.5, 5$ Hz, 1H), 2.84-2.76 (m, 1H), 2.38-2.32 (m, 1H), 1.94-1.84 (m, 1H), 1.75 (d, $J = 3$ Hz, 3H), 1.67 (d, $J = 2.5$ Hz, 3H), 1.66-1.50 (m, 2H), 1.23 (d, $J = 7$ Hz, 3H), 0.98 (d, $J = 6.5$ Hz, 3H), 0.90 (t, $J = 7$ Hz, 3H); ^{13}C NMR (125 MHz, CDCl_3) δ 203.6, 201.7, 175.7, 138.9, 137.7, 128.7 (2), 128.5 (2), 128.1, 128.1 (2), 127.8 (2), 127.7, 103.4, 100.6, 92.5, 88.0, 82.1, 79.3, 74.2, 70.7, 70.4, 44.4, 37.6, 37.0, 27.9, 19.4, 15.4, 15.1, 13.3, 9.8; MS (ESI+) calculated for $[\text{C}_{33}\text{H}_{42}\text{O}_5 + \text{Na}]^+$: 541.3, found: 541.3.



Seco acid **3.21** (280 mg, 0.540 mmol) was dissolved in 20 mL toluene, then triethylamine (273 mg, 2.7 mmol) and 2,4,6-trichlorobenzoyl chloride (658 mg, 2.7 mmol) was added at room temperature. The reaction mixture was then stirred for 6 hours at room temperature. The resulting solution was delivered dropwise by syringe pump over 2 hours into a solution of DMAP (659 mg, 5.40 mmol) in toluene (150 mL) at 80 °C. The mixture was then cooled to room temperature and quenched with aqueous NH_4Cl (100 mL). The organic layer was

separated, washed with water (2 x 100 mL), dried over anhydrous Na₂SO₄, and then concentrated under reduced pressure to give the crude product which upon FCC purification using 5% ethyl acetate in hexanes to afford bis-allenic macrolactone **3.1** (172 mg, 64% yield) as a colorless oil. IR ν_{max} (neat)/cm⁻¹ 2970, 1961, 1731, 1454, 1248; ¹H NMR (500 MHz, CDCl₃) δ 7.45 – 7.29 (m, 8H), 7.29 – 7.19 (m, 2H), 5.41 – 5.32 (m, 1H), 5.27 (t, J = 6.8 Hz, 1H), 5.19 – 5.07 (m, 1H), 4.66 (d, J = 11.7 Hz, 1H), 4.52 (dd, J = 27.5, 11.7 Hz, 2H), 4.35 (d, J = 11.8 Hz, 1H), 3.97 (dd, J = 8.4, 4.0 Hz, 1H), 3.75 (dd, J = 9.3, 5.8 Hz, 1H), 3.55 – 3.38 (m, 1H), 2.87 – 2.67 (m, 1H), 2.21 (dd, J = 5.3, 2.4 Hz, 1H), 2.18 (t, J = 3.9 Hz, 1H), 2.03 – 1.90 (m, 1H), 1.72 (dt, J = 5.6, 2.8 Hz, 4H), 1.70 – 1.65 (m, 1H), 1.65 – 1.49 (m, 3H), 1.38 – 1.24 (m, 4H), 1.22 (t, J = 7.0 Hz, 1H), 1.06 (d, J = 6.7 Hz, 3H), 0.90 (dd, J = 13.5, 5.5 Hz, 3H), 0.89 – 0.75 (m, 2H); ¹³C NMR (125 MHz, CDCl₃) δ 203.65, 201.41, 174.07, 139.32, 138.80, 128.51, 128.41, 127.98, 127.89, 127.71, 127.49, 102.62, 99.24, 91.99, 90.75, 81.84, 76.99, 75.69, 70.74, 68.93, 45.19, 37.91, 36.10, 25.15, 20.40, 15.49, 14.26, 9.85; MS (ESI+) calculated for [C₃₃H₄₀O₄+Na]⁺: 523.3, found: 523.3.

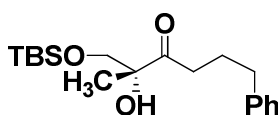
3. Chapter IV

General procedure for catalytic osmylation in acidic solution:

To a solution of the allene (1 equiv.) in *t*-BuOH and H₂O (1:1, 0.1 M) was added OsO₄ solution (4% wt. solution in water, 0.1 equiv.), stirred at rt. for 1 min. then acid (2 equiv.) was added in one portion, stirred at room temperature until the consumption of allene, then quenched with saturated sodium sulfite solution, extracted with ethyl acetate. The organic layer was combined, washed with NaCl solution, dried over Na₂SO₄, filtered and then concentrated to dryness under reduced pressure to give the crude product, which was further purified by FCC to afford the desired product as colorless oil.

Procedure for catalytic osmylation with phenyl boronic acid:

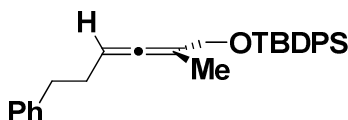
Known allene **4.13** (100 mg, 0.480 mmol) was dissolved in DCM (2.5 mL), then NMO (67.5 mg, 0.576 mmol), phenylboronic acid (70.2 mg, 0.576 mmol) and acetic acid (115 mg, 1.92 mmol) was added. A solution of OsO₄ (12.2 mg, 0.0480 mmol) in 1 mL DCM was added then, stirred at room temperature for 6 hours then quenched with saturated sodium sulfite solution. The mixture was extracted with ethyl acetate (2 x 10 mL), washed with water and then concentrated to dryness under reduced pressure to gave the crude product which was then purified by FCC using 2% ethyl acetate in hexane to afford the desired known product **4.14** as a light yellowish oil (82.0 mg, 0.338 mmol, 70.5%).



4.16

Known racemic allene **4.15** (100mg, 0.331 mmol) was converted to **4.16** using the general procedure for catalytic osmylation in acidic solution, 4-nitrobenzoic acid (163 mg, 1.00 mmol) was employed as the source of acid. FCC using 3% ethyl acetate in hexane afforded the desired racemic **S9** as colorless oil (50.1 mg, 0.149 mmol, 44%): IR ν_{max} (neat)/cm⁻¹ 3482, 2953, 2930, 2857, 1713, 1496, 1447, 1403, 1362, 1256, 1100, 1007; ¹H NMR (500 MHz, CDCl₃) δ 7.31 – 7.24 (m, 2H), 7.19 (t, J = 6.9 Hz, 3H), 3.84 (d, J = 10.1 Hz, 1H), 3.74 (s, 1H), 3.50 (d, J = 10.1 Hz, 1H), 2.74 – 2.65 (m, 1H), 2.65 – 2.59 (m, 2H), 2.57 (t, J = 7.2 Hz, 1H), 2.00 – 1.86 (m, 2H), 1.23 (s, 3H), 0.88 – 0.84 (m, 9H), 0.06 – 0.03 (m, 3H), 0.01 (d, J = 6.9 Hz, 3H); ¹³C NMR (126 MHz, CDCl₃) δ 214.05, 141.85, 128.60 (2), 126.15,

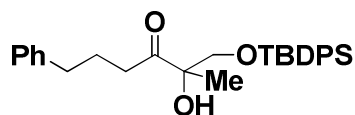
79.77, 69.38, 36.74, 35.35, 26.00, 25.97, 25.04, 21.35, 18.38, -5.32 (q); m/z (ESI-MS) calculated for $[C_{19}H_{32}O_3SiNa]^+$: 359.2, found: 359.2



4.17

Known racemic allene **4.16** (220 mg, 0.728 mmol) was converted to allene **4.17** via a two-step sequence: allene **4.16** was dissolved in 7 mL THF, then TBAF (1.8 mL, 1.0 M solution in THF, 1.8 mmol) was added at 0 °C, warmed to room temperature, stirred for 8 hours then quenched with saturated NH_4Cl solution. The mixture was extracted with ethyl acetate (2 x 10 mL), and the organic layer was combined, dried over Na_2SO_4 , filtered then concentrated to dryness under reduced pressure to give the crude intermediate. This crude intermediate was then dissolved in 7 mL DCM and to this mixture was added TBDPSCl (412 mg, 1.50 mmol) and imidazole (102 mg, 1.50 mmol), stirred at room temperature for 15 mins, and then quenched with saturated NH_4Cl solution. The mixture was extracted with DCM (2 x 5 mL), and the organic layer was combined, washed with saturated NaCl solution, dried over Na_2SO_4 , filtered and then concentrated to dryness under reduced pressure to give the crude product, which upon further purification by FCC using hexane to afford **4.17** as colorless oil (268 mg, 0.628 mmol, 86% over two steps): 1H NMR (500 MHz, $CDCl_3$) δ 7.85 – 7.74 (m, 4H), 7.54 – 7.40 (m, 6H), 7.36 – 7.28 (m, 2H), 7.27 – 7.18 (m, 3H), 5.35 – 5.06 (m, 1H), 4.25 – 4.11 (m, 2H), 2.84 – 2.69 (m, 2H), 2.42 – 2.28 (m, 2H), 1.84 – 1.66 (m, 3H), 1.17 (s, 9H); ^{13}C NMR (126 MHz, $CDCl_3$) δ 201.52, 142.21, 135.91,

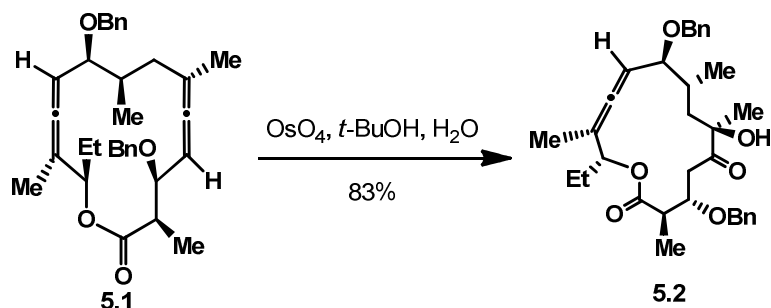
134.18, 129.89, 128.80, 128.52, 127.93, 126.04, 100.15, 91.04, 66.10, 35.78, 31.03, 27.16, 19.65, 16.11; m/z (ESI-MS) calculated for $[C_{29}H_{34}OSiNa]^+$: 449.2, found: 449.2



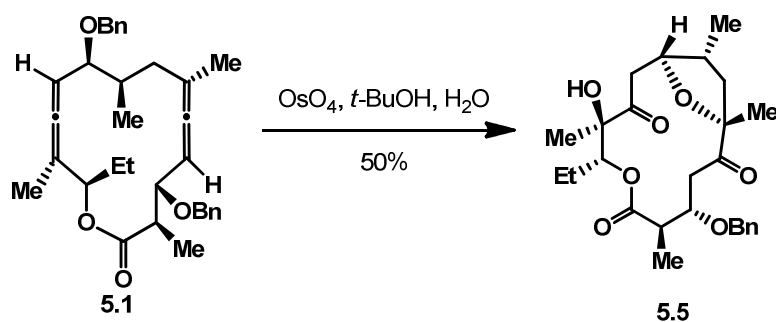
4.18

Racemic allene **4.17** (100mg, 0.234 mmol) was converted to **4.18** using the general procedure for catalytic osmylation in acidic solution, hydrochloric acid (0.120 mL, 1.0M solution in H₂O, 0.12 mmol) was employed as the source of acid. FCC using 3% ethyl acetate in hexane afforded the desired racemic product **S13** as colorless oil (76.2 mg, 0.165 mmol, 71%): IR ν_{\max} (neat)/cm⁻¹ 3482, 3070, 3026, 2931, 2858, 1713, 1496, 1472, 1455, 1428, 1362, 1112, 1009; ¹H NMR (500 MHz, CDCl₃) δ 7.70 – 7.55 (m, 4H), 7.49 – 7.42 (m, 2H), 7.43 – 7.34 (m, 4H), 7.33 – 7.24 (m, 2H), 7.24 – 7.15 (m, 3H), 3.91 (d, J = 10.1 Hz, 1H), 3.91 – 3.83 (bs, 1H), 3.66 – 3.55 (m, 1H), 2.74 – 2.53 (m, 4H), 2.09 – 1.90 (m, 2H), 1.22 (s, 3H), 1.05 – 1.01 (m, 9H); ¹³C NMR (126 MHz, CDCl₃) δ 213.45, 141.75, 135.87, 135.80, 135.74, 135.03, 133.05, 132.81, 130.14, 128.64, 128.63, 128.05, 126.20, 79.95, 69.90, 36.50, 35.39, 27.00, 25.09, 21.39, 19.47; m/z (ESI-MS) calculated for $[C_{29}H_{36}O_3SiNa]^+$: 483.2, found: 483.2

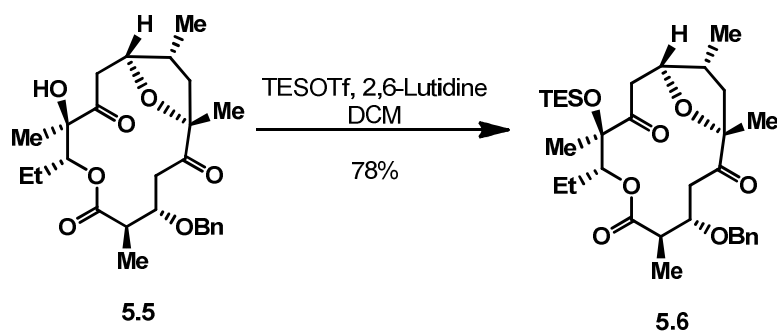
4. Chapter V



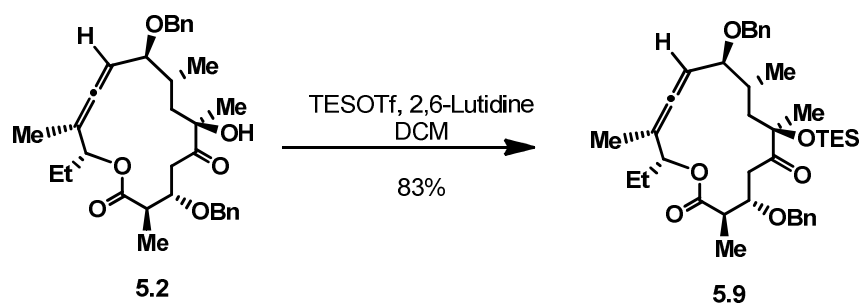
The macro lactone **5.1** (26 mg, 0.052mmol) was dissolved in 2 mL 1:1 mixture of $t\text{-BuOH}$ and water. To this solution was added OsO_4 (0.50 mL, 4% wt. water solution, 0.078mmol) at room temperature, stirred for 45 mins then quenched by 20 mL saturated sodium sulfite solution, extracted with diethyl ether (2 x 20 mL). The organic layer was separated, dried over Na_2SO_4 , and then concentrated under reduced pressure to give the crude product, which was purified by FCC using 10% ethyl acetate in hexane to afford the macro lactone **5.2** as a light yellowish oil (23 mg, 0.043 mmol, 83% yield): IR $\nu_{\text{max}}(\text{neat})/\text{cm}^{-1}$ 3475, 2930, 2872, 1966, 1739, 1496, 1455, 1370; ^1H NMR (500 MHz, CDCl_3) δ 7.26-7.38 (m, 10H), 5.15 (m, 1H), 4.94 (m, 1H), 4.74 (d, $J = 11.6$ Hz, 1H), 4.60 (d, $J = 12.2$ Hz, 1H), 4.56 (d, $J = 11.6$ Hz, 1H), 4.34 (d, $J = 12.2$ Hz, 1H), 4.15 (m, 1H), 3.44 (dd, $J = 6.8, 8.1$ Hz, 1H), 2.96 (dd, $J = 6.9, 17.7$ Hz, 1H), 2.93 (dd, $J = 3.8, 17.7$ Hz, 1H), 2.58 (m, 1H), 1.9 (dd, $J = 6.6, 15.1$ Hz, 1H), 1.79 (d, $J = 2.9$ Hz, 1H), 1.73 (m, 1H), 1.69 (m, 2H), 1.54 (dd, $J = 3.2, 15.1$ Hz, 1H), 1.32 (s, 3H), 1.30 (d, $J = 6.8$ Hz, 3H), 1.05 (d, $J = 6.8$ Hz, 3H), 0.90 (t, $J = 7.4$ Hz, 3H). ^{13}C NMR (126 MHz, CDCl_3) δ 212.1, 204.0, 173.8, 138.6, 138.4, 128.6, 128.5, 128.1, 127.9, 127.7, 126.1, 99.8, 96.7, 82.3, 78.9, 76.5, 76.0, 73.8, 70.0, 45.6, 43.0, 42.6, 34.2, 27.4, 25.3, 18.6, 15.5, 13.7, 9.6; MS (ESI $^{+}$) calculated for $[\text{C}_{33}\text{H}_{42}\text{O}_6 + \text{Na}]^{+}$: 557.3, found: 557.3.



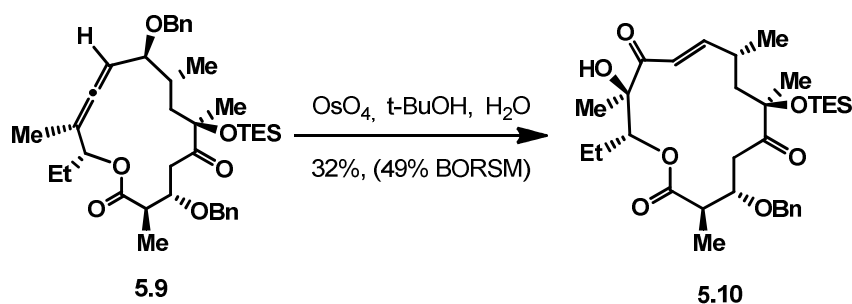
The macro lactone **5.1** (10 mg, 0.02 mmol) was dissolved in a 1:1 mixture solution of $t\text{-BuOH}$ and water (1 mL), then 0.28 ml OsO_4 solution (4% wt. in water) was added at room temperature, stirred for 4 hours then quenched with 15 ml saturated sodium sulfite solution, and then extracted with diethyl ether (2 x 20 mL). The organic layer was combined and dried over Na_2SO_4 then concentrated under reduced pressure to give a crude product, which was purified by FCC using 20% ethyl acetate and hexane to afford macro lactone **5.5** as a colorless oil: (4.4 mg, 0.0092 mmol, 46% yield) IR $\nu_{\text{max}}(\text{neat})/\text{cm}^{-1}$ 3477, 2971, 2934, 2878, 1735, 1711, 1455, 1382; ^1H NMR (600 MHz, CDCl_3) δ 7.35 – 7.30(m, 5H), 4.89 (dd, $J = 9.0, 3.4$ Hz, 1H), 4.63 (m, 1H), 4.57 (d, $J = 11.6$ Hz 1H), 4.59(d, $J = 11.6$ Hz 1H), 3.86 (m, $J = 11.1, 4.7$ Hz, 1H), 3.37 (dd, $J = 14.5, 6.4$ Hz, 1H), 3.08 (dd, $J = 18.7, 10.2$ Hz, 1H), 2.98 – 2.82 (m, 1H), 2.51 – 2.36 (m, 1H), 2.29 (dd, $J = 4.7, 14.5$ Hz, 1H), 1.97 (m, 1H), 1.89 (dd, $J = 12.9, 9.1$ Hz, 1H), 1.79 (dd, $J = 12.9, 7.3$ Hz, 1H), 1.55 (m, 1H), 1.38 (s, 3H), 1.27 (s, 3H), 1.21 (d, $J = 7.3$ Hz, 3H), 0.93 (t, $J = 7.5$ Hz, 3H), 0.67 (d, $J = 7.0$ Hz, 3H); ^{13}C NMR (150 MHz, CDCl_3) δ 213.3, 212.6, 173.2, 137.5, 128.8, 128.4, 128.0, 88.5, 78.9, 78.4, 77.8, 76.3, 72.0, 42.1, 40.5, 39.6, 35.4, 34.9, 25.2, 23.1, 17.0, 15.0, 14.2, 11.0; MS (ESI+) calculated for $[\text{C}_{26}\text{H}_{36}\text{O}_7 + \text{Na}]^+$: 483.3, found: 483.3.



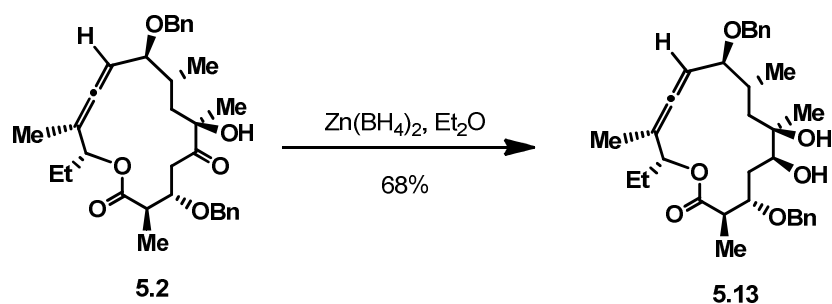
The keto-alcohol **5.5** (4.0 mg, 0.0082 mmol) was dissolved in 1.5 mL DCM then 2,6-lutidine (100 mg) and TESOTf (120 mg) was added respectively at room temperature, stirred at room temperature for 30 mins then quenched by 10mL saturated NH_4Cl solution. Organic layer was diluted with 10 mL DCM, separated then concentrated under reduced pressure to give the crude product, which was Further purified by FCC using 10% ethyl acetate in hexane to afford the product **5.6** as a colorless oil, which could be converted to a white crystalline by slow evaporation at room temperature in 1mL 30% ethyl acetate in hexane (4.0 mg, 78% yield): IR $\nu_{\text{max}}(\text{neat})/\text{cm}^{-1}$ 3444, 2954, 2928, 2875, 1738, 1716, 1456, 1378, 1183, 1164; ^1H NMR (600 MHz, CDCl_3) δ 7.33-7.30 (m, 5H), 5.2 (dd, J = 2.9, 9.5 Hz, 1H), 4.6 (d, J = 10.4 Hz, 1H), 4.48 (m, 1H), 4.44 (d, J = 10.4 Hz, 1H), 3.87 (m, 1H), 3.26 (dd, J = 9.6, 14.9 Hz, 1H), 2.92 (m, 1H), 2.78 (dd, J = 10.5, 19.0 Hz, 1H), 2.35 (dd, J = 1.5, 19.0 Hz, 1H), 2.24 (m, 1H), 2.17 (dd, J = 3.8, 14.9 Hz, 1H), 1.89 (m, 1H), 1.81 (dd, J = 11.4, 12.6 Hz, 1H), 1.73 (dd, J = 7.0, 12.6 Hz, 1H), 1.46 (m, 1H), 1.33 (s, 3H), 1.28 (s, 3H), 1.14 (d, J = 7.0 Hz, 3H), 0.91 (t, J = 7.2 Hz, 3H), 0.89 (dd, J = 7.8, 8.2 Hz, 9H), 0.68 (d, J = 6.9 Hz, 3H), 0.56-0.54 (m, 6H); ^{13}C NMR (150 MHz, CDCl_3) δ 215.5, 211.4, 172.9, 137.7, 129.1, 128.5, 128.3, 88.6, 79.6, 79.4, 78.1, 72.5, 41.6, 41.2, 39.8, 36.3, 35.0, 25.5, 22.7, 17.0, 14.8, 13.9, 11.1, 7.2, 6.4; MS (ESI+) calculated for $[\text{C}_{32}\text{H}_{50}\text{O}_7\text{Si}+\text{Na}]^+$: 597.3, found: 597.3.



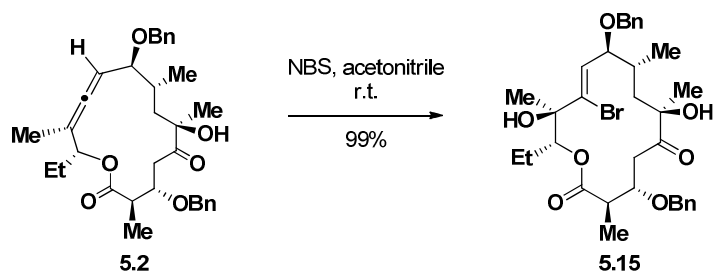
The macrolacton **5.2** (6.0 mg, 0.011 mmol) was dissolved in 1 mL DCM then 2,6-Lutidine and TESOTf was added respectively at room temperature, stirred for 20 mins at room temperature, and then quenched by addition of excess aqueous NH_4Cl solution. The organic layer was diluted with 10mL DCM, separated, and then concentrated under reduced pressure to give the crude product which was purified with FCC (3% ethyl acetate in hexane) to afford the product **5.9** as a colorless oil (6.0 mg, 0.0093mmol, 83% yield): IR $\nu_{\text{max}}(\text{neat})/\text{cm}^{-1}$ 2957, 2934, 2875, 1726, 1455, 1370, 1167, 1072; ^1H NMR (500 MHz, CDCl_3) δ 7.43 – 7.14 (m, 10H), 5.16 (dd, J = 6.2, 5.0 Hz, 1H), 5.04 – 4.90 (m, 1H), 4.60 (q, J = 11.0 Hz, 2H), 4.47 (d, J = 12.1 Hz, 1H), 4.22 (ddd, J = 19.7, 10.9, 5.9 Hz, 1H), 4.12 (d, J = 12.0 Hz, 1H), 4.05 (ddd, J = 8.3, 6.0, 4.3 Hz, 1H), 3.49 – 3.35 (m, 1H), 3.15 (dd, J = 16.9, 8.4 Hz, 1H), 2.88 – 2.82 (m, 1H), 2.82 – 2.75 (m, 1H), 1.91 (dt, J = 10.2, 4.7 Hz, 2H), 1.78 – 1.74 (m, 2H), 1.73 – 1.63 (m, 2H), 1.39 (s, 3H), 1.35 – 1.28 (m, 3H), 1.28 – 1.23 (m, 3H), 1.21 (d, J = 7.0 Hz, 3H), 1.07 (d, J = 6.7 Hz, 3H), 0.98 (dt, J = 6.4, 5.6 Hz, 6H), 0.72 – 0.60 (m, 6H), 0.57 – 0.47 (m, 3H). ^{13}C NMR (101 MHz, CDCl_3) δ 212.9, 204.1, 174.1, 139.2, 138.6, 128.4, 128.4, 128.3, 128.0, 127.8, 127.5, 98.9, 92.4, 83.2, 82.4, 77.7, 77.6, 77.4, 77.2, 76.9, 76.4, 72.9, 70.3, 45.3, 42.7, 41.6, 34.3, 26.9, 25.1, 18.1, 15.7, 13.1, 9.3, 7.5, 7.1, 1.2, 0.2; MS (ESI+) calculated for $[\text{C}_{39}\text{H}_{56}\text{O}_6\text{Si}+\text{Na}]^+$: 671.3, found: 671.3.



The protected ketoalcohol **5.9** (12.8 mg, 0.0200 mmol) was dissolved in 1 mL *t*-BuOH followed by the addition of citric acid (8.0 mg, 0.040 mmol) and the osmium tetroxide solution (0.13mL, 4% wt. in water). The resulting dark purple solution was then stirred at room temperature for 3 hours then the reaction was stopped by adding 10 mL saturated solution of sodium sulfite and extracted with 20 mL ethyl acetate. The organic layer was separated and then concentrated under reduced pressure to give a crude product which was purified by FCC using 10% ethyl acetate in hexane to afford product **5.10** as a colorless oil: (3.7 mg, 0.0064 mmol, 32% yield, 4.5 mg starting material recovered, 49% BORSM) IR $\nu_{\text{max}}(\text{neat})/\text{cm}^{-1}$ 3479, 2921, 2876, 2850, 1731, 1698, 1623, 1455, 1367; ^1H NMR (600 MHz, CDCl_3) δ 7.33-7.28 (m, 5H); 6.64 (d, J = 15.5 Hz, 1H), 6.60 (dd, J = 8.2, 15.5 Hz, 1H), 4.89 (dd, J = 2.5, 11.3 Hz, 1H), 4.56 (d, J = 11.6 Hz, 1H), 4.49 (d, J = 11.6 Hz, 1H), 3.68 (m, 1H), 3.60 (m, 1H), 3.42 (dd, J = 4.3, 18.8 Hz, 1H), 2.58 (m, 1H), 2.44 (dd, J = 3.4, 18.8 Hz, 1H), 2.29 (dd, J = 10.2, 14.3 Hz, 1H), 2.02 (m, 1H), 1.78 (m, 1H), 1.45 (dd, J = 2.1, 14.3 Hz, 1H), 1.31 (s, 3H), 1.23 (s, 3H), 1.21 (d, J = 7.0 Hz, 3H), 1.02 (d, J = 6.6 Hz, 3H), 1.01 (t, J = 7.9, 9H), 0.88 (t, J = 7.4 Hz, 3H), 0.66 (m, 6H); ^{13}C NMR (150 MHz, CDCl_3) δ 212.5, 202.7, 178.5, 154.9, 138.1, 128.6, 128.3, 128.0, 122.7, 84.4, 82.4, 80.8, 77.1, 46.3, 43.0, 37.6, 33.3, 28.3, 23.6, 23.0, 22.5, 16.0, 10.9, 7.5, 7.0; MS (ESI+) calculated for $[\text{C}_{32}\text{H}_{50}\text{O}_7\text{Si}+\text{Na}]^+$: 597.3, found: 597.3

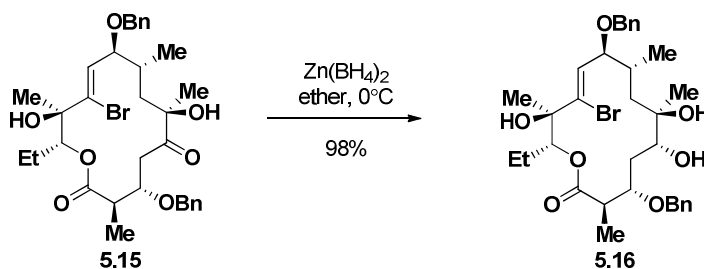


The hydroxyl ketone **5.2** (8.0 mg, 0.015 mmol) was dissolved in 1 mL anhydrous diethyl ether, cooled to 0 °C, then a 0.1 M solution of zinc borohydride (1 mL, 0.1 mmol) was added, stirred for 30mins then quenched with saturated NH_4Cl aqueous solution and extracted with ethyl acetate. The organic layer was dried over Na_2SO_4 , filtered and then concentrated under reduced pressure to give a crude product which was purified by FCC using 20% ethyl acetate in hexane to afford **5.13** as a colorless oil (5.4 mg, 0.010mmol, 68% yield) as product: IR ν_{max} (neat)/ cm^{-1} 3454, 2968, 2933, 2875, 1729, 1455, 1371, 1182, 1067; MS (ESI+) calculated for $[\text{C}_{33}\text{H}_{44}\text{O}_6+\text{Na}]^+$: 559.30, found: 559.30;

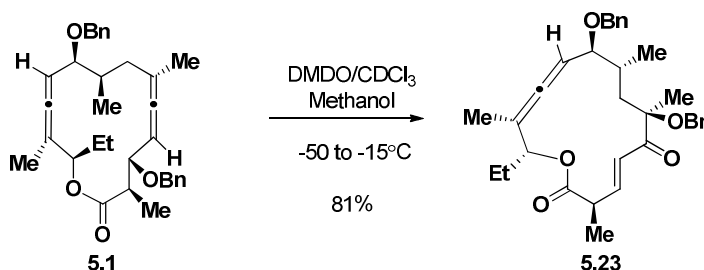


To a stirred solution of macrolactone **5.2** (7.8 mg, 0.015 mmol) in 1.0 mL of acetonitrile was added N-Bromosuccinimide (34 mg, 0.191 mmol) at room temperature then stirred for 5 mins. The reaction mixture was quenched with 1 mL of saturated aqueous solution of $\text{Na}_2\text{S}_2\text{O}_3$ and then extracted with diethyl ether (2 x 5 mL). The organic layer was separated and then concentrated under reduced pressure to give the crude product which was purified by FCC using 14% ethyl acetate in hexane to afford **5.15** as colorless oil: (9.10 mg, 99%

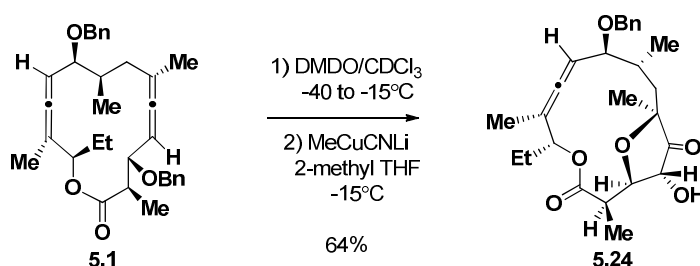
yield). For detailed NMR analysis, see page S32. IR ν_{max} (neat)/ cm^{-1} 3442, 3062, 2956, 2922, 2850, 1728, 1711, 1454, 1376, 1165, 1070; MS (ESI+) calculated for $[\text{C}_{33}\text{H}_{43}\text{BrO}_7+\text{Na}]^+$: 653.3, 655.3, found: 653.2, 655.2; $[\alpha]^{25}_{\text{D}} = 7.6^\circ$ ($c = 0.005$, CHCl_3).



To a stirred solution of macrocyclic lactone **5.15** (5.0 mg, $0.0079\ \mu\text{mol}$) in 1.00 mL of anhydrous diethyl ether was added 0.13 M $\text{Zn}(\text{BH}_4)_2$ solution in anhydrous diethyl ether (0.090 mL, 0.012 mmol) at 0°C . The mixture was stirred for 30 mins at 0°C , quenched with 1 mL of saturated aqueous solution of NH_4Cl , then extracted with diethyl ether (2 x 5 mL). The organic layer was separated, dried over Na_2SO_4 , filtered then concentrated under reduced pressure to give the crude product, which was purified by FCC 20% ethyl acetate in hexane to afford **5.16** (4.9 mg, 98% yield). For detailed NMR analysis, see page S34. IR ν_{max} (neat)/ cm^{-1} 2925, 2851, 1729, 1450, 1375, 1164, 1068; MS (ESI+) calculated for $[\text{C}_{33}\text{H}_{45}\text{O}_7+\text{Na}]^+$: 655.2, 657.2, found: 655.2, 657.2; $[\alpha]^{25}_{\text{D}} = 5.8^\circ$ ($c = 0.005$, CHCl_3).



To a solution of macrolactone **5.1** (12 mg, 0.020 mmol) in methanol (3.0 mL) was added a solution of DMDO (0.38 mL, 0.14 mmol) dropwise at $-50\text{ }^{\circ}\text{C}$. The solution was stirred under inert atmosphere and warmed to $-15\text{ }^{\circ}\text{C}$ over 1 hr 30min. The mixture was concentrated under reduced pressure to give the crude product, which was purified by FCC using 5% ethyl acetate in hexane to afford **5.23** (10 mg, 81%) as colorless oil. For detailed NMR analysis, see page S28. IR ν_{max} (neat)/ cm^{-1} 3442, 3062, 2956, 2922, 2850, 1728, 1711, 1454, 1376, 1165, 1070; MS (ESI+) calculated for $[\text{C}_{33}\text{H}_{40}\text{O}_5+\text{Na}]^+$: 539.3, found: 539.3; $[\alpha]^{25}_{\text{D}} = 3.3^{\circ}$ ($c = 0.005$, CHCl_3).

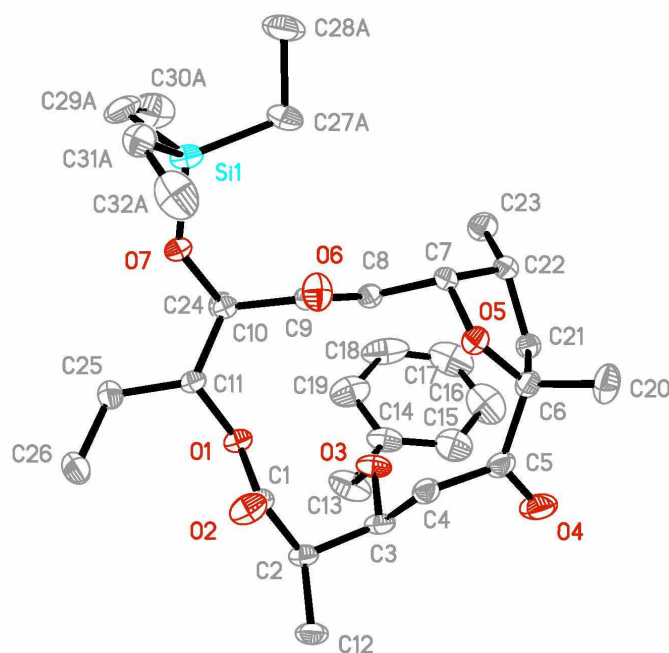


To a solution of macrolactone **5.1** (17.7 mg, 0.0340 mmol) in CDCl_3 (0.5 mL) was added a solution of DMDO (0.56 mL, 0.21 mmol) dropwise at $-40\text{ }^{\circ}\text{C}$, warmed up to $-15\text{ }^{\circ}\text{C}$ over 30min, then lower order methyl cyanocuprate (MeCuCNLi , 0.71 mmol) was added, prepared by addition of MeLi (0.44mL, 0.71 mmol) to a slurry of CuCN (63.30 mg, 0.71 mmol) in 2-methyl THF (5.99 mL) at -78°C and then warming to $-15\text{ }^{\circ}\text{C}$. The mixture was warmed to -2°C over 1 hr 30min, quenched with saturated aqueous solution of NH_4OH and NH_4Cl (1:4 ratio) and then extracted with diethyl ether. The combined organic layer was dried over anhydrous Na_2SO_4 , filtered and then concentrated under reduced pressure to give the crude product, which was purified by FCC using 15% ethyl acetate in hexane to afford **5.24** (10 mg, 64% yield) as a colorless oil. For detailed NMR analysis, see page S30.

IR ν_{max} (neat)/ cm^{-1} 3434, 2968, 2925, 1959, 1764, 1725, 1452, 1370, 1155; MS (ESI+)

calculated for $[\text{C}_{26}\text{H}_{34}\text{O}_6+\text{Na}]^+$: 465.2, found: 465.5; $[\alpha]^{25}_{\text{D}} = 5.9^\circ$ ($c = 0.005$, CHCl_3)

X-ray ORTEP diagram of compound **5.6**



Crystal data:

Table 1. Crystal data and structure refinement for KL-191.

Identification code	KL-191	
Empirical formula	$\text{C}_{32}\text{H}_{50.83}\text{O}_{7.415}\text{Si}$	
Formula weight	582.29	
Temperature	100(2) K	
Wavelength	0.71073 Å	
Crystal system	Monoclinic	
Space group	P2(1)	
Unit cell dimensions	$a = 8.6244(6)$ Å	$\alpha = 90^\circ$.

	$b = 16.3829(11) \text{ \AA}$	$\beta = 110.075(1)^\circ$.
	$c = 12.3896(8) \text{ \AA}$	$\gamma = 90^\circ$.
Volume	$1644.20(19) \text{ \AA}^3$	
Z	2	
Density (calculated)	1.176 Mg/m^3	
Absorption coefficient	0.116 mm^{-1}	
F(000)	632	
Crystal size	$0.32 \times 0.19 \times 0.08 \text{ mm}^3$	
Theta range for data collection	$1.75 \text{ to } 32.03^\circ$	
Index ranges	$-12 \leq h \leq 12, -24 \leq k \leq 24, -18 \leq l \leq 18$	
Reflections collected	21344	
Independent reflections	10801 [$R(\text{int}) = 0.0232$]	
Completeness to $\theta = 32.03^\circ$	99.4 %	
Absorption correction	Semi-empirical from equivalents	
Max. and min. transmission	0.9908 and 0.9639	
Refinement method	Full-matrix least-squares on F^2	
Data / restraints / parameters	10801 / 203 / 400	
Goodness-of-fit on F^2	1.011	
Final R indices [$I > 2\sigma(I)$]	$R1 = 0.0563, wR2 = 0.1340$	
R indices (all data)	$R1 = 0.0638, wR2 = 0.1392$	
Absolute structure parameter	-0.03(10)	
Largest diff. peak and hole	$0.565 \text{ and } -0.257 \text{ e.\AA}^{-3}$	

Table 2. Atomic coordinates ($\times 10^4$) and equivalent isotropic displacement parameters ($\text{\AA}^2 \times 10^3$) for KL-191. $U(\text{eq})$ is defined as one third of the trace of the orthogonalized U^{ij} tensor.

	x	y	z	$U(\text{eq})$
Si(1)	5320(1)	0(1)	-4244(1)	25(1)
O(1)	1438(2)	2254(1)	-3727(1)	20(1)
O(2)	2072(2)	3424(1)	-4443(1)	30(1)
O(3)	1824(2)	2622(1)	-1325(1)	27(1)
O(4)	4111(2)	3950(1)	410(1)	47(1)
O(5)	6462(2)	2679(1)	-787(1)	23(1)
O(6)	5595(2)	1874(1)	-3070(1)	31(1)
O(7)	3705(2)	591(1)	-4381(1)	26(1)
C(1)	1475(2)	3077(1)	-3830(1)	20(1)
C(2)	686(2)	3494(1)	-3056(2)	23(1)
C(3)	1781(2)	3421(1)	-1778(2)	23(1)
C(4)	3583(2)	3630(1)	-1562(1)	24(1)
C(5)	4554(3)	3579(1)	-279(2)	27(1)
C(6)	6115(2)	3054(1)	157(1)	23(1)
C(7)	6458(2)	1799(1)	-690(1)	20(1)
C(8)	4851(2)	1428(1)	-1479(1)	21(1)
C(9)	4626(2)	1506(1)	-2740(1)	21(1)
C(10)	3130(2)	1078(1)	-3652(1)	19(1)
C(11)	2115(2)	1762(1)	-4442(1)	19(1)
C(12)	326(3)	4387(1)	-3405(2)	28(1)
C(13)	339(3)	2341(2)	-1175(2)	42(1)
C(14)	837(2)	1792(1)	-145(2)	31(1)
C(15)	1625(3)	2113(2)	932(2)	43(1)
C(16)	2172(3)	1632(2)	1901(2)	54(1)
C(17)	1898(4)	820(2)	1811(3)	56(1)
C(18)	1106(3)	455(2)	768(3)	52(1)
C(19)	563(3)	952(2)	-247(3)	45(1)
C(20)	7581(3)	3593(1)	810(2)	37(1)
C(21)	5856(2)	2347(1)	888(1)	22(1)
C(22)	6826(2)	1653(1)	596(1)	23(1)
C(23)	6420(3)	806(1)	936(2)	33(1)

C(24)	2101(2)	554(1)	-3136(2)	24(1)
C(25)	705(2)	1456(1)	-5479(2)	26(1)
C(26)	-194(3)	2141(1)	-6287(2)	33(1)
C(27A)	6972(6)	2(4)	-2800(3)	36(1)
C(28A)	8277(10)	-669(7)	-2732(9)	47(1)
C(29A)	4480(12)	-1058(4)	-4630(6)	42(1)
C(30A)	3937(9)	-1481(4)	-3706(7)	56(1)
C(31A)	6070(6)	335(3)	-5440(4)	30(1)
C(32A)	6423(8)	1248(4)	-5420(6)	49(1)
C(27B)	6488(5)	-222(3)	-2695(2)	36(1)
C(28B)	7963(7)	-804(4)	-2524(6)	47(1)
C(29B)	4503(7)	-940(3)	-5054(5)	42(1)
C(30B)	3610(6)	-1507(3)	-4469(5)	56(1)
C(31B)	6796(4)	551(2)	-4806(3)	30(1)
C(32B)	5955(6)	936(3)	-5974(4)	49(1)
O(8W)	7099(5)	3673(3)	-2384(3)	42(1)

Table 3. Bond lengths [\AA] and angles [$^\circ$] for KL-191.

Si(1)-O(7)	1.6563(13)
Si(1)-C(29B)	1.841(5)
Si(1)-C(27A)	1.866(3)
Si(1)-C(27B)	1.872(3)
Si(1)-C(29A)	1.876(6)
Si(1)-C(31B)	1.878(3)
Si(1)-C(31A)	1.890(4)
O(1)-C(1)	1.355(2)
O(1)-C(11)	1.4596(18)
O(2)-C(1)	1.198(2)
O(3)-C(3)	1.420(2)
O(3)-C(13)	1.431(2)
O(4)-C(5)	1.212(2)
O(5)-C(6)	1.441(2)
O(5)-C(7)	1.446(2)
O(6)-C(9)	1.210(2)
O(7)-C(10)	1.4170(19)
C(1)-C(2)	1.517(2)
C(2)-C(12)	1.528(2)
C(2)-C(3)	1.545(2)
C(2)-H(2)	1.0000
C(3)-C(4)	1.523(3)
C(3)-H(3)	1.0000
C(4)-C(5)	1.523(2)
C(4)-H(4A)	0.9900
C(4)-H(4B)	0.9900
C(5)-C(6)	1.531(3)
C(6)-C(20)	1.527(3)
C(6)-C(21)	1.534(2)
C(7)-C(8)	1.522(2)
C(7)-C(22)	1.534(2)
C(7)-H(7)	1.0000
C(8)-C(9)	1.512(2)
C(8)-H(8A)	0.9900
C(8)-H(8B)	0.9900

C(9)-C(10)	1.559(2)
C(10)-C(24)	1.523(2)
C(10)-C(11)	1.547(2)
C(11)-C(25)	1.520(2)
C(11)-H(11)	1.0000
C(12)-H(12A)	0.9800
C(12)-H(12B)	0.9800
C(12)-H(12C)	0.9800
C(13)-C(14)	1.499(3)
C(13)-H(13A)	0.9900
C(13)-H(13B)	0.9900
C(14)-C(15)	1.378(3)
C(14)-C(19)	1.394(3)
C(15)-C(16)	1.377(4)
C(15)-H(15)	0.9500
C(16)-C(17)	1.349(5)
C(16)-H(16)	0.9500
C(17)-C(18)	1.374(5)
C(17)-H(17)	0.9500
C(18)-C(19)	1.435(4)
C(18)-H(18)	0.9500
C(19)-H(19)	0.9500
C(20)-H(20A)	0.9800
C(20)-H(20B)	0.9800
C(20)-H(20C)	0.9800
C(21)-C(22)	1.526(2)
C(21)-H(21A)	0.9900
C(21)-H(21B)	0.9900
C(22)-C(23)	1.526(3)
C(22)-H(22)	1.0000
C(23)-H(23A)	0.9800
C(23)-H(23B)	0.9800
C(23)-H(23C)	0.9800
C(24)-H(24A)	0.9800
C(24)-H(24B)	0.9800
C(24)-H(24C)	0.9800

C(25)-C(26)	1.527(3)
C(25)-H(25A)	0.9900
C(25)-H(25B)	0.9900
C(26)-H(26A)	0.9800
C(26)-H(26B)	0.9800
C(26)-H(26C)	0.9800
C(27A)-C(28A)	1.554(7)
C(27A)-H(27A)	0.9900
C(27A)-H(27B)	0.9900
C(28A)-H(28A)	0.9800
C(28A)-H(28B)	0.9800
C(28A)-H(28C)	0.9800
C(29A)-C(30A)	1.543(7)
C(29A)-H(29A)	0.9900
C(29A)-H(29B)	0.9900
C(30A)-H(30A)	0.9800
C(30A)-H(30B)	0.9800
C(30A)-H(30C)	0.9800
C(31A)-C(32A)	1.525(7)
C(31A)-H(31A)	0.9900
C(31A)-H(31B)	0.9900
C(32A)-H(32A)	0.9800
C(32A)-H(32B)	0.9800
C(32A)-H(32C)	0.9800
C(27B)-C(28B)	1.545(5)
C(27B)-H(27C)	0.9900
C(27B)-H(27D)	0.9900
C(28B)-H(28D)	0.9800
C(28B)-H(28E)	0.9800
C(28B)-H(28F)	0.9800
C(29B)-C(30B)	1.538(6)
C(29B)-H(29C)	0.9900
C(29B)-H(29D)	0.9900
C(30B)-H(30D)	0.9800
C(30B)-H(30E)	0.9800
C(30B)-H(30F)	0.9800

C(31B)-C(32B)	1.516(5)
C(31B)-H(31C)	0.9900
C(31B)-H(31D)	0.9900
C(32B)-H(32D)	0.9800
C(32B)-H(32E)	0.9800
C(32B)-H(32F)	0.9800
O(8W)-H(81)	0.840(10)
O(8W)-H(82)	0.843(10)
O(7)-Si(1)-C(27A)	115.81(19)
O(7)-Si(1)-C(29A)	106.0(3)
O(7)-Si(1)-C(31A)	104.62(16)
O(7)-Si(1)-C(27B)	110.84(13)
O(7)-Si(1)-C(29B)	106.4(2)
O(7)-Si(1)-C(31B)	109.56(12)
C(27A)-Si(1)-C(29A)	110.3(3)
C(27A)-Si(1)-C(31A)	113.4(3)
C(29A)-Si(1)-C(31A)	105.9(3)
C(27B)-Si(1)-C(29B)	111.5(2)
C(27B)-Si(1)-C(31B)	106.17(18)
C(29B)-Si(1)-C(31B)	112.44(19)
C(1)-O(1)-C(11)	117.63(12)
C(3)-O(3)-C(13)	116.38(15)
C(6)-O(5)-C(7)	110.55(12)
C(10)-O(7)-Si(1)	136.94(11)
O(2)-C(1)-O(1)	124.23(15)
O(2)-C(1)-C(2)	124.86(15)
O(1)-C(1)-C(2)	110.91(14)
C(1)-C(2)-C(12)	110.09(14)
C(1)-C(2)-C(3)	111.39(13)
C(12)-C(2)-C(3)	110.92(15)
C(1)-C(2)-H(2)	108.1
C(12)-C(2)-H(2)	108.1
C(3)-C(2)-H(2)	108.1
O(3)-C(3)-C(4)	104.56(13)
O(3)-C(3)-C(2)	113.56(15)
C(4)-C(3)-C(2)	113.01(14)

O(3)-C(3)-H(3)	108.5
C(4)-C(3)-H(3)	108.5
C(2)-C(3)-H(3)	108.5
C(5)-C(4)-C(3)	109.47(15)
C(5)-C(4)-H(4A)	109.8
C(3)-C(4)-H(4A)	109.8
C(5)-C(4)-H(4B)	109.8
C(3)-C(4)-H(4B)	109.8
H(4A)-C(4)-H(4B)	108.2
O(4)-C(5)-C(4)	120.91(17)
O(4)-C(5)-C(6)	119.00(16)
C(4)-C(5)-C(6)	120.09(15)
O(5)-C(6)-C(20)	108.16(15)
O(5)-C(6)-C(5)	110.85(14)
C(20)-C(6)-C(5)	109.29(15)
O(5)-C(6)-C(21)	105.66(13)
C(20)-C(6)-C(21)	112.68(15)
C(5)-C(6)-C(21)	110.14(14)
O(5)-C(7)-C(8)	111.91(13)
O(5)-C(7)-C(22)	103.66(13)
C(8)-C(7)-C(22)	115.02(14)
O(5)-C(7)-H(7)	108.7
C(8)-C(7)-H(7)	108.7
C(22)-C(7)-H(7)	108.7
C(9)-C(8)-C(7)	113.26(14)
C(9)-C(8)-H(8A)	108.9
C(7)-C(8)-H(8A)	108.9
C(9)-C(8)-H(8B)	108.9
C(7)-C(8)-H(8B)	108.9
H(8A)-C(8)-H(8B)	107.7
O(6)-C(9)-C(8)	122.19(15)
O(6)-C(9)-C(10)	118.36(15)
C(8)-C(9)-C(10)	119.42(14)
O(7)-C(10)-C(24)	109.36(14)
O(7)-C(10)-C(11)	104.54(12)
C(24)-C(10)-C(11)	112.89(13)

O(7)-C(10)-C(9)	109.34(13)
C(24)-C(10)-C(9)	113.92(13)
C(11)-C(10)-C(9)	106.31(13)
O(1)-C(11)-C(25)	108.97(13)
O(1)-C(11)-C(10)	105.85(12)
C(25)-C(11)-C(10)	114.20(13)
O(1)-C(11)-H(11)	109.2
C(25)-C(11)-H(11)	109.2
C(10)-C(11)-H(11)	109.2
C(2)-C(12)-H(12A)	109.5
C(2)-C(12)-H(12B)	109.5
H(12A)-C(12)-H(12B)	109.5
C(2)-C(12)-H(12C)	109.5
H(12A)-C(12)-H(12C)	109.5
H(12B)-C(12)-H(12C)	109.5
O(3)-C(13)-C(14)	107.21(17)
O(3)-C(13)-H(13A)	110.3
C(14)-C(13)-H(13A)	110.3
O(3)-C(13)-H(13B)	110.3
C(14)-C(13)-H(13B)	110.3
H(13A)-C(13)-H(13B)	108.5
C(15)-C(14)-C(19)	118.5(2)
C(15)-C(14)-C(13)	119.8(2)
C(19)-C(14)-C(13)	121.7(2)
C(16)-C(15)-C(14)	122.2(3)
C(16)-C(15)-H(15)	118.9
C(14)-C(15)-H(15)	118.9
C(17)-C(16)-C(15)	119.6(3)
C(17)-C(16)-H(16)	120.2
C(15)-C(16)-H(16)	120.2
C(16)-C(17)-C(18)	121.6(3)
C(16)-C(17)-H(17)	119.2
C(18)-C(17)-H(17)	119.2
C(17)-C(18)-C(19)	119.0(2)
C(17)-C(18)-H(18)	120.5
C(19)-C(18)-H(18)	120.5

C(14)-C(19)-C(18)	119.1(3)
C(14)-C(19)-H(19)	120.5
C(18)-C(19)-H(19)	120.5
C(6)-C(20)-H(20A)	109.5
C(6)-C(20)-H(20B)	109.5
H(20A)-C(20)-H(20B)	109.5
C(6)-C(20)-H(20C)	109.5
H(20A)-C(20)-H(20C)	109.5
H(20B)-C(20)-H(20C)	109.5
C(22)-C(21)-C(6)	102.71(13)
C(22)-C(21)-H(21A)	111.2
C(6)-C(21)-H(21A)	111.2
C(22)-C(21)-H(21B)	111.2
C(6)-C(21)-H(21B)	111.2
H(21A)-C(21)-H(21B)	109.1
C(23)-C(22)-C(21)	114.56(16)
C(23)-C(22)-C(7)	116.35(15)
C(21)-C(22)-C(7)	101.25(13)
C(23)-C(22)-H(22)	108.1
C(21)-C(22)-H(22)	108.1
C(7)-C(22)-H(22)	108.1
C(22)-C(23)-H(23A)	109.5
C(22)-C(23)-H(23B)	109.5
H(23A)-C(23)-H(23B)	109.5
C(22)-C(23)-H(23C)	109.5
H(23A)-C(23)-H(23C)	109.5
H(23B)-C(23)-H(23C)	109.5
C(10)-C(24)-H(24A)	109.5
C(10)-C(24)-H(24B)	109.5
H(24A)-C(24)-H(24B)	109.5
C(10)-C(24)-H(24C)	109.5
H(24A)-C(24)-H(24C)	109.5
H(24B)-C(24)-H(24C)	109.5
C(11)-C(25)-C(26)	112.95(15)
C(11)-C(25)-H(25A)	109.0
C(26)-C(25)-H(25A)	109.0

C(11)-C(25)-H(25B)	109.0
C(26)-C(25)-H(25B)	109.0
H(25A)-C(25)-H(25B)	107.8
C(25)-C(26)-H(26A)	109.5
C(25)-C(26)-H(26B)	109.5
H(26A)-C(26)-H(26B)	109.5
C(25)-C(26)-H(26C)	109.5
H(26A)-C(26)-H(26C)	109.5
H(26B)-C(26)-H(26C)	109.5
C(28A)-C(27A)-Si(1)	110.5(5)
C(28A)-C(27A)-H(27A)	109.5
Si(1)-C(27A)-H(27A)	109.5
C(28A)-C(27A)-H(27B)	109.5
Si(1)-C(27A)-H(27B)	109.5
H(27A)-C(27A)-H(27B)	108.1
C(27A)-C(28A)-H(28A)	109.5
C(27A)-C(28A)-H(28B)	109.5
H(28A)-C(28A)-H(28B)	109.5
C(27A)-C(28A)-H(28C)	109.5
H(28A)-C(28A)-H(28C)	109.5
H(28B)-C(28A)-H(28C)	109.5
C(30A)-C(29A)-Si(1)	114.5(4)
C(30A)-C(29A)-H(29A)	108.6
Si(1)-C(29A)-H(29A)	108.6
C(30A)-C(29A)-H(29B)	108.6
Si(1)-C(29A)-H(29B)	108.6
H(29A)-C(29A)-H(29B)	107.6
C(29A)-C(30A)-H(30A)	109.5
C(29A)-C(30A)-H(30B)	109.5
H(30A)-C(30A)-H(30B)	109.5
C(29A)-C(30A)-H(30C)	109.5
H(30A)-C(30A)-H(30C)	109.5
H(30B)-C(30A)-H(30C)	109.5
C(32A)-C(31A)-Si(1)	113.1(4)
C(32A)-C(31A)-H(31A)	109.0
Si(1)-C(31A)-H(31A)	109.0

C(32A)-C(31A)-H(31B)	109.0
Si(1)-C(31A)-H(31B)	109.0
H(31A)-C(31A)-H(31B)	107.8
C(31A)-C(32A)-H(32A)	109.5
C(31A)-C(32A)-H(32B)	109.5
H(32A)-C(32A)-H(32B)	109.5
C(31A)-C(32A)-H(32C)	109.5
H(32A)-C(32A)-H(32C)	109.5
H(32B)-C(32A)-H(32C)	109.5
C(28B)-C(27B)-Si(1)	112.9(3)
C(28B)-C(27B)-H(27C)	109.0
Si(1)-C(27B)-H(27C)	109.0
C(28B)-C(27B)-H(27D)	109.0
Si(1)-C(27B)-H(27D)	109.0
H(27C)-C(27B)-H(27D)	107.8
C(27B)-C(28B)-H(28D)	109.5
C(27B)-C(28B)-H(28E)	109.5
H(28D)-C(28B)-H(28E)	109.5
C(27B)-C(28B)-H(28F)	109.5
H(28D)-C(28B)-H(28F)	109.5
H(28E)-C(28B)-H(28F)	109.5
C(30B)-C(29B)-Si(1)	114.1(3)
C(30B)-C(29B)-H(29C)	108.7
Si(1)-C(29B)-H(29C)	108.7
C(30B)-C(29B)-H(29D)	108.7
Si(1)-C(29B)-H(29D)	108.7
H(29C)-C(29B)-H(29D)	107.6
C(29B)-C(30B)-H(30D)	109.5
C(29B)-C(30B)-H(30E)	109.5
H(30D)-C(30B)-H(30E)	109.5
C(29B)-C(30B)-H(30F)	109.5
H(30D)-C(30B)-H(30F)	109.5
H(30E)-C(30B)-H(30F)	109.5
C(32B)-C(31B)-Si(1)	113.0(3)
C(32B)-C(31B)-H(31C)	109.0
Si(1)-C(31B)-H(31C)	109.0

C(32B)-C(31B)-H(31D)	109.0
Si(1)-C(31B)-H(31D)	109.0
H(31C)-C(31B)-H(31D)	107.8
C(31B)-C(32B)-H(32D)	109.5
C(31B)-C(32B)-H(32E)	109.5
H(32D)-C(32B)-H(32E)	109.5
C(31B)-C(32B)-H(32F)	109.5
H(32D)-C(32B)-H(32F)	109.5
H(32E)-C(32B)-H(32F)	109.5
H(81)-O(8W)-H(82)	110.1(18)

Table 4. Anisotropic displacement parameters ($\text{\AA}^2 \times 10^3$) for KL-191. The anisotropic displacement factor exponent takes the form: $-2\pi^2 [h^2 a^{*2} U^{11} + \dots + 2 h k a^* b^* U^{12}]$

	U^{11}	U^{22}	U^{33}	U^{23}	U^{13}	U^{12}
Si(1)	27(1)	20(1)	32(1)	2(1)	16(1)	4(1)
O(1)	24(1)	17(1)	24(1)	1(1)	13(1)	2(1)
O(2)	40(1)	22(1)	38(1)	0(1)	24(1)	-2(1)
O(3)	27(1)	24(1)	35(1)	12(1)	18(1)	8(1)
O(4)	71(1)	40(1)	27(1)	0(1)	13(1)	31(1)
O(5)	26(1)	22(1)	22(1)	-1(1)	9(1)	-1(1)
O(6)	29(1)	38(1)	28(1)	-2(1)	11(1)	-9(1)
O(7)	26(1)	27(1)	24(1)	-5(1)	8(1)	8(1)
C(1)	21(1)	19(1)	22(1)	0(1)	8(1)	2(1)
C(2)	24(1)	20(1)	27(1)	1(1)	12(1)	7(1)
C(3)	29(1)	19(1)	25(1)	4(1)	14(1)	10(1)
C(4)	32(1)	18(1)	22(1)	1(1)	9(1)	2(1)
C(5)	40(1)	18(1)	23(1)	1(1)	9(1)	5(1)
C(6)	28(1)	20(1)	20(1)	-2(1)	7(1)	-1(1)
C(7)	18(1)	22(1)	20(1)	-1(1)	4(1)	3(1)
C(8)	20(1)	23(1)	20(1)	-2(1)	8(1)	2(1)
C(9)	20(1)	21(1)	22(1)	-1(1)	6(1)	4(1)
C(10)	20(1)	18(1)	20(1)	-2(1)	7(1)	2(1)
C(11)	21(1)	16(1)	21(1)	0(1)	9(1)	2(1)
C(12)	35(1)	21(1)	29(1)	6(1)	10(1)	12(1)
C(13)	28(1)	50(1)	54(1)	24(1)	21(1)	7(1)

C(14)	27(1)	33(1)	43(1)	13(1)	23(1)	8(1)
C(15)	35(1)	51(1)	49(1)	5(1)	24(1)	2(1)
C(16)	44(1)	79(2)	47(1)	14(1)	25(1)	-2(1)
C(17)	45(1)	71(2)	63(2)	29(2)	32(1)	11(1)
C(18)	53(2)	30(1)	95(2)	15(1)	52(2)	8(1)
C(19)	41(1)	40(1)	67(2)	0(1)	35(1)	-1(1)
C(20)	44(1)	31(1)	31(1)	-6(1)	7(1)	-14(1)
C(21)	26(1)	23(1)	17(1)	1(1)	6(1)	4(1)
C(22)	23(1)	24(1)	21(1)	0(1)	4(1)	5(1)
C(23)	46(1)	22(1)	28(1)	5(1)	7(1)	6(1)
C(24)	27(1)	20(1)	25(1)	1(1)	8(1)	-3(1)
C(25)	26(1)	25(1)	23(1)	-2(1)	3(1)	0(1)
C(26)	33(1)	33(1)	26(1)	2(1)	1(1)	2(1)
C(27A)	21(2)	41(2)	44(1)	0(1)	8(1)	11(1)
C(28A)	36(2)	52(3)	53(3)	6(2)	15(2)	23(2)
C(29A)	35(1)	32(2)	59(3)	-19(2)	19(2)	3(1)
C(30A)	45(2)	31(1)	87(3)	0(2)	19(2)	-6(1)
C(31A)	32(1)	36(1)	27(1)	3(1)	15(1)	2(1)
C(32A)	44(2)	66(2)	40(2)	15(2)	19(2)	-5(2)
C(27B)	21(2)	41(2)	44(1)	0(1)	8(1)	11(1)
C(28B)	36(2)	52(3)	53(3)	6(2)	15(2)	23(2)
C(29B)	35(1)	32(2)	59(3)	-19(2)	19(2)	3(1)
C(30B)	45(2)	31(1)	87(3)	0(2)	19(2)	-6(1)
C(31B)	32(1)	36(1)	27(1)	3(1)	15(1)	2(1)
C(32B)	44(2)	66(2)	40(2)	15(2)	19(2)	-5(2)
O(8W)	48(2)	44(2)	39(2)	8(2)	21(2)	-5(2)

Table 5. Hydrogen coordinates ($\times 10^4$) and isotropic displacement parameters ($\text{\AA}^2 \times 10^{-3}$) for KL-191.

	x	y	z	U(eq)
H(2)	-389	3216	-3160	27
H(3)	1347	3803	-1320	28
H(4A)	4049	3244	-1984	29
H(4B)	3666	4189	-1843	29
H(7)	7391	1574	-905	25
H(8A)	4825	842	-1288	25
H(8B)	3914	1699	-1336	25
H(11)	2868	2108	-4710	23
H(12A)	-432	4417	-4201	43
H(12B)	1359	4666	-3340	43
H(12C)	-180	4652	-2898	43
H(13A)	-348	2038	-1866	50
H(13B)	-308	2809	-1053	50
H(15)	1798	2686	1009	51
H(16)	2739	1871	2629	65
H(17)	2262	493	2485	68
H(18)	920	-117	720	63
H(19)	25	712	-978	54
H(20A)	7807	3977	275	55
H(20B)	8555	3251	1166	55
H(20C)	7323	3898	1408	55
H(21A)	6302	2481	1717	26
H(21B)	4672	2206	673	26
H(22)	8028	1757	1006	28
H(23A)	6964	391	620	50
H(23B)	5223	721	631	50
H(23C)	6813	761	1776	50
H(24A)	2802	133	-2645	36
H(24B)	1204	295	-3755	36
H(24C)	1635	899	-2677	36

H(25A)	-95	1159	-5210	31
H(25B)	1146	1064	-5909	31
H(26A)	598	2449	-6536	49
H(26B)	-712	2507	-5884	49
H(26C)	-1045	1906	-6960	49
H(27A)	7516	543	-2653	44
H(27B)	6475	-99	-2200	44
H(28A)	9055	-707	-1943	70
H(28B)	8879	-527	-3249	70
H(28C)	7722	-1195	-2963	70
H(29A)	3522	-1031	-5354	50
H(29B)	5336	-1398	-4777	50
H(30A)	3511	-2027	-3973	83
H(30B)	3069	-1157	-3567	83
H(30C)	4884	-1527	-2992	83
H(31A)	7090	31	-5376	36
H(31B)	5225	193	-6188	36
H(32A)	6817	1385	-6051	73
H(32B)	7269	1393	-4686	73
H(32C)	5409	1553	-5510	73
H(27C)	6901	298	-2290	44
H(27D)	5727	-469	-2343	44
H(28D)	8544	-889	-1700	70
H(28E)	8721	-564	-2870	70
H(28F)	7558	-1329	-2892	70
H(29C)	3726	-789	-5823	50
H(29D)	5428	-1244	-5166	50
H(30D)	3196	-1988	-4952	83
H(30E)	2682	-1215	-4362	83
H(30F)	4381	-1680	-3719	83
H(31C)	7367	982	-4252	36
H(31D)	7643	161	-4861	36
H(32D)	6780	1215	-6222	73
H(32E)	5130	1331	-5923	73
H(32F)	5412	511	-6532	73
H(81)	6940(90)	3360(40)	-1900(40)	63

H(82)	6590(90)	3500(40)	-3050(20)	63
-------	----------	----------	-----------	----

Table 6. Torsion angles [°] for KL-191.

C(29B)-Si(1)-O(7)-C(10)	134.6(2)
C(27A)-Si(1)-O(7)-C(10)	-6.2(3)
C(27B)-Si(1)-O(7)-C(10)	13.3(2)
C(29A)-Si(1)-O(7)-C(10)	116.5(3)
C(31B)-Si(1)-O(7)-C(10)	-103.6(2)
C(31A)-Si(1)-O(7)-C(10)	-131.8(2)
C(11)-O(1)-C(1)-O(2)	-2.4(2)
C(11)-O(1)-C(1)-C(2)	178.44(13)
O(2)-C(1)-C(2)-C(12)	15.7(2)
O(1)-C(1)-C(2)-C(12)	-165.14(15)
O(2)-C(1)-C(2)-C(3)	-107.8(2)
O(1)-C(1)-C(2)-C(3)	71.39(18)
C(13)-O(3)-C(3)-C(4)	166.30(17)
C(13)-O(3)-C(3)-C(2)	-70.1(2)
C(1)-C(2)-C(3)-O(3)	-71.76(18)
C(12)-C(2)-C(3)-O(3)	165.24(14)
C(1)-C(2)-C(3)-C(4)	47.13(19)
C(12)-C(2)-C(3)-C(4)	-75.87(17)
O(3)-C(3)-C(4)-C(5)	-58.42(17)
C(2)-C(3)-C(4)-C(5)	177.59(14)
C(3)-C(4)-C(5)-O(4)	-53.2(2)
C(3)-C(4)-C(5)-C(6)	126.84(17)
C(7)-O(5)-C(6)-C(20)	120.24(15)
C(7)-O(5)-C(6)-C(5)	-119.96(14)
C(7)-O(5)-C(6)-C(21)	-0.65(17)
O(4)-C(5)-C(6)-O(5)	-178.62(19)
C(4)-C(5)-C(6)-O(5)	1.3(2)
O(4)-C(5)-C(6)-C(20)	-59.5(2)
C(4)-C(5)-C(6)-C(20)	120.46(18)
O(4)-C(5)-C(6)-C(21)	64.8(2)
C(4)-C(5)-C(6)-C(21)	-115.24(18)
C(6)-O(5)-C(7)-C(8)	100.85(15)
C(6)-O(5)-C(7)-C(22)	-23.68(16)
O(5)-C(7)-C(8)-C(9)	68.37(17)
C(22)-C(7)-C(8)-C(9)	-173.69(14)

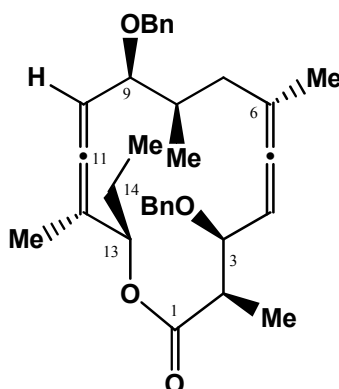
C(7)-C(8)-C(9)-O(6)	-4.3(2)
C(7)-C(8)-C(9)-C(10)	173.83(13)
Si(1)-O(7)-C(10)-C(24)	-87.89(19)
Si(1)-O(7)-C(10)-C(11)	150.97(15)
Si(1)-O(7)-C(10)-C(9)	37.5(2)
O(6)-C(9)-C(10)-O(7)	50.8(2)
C(8)-C(9)-C(10)-O(7)	-127.40(15)
O(6)-C(9)-C(10)-C(24)	173.47(16)
C(8)-C(9)-C(10)-C(24)	-4.7(2)
O(6)-C(9)-C(10)-C(11)	-61.56(19)
C(8)-C(9)-C(10)-C(11)	120.27(15)
C(1)-O(1)-C(11)-C(25)	-99.37(16)
C(1)-O(1)-C(11)-C(10)	137.38(14)
O(7)-C(10)-C(11)-O(1)	177.37(12)
C(24)-C(10)-C(11)-O(1)	58.60(16)
C(9)-C(10)-C(11)-O(1)	-67.01(15)
O(7)-C(10)-C(11)-C(25)	57.49(17)
C(24)-C(10)-C(11)-C(25)	-61.28(18)
C(9)-C(10)-C(11)-C(25)	173.11(14)
C(3)-O(3)-C(13)-C(14)	-147.23(18)
O(3)-C(13)-C(14)-C(15)	67.9(3)
O(3)-C(13)-C(14)-C(19)	-110.3(2)
C(19)-C(14)-C(15)-C(16)	1.1(3)
C(13)-C(14)-C(15)-C(16)	-177.2(2)
C(14)-C(15)-C(16)-C(17)	-1.7(4)
C(15)-C(16)-C(17)-C(18)	1.1(4)
C(16)-C(17)-C(18)-C(19)	0.2(4)
C(15)-C(14)-C(19)-C(18)	0.2(3)
C(13)-C(14)-C(19)-C(18)	178.41(19)
C(17)-C(18)-C(19)-C(14)	-0.8(3)
O(5)-C(6)-C(21)-C(22)	24.74(17)
C(20)-C(6)-C(21)-C(22)	-93.16(18)
C(5)-C(6)-C(21)-C(22)	144.52(14)
C(6)-C(21)-C(22)-C(23)	-163.95(15)
C(6)-C(21)-C(22)-C(7)	-37.91(16)
O(5)-C(7)-C(22)-C(23)	162.82(15)

C(8)-C(7)-C(22)-C(23)	40.3(2)
O(5)-C(7)-C(22)-C(21)	37.97(16)
C(8)-C(7)-C(22)-C(21)	-84.52(17)
O(1)-C(11)-C(25)-C(26)	66.07(19)
C(10)-C(11)-C(25)-C(26)	-175.82(15)
O(7)-Si(1)-C(27A)-C(28A)	171.5(5)
C(29A)-Si(1)-C(27A)-C(28A)	51.1(6)
C(31A)-Si(1)-C(27A)-C(28A)	-67.5(6)
O(7)-Si(1)-C(29A)-C(30A)	-74.4(6)
C(27A)-Si(1)-C(29A)-C(30A)	51.7(7)
C(31A)-Si(1)-C(29A)-C(30A)	174.8(6)
O(7)-Si(1)-C(31A)-C(32A)	54.7(4)
C(27A)-Si(1)-C(31A)-C(32A)	-72.4(5)
C(29A)-Si(1)-C(31A)-C(32A)	166.5(5)
O(7)-Si(1)-C(27B)-C(28B)	177.3(3)
C(29B)-Si(1)-C(27B)-C(28B)	59.0(4)
C(31B)-Si(1)-C(27B)-C(28B)	-63.8(4)
O(7)-Si(1)-C(29B)-C(30B)	-73.1(4)
C(27B)-Si(1)-C(29B)-C(30B)	47.8(5)
C(31B)-Si(1)-C(29B)-C(30B)	166.9(4)
O(7)-Si(1)-C(31B)-C(32B)	-47.9(3)
C(29B)-Si(1)-C(31B)-C(32B)	70.2(4)
C(27B)-Si(1)-C(31B)-C(32B)	-167.7(3)

Table 7. Hydrogen bonds for KL-191 [\AA and $^\circ$].

D-H...A	d(D-H)	d(H...A)	d(D...A)	$\angle(\text{DHA})$
O(8W)-H(81)...O(5)	0.840(10)	1.921(12)	2.760(4)	176(8)
O(8W)-H(82)...O(6)	0.843(10)	2.80(6)	3.214(5)	112(5)

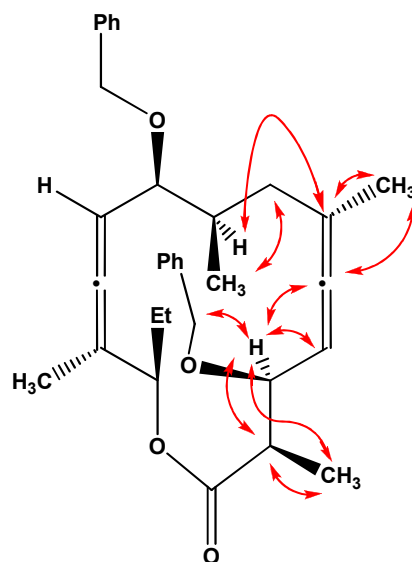
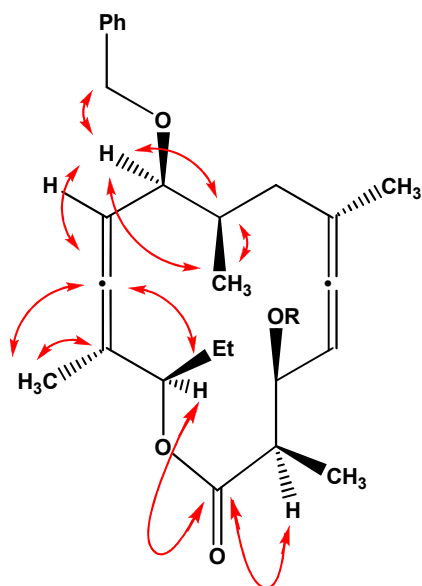
Detailed NMR analysis for compounds 5.1



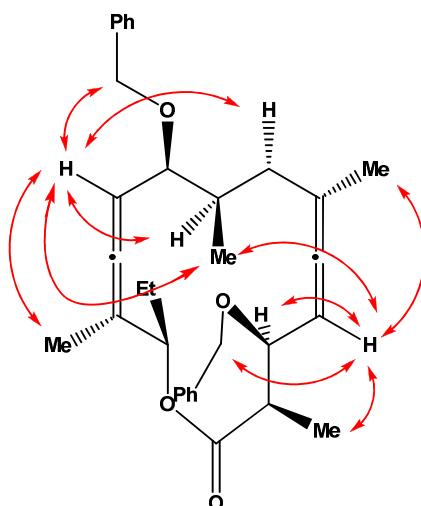
5.1

¹ H NMR chemical shifts (d/ppm) and coupling constant (J/Hz)	¹³ C NMR chemical shift (d/ppm)
2.78 (dq, J _{H2, H3} = 8.4Hz, J _{H2, 2-CH3} = 7.1Hz, H2)	173.8 ----- C1
1.26 (d, J _{2-CH3, H2} = 7.1Hz, 2-CH ₃)	44.5 ----- C2
3.95 (dd, J _{H3, H2} = 8.4Hz, J _{H3, H4} = 4.0Hz, H3)	77.2 ----- C3
5.33 (m, J _{H4, H3} = 4.0Hz, J _{H4, 6-CH3} = 2.9Hz, J _{H4, H7α} = 2.7Hz, J _{H4, H7β} = 3.4Hz, H4)	90.5 ----- C4
1.70 (d, 6-CH ₃)	201.2 ----- C5
1.61 (m, J _{H7β, H8} = 5.4Hz, J _{H7β, H7α} = 15.4Hz, J _{H4, H7β} = 3.4Hz, H7β)	102.4 ----- C6
2.18 (m, J _{H7α, H8} = 5.7Hz, J _{H7α, H7β} = 15.4Hz, J _{H4, H7α} = 2.7Hz, H7α)	37.7 ----- C7
1.96 (m, J _{H7α, H8} = 5.7Hz, J _{H7β, H8} = 5.4Hz, J _{H8, 8-CH3} = 6.7Hz, J _{H8, H9} = 7.2Hz, H8)	35.9 ----- C8
1.05 (d, J _{8-CH3, H8} = 6.7Hz, 8-CH ₃)	81.6 ----- C9
3.74 (dd, J _{H9, H8} = 7.2Hz, J _{H9, H10} = 7.8Hz, H9)	91.7 ----- C10
5.13 (m, J _{H9, H10} = 7.8Hz, J _{H10, 12-CH3} = 2.9Hz, J _{H10, H13} = 1.1Hz, H10)	203.4 ----- C11
1.71 (d, J _{H10, 12-CH3} = 2.9Hz, 12-CH ₃)	99.0 ----- C12
5.26 (dt, J _{H10, H13} = 1.1Hz, J _{H13, H14} = 6.8Hz, H13)	75.5 ----- C13
1.69, 1.67 (m, 14-CH ₂)	24.9 ----- C14
0.90 (t, J _{14-CH3, H14} = 7.5Hz, 14-CH ₃)	15.2 ----- 2-CH ₃
4.64 (d, J = 11.7Hz, 3-Bn-CH ₂ a)	20.2 ----- 6-CH ₃
4.48 (d, J = 11.7Hz, 3-Bn-CH ₂ b)	17.6 ----- 8-CH ₃
4.54 (d, J = 11.9Hz, 9-Bn-CH ₂ a)	14.0 ----- 12-CH ₃
4.34 (d, J = 11.9Hz, 9-Bn-CH ₂ b)	9.6 ----- 14-CH ₃
7.22-7.35 (two phenyl)	

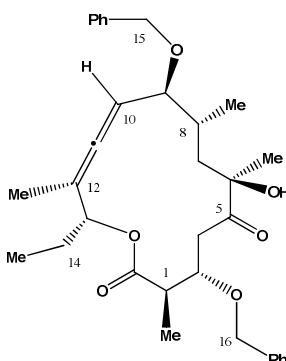
HMBC



NOESY

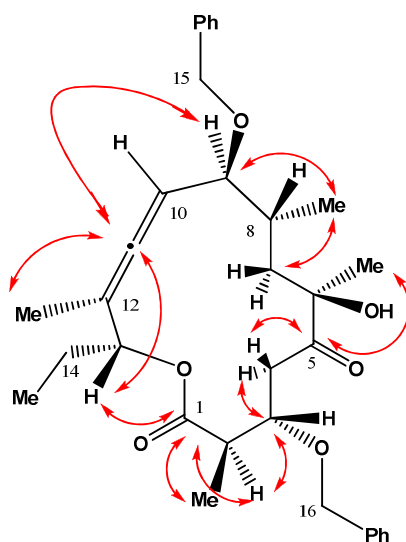


Detailed NMR analysis for compounds 5.2

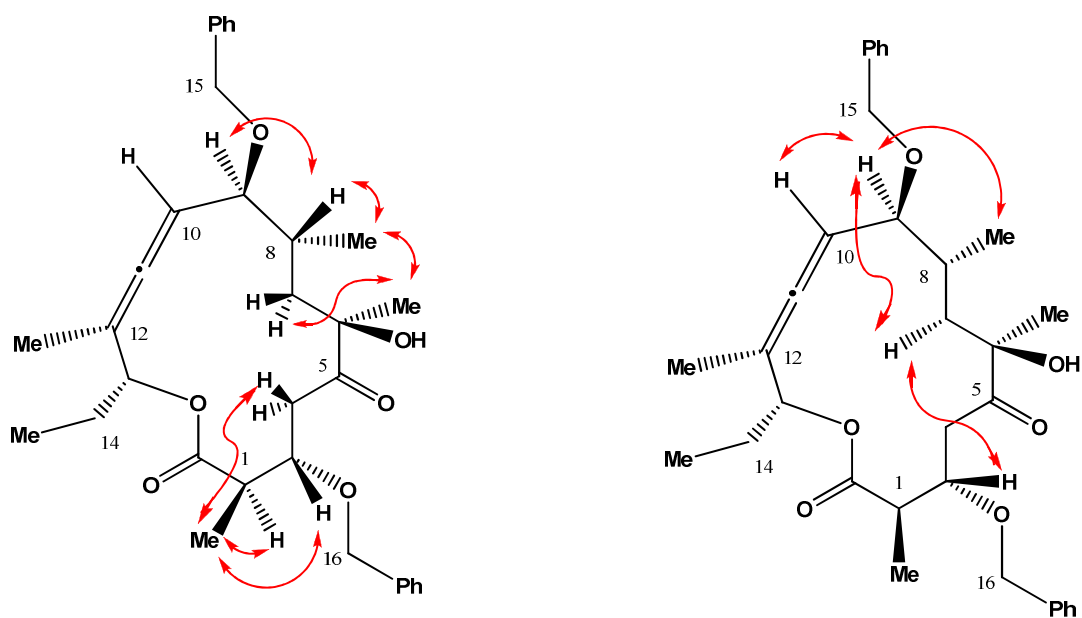


1H NMR chemical shifts (d/ppm) and coupling constant (J/Hz)	13C NMR chemical shift (d/ppm)
2.58 (dq, $J_{H_2, H_3} = 8.7\text{Hz}$, $J_{H_2, 2-\text{CH}_3} = 6.8\text{Hz}$, H2)	173.84 ---- C1
1.30 (d, $J_{2-\text{CH}_3, H_2} = 6.8\text{Hz}$, 2-CH ₃)	45.56 ---- C2
4.15 (m, $J_{H_3, H_2} = 8.7\text{Hz}$, $J_{H_3, H_{4\alpha}} = 3.8\text{Hz}$, $J_{H_3, H_{4\beta}} = 6.9\text{Hz}$, H3)	76.0 ---- C3
2.93 (dd, $J_{H_{4\alpha}, H_3} = 3.8\text{Hz}$, $J_{H_{4\alpha}, H_{4\beta}} = 17.7$, H4 α)	42.6 ---- C4
2.96 (dd, $J_{H_{4\beta}, H_3} = 6.9\text{Hz}$, $J_{H_{4\alpha}, H_{4\beta}} = 17.7$, H4 β)	212.1 ---- C5
1.32 (s, 6-CH ₃)	78.9 ---- C6
1.90 (dd, $J_{H_{7\beta}, H_8} = 6.6\text{Hz}$, $J_{H_{7\beta}, H_{7\alpha}} = 15.1\text{Hz}$, H7 β)	43.0 ---- C7
1.54 (dd, $J_{H_{7\alpha}, H_8} = 3.2\text{Hz}$, $J_{H_{7\alpha}, H_{7\beta}} = 15.1\text{Hz}$, H7 α)	34.2 ---- C8
1.69 (m, $J_{H_{7\alpha}, H_8} = 3.2\text{Hz}$, $J_{H_{7\beta}, H_8} = 6.6\text{Hz}$, $J_{H_8, 8-\text{CH}_3} = 6.8\text{Hz}$, $J_{H_8, H_9} = 6.8\text{Hz}$, H8)	82.3 ---- C9
1.05 (d, $J_{8-\text{CH}_3, H_8} = 6.8\text{Hz}$, 8-CH ₃)	96.7 ---- C10
3.44 (dd, $J_{H_9, H_8} = 6.8\text{Hz}$, $J_{H_9, H_{10}} = 8.1\text{Hz}$, H9)	204.0 ---- C11
4.94 (m, $J_{H_9, H_{10}} = 8.1\text{Hz}$, $J_{H_{10}, H_{13}} = 1.1\text{Hz}$, $J_{H_{10}, 12-\text{CH}_3} = 2.9\text{Hz}$, H10)	99.8 ---- C12
1.79 (d, $J_{H_{10}, 12-\text{CH}_3} = 2.9\text{Hz}$, 12-CH ₃)	76.5 ---- C13
5.15 (m, $J_{H_{13}, H_{14}} = 7.0\text{ Hz}$, $J_{H_{10}, H_{13}} = 1.1\text{Hz}$ H13)	25.3 ---- C14
1.69, 1.73 (m, 14-CH ₂)	13.7 ---- 2-CH ₃
0.90 (t, $J_{14-\text{CH}_3, H_{14}} = 7.4\text{Hz}$, 14-CH ₃)	27.4 ---- 6-CH ₃
4.34 (d, $J_{H_{15a}, H_{15b}} = 12.2$, H15a)	18.6 ---- 8-CH ₃
4.60 (d, $J_{H_{15a}, H_{15b}} = 12.2$, H15b)	15.5 ---- 12-CH ₃
4.56 (d, $J = 11.6\text{Hz}$, H16a)	9.6 ---- 14-CH ₃
4.74 (d, $J = 11.6\text{Hz}$, H16b)	73.8 ---- C16
7.26-7.38 (m, 10H, two phenyl)	70.0 ---- C15
	138.6 ---- ipsoC-15
	128.1 ---- orthoC-15
	128.6 ---- metaC-15
	127.9 ---- paraC-15
	138.4 ---- ipsoC-16
	126.1 ---- orthoC-16
	128.5 ---- metaC-16
	127.7 ---- paraC-16

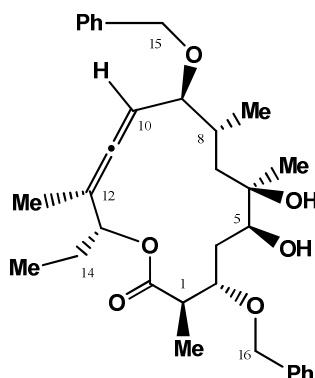
HMBC



NOESY

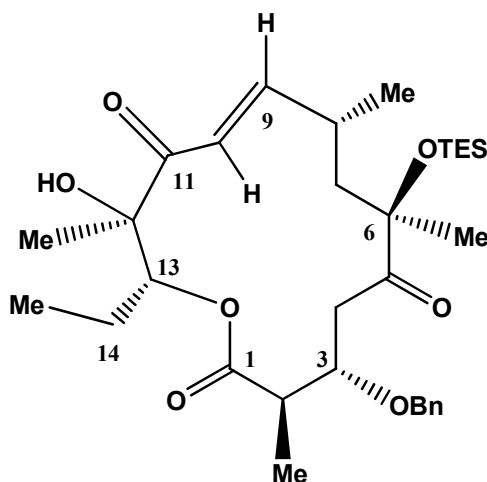


Detailed NMR analysis for compounds 5.13



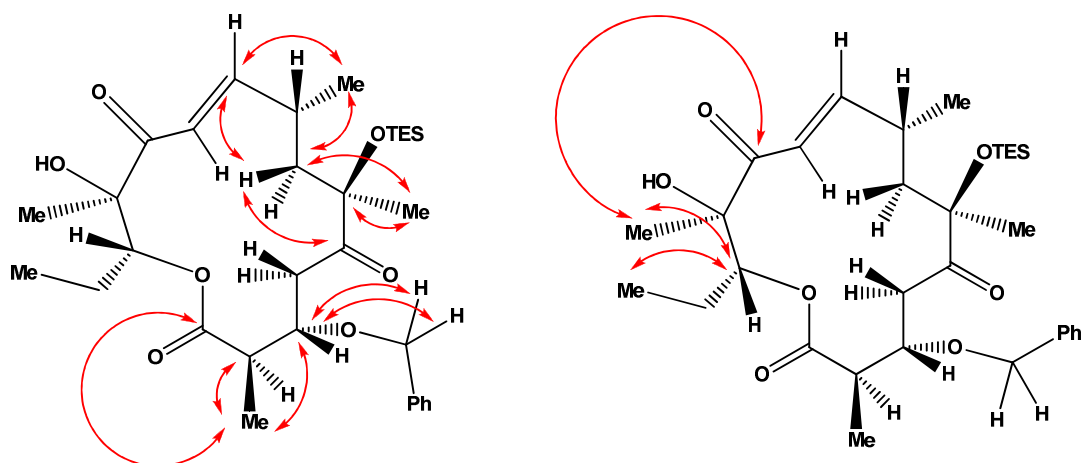
1H NMR chemical shifts (d/ppm) and coupling constant (J/Hz)	13C NMR chemical shift (d/ppm)
2.76 (dq, $J_{H2, H3} = 7.2\text{Hz}$, $J_{H2, 2-CH3} = 6.9\text{Hz}$, H2)	174.8 ---- C1
1.24 (d, $J_{2-CH3, H2} = 6.9\text{Hz}$, 2-CH ₃)	44.0 ---- C2
3.92 (m, $J_{H3, H2} = 7.2\text{Hz}$, $J_{H3, H4\alpha} = 3.4\text{Hz}$, $J_{H3, H4\beta} = 7.1\text{Hz}$, H3)	79.7 ---- C3
1.86 (dd, $J_{H4\alpha, H3} = 3.4\text{Hz}$, $J_{H4\alpha, H4\beta} = 15.0$, H4 α)	33.5 ---- C4
1.83 (dd, $J_{H4\beta, H3} = 7.1\text{Hz}$, $J_{H4\alpha, H4\beta} = 15.0$, H4 β)	74.6 ---- C5
3.59 (m, $J_{H4\alpha, H5} = 9.6\text{Hz}$, $J_{H4\beta, H5} = 2.1\text{Hz}$, $J_{H5-5-OH} = 6.21\text{Hz}$, H5)	73.7 ---- C6
1.16 (s, 6-CH ₃)	39.8 ---- C7
2.89 (s, 6-OH)	34.1 ---- C8
1.99 (dd, $J_{H7\beta, H8} = 5.3\text{Hz}$, $J_{H7\beta, H7\alpha} = 14.8\text{Hz}$, H7 β)	80.6 ---- C9
1.07 (dd, $J_{H7\alpha, H8} = 3.8\text{Hz}$, $J_{H7\alpha, H7\beta} = 14.8\text{Hz}$, H7 α)	91.7 ---- C10
2.06 (m, $J_{H7\alpha, H8} = 3.8\text{Hz}$, $J_{H7\beta, H8} = 5.3\text{Hz}$, $J_{H8, 8-CH3} = 6.9\text{Hz}$, $J_{H8, H9} = 5.5\text{Hz}$, H8)	204.2 ---- C11
1.00 (d, $J_{8-CH3, H8} = 6.9\text{Hz}$, 8-CH ₃)	99.5 ---- C12
3.69 (dd, $J_{H9, H8} = 5.5\text{Hz}$, $J_{H9, H10} = 7.5\text{Hz}$, H9)	76.3 ---- C13
5.21 (m, $J_{H9, H10} = 7.5\text{Hz}$, $J_{H10, H13} = 1.2\text{Hz}$, $J_{H10, 12-CH3} = 3.0\text{Hz}$, H10)	25.2 ---- C14
1.74 (d, $J_{H10, 12-CH3} = 3.0\text{Hz}$, 12-CH ₃)	14.2 ---- 2-CH ₃
5.38 (m, $J_{H13, H14} = 6.8\text{Hz}$, $J_{H10, H13} = 1.2\text{Hz}$, H13)	27.1 ---- 6-CH ₃
1.72 (m, 14-CH ₂)	19.9 ---- 8-CH ₃
0.91 (t, $J_{14-CH3, H14} = 7.3\text{Hz}$, 14-CH ₃)	14.6 ---- 12-CH ₃
4.59 (d, $J_{H15a, H15b} = 11.1$, H15a)	9.7 ---- 14-CH ₃
4.60 (d, $J_{H15a, H15b} = 11.1$, H15b)	73.1 ---- C16
4.42 (d, $J = 12.3\text{Hz}$, H16a)	70.6 ---- C15
4.74 (d, $J = 12.3\text{Hz}$, H16b)	
7.27-7.37 (m, 10H, two phenyl)	

Detailed NMR analysis for compounds 5.10

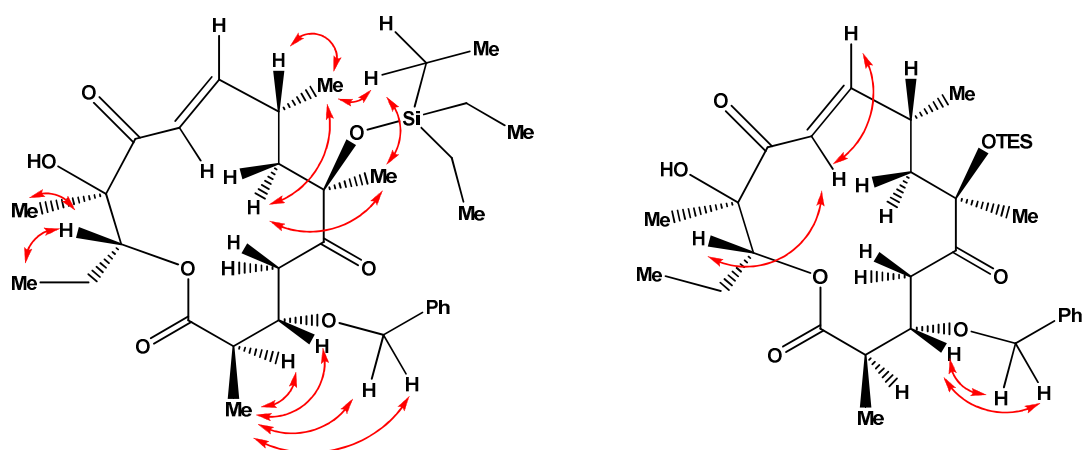

¹H NMR chemical shifts (d/ppm) and coupling constant (J/Hz)
¹³C NMR chemical shift (d/ppm)

3.60 (dq, $J_{H2, H3} = 9.7\text{Hz}$, $J_{H2, 2-CH3} = 7.0\text{Hz}$, H2)	178.5 ---- C1
1.21 (d, $J_{2-CH3, H2} = 7.0\text{Hz}$, 2-CH ₃)	43.0 ---- C2
3.68 (ddd, $J_{H3, H2} = 9.7\text{Hz}$, $J_{H3, H4\alpha} = 3.4\text{Hz}$, $J_{H3, H4\beta} = 4.3\text{Hz}$, H3)	77.1 ---- C3
2.44 (dd, $J_{H4\alpha, H3} = 3.4\text{Hz}$, $J_{H4\alpha, H4\beta} = 18.8$, H4 α)	37.6 ---- C4
3.42 (dd, $J_{H4\beta, H3} = 4.3\text{Hz}$, $J_{H4\beta, H4\alpha} = 18.8$, H4 β)	212.5 ---- C5
1.23 (s, 6-CH ₃)	82.4 ---- C6
2.29 (dd, $J_{H7\beta, H8} = 10.2\text{Hz}$, $J_{H7\beta, H7\alpha} = 14.3\text{Hz}$, H7 β)	46.3 ---- C7
1.45 (dd, $J_{H7\alpha, H8} = 2.1\text{Hz}$, $J_{H7\alpha, H7\beta} = 14.3\text{Hz}$, H7 α)	33.3 ---- C8
2.58 (m, $J_{H8, 8-CH3} = 6.6\text{Hz}$, $J_{H8, H9} = 8.2\text{Hz}$, H8)	154.9 ---- C9
1.02 (d, $J_{8-CH3, H8} = 6.6\text{Hz}$, 8-CH ₃)	122.7 ---- C10
6.60 (dd, $J_{H9, H8} = 8.2\text{Hz}$, $J_{H9, H10} = 15.5\text{Hz}$, H9)	202.7 ---- C11
6.64 (d, $J_{H9, H10} = 15.5\text{Hz}$, H10)	80.8 ---- C12
1.31 (s, 12-CH ₃)	84.4 ---- C13
4.89 (dd, $J_{H13, H14} = 2.5, 11.3\text{Hz}$, H13)	23.6 ---- C14
1.78, 2.02 (m, 14-CH ₂)	16.0 ---- 2-CH ₃
0.88 (t, $J_{14-CH3, H14} = 7.4\text{Hz}$, 14-CH ₃)	28.3 ---- 6-CH ₃
4.49 (d, $J=11.6\text{Hz}$, Bn-CH ₂ a)	22.5 ---- 8-CH ₃
4.56 (d, $J=11.6\text{Hz}$, Bn-CH ₂ b)	23.0 ---- 12-CH ₃
0.66 (m, $J=7.9, 15.1$, TES-CH ₂)	10.9 ---- 14-CH ₃
1.01 (t, $J=7.9$, TES-CH ₃)	138.1 ---- ipsoC
	128.3 ---- orthoC
	128.6 ---- metaC
	128.0 ---- paraC
	7.01 ---- TES-CH ₂
	7.45 ---- TES-CH ₃

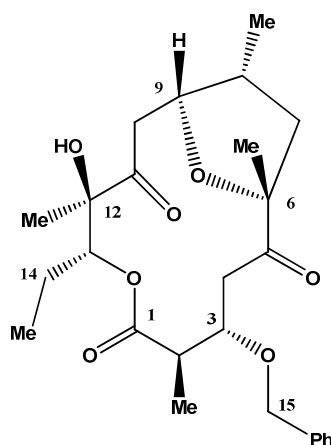
HMBC



NOESY

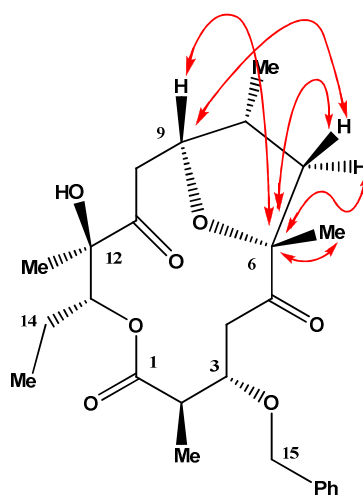


Detailed NMR analysis for compounds 5.5

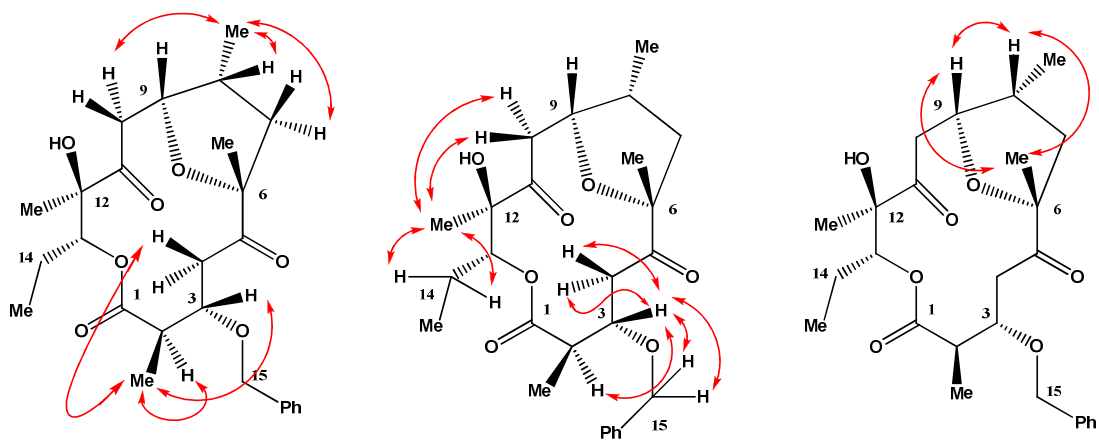


¹ H NMR chemical shifts (d/ppm) and coupling constant (J/Hz)	¹³ C NMR chemical shift (d/ppm)
2.89 (dq, J _{H2, H3} = 11.1Hz, J _{H2, 2-CH3} = 7.3Hz, H2)	173.2 ---- C1
1.21 (d, J _{2-CH3, H2} = 7.3Hz, 2-CH ₃)	42.1 ---- C2
3.86 (m, J _{H3, H2} = 11.1Hz, J _{H3, H4α} = 4.7Hz, J _{H3, H4β} = 6.4Hz, H3)	78.4 ---- C3
2.29 (dd, J _{H4α, H3} = 4.7Hz, J _{H4α, H4β} = 14.5, H4α)	35.4 ---- C4
3.37 (dd, J _{H4β, H3} = 6.4Hz, J _{H4α, H4β} = 14.5, H4β)	212.6 ---- C5
1.27 (s, 6-CH ₃)	88.5 ---- C6
1.89 (dd, J _{H7β, H8} = 9.1Hz, J _{H7β, H7α} = 12.9Hz, H7β)	40.5 ---- C7
1.79 (dd, J _{H7α, H8} = 7.3Hz, J _{H7α, H7β} = 12.9Hz, H7α)	34.9 ---- C8
2.40 (m, J _{H7α, H8} = 7.3Hz, J _{H7β, H8} = 9.1Hz, J _{H8, 8-CH3} = 7.0Hz, J _{H8, H9} = 6.9Hz, H8)	76.3 ---- C9
0.67 (d, J _{8-CH3, H8} = 7.0Hz, 8-CH ₃)	39.6 ---- C10
4.63 (ddd, J _{H9, H8} = 6.9Hz, J _{H9, H10α} = 10.2Hz, J _{H9, H10β} = 1.5Hz H9)	213.3 ---- C11
3.08 (dd, J _{H9, H10β} = 10.2Hz, J _{10β, H10α} = 18.7Hz H10β)	77.8 ---- C12
2.29 (dd, J _{H9, H10α} = 1.5Hz, J _{10α, H10β} = 18.7Hz H10α)	78.9 ---- C13
1.38 (s, 12-CH ₃)	23.1 ---- C14
4.89 (dd, J _{H13, H14} = 3.4, 9.0 Hz, H13)	15.0 ---- 2-CH ₃
1.55, 1.97 (m, 14-CH ₂)	25.2 ---- 6-CH ₃
0.93 (t, J _{14-CH3, H14} = 7.5Hz, 14-CH ₃)	14.2 ---- 8-CH ₃
4.57 (d, J=11.6Hz, Bn-CH ₂ a)	17.0 ---- 12-CH ₃
4.59 (d, J=11.6Hz, Bn-CH ₂ b)	11.0 ---- 14-CH ₃
7.35 (^o H/Ph)	137.5 ---- ipsoC
7.34 (^m H/Ph)	128.8 ---- orthoC
7.30 (^p H/Ph)	128.4 ---- metaC
	128.0 ---- paraC
	72.0 ---- 15-CH ₂

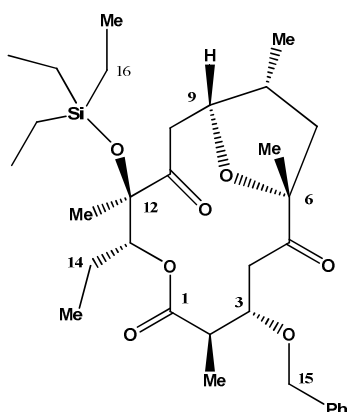
HMBC



NOESY

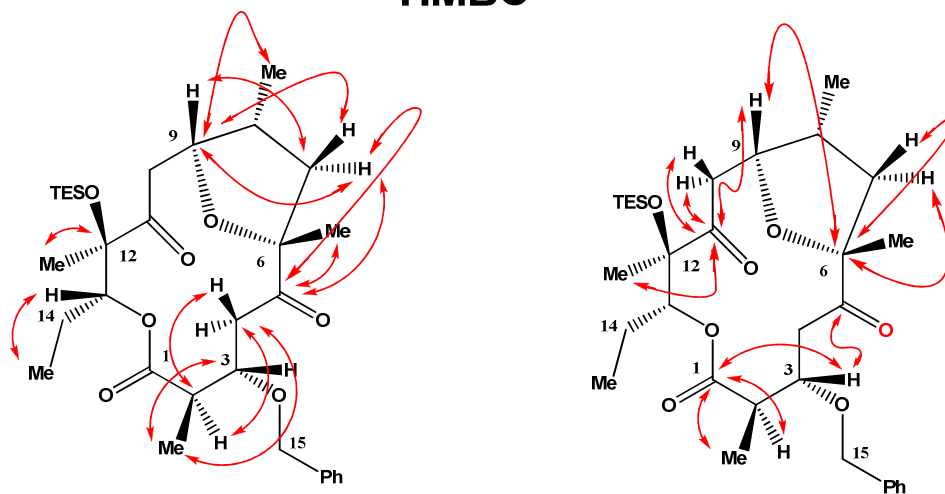


Detailed NMR analysis for compounds 5.6

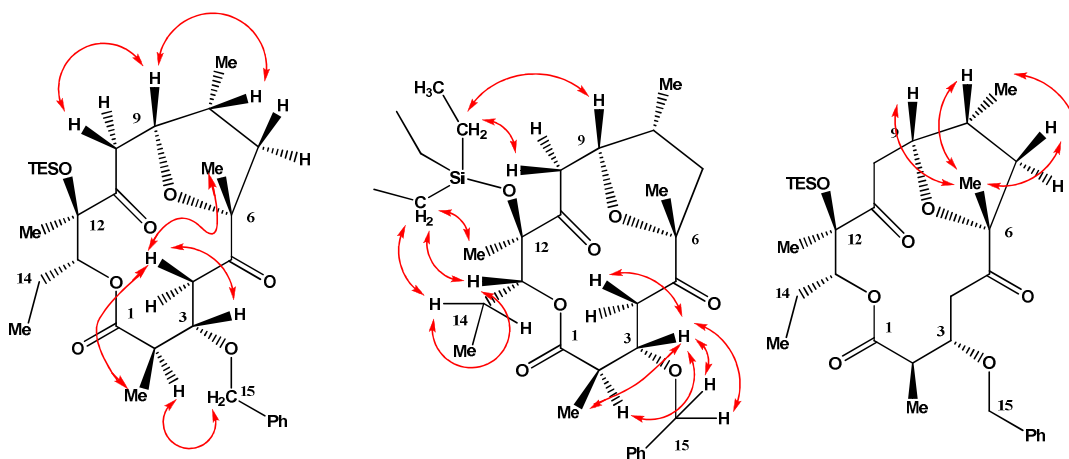


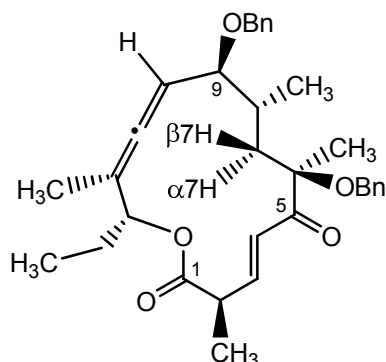
1H NMR chemical shifts (d/ppm) and coupling constant (J/Hz)	13C NMR chemical shift (d/ppm)
2.92 (dq, $J_{H2, H3} = 5.0\text{Hz}$, $J_{H2, 2-CH3} = 7.0\text{Hz}$, H2)	172.9 ---- C1
1.14 (d, $J_{2-CH3, H2} = 7.0\text{Hz}$, 2-CH ₃)	41.6 ---- C2
3.87 (m, $J_{H3, H2} = 5.0\text{Hz}$, $J_{H3, H4\alpha} = 3.8\text{Hz}$, $J_{H3, H4\beta} = 9.6\text{Hz}$, H3)	79.6 ---- C3
2.17 (dd, $J_{H4\alpha, H3} = 3.8\text{Hz}$, $J_{H4\alpha, H4\beta} = 14.9$, H4 α)	36.3 ---- C4
3.26 (dd, $J_{H4\beta, H3} = 9.6\text{Hz}$, $J_{H4\alpha, H4\beta} = 14.9$, H4 β)	215.5 ---- C5
1.28 (s, 6-CH ₃)	88.6 ---- C6
1.73 (dd, $J_{H7\beta, H8} = 7.0\text{Hz}$, $J_{H7\beta, H7\alpha} = 12.6\text{Hz}$, H7 β)	41.2 ---- C7
1.81 (dd, $J_{H7\alpha, H8} = 11.4\text{Hz}$, $J_{H7\alpha, H7\beta} = 12.6\text{Hz}$, H7 α)	35.0 ---- C8
2.24 (m, $J_{H7\alpha, H8} = 11.4\text{Hz}$, $J_{H7\beta, H8} = 7.0\text{Hz}$, $J_{H8, 8-CH3} = 6.9\text{Hz}$, $J_{H8, H9} = 7.4\text{Hz}$, H8)	78.1 ---- C9
0.68 (d, $J_{8-CH3, H8} = 6.9\text{Hz}$, 8-CH ₃)	39.8 ---- C10
4.48 (ddd, $J_{H9, H8} = 7.4\text{Hz}$, $J_{H9, H10\alpha} = 1.5\text{Hz}$, $J_{H9, H10\beta} = 10.5\text{Hz}$ H9)	211.4 ---- C11
2.78 (dd, $J_{H9, H10\beta} = 10.5\text{Hz}$, $J_{10\beta, H10\alpha} = 19.0\text{Hz}$ H10 β)	79.4 ---- C12
2.35 (dd, $J_{H9, H10\alpha} = 1.5\text{Hz}$, $J_{10\alpha, H10\beta} = 19.0\text{Hz}$ H10 α)	79.6 ---- C13
1.33 (s, 12-CH ₃)	22.7 ---- C14
5.20 (dd, $J_{H13, H14} = 2.9, 9.5\text{ Hz}$, H13)	14.8 ---- 2-CH ₃
1.46, 1.89 (m, 14-CH ₂)	25.5 ---- 6-CH ₃
0.91 (t, $J_{14-CH3, H14} = 7.2, 7.6\text{Hz}$, 14-CH ₃)	13.9 ---- 8-CH ₃
4.44 (d, $J=10.4\text{Hz}$, Bn-CH _{2a})	17.0 ---- 12-CH ₃
4.60 (d, $J=10.4\text{Hz}$, Bn-CH _{2b})	11.1 ---- 14-CH ₃
0.54, 0.56(m, H16)	137.7 ---- ipsoC
0.89 (dd, $J= 8.2, 7.8\text{Hz}$, 16-CH ₃)	129.1 ---- orthoC
7.33 (^o H/Ph)	128.5 ---- metaC
7.33 (^m H/Ph)	128.3 ---- paraC
7.30 (^p H/Ph)	72.5 ---- 15-CH ₂
	6.4 ---- C16
	7.2 ---- 16-CH ₃

HMBC

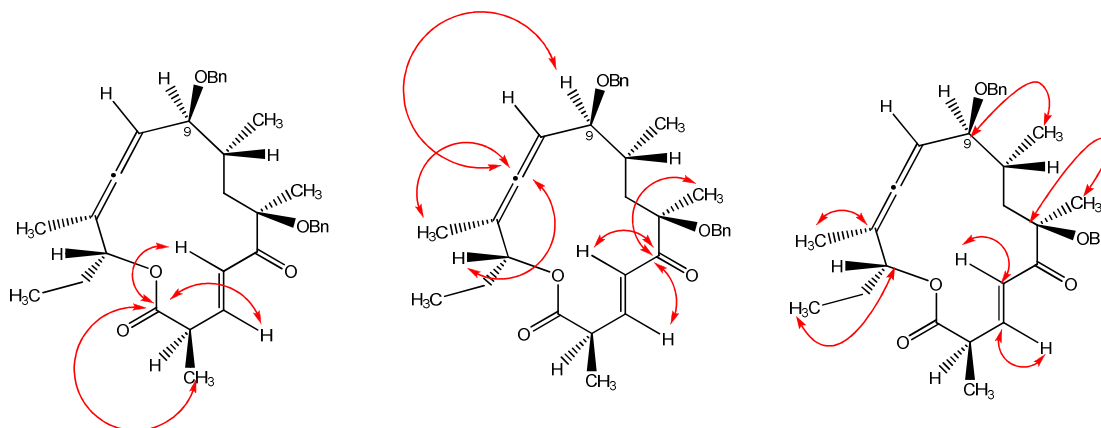
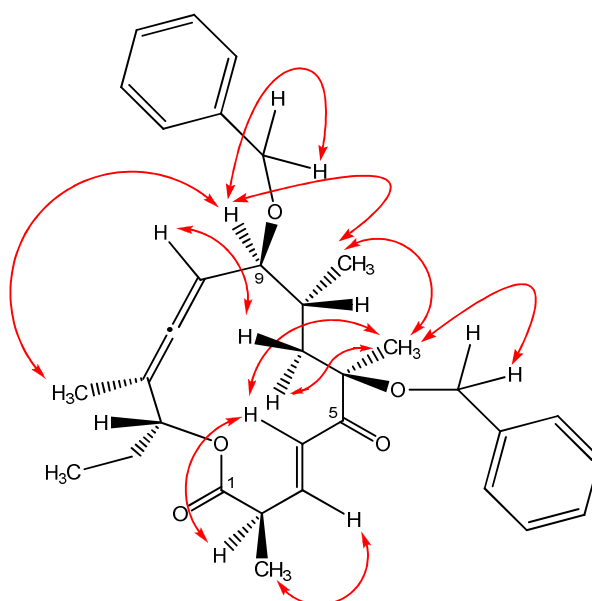


NOESY

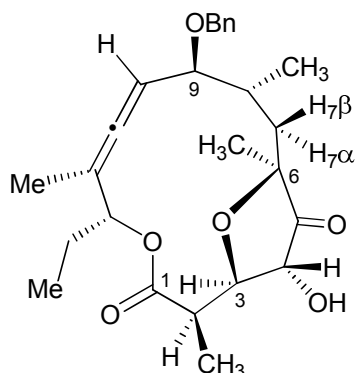




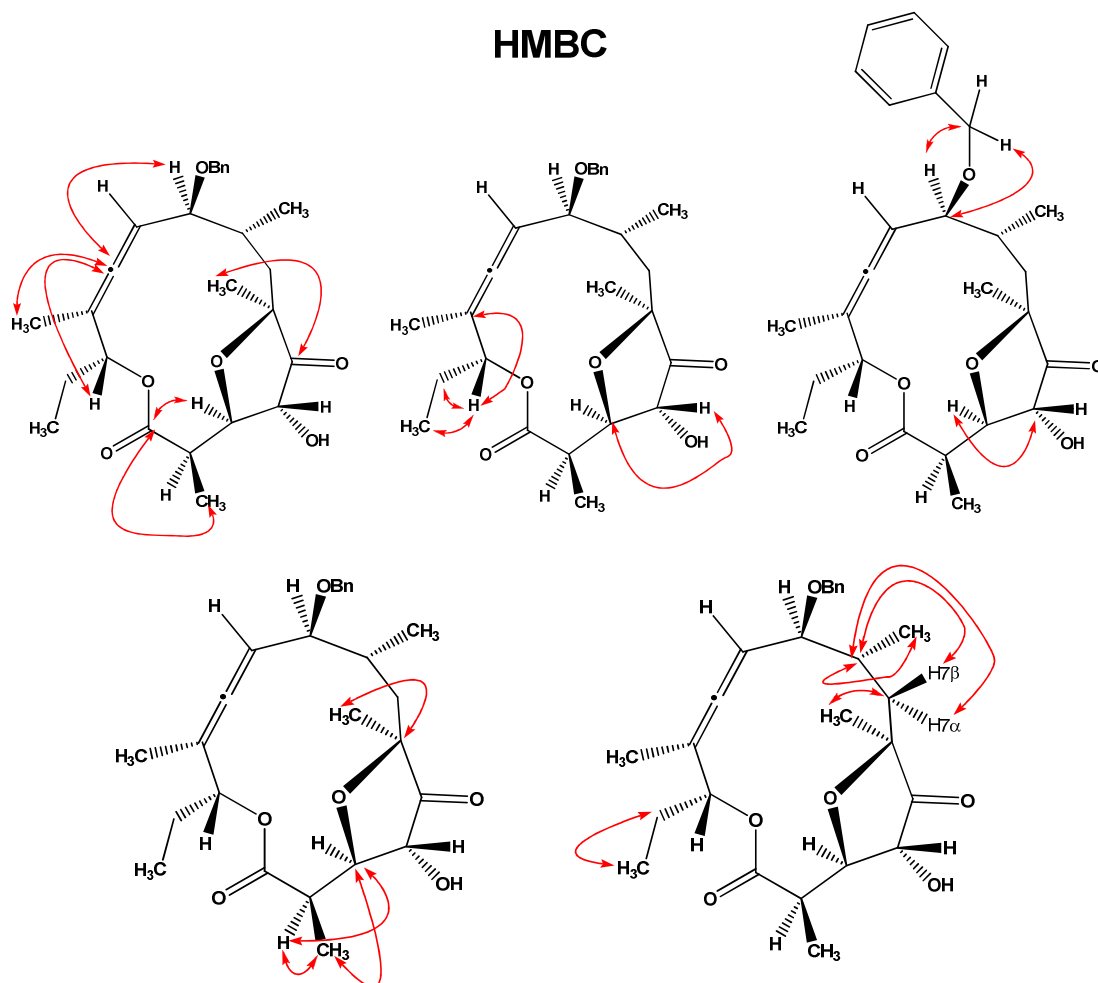
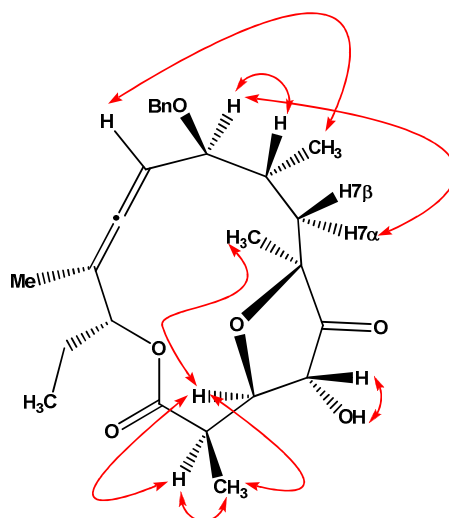
¹H NMR chemical shifts (d/ppm) & coupling constant (J/Hz)	¹³C NMR chemical shift (d/ppm)
3.30 (ddd, J_{H2, H3} = 8.2Hz, J_{H2, 2-CH3} = 6.8Hz, J_{H2, H4} = 1.1Hz, H2)	171.9 ---- C1
1.32 (d, J_{2-CH3, H2} = 6.8Hz, 2-CH₃)	42.3 ---- C2
6.73 (dd, J_{H3, H4} = 15.7Hz, J_{H3, H2} = 8.3Hz, H3)	145.3 ---- C3
7.05 (dd, J_{H4, H3} = 15.7Hz, J_{H4, H2} = 1.2Hz, H4)	127.8 ---- C4
1.44 (s, 6-CH₃)	202.1 ---- C5
4.26 (d, J_{AB} = 11.5Hz, 6-OCH₂)	84.9 ---- C6
4.56 (d, J_{AB} = 12.0Hz, 6-OCH₂)	41.4 ---- C7
1.95 (dd, J_{H7α, H7β} = 14.2Hz, H7β)	33.5 ---- C8
1.48 (dd, J_{H7β, H8} = 6.85 Hz, J_{H7β, H7α} = 14.4Hz, H7α)	83.0 ---- C9
1.41 (m, H8)	93.9 ---- C10
1.09 (d, J_{8-CH3, H8} = 6.6Hz, 8-CH₃)	202.6 ---- C11
3.24 (t, J_{H9, H8} = 9.1Hz, H9)	101.1 ---- C12
4.24 (d, J_{AB} = 11.5Hz, 9-OCH₂)	75.8 ---- C13
4.57 (d, J_{AB} = 11.0Hz, 9-OCH₂)	26.4 ---- C14
4.62 (dq, J = 9.31Hz, H10)	14.6 ---- 2-CH₃
1.82 (d, J_{12-CH3, H10} = 2.9Hz, 12-CH₃)	17.4 ---- 6-CH₃
4.71 (ddd, J_{H13, 14-CH2} = 6.6Hz, J_{H13, H10} = 1.6Hz, H13)	19.9 ---- 8-CH₃
1.68 - 1.78 (m, 14-CH₂)	18.0 ---- 12-CH₃
0.99 (t, J_{14-CH3, 13-CH2} = 7.3Hz, 14-CH₃)	9.7 ---- 14-CH₃
7.48 - 7.17 (m, 8H, Ph)	66.3 ---- 6-OCH₃
	69.8 ---- 9-OCH₃

HMBC**NOESY**

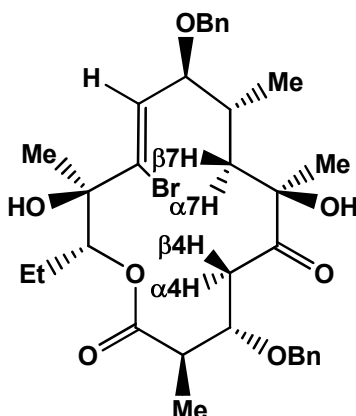
Detailed NMR analysis for compound 5.24



¹H NMR chemical shifts (d/ppm) & coupling constant (J/Hz)	¹³C NMR chemical shift (d/ppm)
3.06 dq, $J_{H2, H3} = 4.4\text{Hz}$, $J_{H2, 2-CH3} = 7.4\text{Hz}$, H2)	171.0 ---- C1
1.35 (d, $J_{2-CH3, H2} = 7.4\text{Hz}$, 2-CH₃)	40.2 ---- C2
3.90 (dd, $J_{H3, H2} = 4.4\text{Hz}$, $J_{H3, H4} = 8.7\text{Hz}$, H3)	79.7 ---- C3
5.07 (d, $J_{H4, H3} = 8.7\text{Hz}$, H4)	72.5 ---- C4
1.14 (s, 6-CH₃)	218.9 ---- C5
1.65 (dd, $J_{H7\beta, H8} = 3.9\text{ Hz}$, $J_{H7\beta, H7\alpha} = 15.0\text{Hz}$, H7β)	83.4 ---- C6
1.87 (dd, $J_{H7\alpha, H8} = 5.8\text{ Hz}$, $J_{H7\alpha, H7\beta} = 15.0\text{Hz}$, H7α)	42.9 ---- C7
1.70 (m, H8)	34.0 ---- C8
0.88 (d, $J_{8-CH3, H8} = 7.0\text{Hz}$, 8-CH₃)	82.3 ---- C9
3.83 (dd, $J_{H9, H8} = 2.6\text{Hz}$, $J_{H9, H10} = 8.1\text{Hz}$, H9)	90.7 ---- C10
4.62, 4.36 (d, $J_{AB} = 12.1\text{Hz}$, 9-OCH₂)	206.6 ---- C11
5.07 (qd, H10)	99.0 ---- C12
1.80 (d, 12-CH₃)	76.6 ---- C13
5.60 (dd, $J_{H13, H14} = 6.3, 8.1\text{Hz}$, H13)	24.3 ---- C14
1.65, 1.70 (m, 14-CH₂)	13.8 ---- 2-CH ₃
0.93 (t, $J_{14-CH3, H14} = 7.6\text{Hz}$, 14-CH₃)	22.8 ---- 6-CH ₃
	14.5 ---- 8-CH ₃
	13.6 ---- 12-CH ₃
	10.0 ---- 14-CH ₃
	70.2 ---- 9-OCH ₃

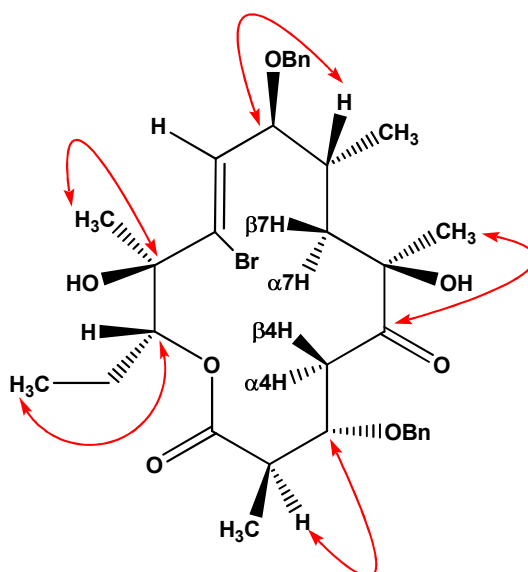
HMBC**NOESY**

Detailed NMR analysis for compound 5.15

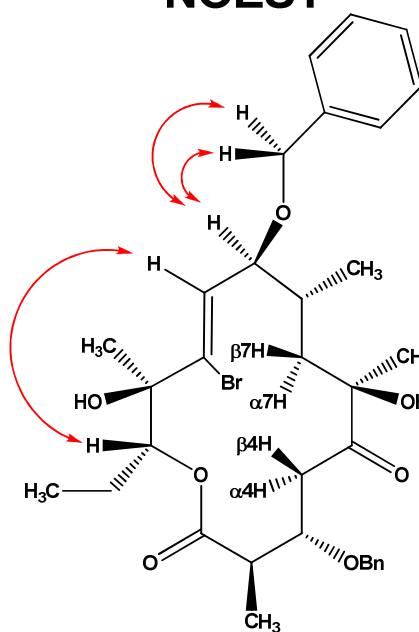


1H NMR chemical shifts (d/ppm) & coupling constant (J/Hz)	13C NMR chemical shift (d/ppm)
2.56 (quintet, $J_{H2, 2-CH3} = 6.9\text{Hz}$, H2)	174.6 ---- C1
1.20 (d, $J_{2-CH3, H2} = 6.9\text{Hz}$, 2-CH ₃)	42.5 ---- C2
4.34 (m, H3)	76.1 ---- C3
4.64, 4.52 (d, $J_{AB} = 11.1\text{Hz}$, C3-OCH ₂)	44.8 ---- C4
3.11 (dd, $J_{H4\alpha, H4\beta} = 15.6\text{Hz}$, $J_{H4\alpha, H3} = 6.4\text{Hz}$, H4 α)	212.7 ---- C5
2.47 (dd, $J_{H4\beta, H4\alpha} = 15.6\text{Hz}$, $J_{H4\beta, H3} = 5.7\text{Hz}$, H4 β)	79.4 ---- C6
1.23 (s, 6-CH ₃)	41.3 ---- C7
1.79 (dd, $J_{H7\beta, H7\alpha} = 14.4\text{Hz}$, H7 β)	35.0 ---- C8
1.45 ($J_{H7\alpha, H8} = 5.90\text{ Hz}$, $J_{H7\alpha, H7\beta} = 14.4\text{Hz}$, H7 α)	84.0 ---- C9
1.70-1.85 (m, H8)	131.2 ---- C10
1.05 (d, $J_{8-CH3, H8} = 6.6\text{Hz}$, 8-CH ₃)	134.2 ---- C11
4.00 (dd, $J_{H9, H10} = 8.3\text{Hz}$, $J_{H9, H8} = 6.1\text{Hz}$, H9)	77.1 ---- C12
4.52, 4.40 (d, $J_{AB} = 12.3\text{Hz}$, 9-OCH ₂)	79.3 ---- C13
6.14 (d, $J = 8.4\text{Hz}$, H10)	24.4 ---- C14
1.44 (s, 12-CH ₃)	12.6 ---- 2-CH ₃
4.89 (dd, $J_{H13, H14} = 2.4, 10.9\text{Hz}$, H13)	26.8 ---- 6-CH ₃
1.75-1.82, 1.47-1.55 (m, 14-CH ₂)	19.6 ---- 8-CH ₃
0.80 (t, $J_{14-CH3, H14} = 7.4\text{Hz}$, 14-CH ₃)	25.1 ---- 12-CH ₃
	11.1 ---- 14-CH ₃
	73.3 ---- 6-OCH ₃
	72.2 ---- 9-OCH ₃

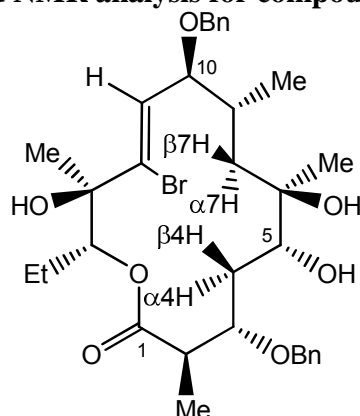
HMBC



NOESY

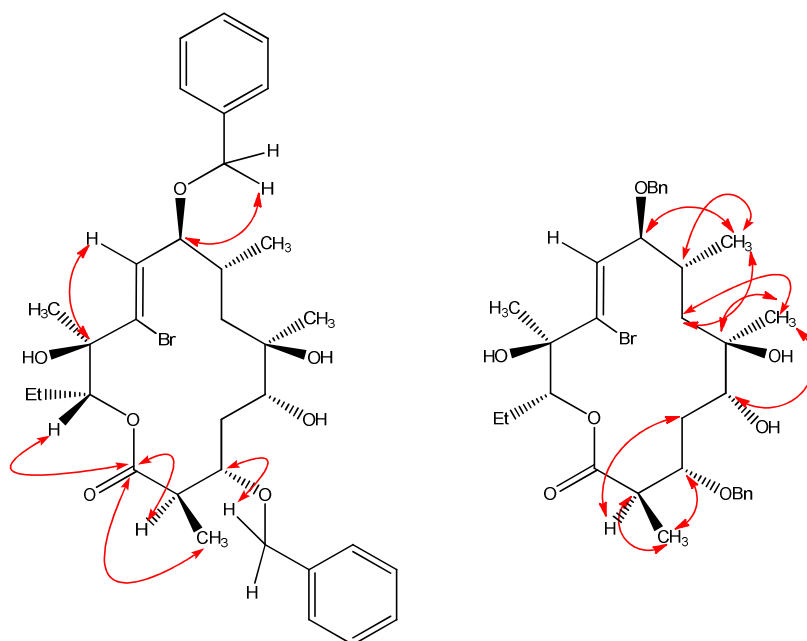


Detailed NMR analysis for compound 5.16

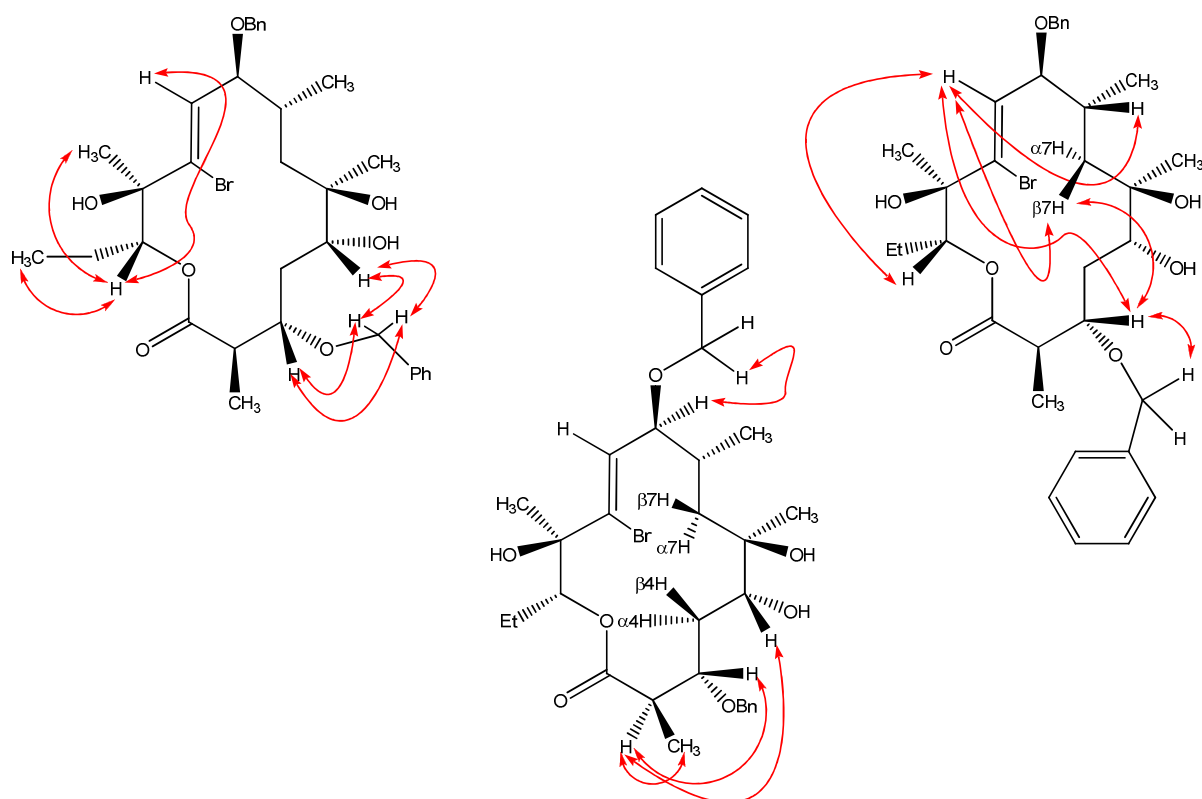


¹ H NMR chemical shifts (δ/ppm) & coupling constant (J/Hz)	¹³ C NMR chemical shift (δ/ppm)
2.65 (qd, J _{H2, 2-CH3} = 6.9Hz, J _{H2, H3} = 13.4Hz, H2)	176.8 ---- C1
1.27 (d, J _{2-CH3, H2} = 7.0Hz, 2-CH ₃)	44.8 ---- C2
4.36 (ddd, J _{H3, H2} = 8.6Hz, J _{H3, H4α} = 6.2Hz, J _{H3, H4β} = 2.9Hz, H3)	78.2 ---- C3
4.58, 4.51 (d, J _{AB} = 10.7Hz, C3-OCH ₂)	35.9 ---- C4
1.83 (dd, J _{H4α, H4β} = 15.0Hz, J _{H4α, H3} = 8.5 Hz, H4α)	75.2 ---- C5
1.77 (dd, J _{H4β, H4α} = 15.0Hz, J _{H4β, H3} = 3.0 Hz, H4β)	73.7 ---- C6
3.51 (dd, J _{H5, H4α} = 2.4 Hz, J _{H5, H4β} = 7.0 Hz, H5)	40.8 ---- C7
1.28 (s, 6-CH ₃)	34.6 ---- C8
1.61 (dd, J _{H7β, H8} = 6.1 Hz, J _{H7β, H7α} = 14.7Hz, H7β)	84.7 ---- C9
1.17 (dd, J _{H7α, H8} = 7.0 Hz, J _{H7α, H7β} = 14.9Hz, H7α)	131.4 ---- C10
2.31 (dt, J _{H8, 8-CH3} = 6.4Hz, H8)	133.0 ---- C11
1.12 (d, J _{8-CH3, H8} = 6.7Hz, 8-CH ₃)	77.6 ---- C12
4.11 (dd, J _{H9, H10} = 8.6Hz, J _{H9, H8} = 6.6Hz, H9)	81.3 ---- C13
4.58, 4.47 (d, J _{AB} = 12.4Hz, 9-OCH ₂)	24.7 ---- C14
6.38 (d, J _{H10, H9} = 8.6Hz, H10)	12.4 ---- 2-CH ₃
1.50 (s, 12-CH ₃)	27.7 ---- 6-CH ₃
4.88 (dd, J _{H13, H14} = 2.3, 11.0Hz, H13)	20.0 ---- 8-CH ₃
1.73-1.85 (m, 14-CH ₂)	26.0 ---- 12-CH ₃
0.89 (t, J _{14-CH3, H14} = 7.4Hz, 14-CH ₃)	11.4 ---- 14-CH ₃
	73.1 ---- 6-OCH ₃
	71.9 ---- 9-OCH ₃
	137.9, 139.0 ---- ipsoC (C ₃ , C ₉)
	128.1, 128.0 ---- orthoC (C ₃ , C ₉)
	126.5, 128.3 ---- metaC (C ₃ , C ₉)
	127.9, 127.6 ---- paraC (C ₃ , C ₉)

HMBC



NOESY



5. Chapter VI

General procedure of stoichiometric osmylation-fluorination:

The Selectfluor® (5 equiv.) was dissolved in *t*-BuOH and H₂O (1:1, 0.05 M), then allene (1 equiv.) was added, stirred at rt. for 1 min. and then OsO₄ solution (4% wt. solution in water, 1.1 equiv.) was added. The resulting dark solution was stirred at rt. for 1 hour, diluted with water, and then sodium sulfite was added. Extracted with ethyl acetate, then the combined organic layer was washed with saturated NaCl solution, dried over Na₂SO₄, filtered and then concentrated to dryness under reduced pressure to give the crude product which was further purified by FCC.

General procedure of stoichiometric osmylation-chlorination:

To a solution of the allene (1 equiv.) in *t*-BuOH and H₂O (1:1, 0.05 M) was added OsO₄ solution (4% wt. solution in water, 1.1 equiv.), stirred at rt. then N-chlorosuccinimide solution (2 equiv.) in *t*-BuOH, H₂O and acetone (1:1:1, 0.05 M) was added in one portion, stirred for 1 hr then quenched with saturated sodium sulfite solution and extracted with ethyl acetate. The organic layer was combined, washed with NaCl solution, dried over Na₂SO₄, filtered and then concentrated to dryness under reduced pressure to give the crude product, which was further purified by FCC.

General procedure of stoichiometric osmylation-bromination:

To a solution of the allene (1 equiv.) in *t*-BuOH (0.1 M) was added OsO₄ solution (4% wt. solution in water, 1.1 equiv.), stirred at rt. for 1 min. then N-bromosuccinimide (2 equiv.)

was added in one portion, stirred for 30 min. then quenched with saturated sodium sulfite solution, extracted with ethyl acetate. The organic layer was combined, washed with NaCl solution, dried over Na₂SO₄, filtered and then concentrated to dryness under reduced pressure to give the crude product, which was further purified by FCC to afford the desired product as colorless oil.

General procedure of catalytic osmylation-Fluorination:

The Selectfluor® (5 equiv.) was dissolved in 1:1 *t*-BuOH and H₂O (0.05 M), then NMO (2 equiv.) was added followed by the addition of allene (1 equiv.), stirred at room temperature until the Selectfluor® was dissolved, and then OsO₄ solution (4% wt. solution in H₂O, 0.1 equiv.) was added. The resulting dark solution was stirred at rt. for 8 hrs, diluted with water, and then sodium sulfite was added. Extracted with ethyl acetate twice, then the combined organic layer was washed with saturated NaCl solution, dried over Na₂SO₄, filtered and then concentrated to dryness under reduced pressure to give the crude product, which was further purified by FCC to afford the desired product.

General procedure of catalytic osmylation-Chlorination:

To a solution of the allene (1 equiv.) in *t*-BuOH and H₂O (1:1, 0.05 M) was added OsO₄ solution (4% wt. solution in water, 0.1 equiv.), stirred at rt. then N-chlorosuccinimide solution (2 equiv.) in *t*-BuOH, H₂O and acetone (1:1:1, 0.05 M) was delivered by syringe pump over 5 hours, stirred for an extra 1 hr then quenched with saturated sodium sulfite solution and extracted with ethyl acetate. The organic layer was combined, washed with

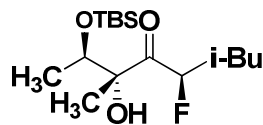
NaCl solution, dried over Na₂SO₄, filtered and then concentrated to dryness under reduced pressure to give the crude product, which was further purified by FCC.

General procedure of catalytic osmylation-Bromination:

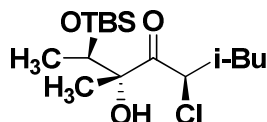
To a solution of the allene (1 equiv.) in *t*-BuOH and H₂O (1:1, 0.05 M) was added OsO₄ solution (4% wt. solution in water, 0.1 equiv.), stirred at rt. then *N*-bromosuccinimide solution (1 equiv.) in *t*-BuOH, H₂O and acetone (1:1:1, 0.05 M) was delivered by syringe pump over 6 hours, stirred for an extra 1 hr then quenched with saturated sodium sulfite solution and extracted with ethyl acetate. The organic layer was combined, washed with NaCl solution, dried over Na₂SO₄, filtered and then concentrated to dryness under reduced pressure to give the crude product, which was further purified by FCC.

General procedure of allene aminohydroxylation:

To a solution of K₂OsO₄ (0.05 equiv.) in *t*-BuOH and H₂O (1:1, 0.1 M) was added LiOH (3.0 equiv.) and *N*-bromoacetamide (3.0 equiv.). The resulting solution was stirred vigorously until it becomes a nearly clear colorless solution. Allene (1 equiv.) was then added to this solution and stirred until the completion of reaction indicated by TLC. The reaction was then quenched with saturated sodium sulfite solution and extracted with ethyl acetate. The organic layer was combined, washed with NaCl solution, dried over Na₂SO₄, filtered and then concentrated to dryness under reduced pressure to give the crude product, which was further purified by FCC.

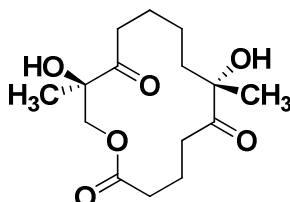
**6.9**

Known allene **6.8** (17.5 mg, 0.0652 mmol) was converted to **6.9** using the general procedure for stoichiometric osmylation-fluorination. FCC using 2% ethyl acetate in hexane gave **6.9** as a mixture of diastereomers (13.4 mg, 0.0418 mmol, 64%, d.r. = 5.9:1): IR ν_{max} (neat)/ cm^{-1} 3546, 2958, 2931, 2858, 1733, 1464, 1374, 1256, 1159, 1120, 1037, 982, 836. ^1H NMR (500 MHz, CDCl_3) δ 5.48 (1H, m), 4.05 (1H, q, $J = 6.11$ Hz), 2.83 (1H, s), 1.96 – 1.88 (1H, m), 1.81 – 1.68 (2H, m), 1.35 (3H, s), 1.08 (3H, d, $J = 6.36$ Hz), 1.01 (3H, d, $J = 6.85$ Hz), 0.98 (6H, d, $J = 6.26$ Hz), 0.90 (9H, s), 0.86 (3H, s); ^{13}C NMR (125 MHz, CDCl_3) δ 210.4 (d, $J = 16.75$), 92.2, 82.1, 72.4, 39.7, 25.8 (3), 25.7, 24.7, 23.3, 21.2, 18.6, 18.0, –4.3, –4.9; m/z (HRMS) calculated for $[\text{C}_{16}\text{H}_{33}\text{FO}_3\text{SiNa}]^+$: 343.2, found: 343.2; $[\alpha]_{\text{D}}^{25} = -46.5^\circ$ ($c = 0.01$, CHCl_3).

**6.10**

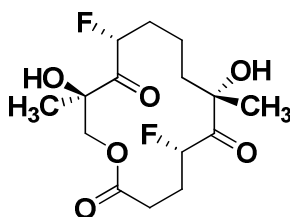
Known allene **6.8** (17.5 mg, 0.0652 mmol) was converted to **6.10** using the general procedure for stoichiometric osmylation-chlorination. FCC using 2% ethyl acetate in hexane gave **6.10** as a mixture of diastereomers (17.1 mg, 0.0509 mmol, 78%, d.r. = 5.3:1): IR ν_{max} (neat)/ cm^{-1} 3544, 2958, 2931, 2858, 1723, 1464, 1375, 1257, 1169, 1104, 1029, 1008, 837. ^1H NMR (500 MHz, CDCl_3) δ 5.02 (1H, dd, $J = 4.7, 10.2$ Hz), 3.97 (1H, q, $J = 6.3$ Hz), 2.77 (1H, s), 1.90 – 1.82 (1H, m), 1.71 – 1.66 (2H, m), 1.42 (3H, s), 1.04 (3H, d, $J = 6.3$ Hz), 0.97 (3H, d, $J = 6.7$ Hz), 0.93 (3H, d, $J = 6.3$ Hz), 0.91 (3H, s), 0.90 (9H, s), 0.88

(3H, s); ^{13}C NMR (125 MHz, CDCl_3) δ 208.2, 82.1, 73.3, 55.7, 40.9, 25.8 (3), 25.7, 24.8, 23.1, 21.1, 18.4, 18.0, -4.26 , -4.81 ; m/z (HRMS) calculated for $[\text{C}_{16}\text{H}_{33}\text{ClO}_3\text{SiNa}]^+$: 359.2, found: 359.2; $[\alpha]_D^{25} = 24.8^\circ$ ($c = 0.01$, CHCl_3).

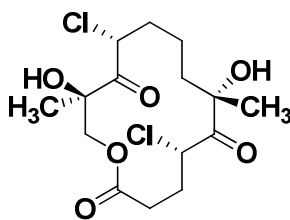


S1 (Table VI.4, entry 1)

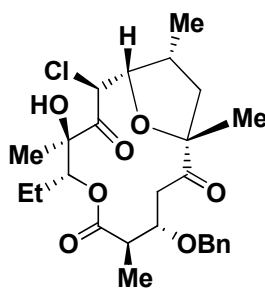
Known racemic allene **6.21** (8.0 mg, 0.034 mmol) was dissolved in 1.5 mL *t*-BuOH and 1.0 mL H_2O , then 12 mg acetic acid was added, stirred for 20 mins then OsO_4 (0.48 mL, 4% wt. solution in water, 2.2 equiv.) was added, stirred for another 30 mins then quenched by 20 mg Na_2SO_3 . The reaction mixture was diluted with 5 mL H_2O and extracted with ethyl acetate (2 x 3 mL). The organic layer was concentrated to dryness under reduced pressure to give the crude product, which upon further purification by FCC using 30% ethyl acetate to afford the racemic product **S1** as colorless oil (4.6 mg, 0.015 mmol, 45%): IR ν_{max} (neat)/ cm^{-1} 3479, 2923, 2851, 1713, 1458, 1374, 1133; ^1H NMR (500 MHz, CDCl_3) δ 4.43 (1H, d, $J = 11.7$ Hz), 4.18 (1H, s), 4.16 (1H, d, $J = 11.7$ Hz), 3.94 (1H, s), 2.62 (1H, m), 2.56 (1H, m), 2.50 (1H, m), 2.31 (3H, m), 2.19 (1H, m), 1.91 (2H, m), 1.74 (1H, m), 1.62 (1H, m), 1.52 (1H, m), 1.36 (3H, s), 1.35 (3H, s), 1.25 (1H, m), 0.54 (1H, m); ^{13}C NMR (125 MHz, CDCl_3) δ 213.0, 210.0, 172.4, 80.5, 78.4, 69.7, 39.7, 33.6, 33.5, 32.3, 25.9, 21.8, 21.6, 21.5, 18.2; m/z (HRMS) calculated for $[\text{C}_{15}\text{H}_{24}\text{O}_6\text{Na}]^+$: 323.2, found: 323.2

**S2** (Table VI.4, entry 2)

Known racemic allene **6.21** (10.4 mg, 0.0448 mmol) was dissolved in 1.0 mL *t*-BuOH and 0.5 mL H₂O, and then Selectfluor® (64 mg, 0.18 mmol) was added followed by the addition of OsO₄ solution (0.636 mL, 4% wt. solution in H₂O, 0.1 mmol) at room temperature, stirred for 90 mins then quenched by adding 20 mg Na₂SO₃. Diluted with 10 mL H₂O, extracted with ethyl acetate (2 x 8 mL). Organic layer was separated, dried with Na₂SO₄, filtered, concentrated to dryness under reduced pressure to gave the crude product, which upon further purification by FCC using 40% ethyl acetate in hexane to give the racemic product **S2** as a colorless oil (8.4 mg, 0.025 mmol, 56%): IR ν_{max} (neat)/cm⁻¹ 3479, 2927, 2853, 1727, 1455, 1372, 1162; ¹H NMR (500 MHz, CDCl₃) δ 5.43 (1H, ddd, *J* = 46.4, 8.14, 3.25), 5.28 (1H, ddd, *J* = 47.1, 5.7, 2.7 Hz), 4.54 (1H, dd, *J* = 11.3, 1.8 Hz), 4.22 (1H, dd, *J* = 11.3, 3.8 Hz), 3.80 (2H, s), 2.46 (1H, m), 2.35 (1H, s), 2.29 (1H, m), 2.26 (1H, m), 2.08 (2H, m), 1.89 (1H, m), 1.64 (1H, m), 1.46 (6H, s), 1.46 (1H, m) 0.89 (1H, m); ¹³C NMR (125 MHz, CDCl₃) δ 209.9, 209.4, 171.7, 94.9, 90.9, 80.1, 78.5, 69.2, 40.4, 31.7, 28.2, 28.0, 25.0, 21.1, 17.4; *m/z* (HRMS) calculated for [C₁₅H₂₂F₂O₆Na]⁺: 359.1, found: 359.1.

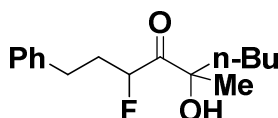
**S3** (Table VI.4, entry 3)

Known racemic allene **6.21** (14.0 mg, 0.0603 mmol) was dissolved in 2.0 mL *t*-BuOH and 1.0 mL H₂O, and then N-chlorosuccinimide (32.0 mg, 0.241 mmol) was added followed by the addition of OsO₄ solution (0.843 mL, 4% wt. solution in H₂O, 0.133 mmol) at room temperature, stirred for 90 mins then quenched by adding 20 mg Na₂SO₃. Diluted with 10 mL H₂O, extracted with ethyl acetate (2 x 8 mL). Organic layer was separated, dried with Na₂SO₄, filtered, concentrated to dryness under reduced pressure to gave the crude product, which upon further purification by FCC using 40% ethyl acetate in hexane to give the racemic product **S3** as a colorless oil, which could be crystallized by slow evaporation of solvent (20% diethyl ether in hexane at room temperature) to afford a white needle crystal (11.2 mg, 0.0304 mmol, 52%, see below for X-ray structure): IR ν_{max} (neat)/cm⁻¹ 3433, 2920, 2850, 1739, 1462, 1375, 1241, 1157; ¹H NMR (500 MHz, CDCl₃) δ 4.93 (1H, dd, J = 11.4, 3.8 Hz), 4.87 (1H, dd, J = 10.5, 3.9 Hz), 4.59 (1H, d, J = 11.1 Hz), 3.88 (1H, d, J = 11.1 Hz), 2.71 (1H, s), 2.47 (1H, m), 2.32 (1H, m), 2.29 (1H, m), 2.21 (1H, m), 2.18 (1H, m), 2.11 (1H, s), 1.97 (1H, m), 1.73 (1H, m), 1.49 (6H, s), 1.47 (1H, m), 1.41 (1H, m), 0.69 (1H, m); ¹³C NMR (125 MHz, CDCl₃) δ 209.8, 207.5, 171.4, 80.5, 79.1, 71.4, 54.0, 53.4, 41.6, 33.2, 30.8, 29.9, 27.6, 24.3, 21.7; *m/z* (HRMS) calculated for [C₁₅H₂₂Cl₂O₆H]⁺: 367.1, 369.1, 372.1, found: 367.1, 369.1, 372.1.

**6.23**

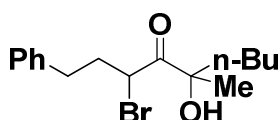
Known allene **6.22** (13.2 mg, 0.0264 mmol) was dissolved in 1 mL *t*-BuOH and 0.5 mL H₂O, then OsO₄ (0.335 mL, 4% wt. solution in H₂O, 0.0528 mmol) was added, stirred at room temperature for 5 mins then N-chlorosuccinimide (10.5 mg, 0.0792 mmol) in 0.5 mL acetone was added, stirred at room temperature for 18 hours then quenched by addition of 10 mg Na₂SO₃. The *t*-BuOH solvent was removed under reduced pressure, and the aqueous residue was extracted with diethyl ether (2 x 3 mL). Organic layer was combined, dried over Na₂SO₄, filtered and then concentrated under reduced pressure to gave the crude product, which upon further purification by FCC using 10% ethyl acetate in hexane to afford **6.23** as a colorless oil (7.7 mg, 0.016 mmol, 59%): IR ν_{max} (neat)/cm⁻¹ 2971, 2936, 1740, 1717, 1456, 1375, 1300, 1168, 1102, 1071; ¹H NMR (500 MHz, CDCl₃) δ 7.39 (2H, m), 7.34 (2H, m), 7.29 (1H, m), 4.93 (1H, d, *J* = 11.6 Hz), 4.68 (1H, dd, *J* = 8.1, 4.0 Hz), 4.51 (1H, dd, *J* = 10.3, 4.0 Hz), 4.48 (1H, d, *J* = 10.3 Hz), 4.46 (1H, d, *J* = 11.6 Hz), 3.77 (1H, ddd, *J* = 10.7, 6.4, 1.7 Hz), 3.68 (1H, s), 3.29 (1H, dd, *J* = 1.7 Hz), 2.65 (1H, dd, *J* = 13.8, 6.4 Hz), 2.54 (1H, dd, *J* = 0.8 Hz), 2.50 (1H, m), 2.49 (1H, m), 1.95 (1H, m), 1.82 (1H, dd, *J* = 13.8, 7.7 Hz), 1.68 (3H, s), 1.56 (1H, m), 1.30 (3H, d, *J* = 7.3 Hz), 1.28 (3H, s), 0.93 (3H, t, *J* = 7.5 Hz), 0.89 (3H, d, *J* = 7.1 Hz); ¹³C NMR (125 MHz, CDCl₃) δ 206.8, 205.8, 173.7, 138.0, 128.6, 128.3, 127.7, 90.1, 79.5, 79.1, 78.3, 76.3, 70.9, 51.7, 43.9, 38.9, 34.7,

34.6, 24.8, 23.2, 17.0, 16.2, 14.2, 10.9; m/z (HRMS) calculated for $[C_{26}H_{35}ClO_7Na]^+$: 517.2, found: 517.2.



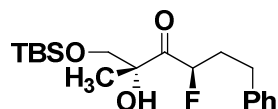
S4 (Table VI.2, entry 2)

Known racemic allene **6.11** (100 mg, 0.467 mmol) was converted to **S4** using the general procedure for catalytic osmylation-fluorination. FCC using 2% ethyl acetate in hexane afforded racemic **S4** as colorless oil (72.7 mg, 0.273 mmol, 58%, inseparable mixture of diastereomers, d.r. = 1.8:1): IR ν_{\max} (neat)/ cm^{-1} 3501, 3028, 2958, 2932, 2871, 1724, 1604, 1497, 1455, 1373, 1222, 1162, 1072, 1030, 1009; ^1H NMR (500 MHz, CDCl_3) δ 7.42 – 7.25 (2H, m), 7.21 (3H, m), 5.15 – 5.05 (m, 1H), 3.84 (1H, s), 2.93 – 2.81 (m, 1H), 2.77 (m, 1H), 2.66 (dd, $J = 17.5, 9.9$ Hz, 2H), 2.51 (m, 2H), 2.07 – 1.91 (m, 2H), 1.64 (m, 1H), 1.40 (t, $J = 3.7$ Hz, 1H), 1.31 (s, 3H), 0.88 – 0.76 (m, 3H); ^{13}C NMR (126 MHz, CDCl_3) δ 214.50, 141.52, 128.84, 128.66, 126.28, 78.91, 39.56, 38.79, 35.04, 33.96, 33.79, 31.13, 25.93, 25.74, 25.21, 23.10, 14.13; m/z (ESI-MS) calculated for $[C_{16}H_{23}FO_2Na]^+$: 289.2, found: 289.2



S5 (Table VI.2, entry 3)

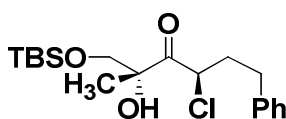
Known racemic allene **6.11** (100 mg, 0.467 mmol) was converted to **S5** using the general procedure for catalytic osmylation-bromination. FCC using 2% ethyl acetate in hexane afforded racemic **S5** as colorless oil (98.6 mg, 0.302 mmol, 64%, inseparable mixture of diastereomers, d.r. = 2:1 by crude ^1H NMR): IR ν_{max} (neat)/ cm^{-1} 3505, 3027, 2957, 2932, 2862, 1714, 1603, 1497, 1454, 1371, 1229, 1178, 1091, 1030, 1003; ^1H NMR (500 MHz, CDCl_3) δ 7.37 – 7.28 (m, 2H), 7.23 – 7.15 (m, 3H), 4.81 – 4.72 (m, 1H), 2.94 – 2.80 (m, 2H), 2.75 – 2.65 (m, 1H), 2.42 – 2.27 (m, 1H), 2.27 – 2.16 (m, 1H), 1.73 – 1.62 (m, 1H), 1.62 – 1.51 (m, 1H), 1.45 – 1.39 (s, 3H), 1.31 – 1.21 (m, 2H), 1.21 – 1.02 (m, 1H), 0.88 (t, $J = 7.3$ Hz, 3H); ^{13}C NMR (126 MHz, CDCl_3) δ 209.07, 140.22, 128.86, 128.63, 126.66, 79.95, 48.37, 45.29, 40.20, 39.59, 35.13, 33.31, 26.86, 25.79, 23.07, 14.15; m/z (ESI-MS) calculated for $[\text{C}_{16}\text{H}_{23}\text{BrO}_2\text{Na}]^+$: 349.2, 351.2, found: 349.2, 351.2



S6 (Table VI.2, entry 5)

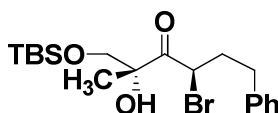
Known racemic allene **6.12** (100mg, 0.331 mmol) was converted to **S6** using the general procedure for catalytic osmylation-fluorination. FCC using 1% ethyl acetate in hexane afforded the desired racemic **S6** as colorless oil (68.2 mg, 0.193 mmol, 57%, d.r. = 5:1): IR ν_{max} (neat)/ cm^{-1} 3507, 3028, 2955, 2929, 2857, 1716, 1497, 1471, 1463, 1362, 1258, 1100, 1016; ^1H NMR (500 MHz, CDCl_3) δ 7.35 – 7.25 (m, 2H), 7.25 – 7.11 (m, 3H), 5.21 (ddd, $J = 49.6, 9.2, 3.2$ Hz, 1H), 4.09 (dd, $J = 9.9, 1.3$ Hz, 1H), 3.53 (s, 1H), 3.51 (dd, $J = 10.0, 2.3$ Hz, 1H), 2.93 – 2.83 (m, 1H), 2.81 – 2.71 (m, 1H), 2.20 – 2.06 (m, 2H), 1.31 (s, 3H), 0.84 (s, 9H), 0.06 – 0.04 (m, 3H), 0.02 (d, $J = 3.0$ Hz, 3H); ^{13}C NMR (126 MHz, CDCl_3) δ 210.77

(d, $J = 20.0$ Hz), 140.54, 128.76, 128.71, 126.48, 93.32 (d, $J = 183.8$ Hz), 80.39, 68.77, 33.62 (d, $J = 21.3$ Hz), 29.89 (d, $J = 37.5$ Hz), 25.97, 21.26 (d, $J = 3.8$ Hz), 18.41, -5.31; m/z (ESI-MS) calculated for $[C_{19}H_{31}FO_3SiNa]^+$: 377.2, found: 377.2



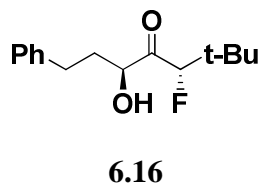
S7 (Table VI.2, entry 6)

Known racemic allene **6.12** (100mg, 0.331 mmol) was converted to **S7** using the general procedure for catalytic osmylation-fluorination. FCC using 1% ethyl acetate in hexane afforded the desired racemic **S7** as colorless oil (67.8 mg, 0.183 mmol, 55%): IR ν_{\max} (neat)/ cm^{-1} 3535, 3028, 2954, 2929, 2857, 1726, 1497, 1471, 1455, 1362, 1258, 1097, 1006; ^1H NMR (500 MHz, CDCl_3) δ 7.29 (dd, $J = 10.3, 4.4$ Hz, 2H), 7.24 – 7.14 (m, 3H), 4.92 (dd, $J = 9.3, 4.5$ Hz, 1H), 3.93 (d, $J = 9.7$ Hz, 1H), 3.42 (d, $J = 9.7$ Hz, 1H), 3.30 (bs, 1H), 2.86 (m, 1H), 2.77 – 2.62 (m, 1H), 2.25 – 2.15 (m, 1H), 2.11 (ddd, $J = 14.3, 9.7, 5.0$ Hz, 1H), 1.30 (s, 3H), 0.85 – 0.76 (s, 9H), 0.04 (s, $J = 5.0$ Hz, 3H), 0.03 – -0.02 (s, 3H); ^{13}C NMR (126 MHz, CDCl_3) δ 208.69, 140.53, 128.79, 128.66, 126.51, 80.19, 69.19, 56.42, 34.86, 32.37, 25.99, 22.79, 18.40, 14.35, -5.32, -5.38; m/z (ESI-MS) calculated for $[C_{19}H_{31}ClO_3SiNa]^+$: 393.2, found: 393.2



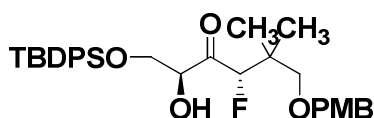
S8 (Table VI.2, entry 7)

Known racemic allene **6.12** (100mg, 0.331 mmol) was converted to **S8** using the general procedure for catalytic osmylation-bromination. FCC using 1% ethyl acetate in hexane afforded the desired racemic **S8** as colorless oil (64.0 mg, 0.154 mmol, 46%): IR ν_{max} (neat)/ cm^{-1} 3537, 2954, 2929, 2857, 1718, 1497, 1455, 1362, 1254, 1093, 1006; ^1H NMR (500 MHz, CDCl_3) δ 7.33 – 7.27 (m, 2H), 7.21 (m, 3H), 4.91 (dd, $J = 8.8, 5.5$ Hz, 1H), 3.89 (t, $J = 9.4$ Hz, 1H), 3.42 (t, $J = 8.8$ Hz, 1H), 3.24 (bs, 1H), 2.91 – 2.77 (m, 1H), 2.75 – 2.60 (m, 1H), 2.32 – 2.13 (m, 2H), 1.40 (s, 3H), 0.86 – 0.75 (s, 9H), 0.06 – 0.03 (s, 3H), 0.03 – 0.01 (s, 3H); ^{13}C NMR (126 MHz, CDCl_3) δ 208.84, 140.54, 128.79, 128.64, 126.51, 80.12, 69.71, 46.07, 34.75, 33.40, 26.01, 23.64, 18.41, -5.31, -5.36; m/z (ESI-MS) calculated for $[\text{C}_{19}\text{H}_{31}\text{BrO}_3\text{SiNa}]^+$: 439.1, 437.1, found: 439.1, 437.1.



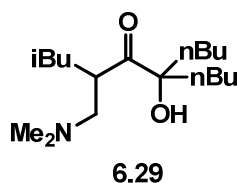
Known racemic allene **6.13** (50mg, 0.25 mmol) was converted to **6.16** using the general procedure for catalytic osmylation-fluorination. FCC using 5% ethyl acetate in hexane afforded the racemic product **6.16** as colorless oil (34.4 mg, 0.137 mmol, 54%, single anti-diastereomer): IR ν_{max} (neat)/ cm^{-1} 3496, 3028, 2961, 2872, 1720, 1603, 1497, 1481, 1455, 1398, 1368, 1253, 1127, 1088, 1071, 1057, 1011; ^1H NMR (500 MHz, CDCl_3) δ 7.30 (t, $J = 7.2$ Hz, 2H), 7.22 (dd, $J = 14.5, 7.3$ Hz, 3H), 4.59 (t, $J = 31.8$ Hz, 1H), 4.41 (d, $J = 8.3$ Hz, 1H), 3.26 (s, 1H), 2.94 – 2.85 (m, 1H), 2.85 – 2.70 (m, 1H), 2.24 (dd, $J = 19.9, 9.3$ Hz, 1H), 1.72 – 1.59 (m, 1H), 1.12 – 1.01 (m, 9H); ^{13}C NMR (126 MHz, CDCl_3) δ 210.90 (d),

141.25, 128.80, 128.70, 126.33, 100.68 (d), 74.99 (d), 36.11 (d), 35.04 (d), 32.01, 26.04 (d).



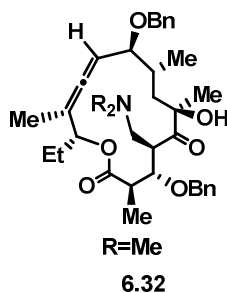
S15 (Table 3, entry 10)

Known allene **6.17** (35.0mg, 0.0700 mmol) was converted to **6.18** using the general procedure for catalytic osmylation-fluorination. FCC using 10% ethyl acetate in hexane afforded the desired product **6.18** as colorless oil (23.8 mg, 0.0431 mmol, 62%): IR ν_{max} (neat)/ cm^{-1} 3071, 3048, 2957, 2931, 2857, 1725, 1427, 1362, 1247, 1173, 1112, 1035, 1008, 736, 702; ^1H NMR (500 MHz, CDCl_3) δ 7.67 – 7.63 (4H, m), 7.45 – 7.36 (6H, m), 7.21 – 7.18 (2H, m), 6.87 – 6.84 (2H, m), 5.16 (1H, d, $J = 47.2$ Hz), 4.49 – 4.46 (1H, m), 4.37 (2H, s), 3.96 (1H, ddd, $J = 1.0, 3.4, 10.8$ Hz), 3.89 (1H, ddd, $J = 1.0, 4.4, 10.8$ Hz), 3.80 (3H, s), 3.53 (1H, dd, $J = 6.9$ Hz), 3.19 (1H, dd, $J = 9.3$ Hz), 1.02 (9H, s), 1.00 (6H, s); ^{13}C NMR (125 MHz, CDCl_3) δ 208.0, 207.8, 159.2, 135.7, 135.6, 132.9, 132.6, 129.8, 129.1, 127.7, 113.7, 97.0, 95.5, 76.5, 75.0, 72.8, 65.2, 55.2, 40.2, 40.1, 26.7, 20.9, 19.2; m/z (HRMS) calculated for $[\text{C}_{32}\text{H}_{41}\text{FO}_5\text{SiNa}]^+$: 575.3, found: 575.3; $[\alpha]_D^{25} = 18.4^\circ$ ($c = 0.01$, CHCl_3).



To the solution of known allene (30.0 mg, 0.140 mmol) **6.4** in anhydrous DCM (3 mL), dimethylmethylenediammonium chloride (70.0 mg, 0.700 mmol), and OsO_4 solution (3.0

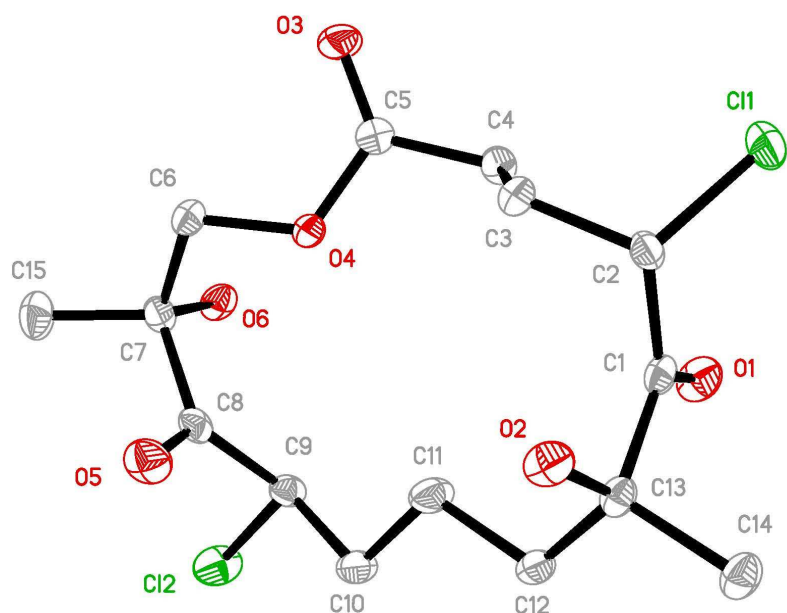
mL, 0.15 mmol, 0.050 M in DCM) were added at room temperature. The mixture was stirred for 1 hour, and then quenched by saturated solution of Na₂SO₃. The organic layer was extracted in DCM. The crude product was purified by FCC to give **6.29** as a slight yellowish oil (27.3 mg, 63% yield): ¹H NMR (500 MHz, CDCl₃) 3.92 (1H, s), 3.50 – 3.38 (1H, m), 2.46 (2H, t, *J* = 7.6), 2.30 (6H, s), 1.76 – 1.00 (15H, m), 0.96 – 0.84 (12H, m); ¹³C NMR (125 MHz, CDCl₃) δ 219.7, 81.2, 64.4, 45.6, 42.3, 39.0, 38.7, 37.4, 26.3, 25.6, 25.5, 23.2, 23.1, 23.0, 22.7, 14.1, 13.9; *m/z* (HRMS) calculated for [C₁₈H₃₇NO₂H]⁺: 300.3, found: 300.3.



To the solution of known allene (15.0 mg, 0.030 mmol) **3.1** in anhydrous DCM (1 mL), dimethylmethyldeneammonium chloride (7.0 mg, 0.070 mmol), and OsO₄ solution (0.8 mL, 0.040 mmol, 0.050 M in DCM) were added at room temperature. The mixture was stirred for 1 hour, and then quenched by saturated solution of Na₂SO₃. The organic layer was extracted in DCM. The crude product was purified by FCC to give **6.29** as a slight yellowish oil (8.3 mg, 0.014 mmol, 46%): ¹H NMR (500 MHz, Chloroform-d) δ 7.41 – 7.19 (m, 10H), 5.15 (dd, *J* = 14.2, 3.4 Hz, 2H), 4.71 (d, *J* = 12.1 Hz, 1H), 4.63 – 4.52 (m, 2H), 4.46 – 4.34 (m, 2H), 3.37 (t, *J* = 9.2 Hz, 1H), 3.09 (td, *J* = 9.4, 8.9, 6.0 Hz, 1H), 3.01 (dd, *J* = 12.1, 10.2 Hz, 1H), 2.66 (d, *J* = 8.2 Hz, 1H), 2.49 – 2.40 (m, 1H), 2.37 (dd, *J* = 12.1, 6.1 Hz, 1H), 2.14 (s, 3H), 2.03 – 1.95 (m, 1H), 1.90 (m, *J* = 15.4, 7.7, 4.2 Hz, 1H), 1.76 (d, *J* = 2.5 Hz, 2H), 1.61 (dq, *J* = 14.9, 7.3, 4.8 Hz, 2H), 1.32 (s, 2H), 1.29 – 1.24 (m, 2H),

1.20 (dd, $J = 9.1, 6.8$ Hz, 3H), 1.18 – 1.12 (m, 3H), 1.09 (t, $J = 7.1$ Hz, 3H), 0.92 – 0.80 (m, 3H), 0.77 (t, $J = 7.4$ Hz, 3H); ^{13}C NMR (126 MHz, CDCl_3) δ 217.92, 203.41, 174.52, 138.72, 138.13, 128.78, 128.55, 128.51, 128.49, 128.19, 127.99, 127.72, 127.20, 98.36, 93.46, 85.16, 81.29, 77.98, 77.96, 74.53, 70.45, 59.10, 57.80, 46.08, 45.81, 42.65, 41.33, 40.89, 33.73, 31.81, 29.92, 25.60, 24.29, 22.88, 20.88, 16.12, 14.34, 9.97, 7.84.

X-ray ORTEP diagram of compound **S3**:



X-ray crystallography data of **S3**:

Table 1. Crystal data and structure refinement for kl2076.

Identification code	kl2076	
Empirical formula	C ₁₅ H ₂₂ Cl ₂ O ₆	
Formula weight	369.23	
Temperature	100(2) K	
Wavelength	0.71073 Å	
Crystal system	Monoclinic	
Space group	P2(1)/c	
Unit cell dimensions	a = 9.8209(9) Å	α = 90°.
	b = 18.5191(18) Å	β = 102.619(2)°.
	c = 9.5660(9) Å	γ = 90°.
Volume	1697.8(3) Å ³	
Z	4	
Density (calculated)	1.445 Mg/m ³	
Absorption coefficient	0.409 mm ⁻¹	

F(000)	776
Crystal size	1.00 x 0.02 x 0.01 mm ³
Theta range for data collection	2.13 to 28.28°.
Index ranges	-13<=h<=13, -24<=k<=24, -12<=l<=12
Reflections collected	15055
Independent reflections	4203 [R(int) = 0.0537]
Completeness to theta = 28.28°	99.8 %
Absorption correction	Semi-empirical from equivalents
Max. and min. transmission	0.9959 and 0.6850
Refinement method	Full-matrix least-squares on F ²
Data / restraints / parameters	4203 / 0 / 222
Goodness-of-fit on F ²	1.005
Final R indices [I>2sigma(I)]	R1 = 0.0544, wR2 = 0.1146
R indices (all data)	R1 = 0.0814, wR2 = 0.1263
Largest diff. peak and hole	0.581 and -0.261 e.Å ⁻³

Table 2. Atomic coordinates ($\times 10^4$) and equivalent isotropic displacement parameters ($\text{\AA}^2 \times 10^3$)

for kl2076. $U(\text{eq})$ is defined as one third of the trace of the orthogonalized U_{ij} tensor.

	x	y	z	$U(\text{eq})$
Cl(1)	2478(1)	3446(1)	4751(1)	31(1)
Cl(2)	10966(1)	1346(1)	5794(1)	30(1)
O(1)	5347(2)	3626(1)	4328(2)	26(1)
O(2)	6265(2)	3700(1)	8086(2)	22(1)
O(3)	3946(2)	743(1)	5584(2)	27(1)
O(4)	6065(2)	1236(1)	6319(2)	19(1)
O(5)	9164(2)	1353(1)	8370(2)	28(1)
O(6)	7973(2)	413(1)	5133(2)	21(1)
C(1)	5296(2)	3610(1)	5576(3)	17(1)
C(2)	4041(2)	3310(1)	6086(3)	18(1)
C(3)	4244(2)	2510(1)	6484(2)	17(1)
C(4)	4267(2)	2013(1)	5211(3)	18(1)
C(5)	4703(2)	1260(1)	5709(2)	17(1)
C(6)	6652(2)	568(1)	6964(3)	19(1)
C(7)	8098(2)	494(1)	6638(3)	17(1)
C(8)	8889(2)	1198(1)	7118(3)	18(1)
C(9)	9306(2)	1695(1)	6003(3)	19(1)
C(10)	9412(2)	2480(1)	6437(3)	22(1)
C(11)	7969(2)	2771(1)	6497(3)	26(1)
C(12)	7917(2)	3589(1)	6526(3)	20(1)
C(13)	6522(2)	3900(1)	6725(2)	17(1)
C(14)	6520(3)	4720(1)	6552(3)	22(1)
C(15)	8863(3)	-144(1)	7456(3)	29(1)

Table 3. Bond lengths [Å] and angles [°] for kl2076.

Cl(1)-C(2)	1.787(2)
Cl(2)-C(9)	1.806(2)
O(1)-C(1)	1.206(3)
O(2)-C(13)	1.428(3)
O(2)-H(2O)	0.76(3)
O(3)-C(5)	1.203(3)
O(4)-C(5)	1.338(3)
O(4)-C(6)	1.446(3)
O(5)-C(8)	1.204(3)
O(6)-C(7)	1.426(3)
O(6)-H(6O)	0.74(3)
C(1)-C(2)	1.526(3)
C(1)-C(13)	1.539(3)
C(2)-C(3)	1.532(3)
C(2)-H(2)	0.98(3)
C(3)-C(4)	1.530(3)
C(3)-H(3A)	0.9900
C(3)-H(3B)	0.9900
C(4)-C(5)	1.504(3)
C(4)-H(4A)	0.9900
C(4)-H(4B)	0.9900
C(6)-C(7)	1.525(3)
C(6)-H(6A)	0.9900
C(6)-H(6B)	0.9900
C(7)-C(15)	1.521(3)
C(7)-C(8)	1.535(3)
C(8)-C(9)	1.531(3)
C(9)-C(10)	1.509(3)
C(9)-H(9)	0.95(3)
C(10)-C(11)	1.528(3)
C(10)-H(10A)	0.9900
C(10)-H(10B)	0.9900
C(11)-C(12)	1.517(3)
C(11)-H(11A)	0.9900
C(11)-H(11B)	0.9900

C(12)-C(13)	1.536(3)
C(12)-H(12A)	0.9900
C(12)-H(12B)	0.9900
C(13)-C(14)	1.527(3)
C(14)-H(14A)	0.9800
C(14)-H(14B)	0.9800
C(14)-H(14C)	0.9800
C(15)-H(15A)	0.9800
C(15)-H(15B)	0.9800
C(15)-H(15C)	0.9800
C(13)-O(2)-H(2O)	110(2)
C(5)-O(4)-C(6)	118.80(17)
C(7)-O(6)-H(6O)	109(2)
O(1)-C(1)-C(2)	122.5(2)
O(1)-C(1)-C(13)	120.2(2)
C(2)-C(1)-C(13)	117.3(2)
C(1)-C(2)-C(3)	111.17(18)
C(1)-C(2)-Cl(1)	110.40(17)
C(3)-C(2)-Cl(1)	110.99(16)
C(1)-C(2)-H(2)	111.1(16)
C(3)-C(2)-H(2)	110.2(16)
Cl(1)-C(2)-H(2)	102.7(16)
C(4)-C(3)-C(2)	114.04(19)
C(4)-C(3)-H(3A)	108.7
C(2)-C(3)-H(3A)	108.7
C(4)-C(3)-H(3B)	108.7
C(2)-C(3)-H(3B)	108.7
H(3A)-C(3)-H(3B)	107.6
C(5)-C(4)-C(3)	110.95(19)
C(5)-C(4)-H(4A)	109.4
C(3)-C(4)-H(4A)	109.4
C(5)-C(4)-H(4B)	109.4
C(3)-C(4)-H(4B)	109.4
H(4A)-C(4)-H(4B)	108.0
O(3)-C(5)-O(4)	123.6(2)
O(3)-C(5)-C(4)	125.5(2)

O(4)-C(5)-C(4)	110.92(19)
O(4)-C(6)-C(7)	106.94(18)
O(4)-C(6)-H(6A)	110.3
C(7)-C(6)-H(6A)	110.3
O(4)-C(6)-H(6B)	110.3
C(7)-C(6)-H(6B)	110.3
H(6A)-C(6)-H(6B)	108.6
O(6)-C(7)-C(15)	111.24(19)
O(6)-C(7)-C(6)	109.73(19)
C(15)-C(7)-C(6)	109.9(2)
O(6)-C(7)-C(8)	108.50(19)
C(15)-C(7)-C(8)	110.1(2)
C(6)-C(7)-C(8)	107.21(18)
O(5)-C(8)-C(9)	120.9(2)
O(5)-C(8)-C(7)	119.3(2)
C(9)-C(8)-C(7)	119.8(2)
C(10)-C(9)-C(8)	113.6(2)
C(10)-C(9)-Cl(2)	111.48(16)
C(8)-C(9)-Cl(2)	104.28(15)
C(10)-C(9)-H(9)	110.7(17)
C(8)-C(9)-H(9)	111.6(17)
Cl(2)-C(9)-H(9)	104.7(17)
C(9)-C(10)-C(11)	109.94(19)
C(9)-C(10)-H(10A)	109.7
C(11)-C(10)-H(10A)	109.7
C(9)-C(10)-H(10B)	109.7
C(11)-C(10)-H(10B)	109.7
H(10A)-C(10)-H(10B)	108.2
C(12)-C(11)-C(10)	112.83(19)
C(12)-C(11)-H(11A)	109.0
C(10)-C(11)-H(11A)	109.0
C(12)-C(11)-H(11B)	109.0
C(10)-C(11)-H(11B)	109.0
H(11A)-C(11)-H(11B)	107.8
C(11)-C(12)-C(13)	114.31(18)
C(11)-C(12)-H(12A)	108.7

C(13)-C(12)-H(12A)	108.7
C(11)-C(12)-H(12B)	108.7
C(13)-C(12)-H(12B)	108.7
H(12A)-C(12)-H(12B)	107.6
O(2)-C(13)-C(14)	111.17(19)
O(2)-C(13)-C(12)	110.87(19)
C(14)-C(13)-C(12)	109.84(18)
O(2)-C(13)-C(1)	107.09(18)
C(14)-C(13)-C(1)	106.69(19)
C(12)-C(13)-C(1)	111.08(19)
C(13)-C(14)-H(14A)	109.5
C(13)-C(14)-H(14B)	109.5
H(14A)-C(14)-H(14B)	109.5
C(13)-C(14)-H(14C)	109.5
H(14A)-C(14)-H(14C)	109.5
H(14B)-C(14)-H(14C)	109.5
C(7)-C(15)-H(15A)	109.5
C(7)-C(15)-H(15B)	109.5
H(15A)-C(15)-H(15B)	109.5
C(7)-C(15)-H(15C)	109.5
H(15A)-C(15)-H(15C)	109.5
H(15B)-C(15)-H(15C)	109.5

Table 4. Anisotropic displacement parameters ($\text{\AA}^2 \times 10^3$) for kl2076. The anisotropic displacement factor exponent takes the form: $-2\pi^2 [h^2 a^{*2} U^{11} + \dots + 2 h k a^* b^* U^{12}]$

	U ¹¹	U ²²	U ³³	U ²³	U ¹³	U ¹²
Cl(1)	21(1)	27(1)	41(1)	5(1)	-5(1)	3(1)
Cl(2)	22(1)	26(1)	48(1)	-6(1)	18(1)	1(1)
O(1)	34(1)	25(1)	18(1)	1(1)	5(1)	-6(1)
O(2)	27(1)	24(1)	15(1)	-1(1)	4(1)	-6(1)
O(3)	20(1)	18(1)	42(1)	-2(1)	4(1)	-5(1)
O(4)	16(1)	13(1)	27(1)	1(1)	3(1)	-1(1)
O(5)	30(1)	34(1)	19(1)	-5(1)	3(1)	-4(1)
O(6)	26(1)	16(1)	21(1)	-3(1)	6(1)	-2(1)
C(1)	19(1)	12(1)	19(1)	0(1)	5(1)	2(1)
C(2)	15(1)	18(1)	19(1)	-1(1)	2(1)	2(1)
C(3)	18(1)	16(1)	16(1)	0(1)	5(1)	0(1)
C(4)	16(1)	18(1)	18(1)	-2(1)	2(1)	1(1)
C(5)	19(1)	18(1)	15(1)	-2(1)	6(1)	0(1)
C(6)	21(1)	14(1)	22(1)	2(1)	5(1)	-1(1)
C(7)	17(1)	17(1)	17(1)	-1(1)	2(1)	2(1)
C(8)	13(1)	17(1)	24(1)	-1(1)	3(1)	4(1)
C(9)	14(1)	19(1)	23(1)	-2(1)	5(1)	1(1)
C(10)	17(1)	18(1)	30(1)	-3(1)	7(1)	-3(1)
C(11)	17(1)	16(1)	45(2)	-3(1)	8(1)	-2(1)
C(12)	17(1)	15(1)	27(1)	0(1)	6(1)	-2(1)
C(13)	21(1)	14(1)	16(1)	0(1)	6(1)	0(1)
C(14)	28(1)	15(1)	23(1)	-2(1)	6(1)	0(1)
C(15)	30(1)	23(1)	32(2)	5(1)	4(1)	8(1)

Table 5. Hydrogen coordinates ($\times 10^4$) and isotropic displacement parameters ($\text{\AA}^2 \times 10^3$) for kl2076.

	x	y	z	U(eq)
H(2O)	6700(30)	3936(17)	8670(30)	33
H(6O)	7620(30)	67(17)	4900(30)	32
H(2)	3860(30)	3586(14)	6900(30)	26
H(3A)	5133	2453	7198	20
H(3B)	3480	2354	6942	20
H(4A)	3326	1999	4573	21
H(4B)	4925	2207	4656	21
H(6A)	6056	155	6557	23
H(6B)	6722	579	8012	23
H(9)	8710(30)	1638(15)	5090(30)	28
H(10A)	9800	2763	5737	26
H(10B)	10049	2531	7389	26
H(11A)	7280	2594	5651	31
H(11B)	7698	2579	7364	31
H(12A)	8105	3776	5617	24
H(12B)	8671	3765	7315	24
H(14A)	5650	4918	6733	33
H(14B)	6596	4842	5574	33
H(14C)	7314	4927	7237	33
H(15A)	8285	-578	7246	43
H(15B)	9048	-44	8486	43
H(15C)	9748	-220	7163	43

Table 6. Torsion angles [°] for kl2076.

O(1)-C(1)-C(2)-C(3)	93.3(3)
C(13)-C(1)-C(2)-C(3)	-86.9(2)
O(1)-C(1)-C(2)-Cl(1)	-30.3(3)
C(13)-C(1)-C(2)-Cl(1)	149.46(16)
C(1)-C(2)-C(3)-C(4)	-66.8(2)
Cl(1)-C(2)-C(3)-C(4)	56.5(2)
C(2)-C(3)-C(4)-C(5)	170.64(18)
C(6)-O(4)-C(5)-O(3)	-4.9(3)
C(6)-O(4)-C(5)-C(4)	175.25(19)
C(3)-C(4)-C(5)-O(3)	108.0(3)
C(3)-C(4)-C(5)-O(4)	-72.1(2)
C(5)-O(4)-C(6)-C(7)	141.9(2)
O(4)-C(6)-C(7)-O(6)	-65.2(2)
O(4)-C(6)-C(7)-C(15)	172.16(19)
O(4)-C(6)-C(7)-C(8)	52.5(2)
O(6)-C(7)-C(8)-O(5)	-176.7(2)
C(15)-C(7)-C(8)-O(5)	-54.7(3)
C(6)-C(7)-C(8)-O(5)	64.9(3)
O(6)-C(7)-C(8)-C(9)	3.9(3)
C(15)-C(7)-C(8)-C(9)	125.9(2)
C(6)-C(7)-C(8)-C(9)	-114.5(2)
O(5)-C(8)-C(9)-C(10)	-27.6(3)
C(7)-C(8)-C(9)-C(10)	151.8(2)
O(5)-C(8)-C(9)-Cl(2)	94.0(2)
C(7)-C(8)-C(9)-Cl(2)	-86.6(2)
C(8)-C(9)-C(10)-C(11)	-66.6(3)
Cl(2)-C(9)-C(10)-C(11)	175.89(18)
C(9)-C(10)-C(11)-C(12)	-164.4(2)
C(10)-C(11)-C(12)-C(13)	-174.7(2)
C(11)-C(12)-C(13)-O(2)	63.8(3)
C(11)-C(12)-C(13)-C(14)	-173.0(2)
C(11)-C(12)-C(13)-C(1)	-55.2(3)
O(1)-C(1)-C(13)-O(2)	-170.5(2)
C(2)-C(1)-C(13)-O(2)	9.7(3)
O(1)-C(1)-C(13)-C(14)	70.4(3)

C(2)-C(1)-C(13)-C(14)	-109.4(2)
O(1)-C(1)-C(13)-C(12)	-49.3(3)
C(2)-C(1)-C(13)-C(12)	130.9(2)

Table 7. Hydrogen bonds for kl2076 [\AA and $^\circ$].

D-H...A	d(D-H)	d(H...A)	d(D...A)	$\angle(\text{DHA})$
O(2)-H(2O)...O(6)#1	0.76(3)	2.05(3)	2.812(3)	175(3)
O(6)-H(6O)...O(3)#2	0.74(3)	2.13(3)	2.835(2)	161(3)

Symmetry transformations used to generate equivalent atoms:

#1 $x, -y+1/2, z+1/2$ #2 $-x+1, -y, -z+1$

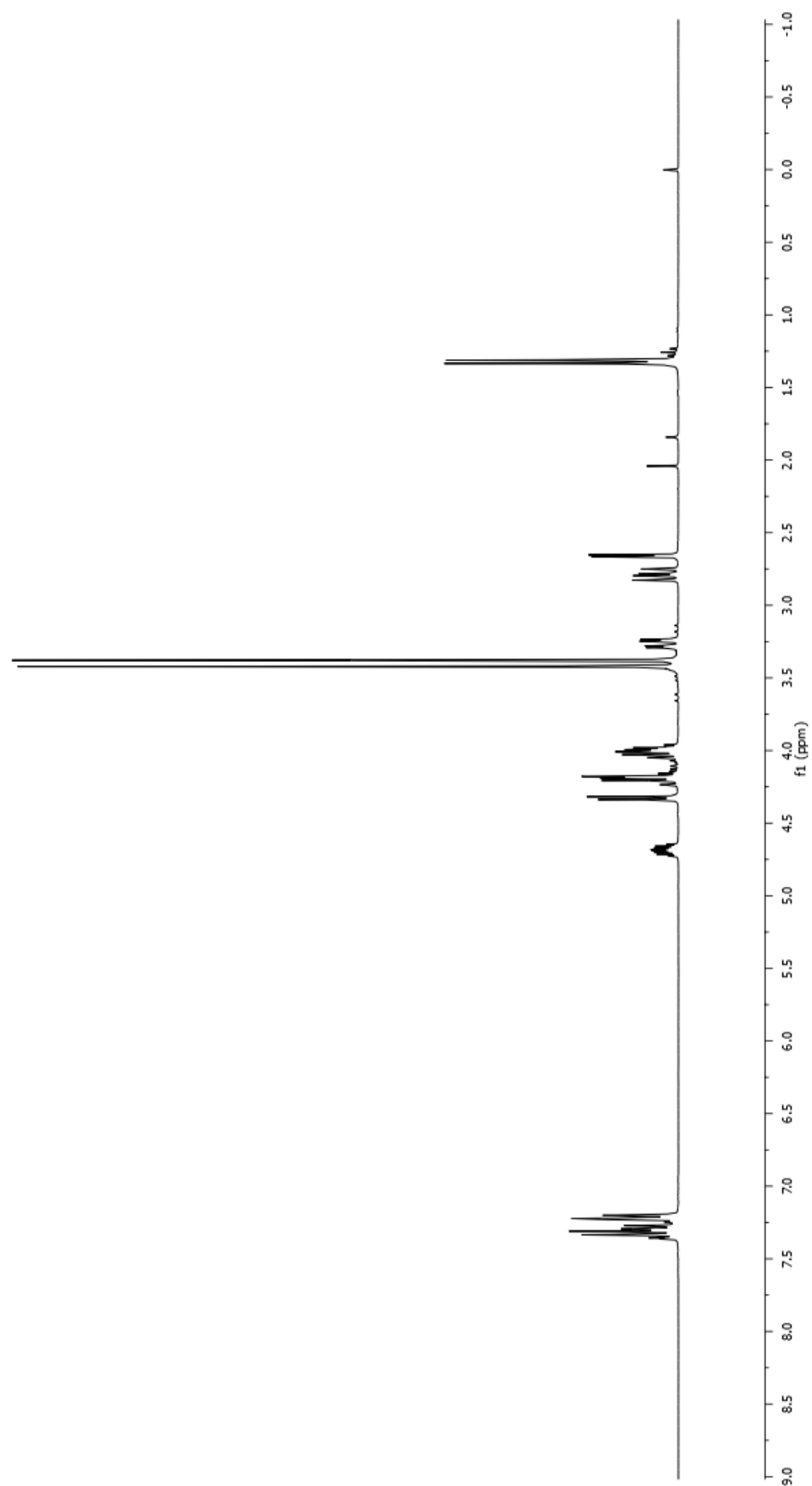
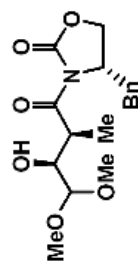
6. Reference

1. Li, J. J.; Wang, Y. A.; Guo, W.; Keay, J. C.; Mishima, T. D.; Johnson, M. B.; Peng, X. *J. Am. Chem. Soc.* **2003**, *125*, 12567.
2. Xie, R.; Kolb, U.; Li, J.; Basch, T.; Mews, A. *J. Am. Chem. Soc.* **2005**, *127*, 7480.

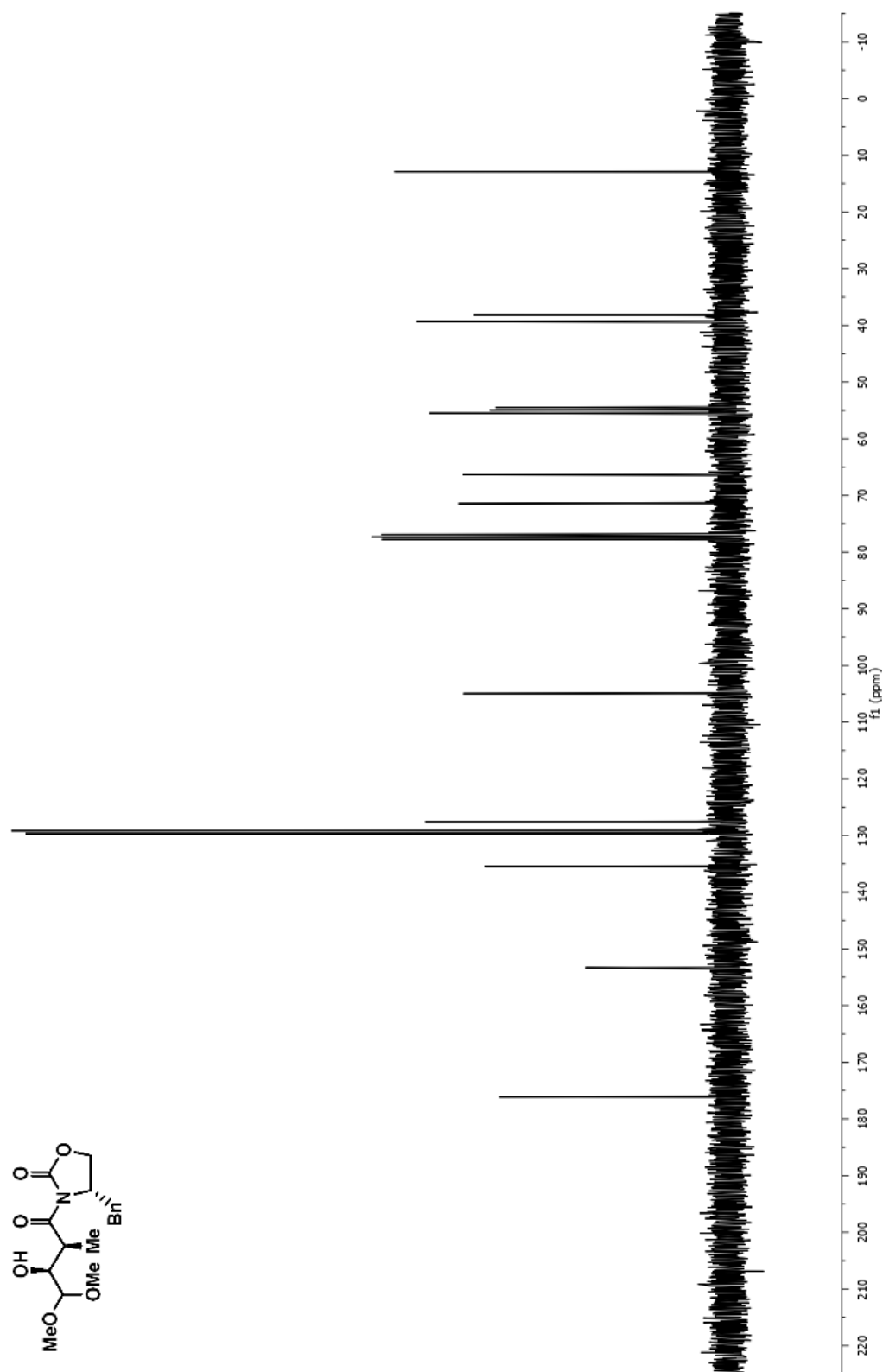
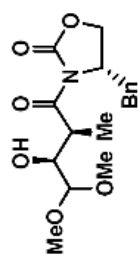
Appendix I

Spectra of Compounds

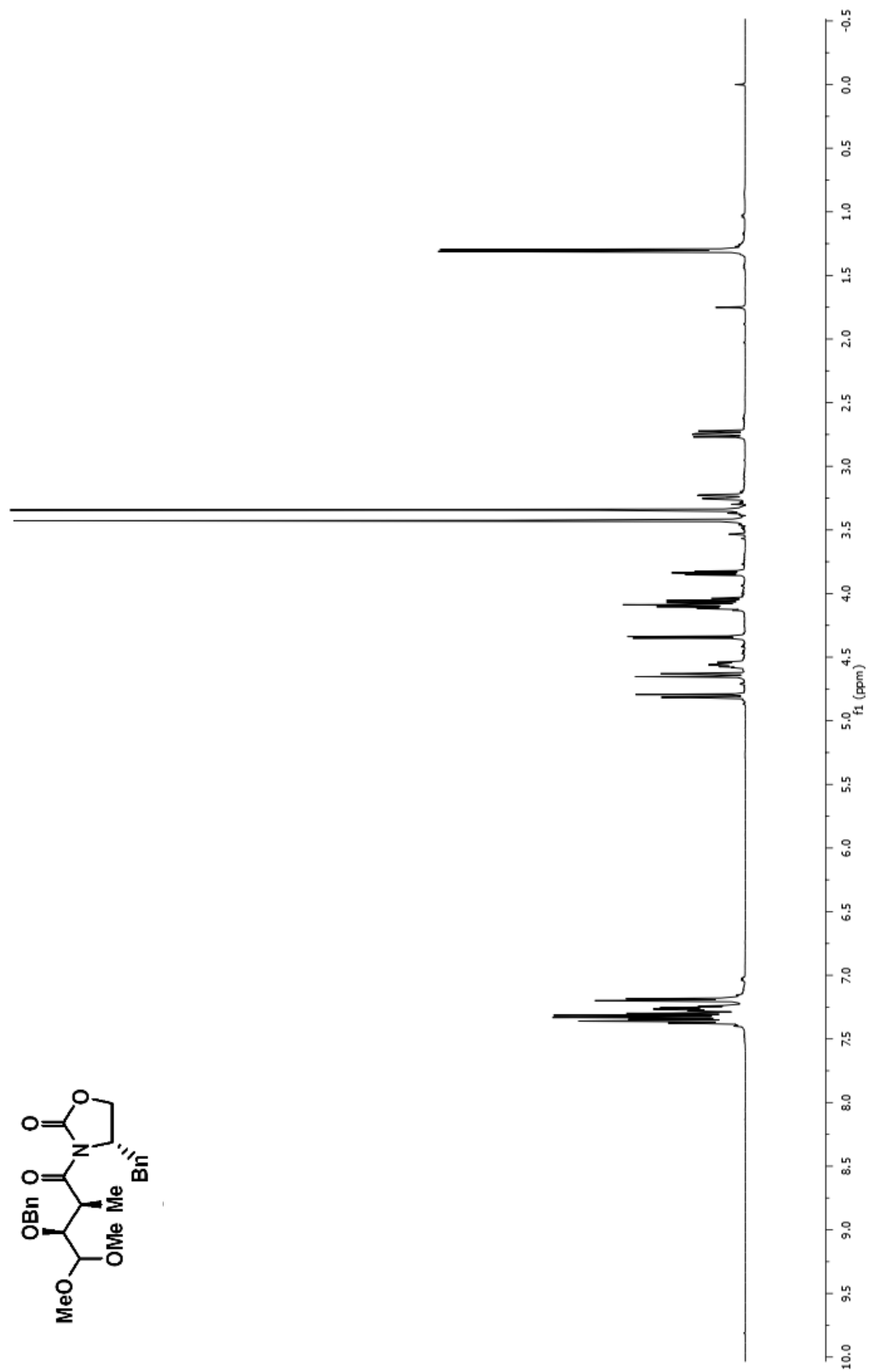
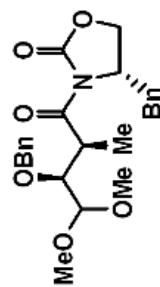
¹H NMR (500MHz, CDCl₃)



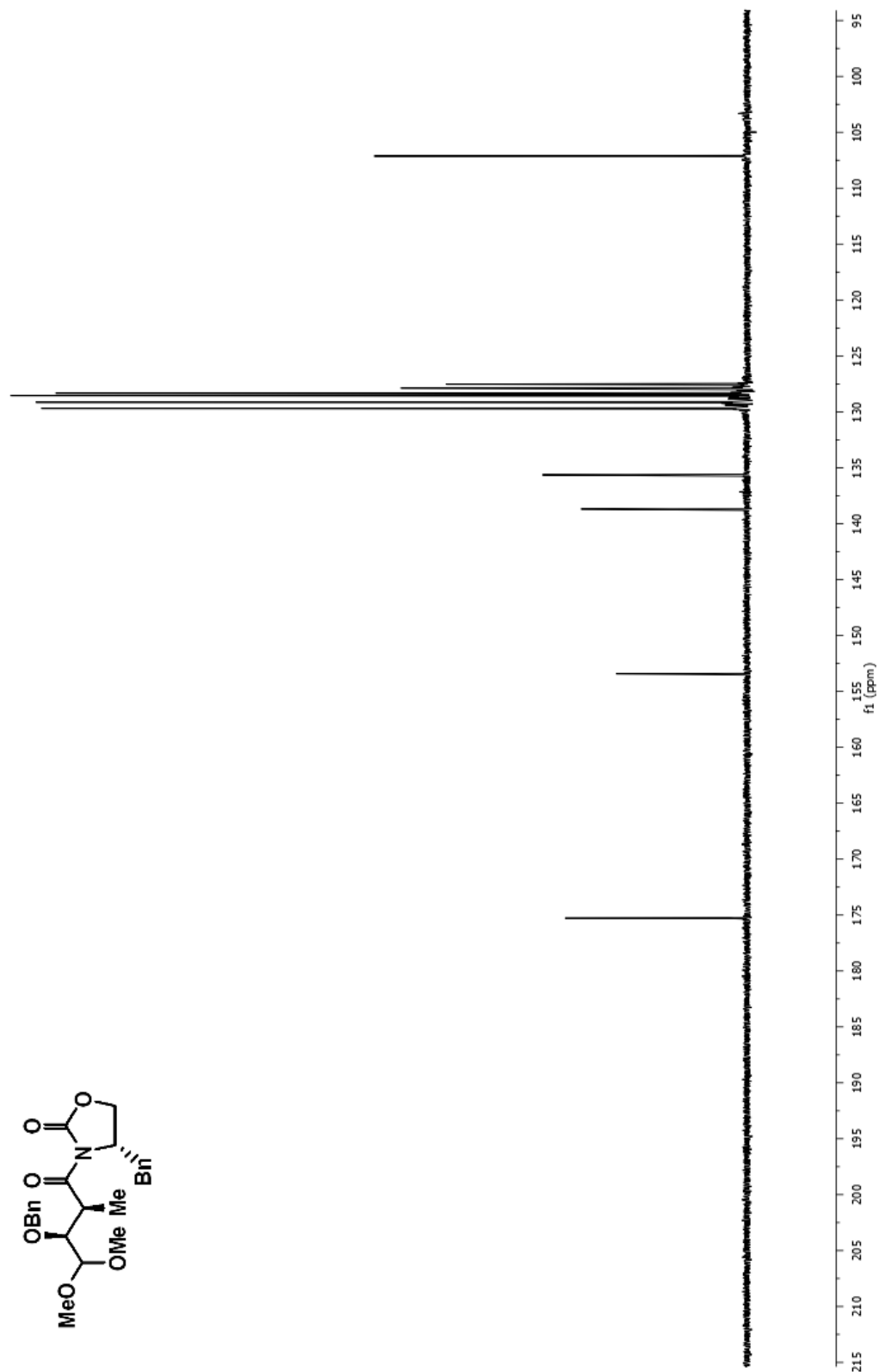
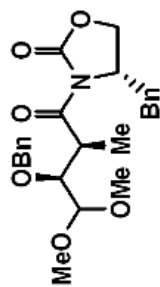
^{13}C NMR (125MHz, CDCl_3)



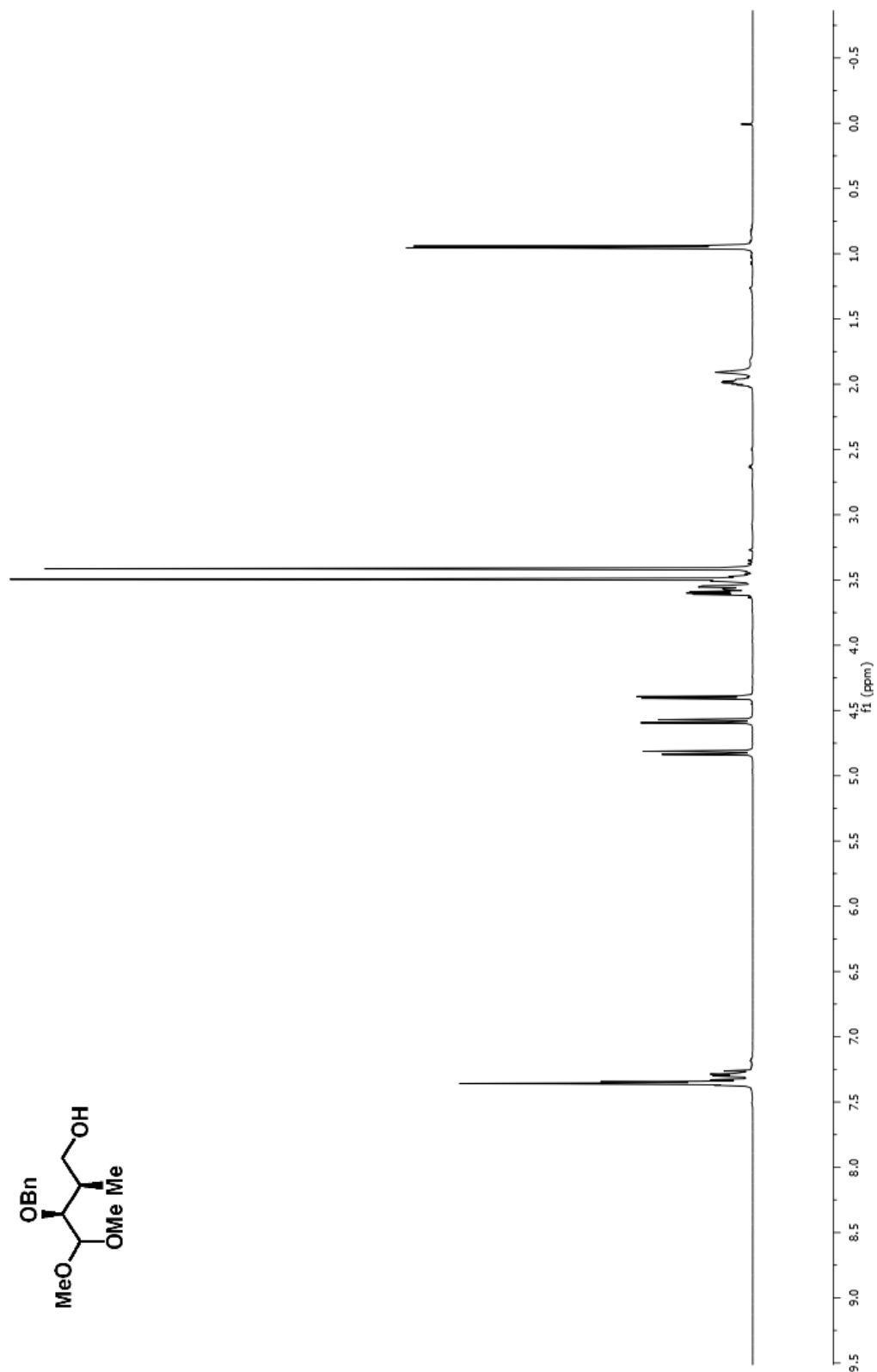
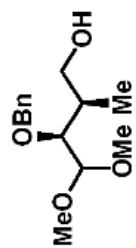
^1H NMR (500MHz, CDCl_3)



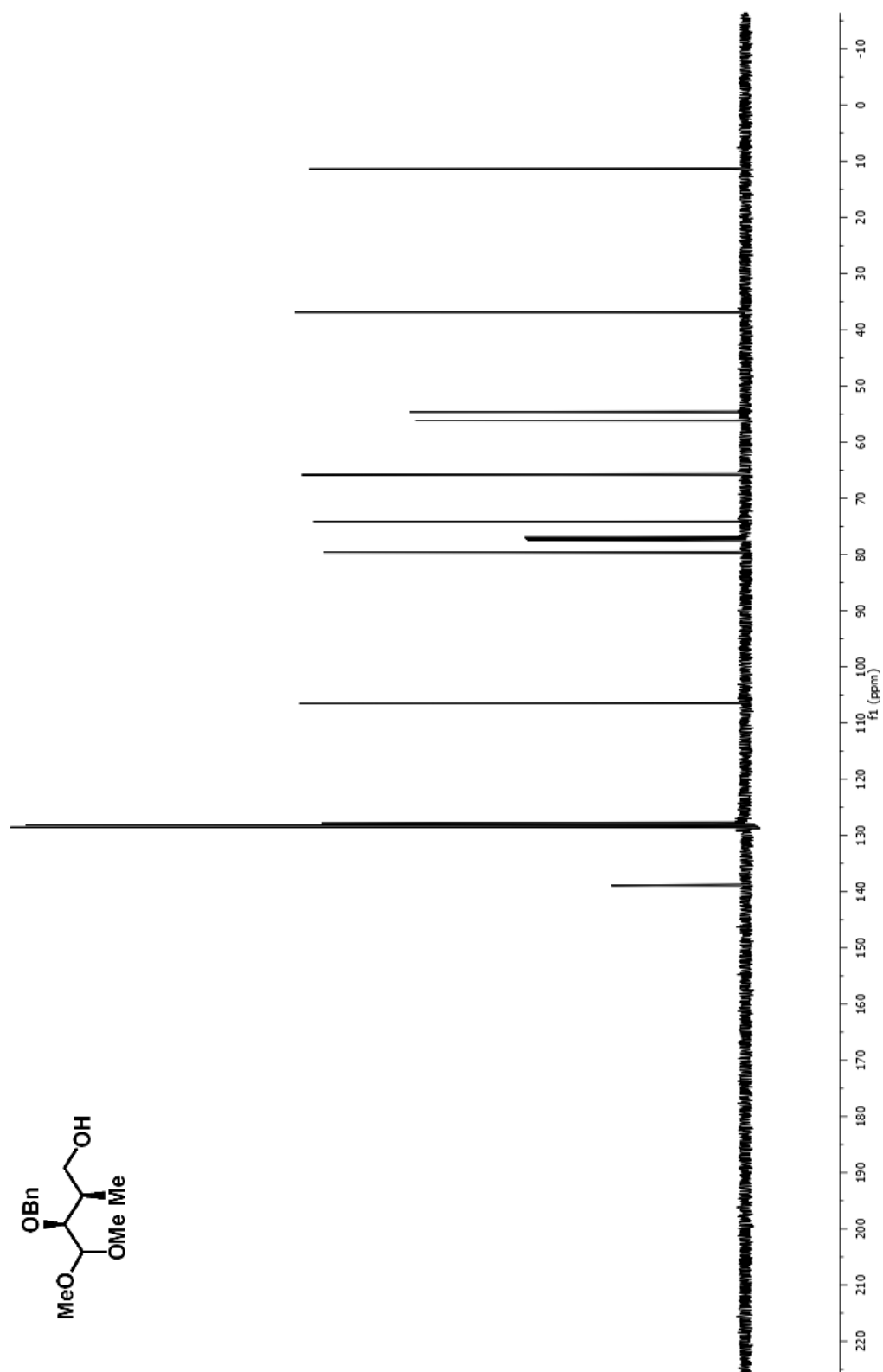
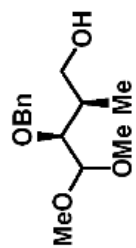
^{13}C NMR (125MHz, CDCl_3)



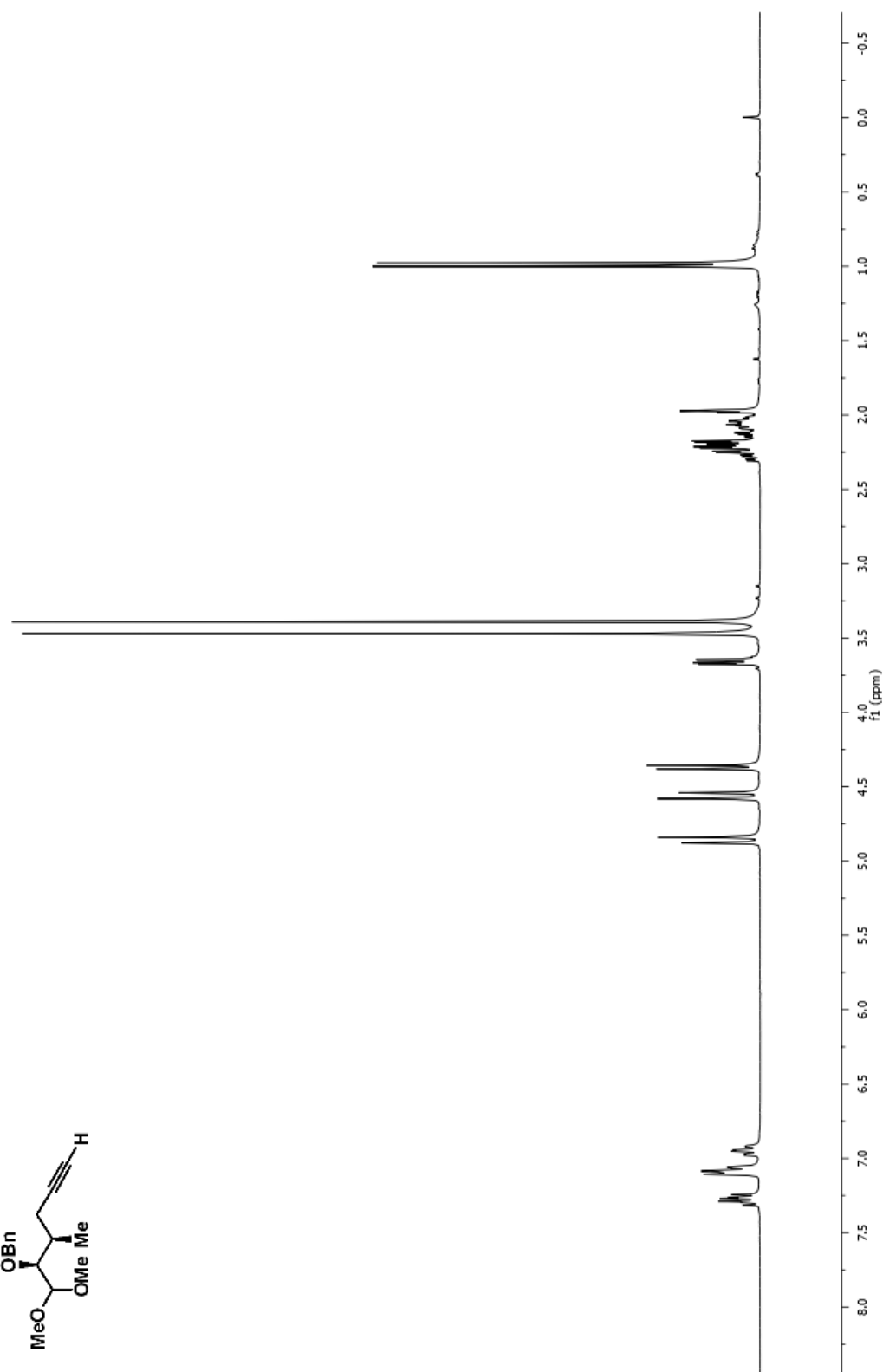
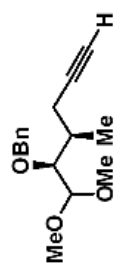
^1H NMR (500MHz, CDCl_3)



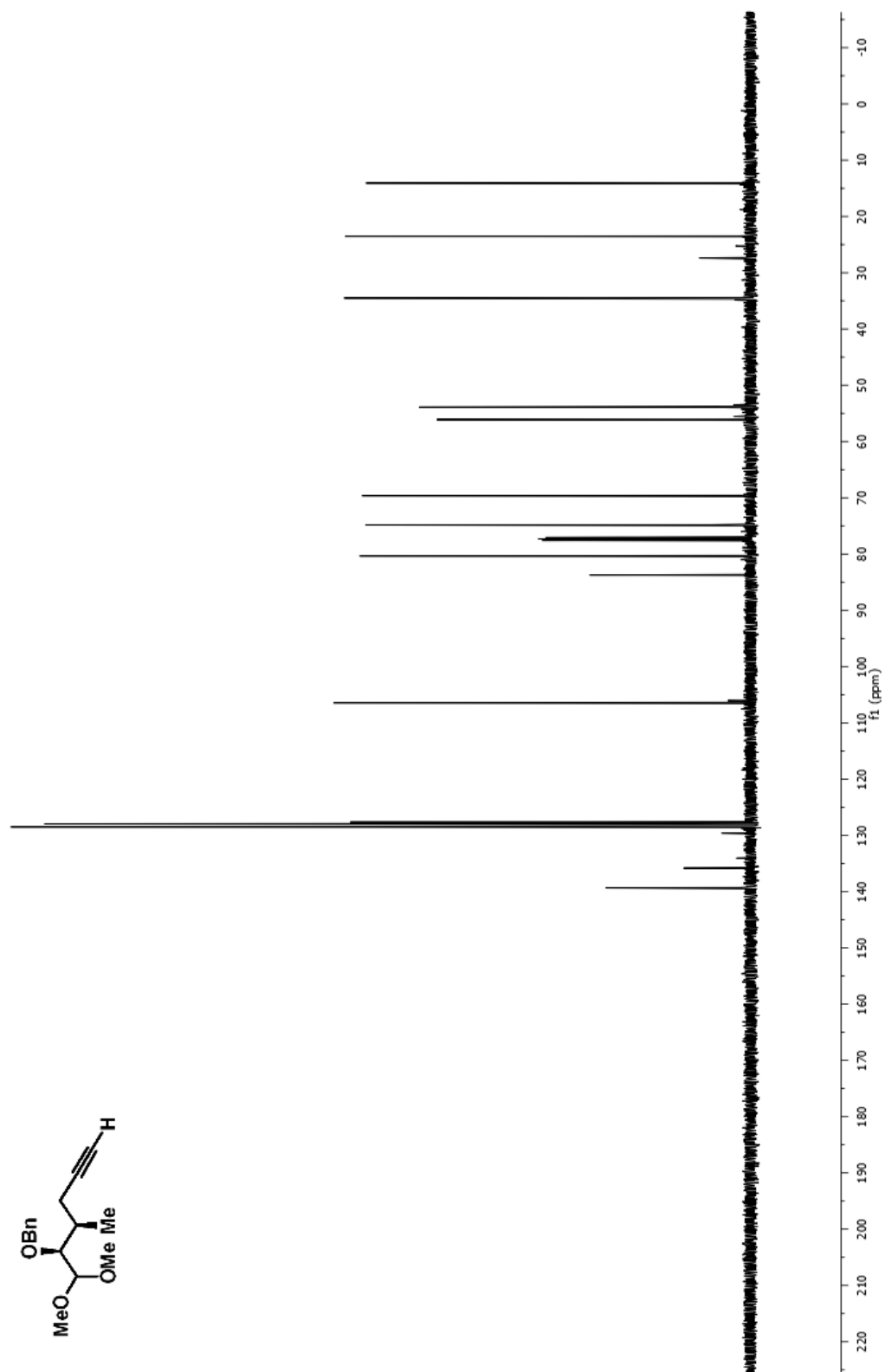
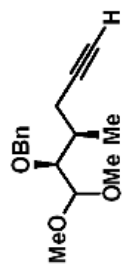
^{13}C NMR (125MHz, CDCl_3)



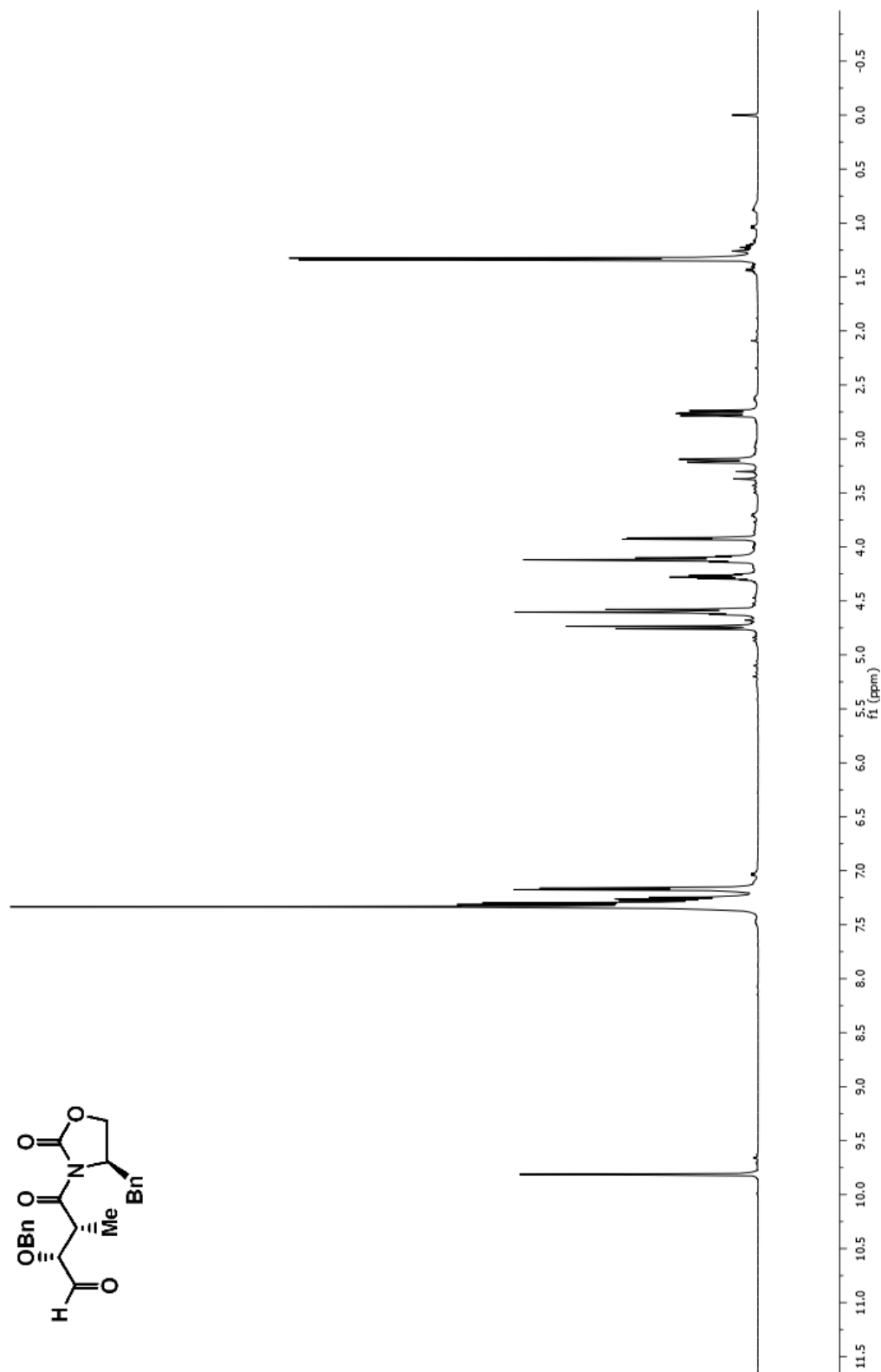
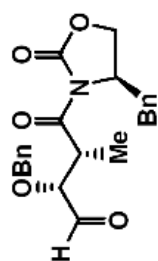
¹H NMR (500MHz, CDCl₃)



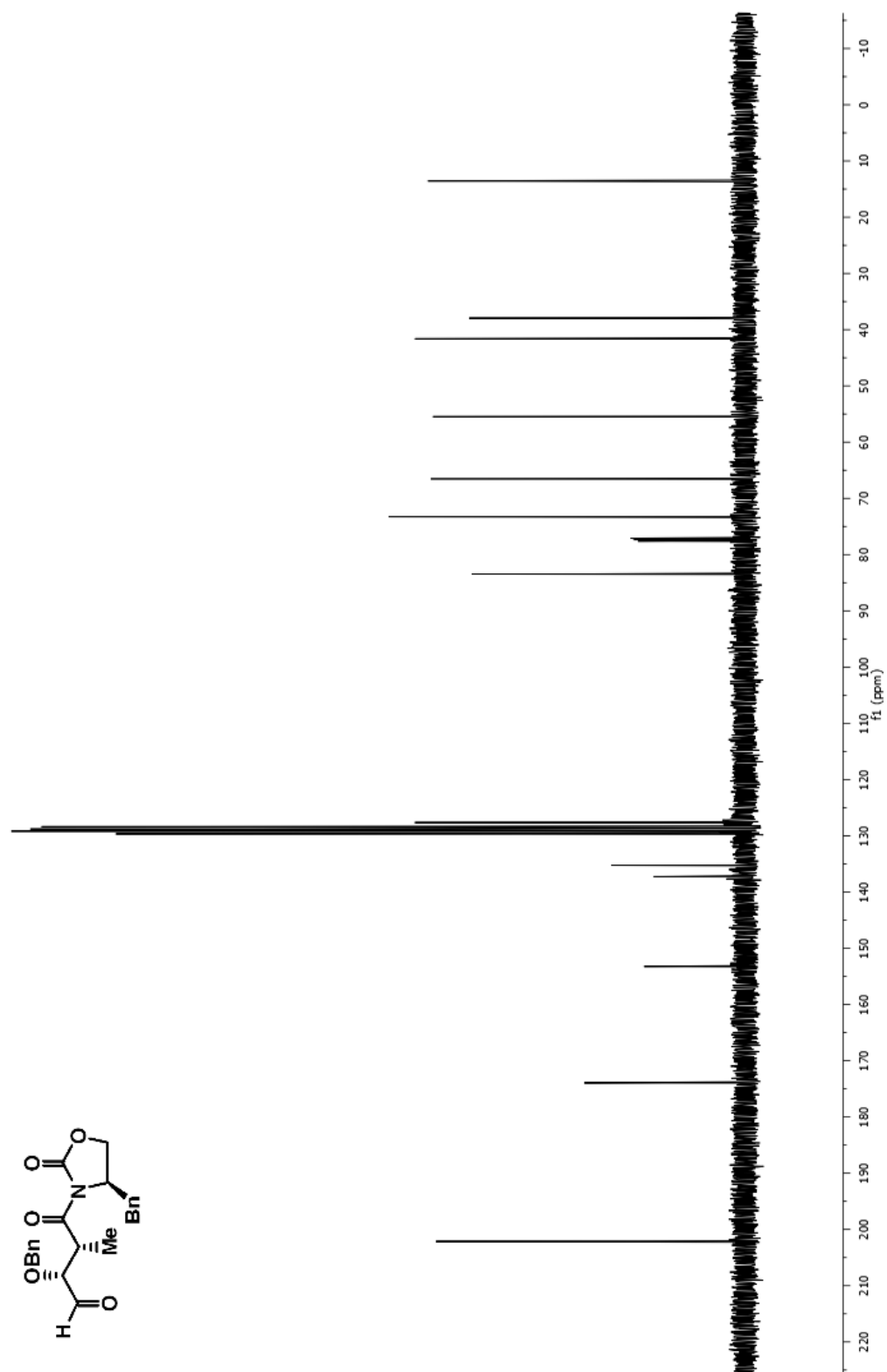
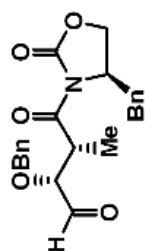
^{13}C NMR (125MHz, CDCl_3)

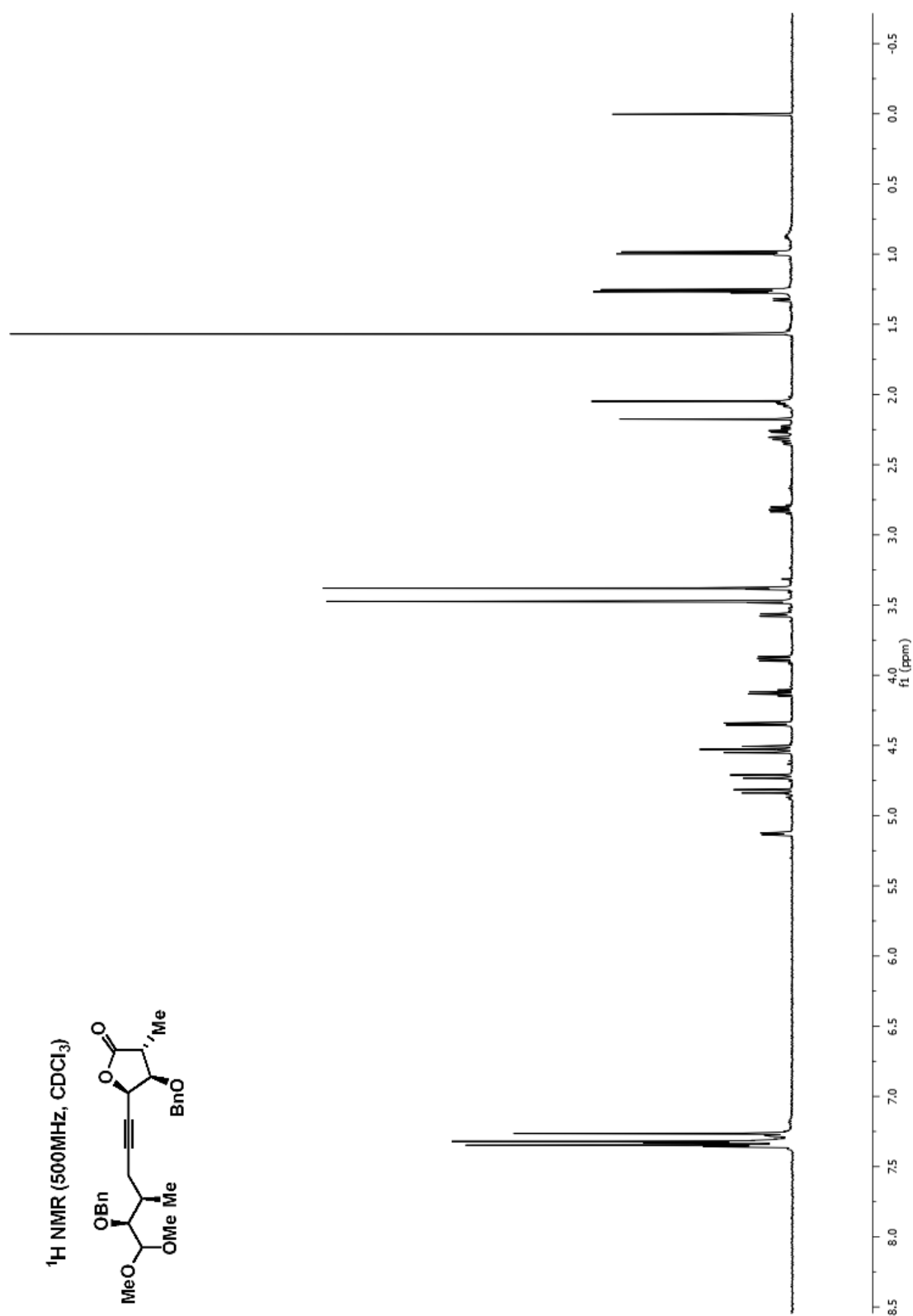


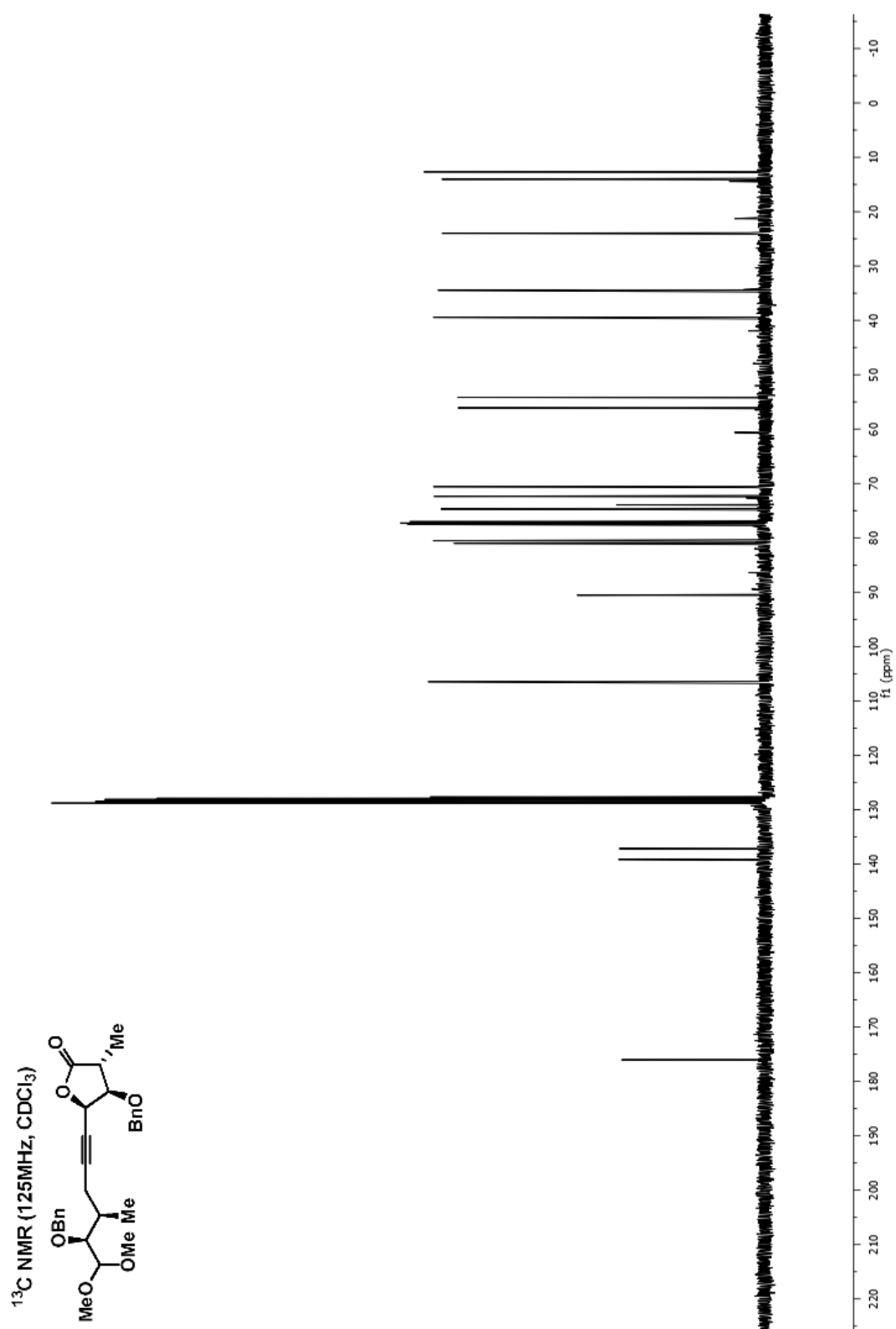
¹H NMR (500MHz, CDCl₃)

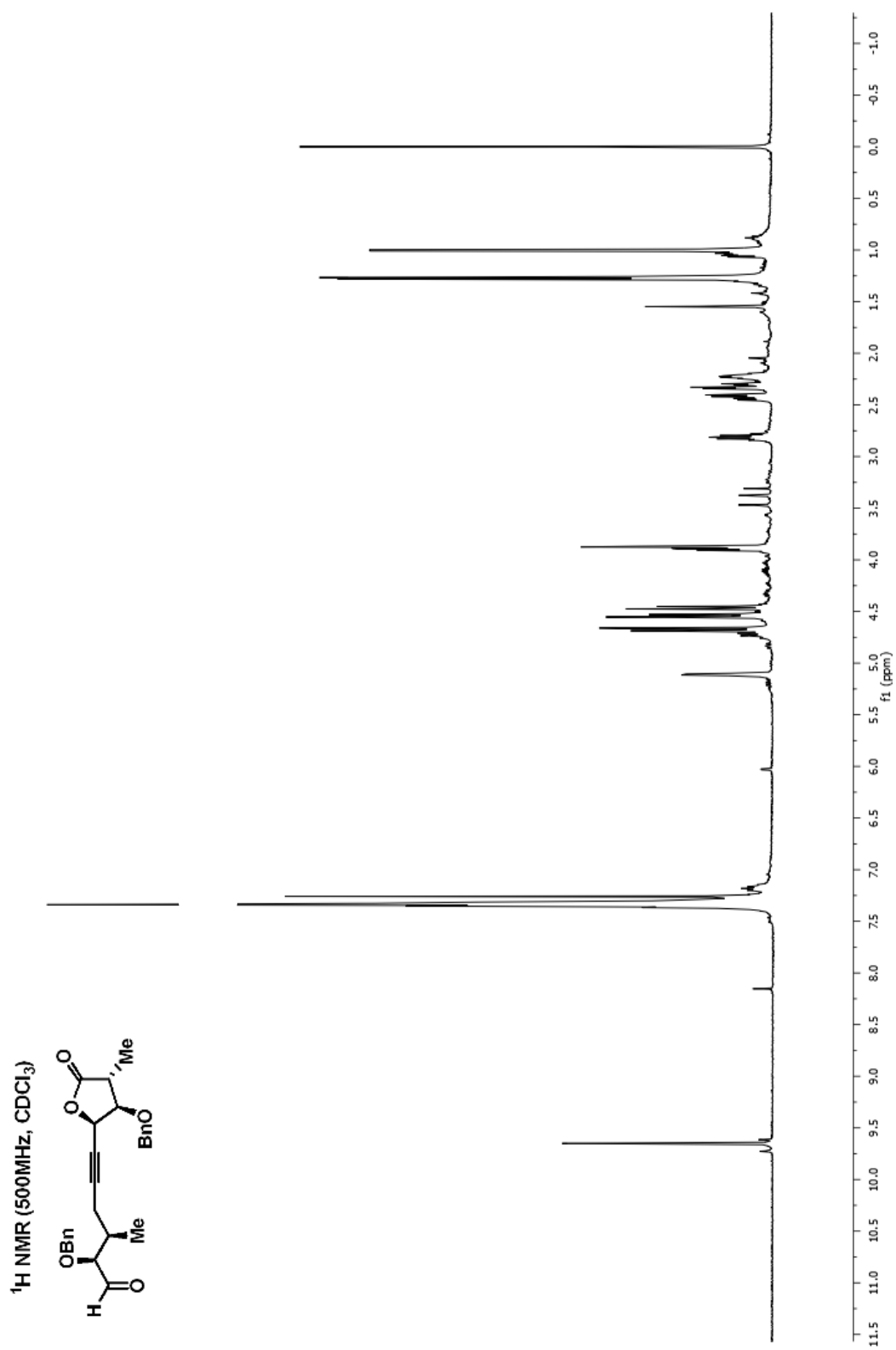


^{13}C NMR (125MHz, CDCl_3)

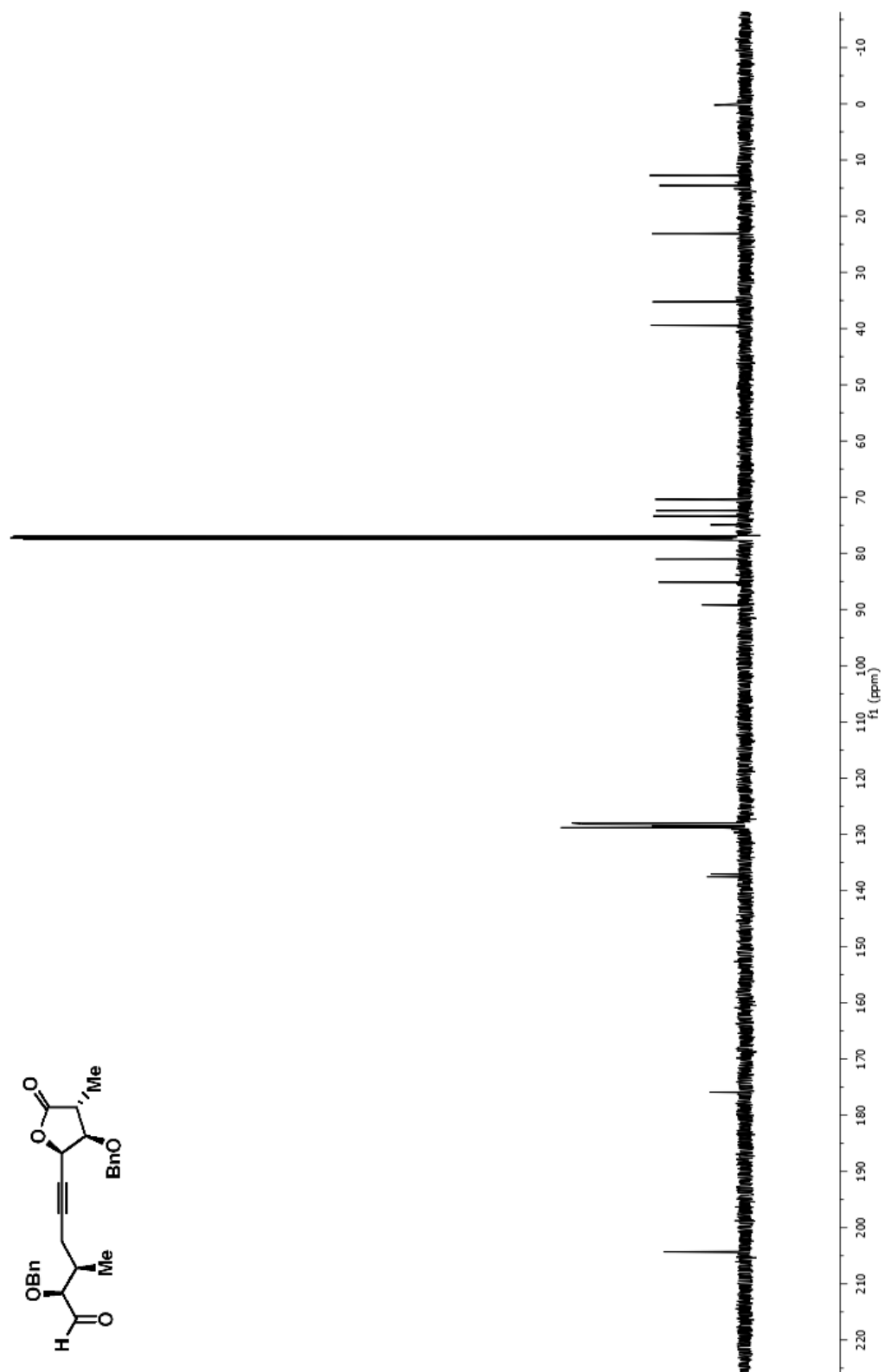
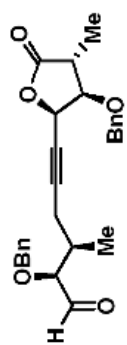


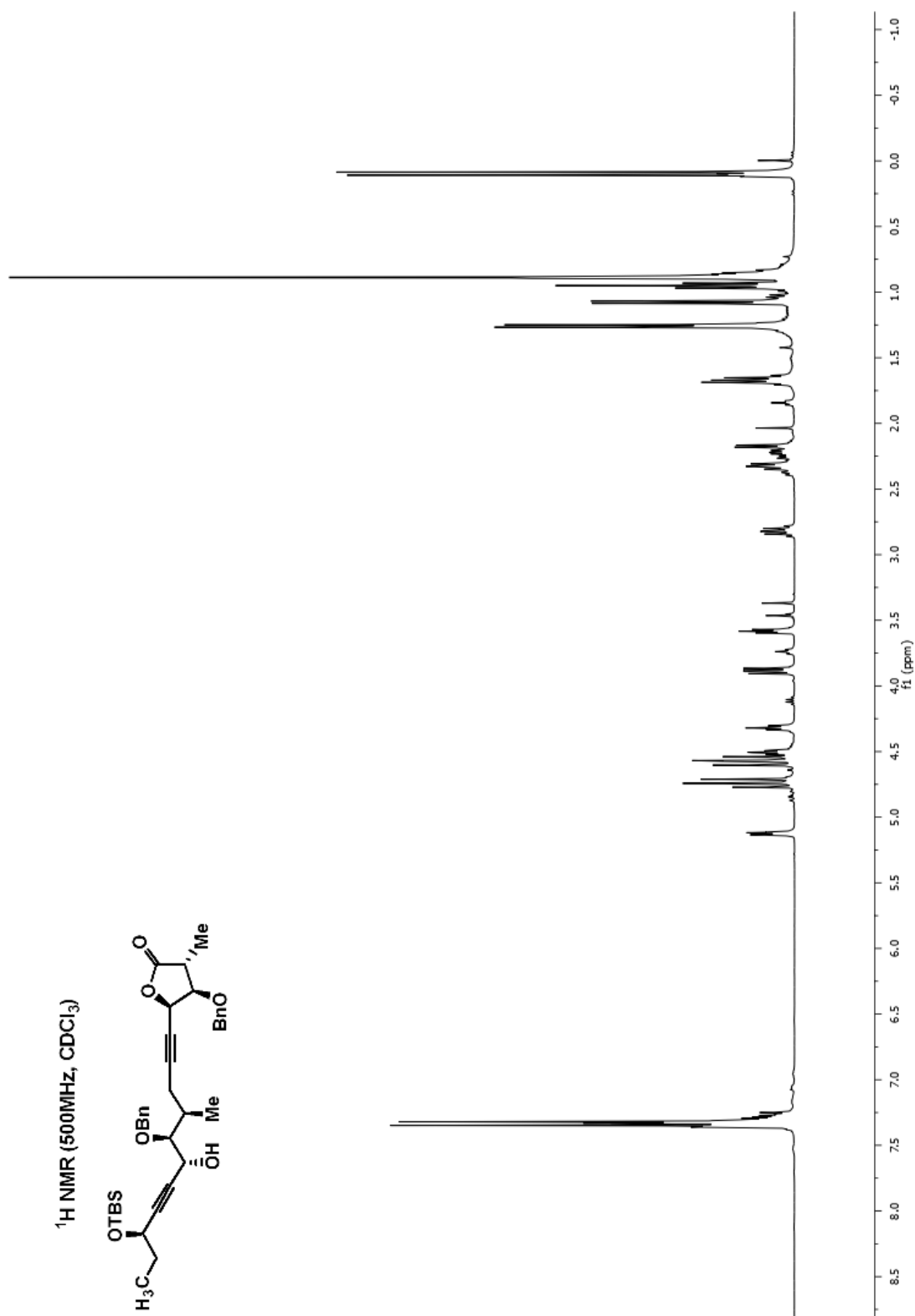


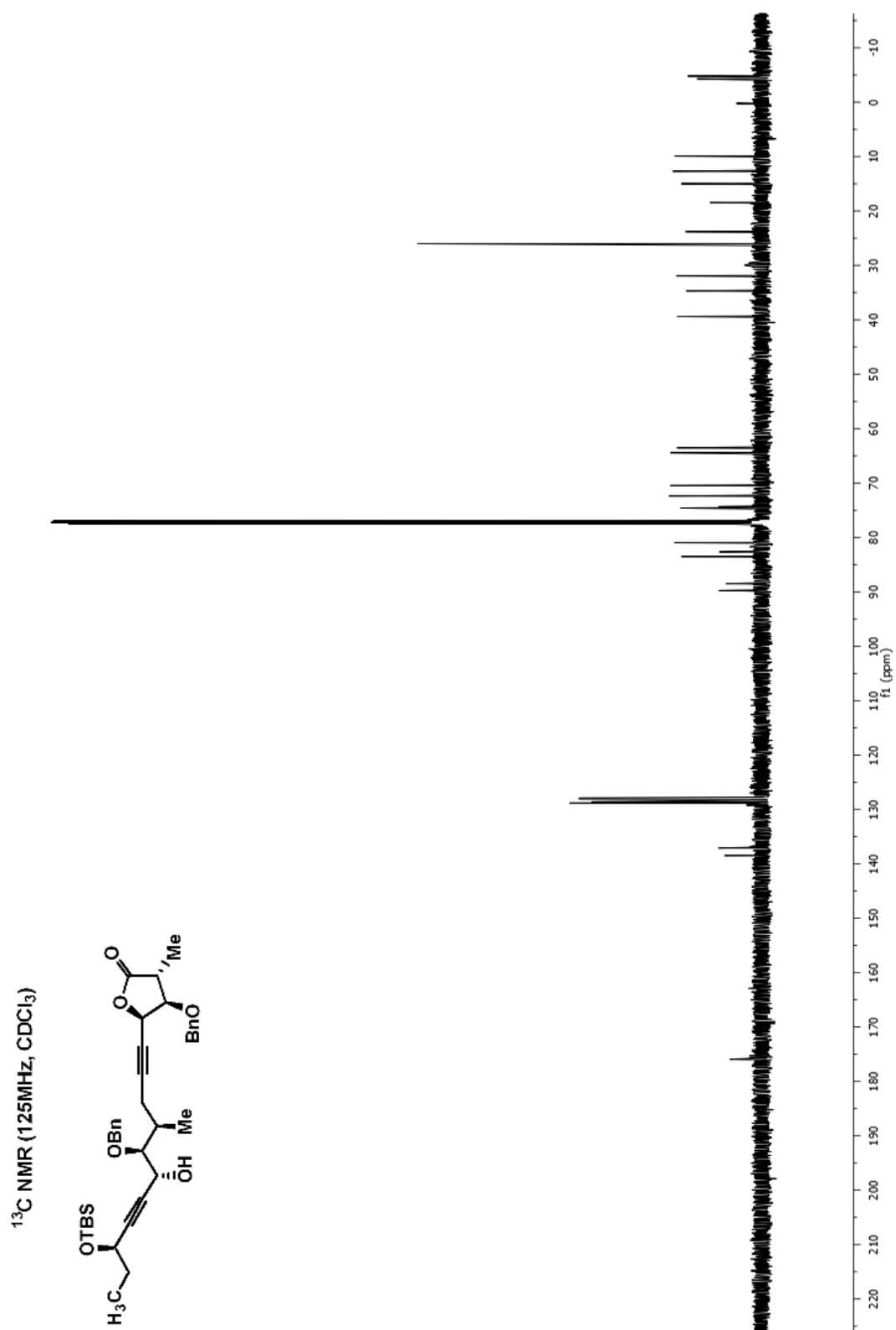


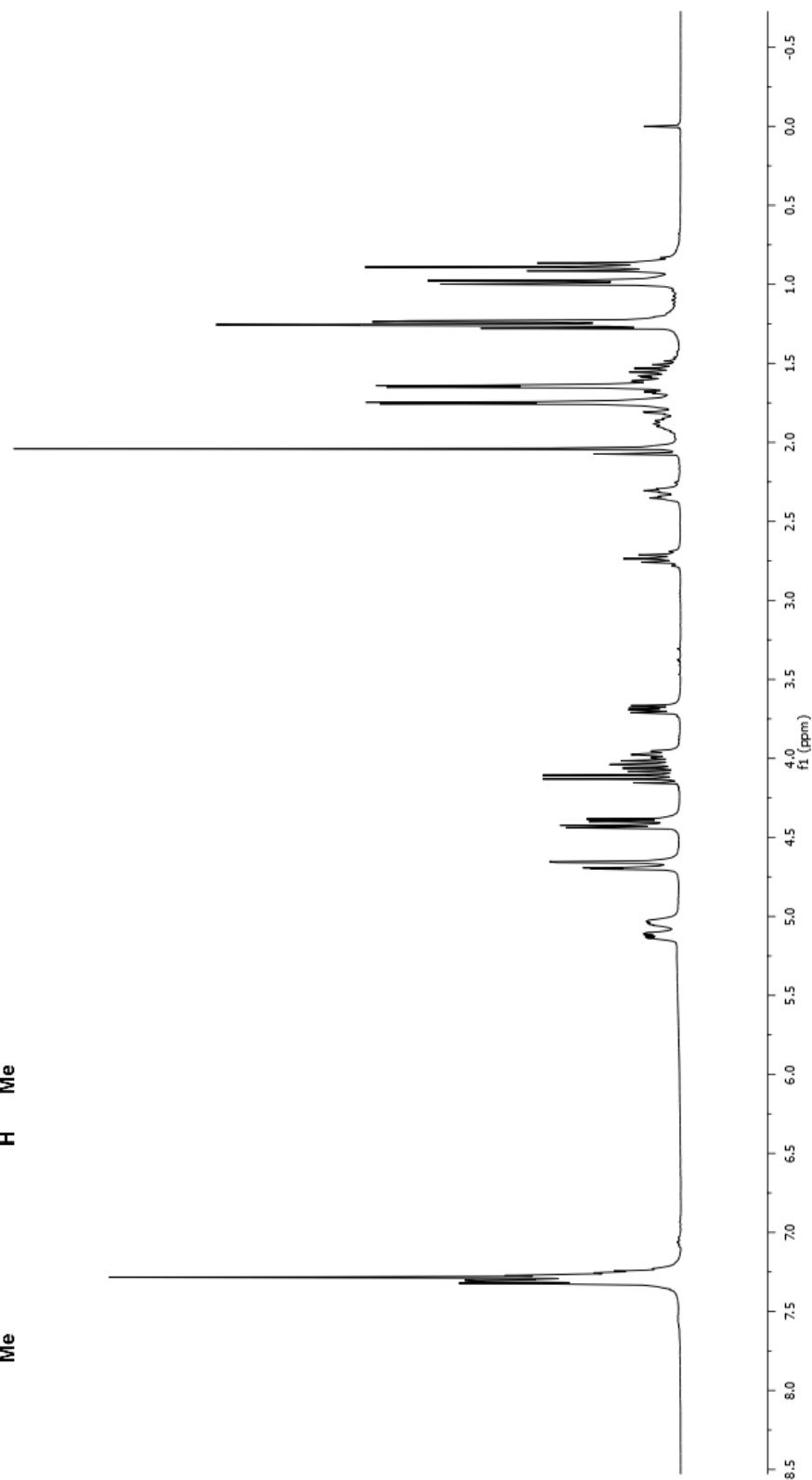
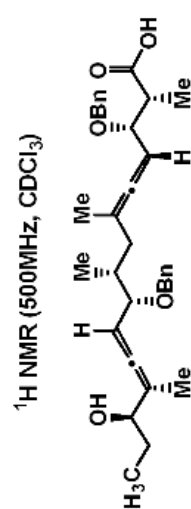


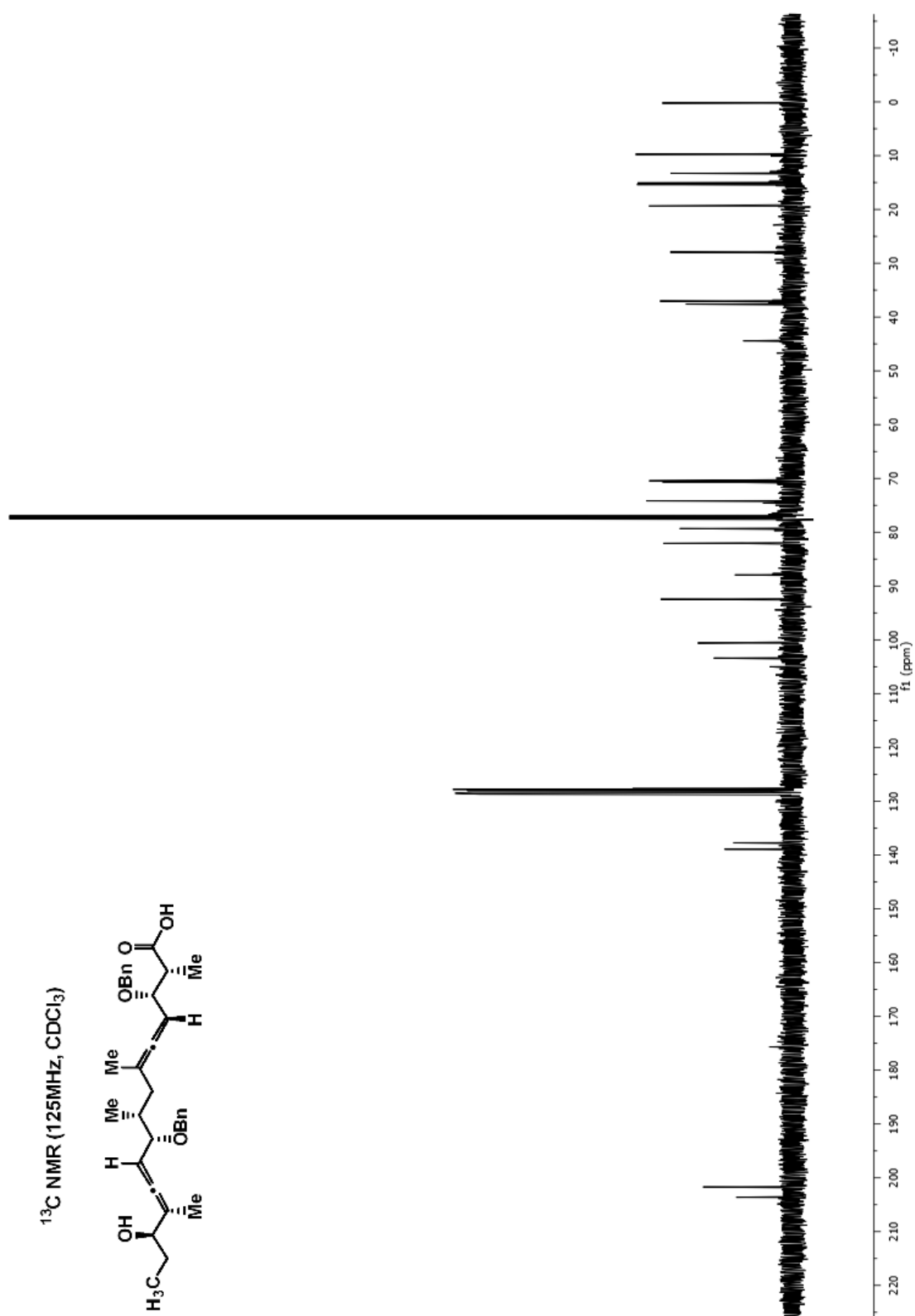
^{13}C NMR (125MHz, CDCl_3)



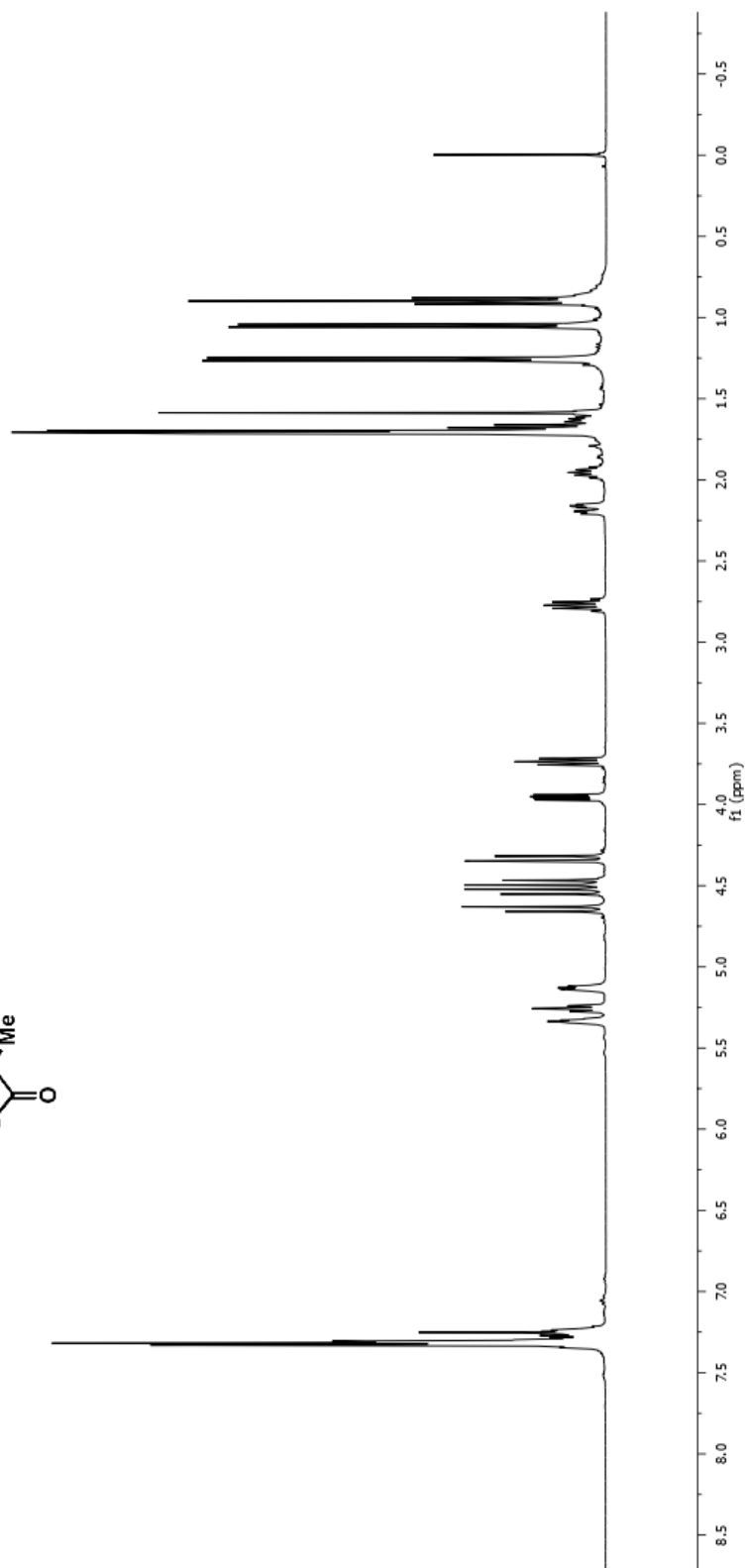
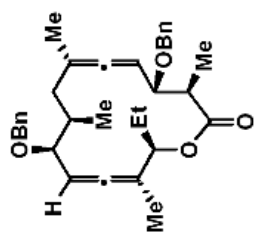




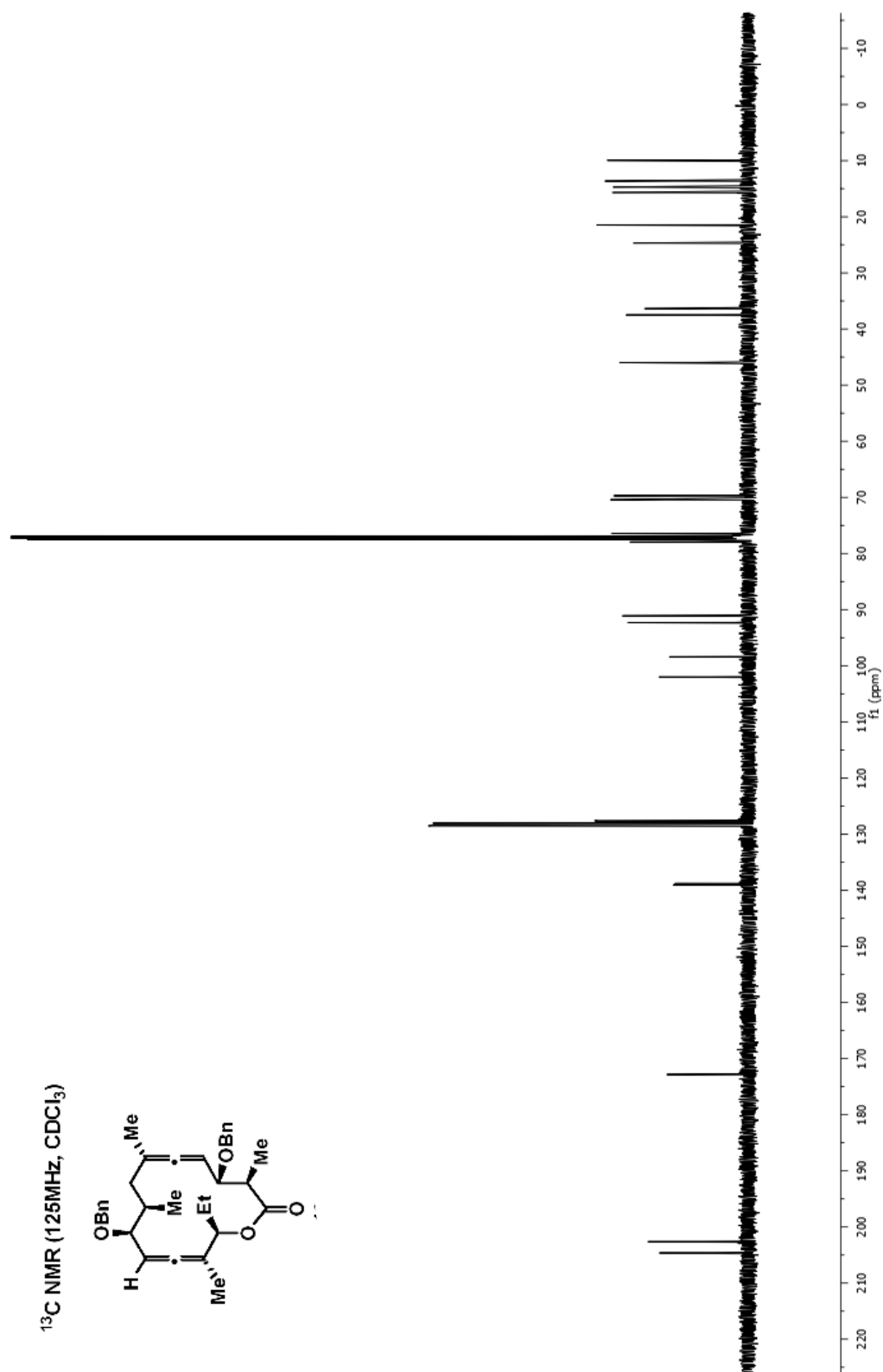
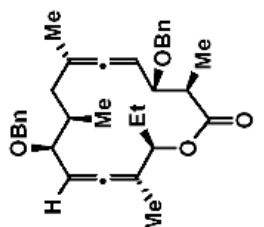


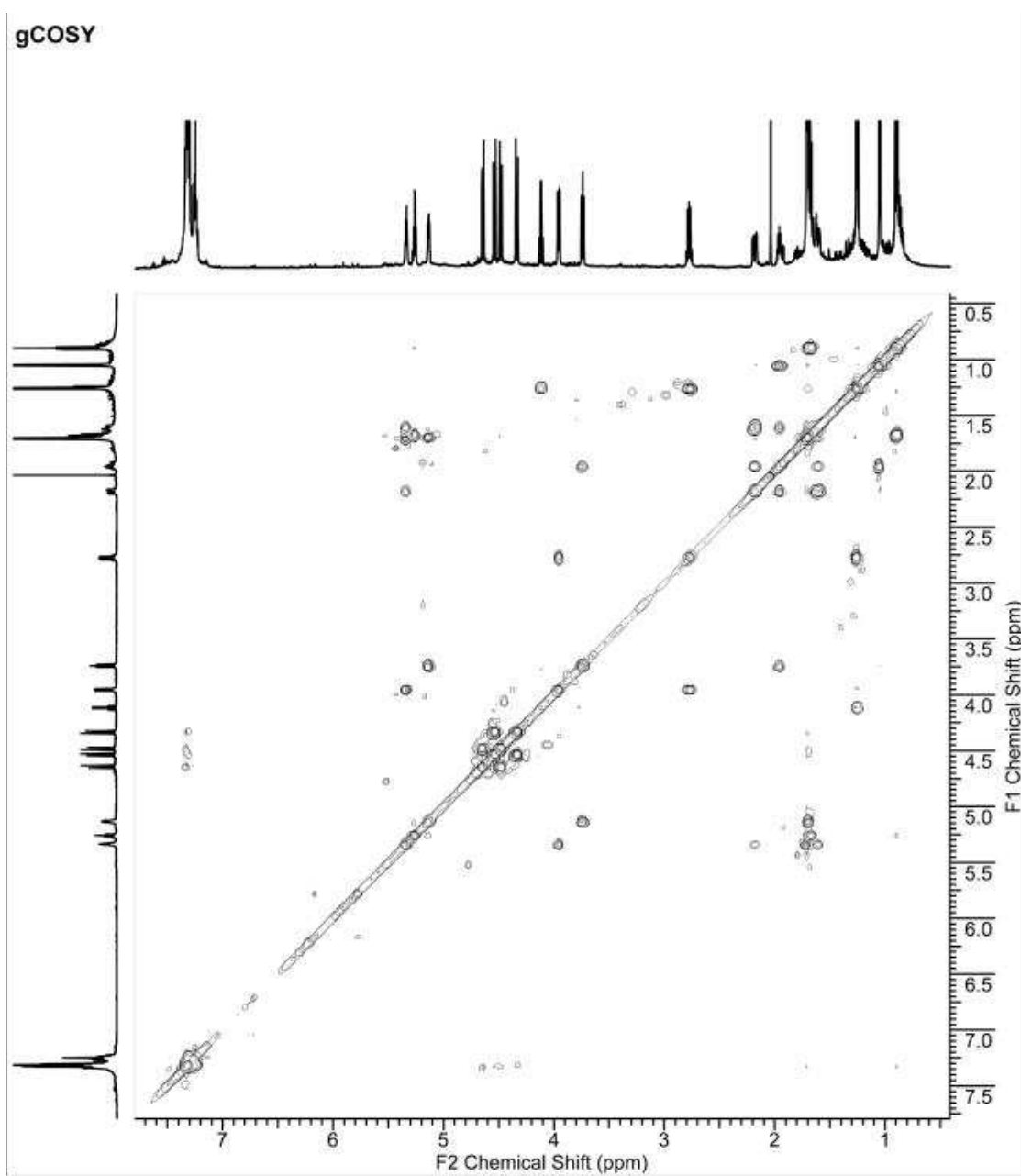


¹H NMR (500MHz, CDCl₃)

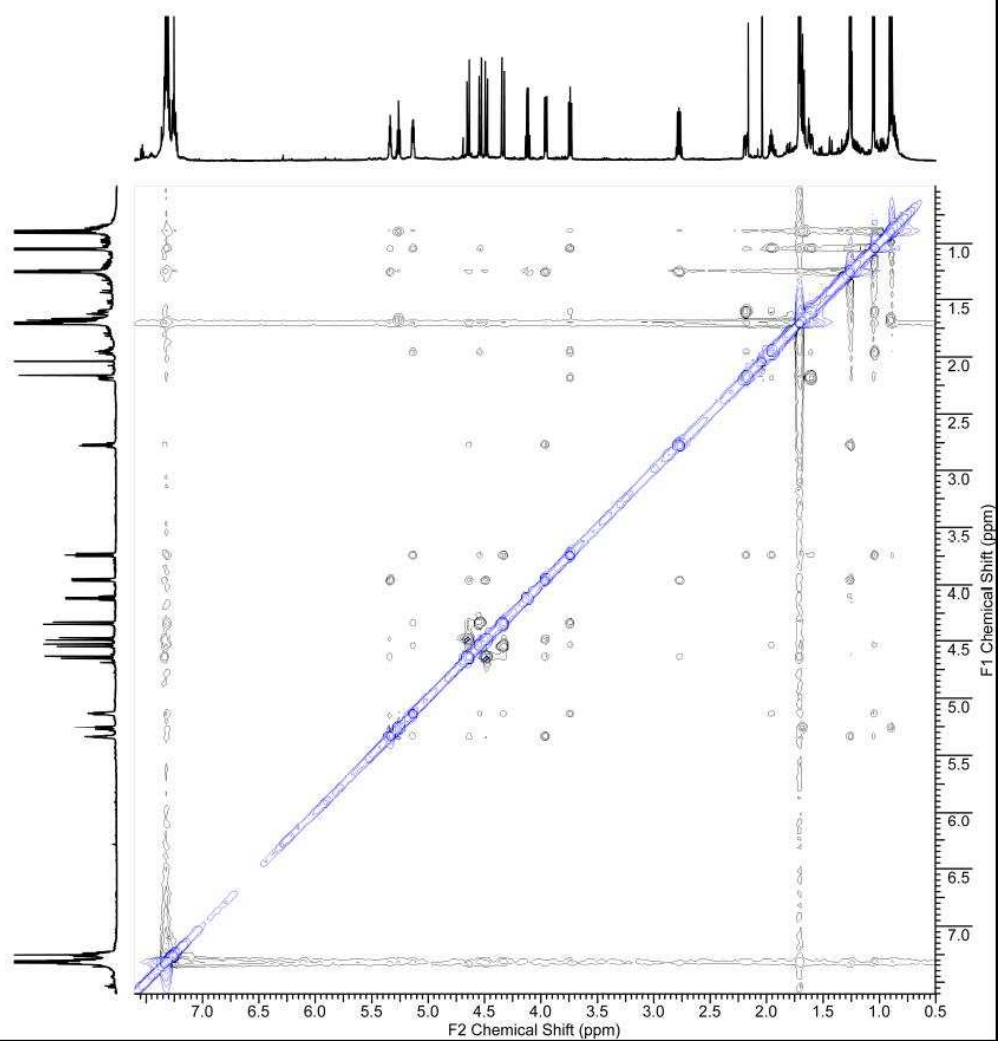


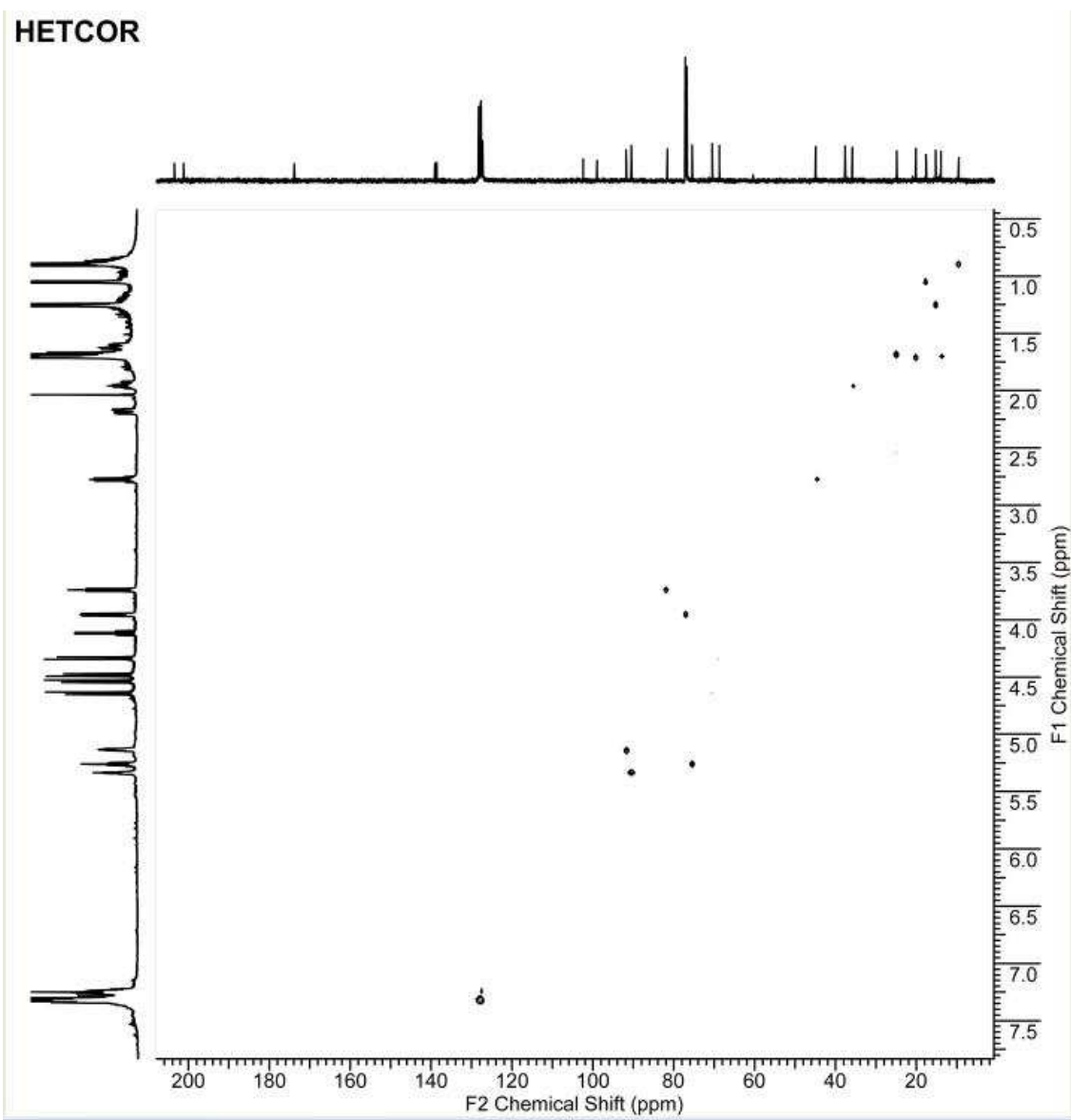
^{13}C NMR (125MHz, CDCl_3)

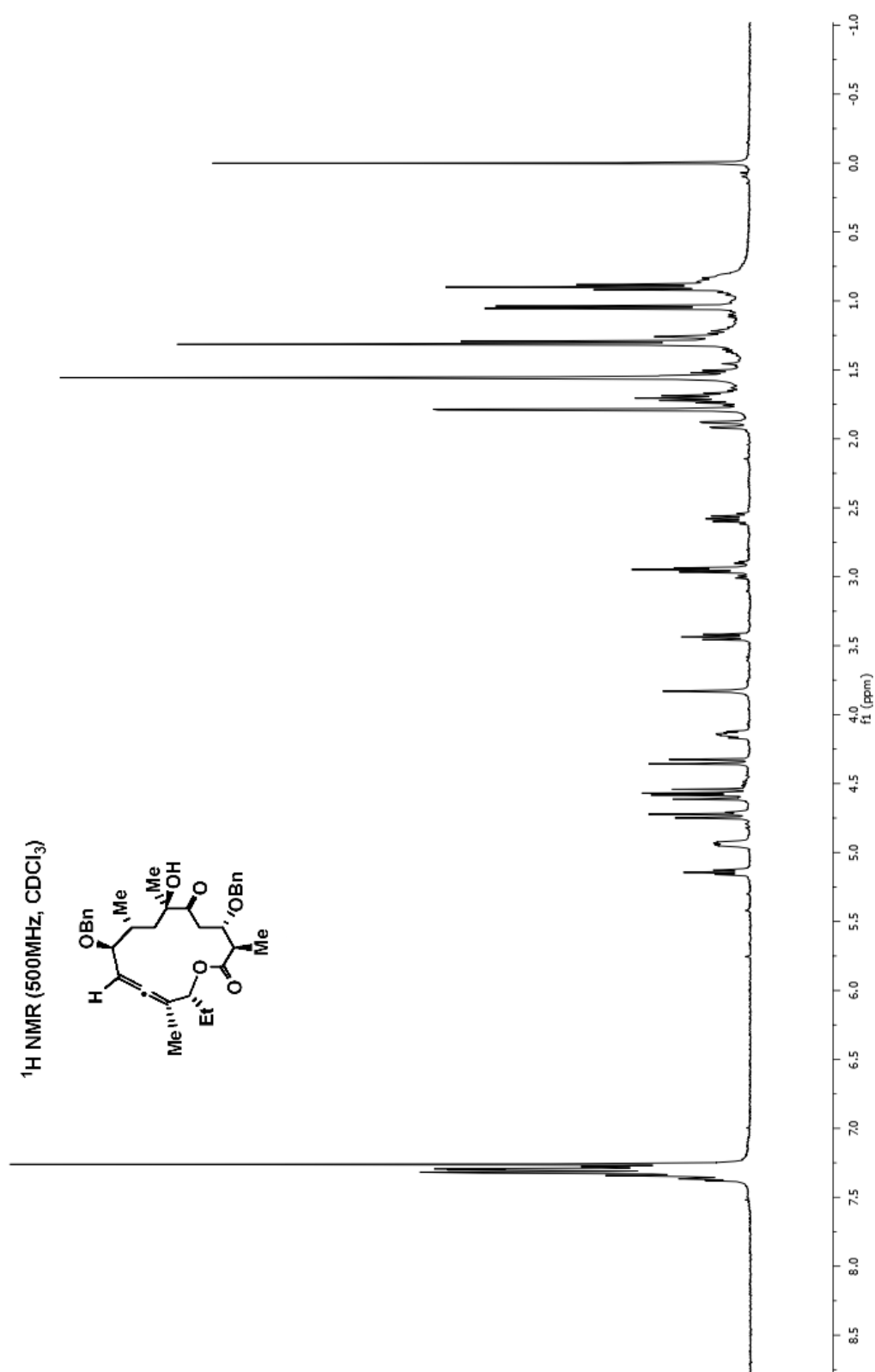




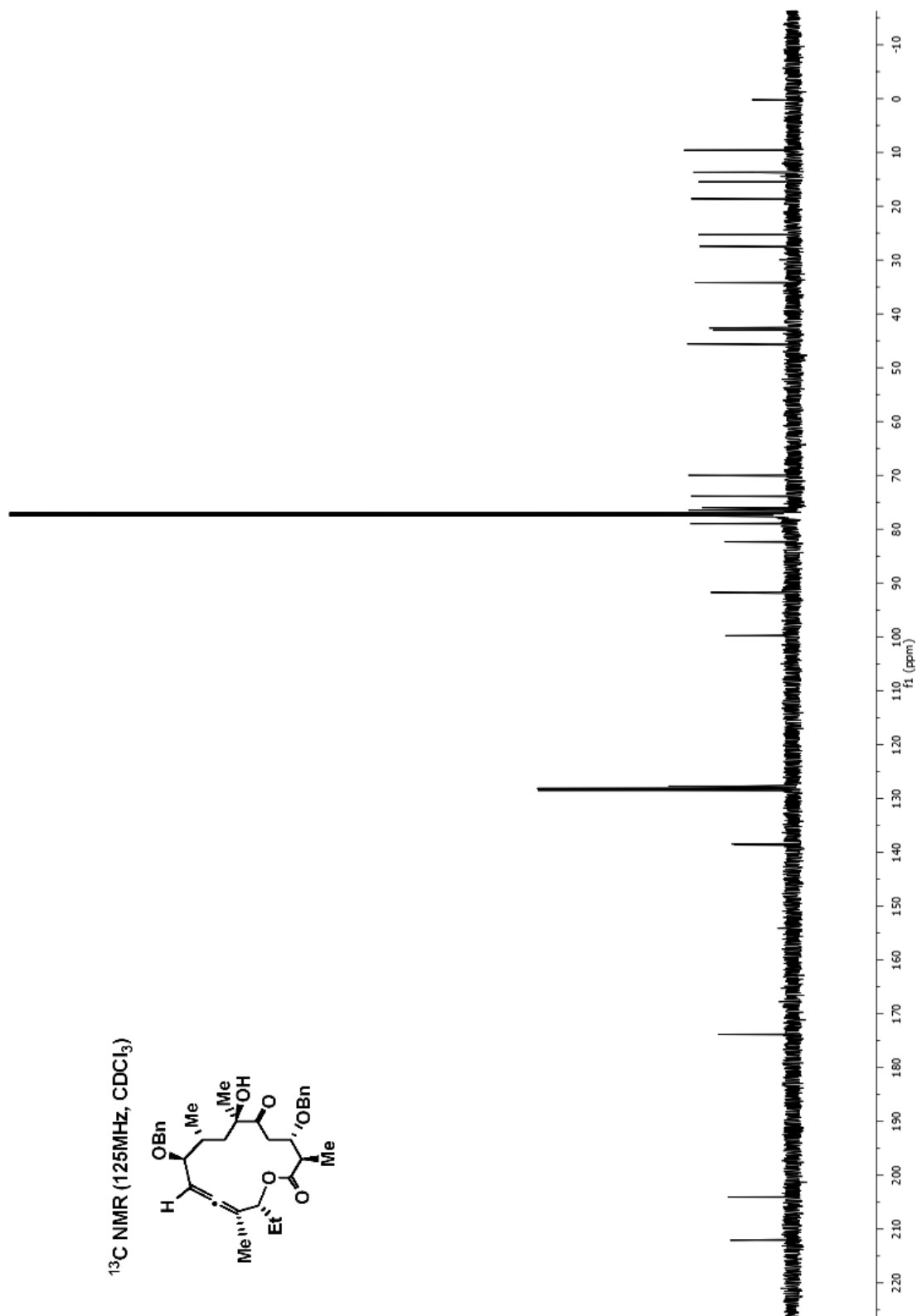
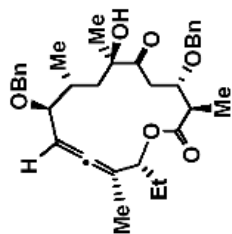
NOESY

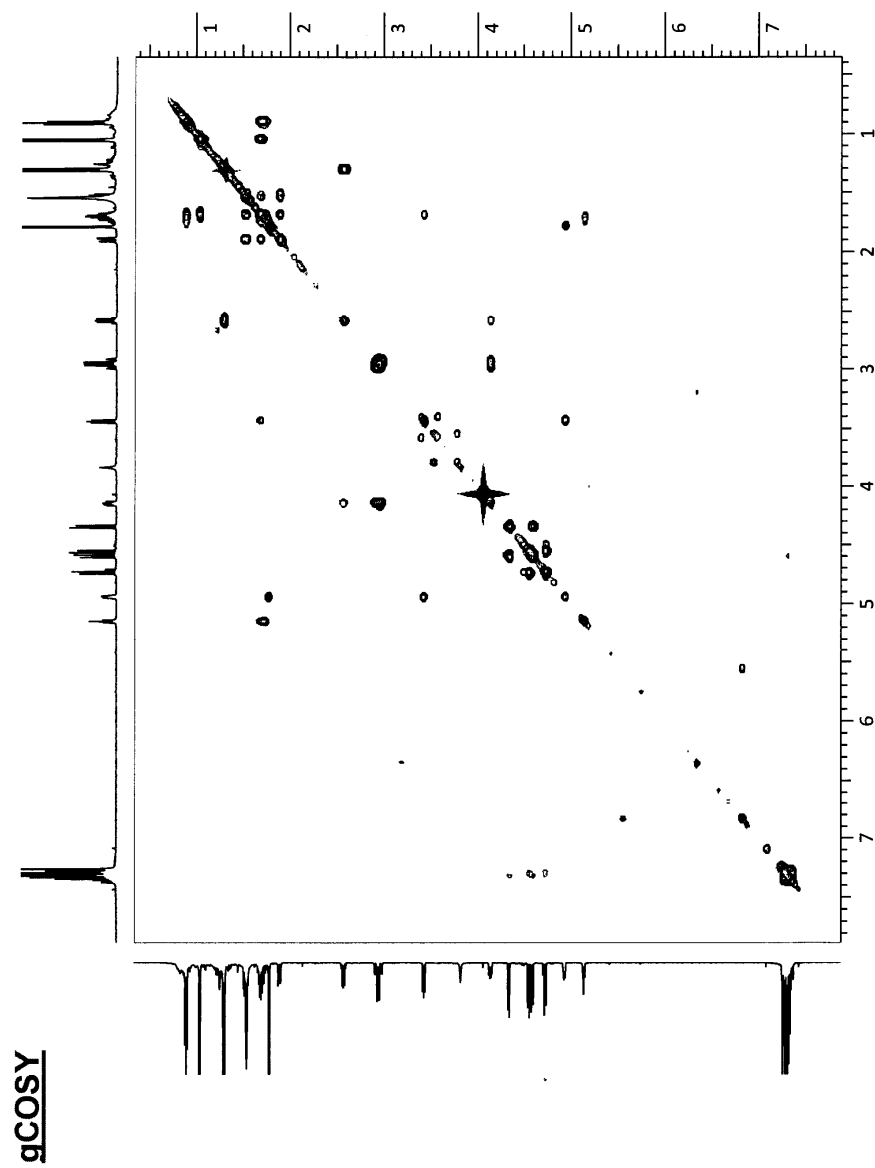




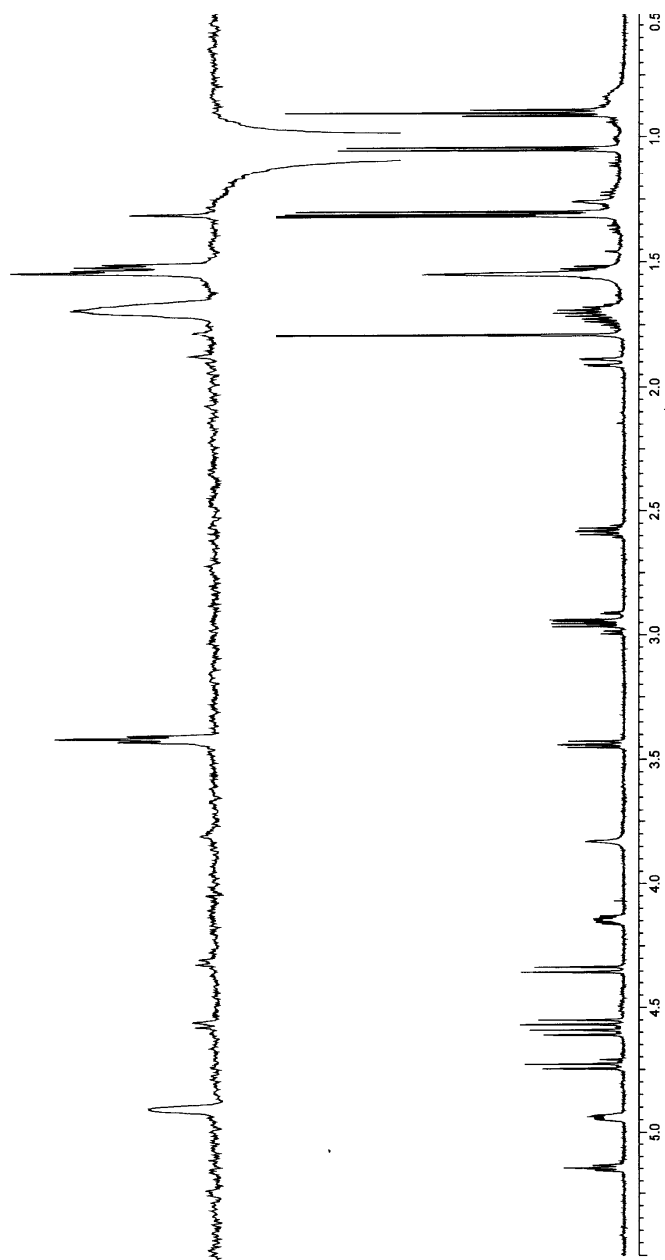


^{13}C NMR (125MHz, CDCl_3)

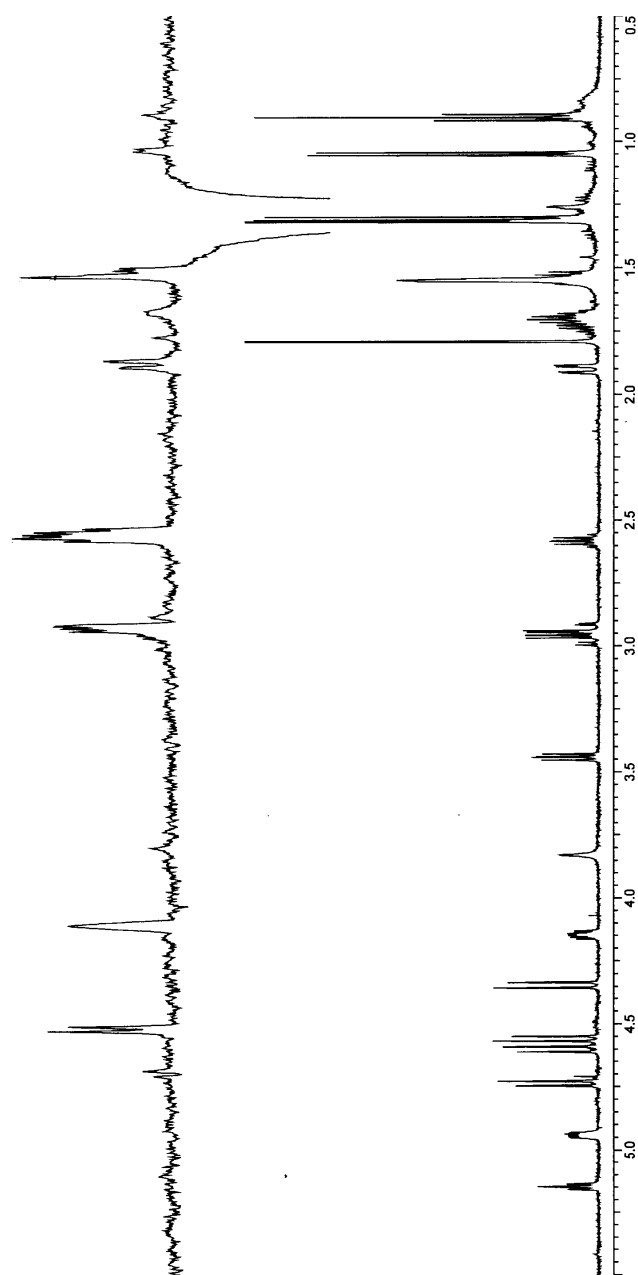




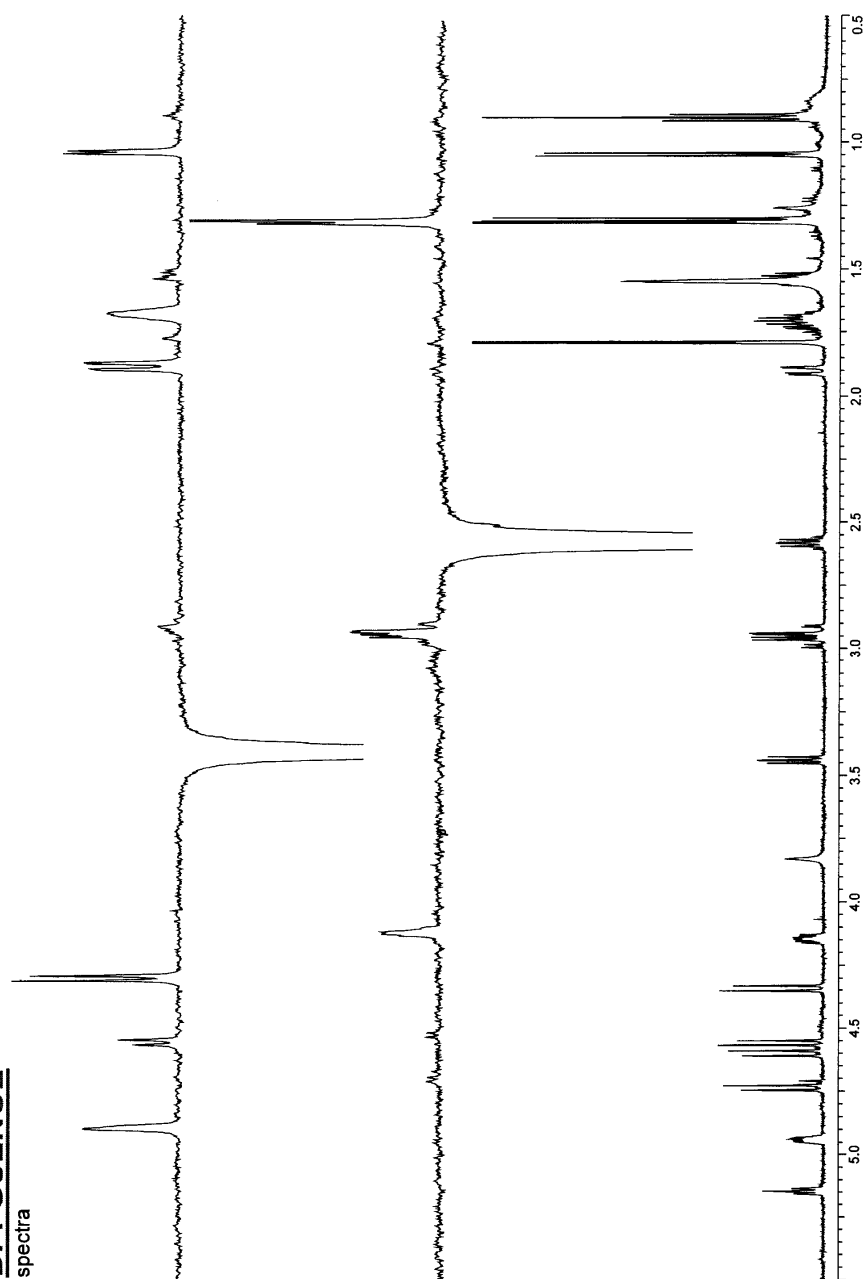
DPFGSENOE
spectrum



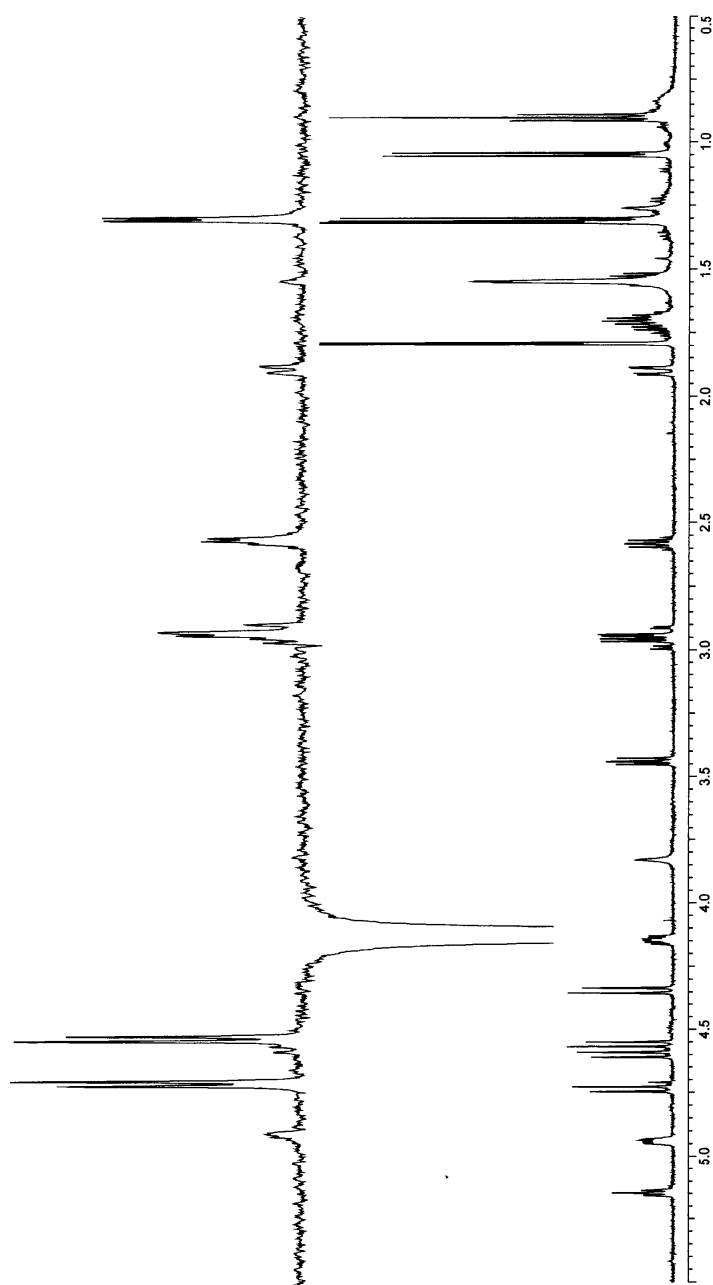
DPFGSENOE
spectrum

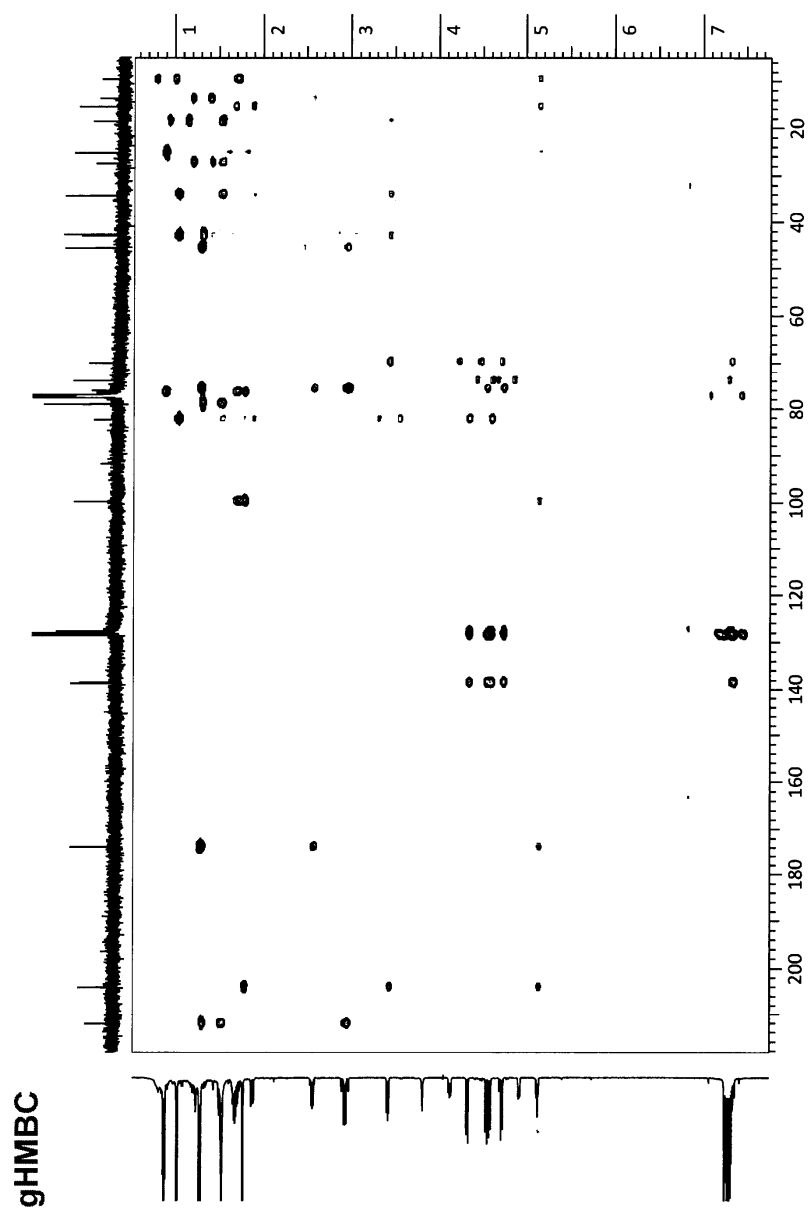


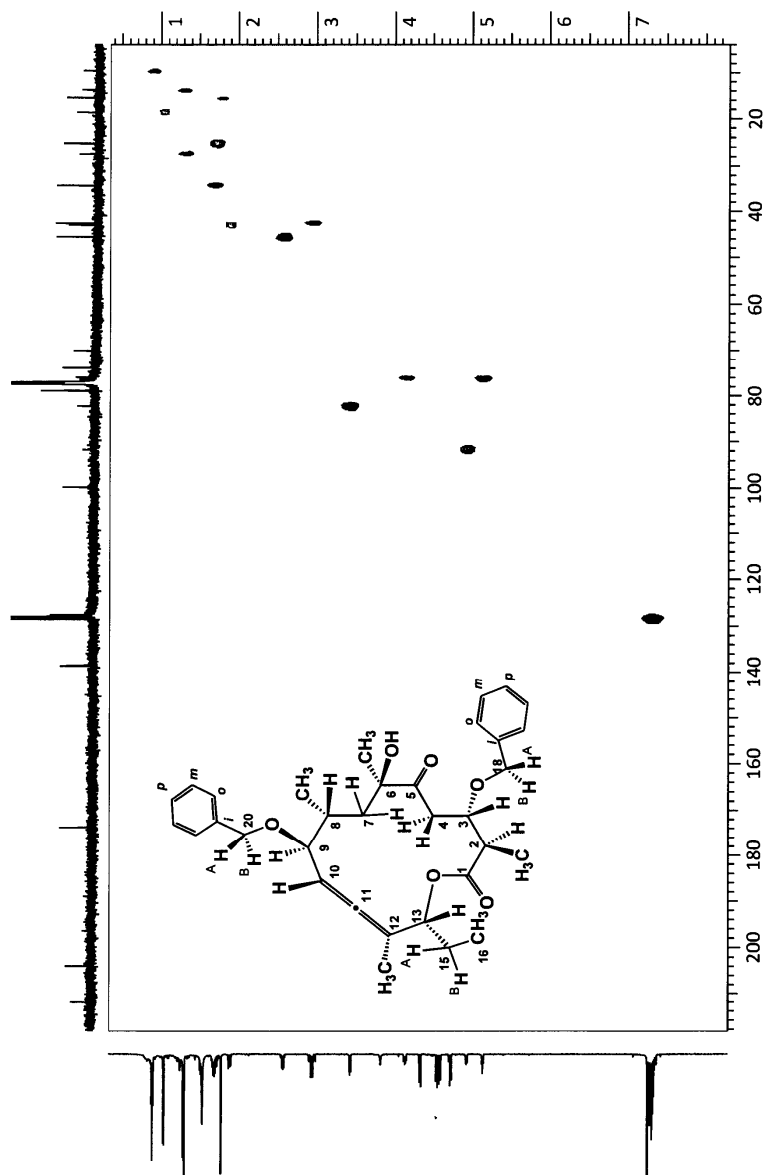
DPFGSENOE
spectra



DPFGSENOE
spectrum

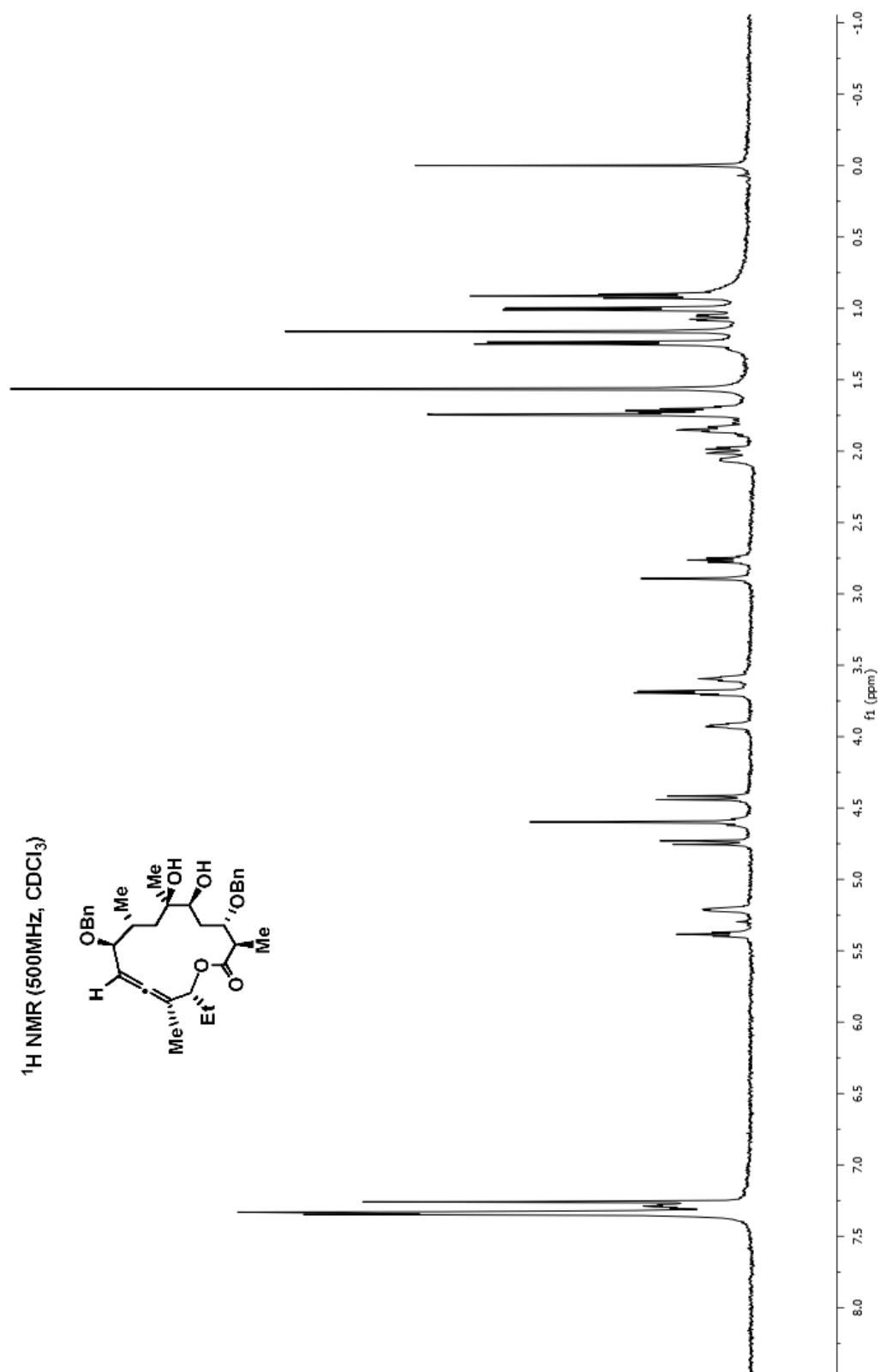
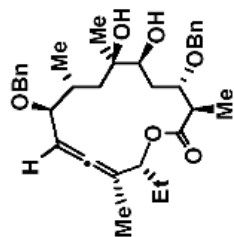




HETCOR

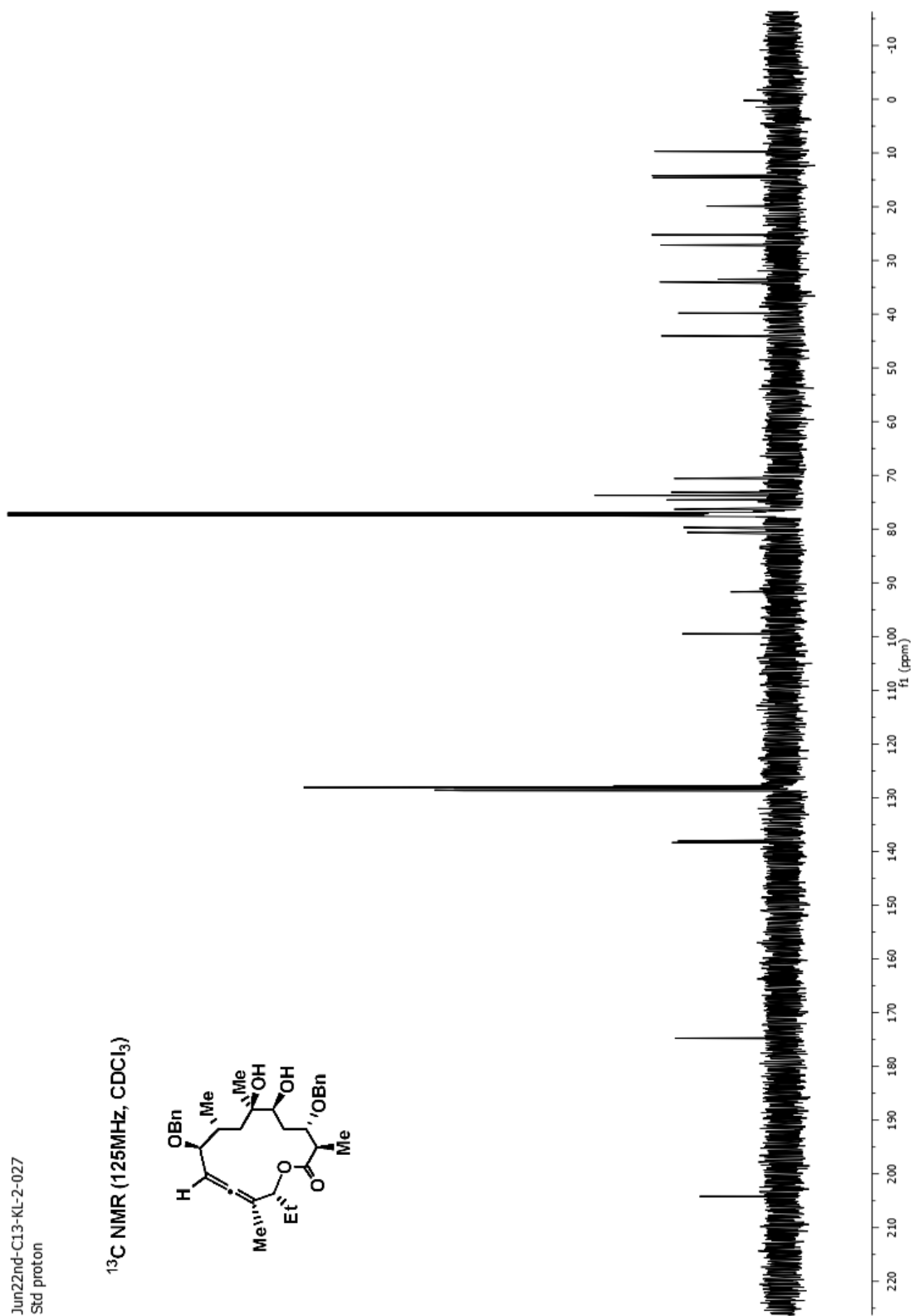
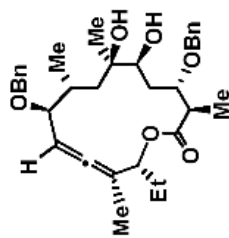
Jun22nd-H1-KL-2-027
Std proton

^1H NMR (500MHz, CDCl_3)

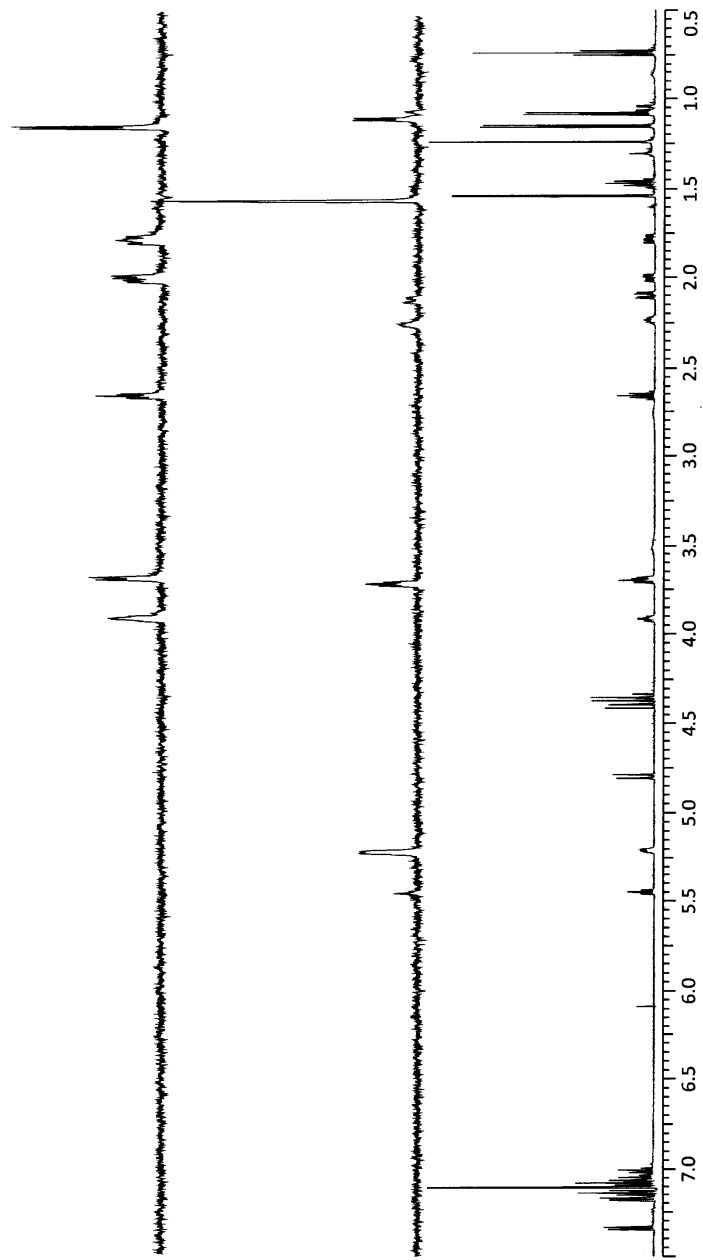


Jun22nd-C13-KL-2-027
Std proton

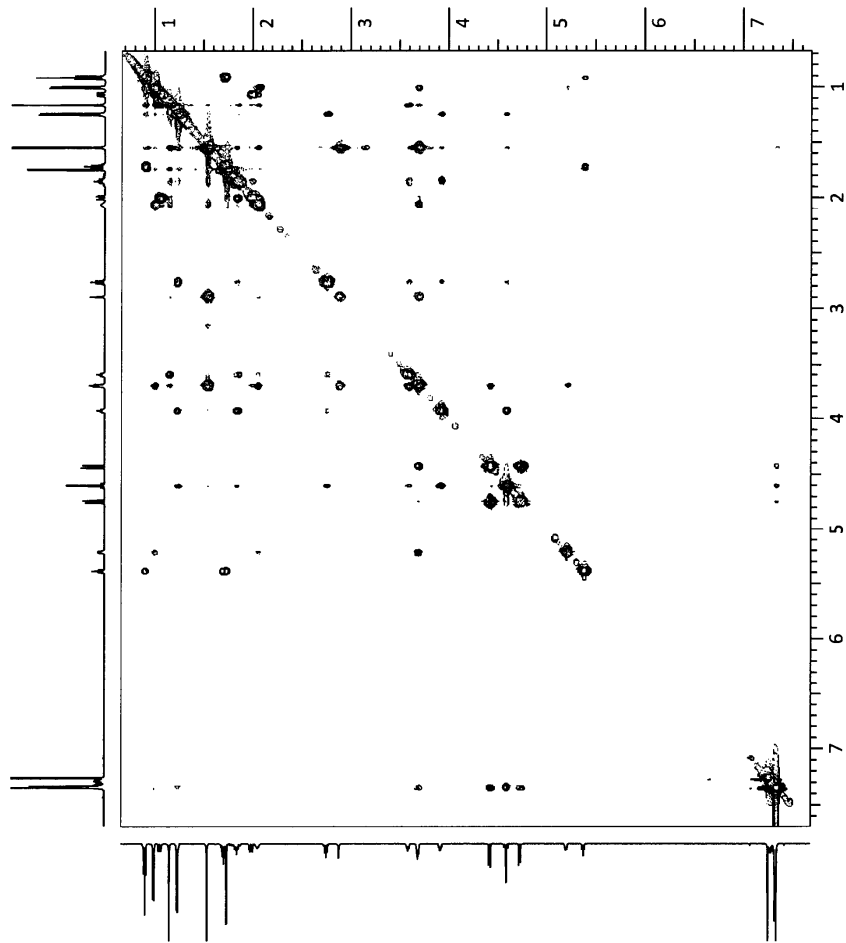
^{13}C NMR (125MHz, CDCl_3)



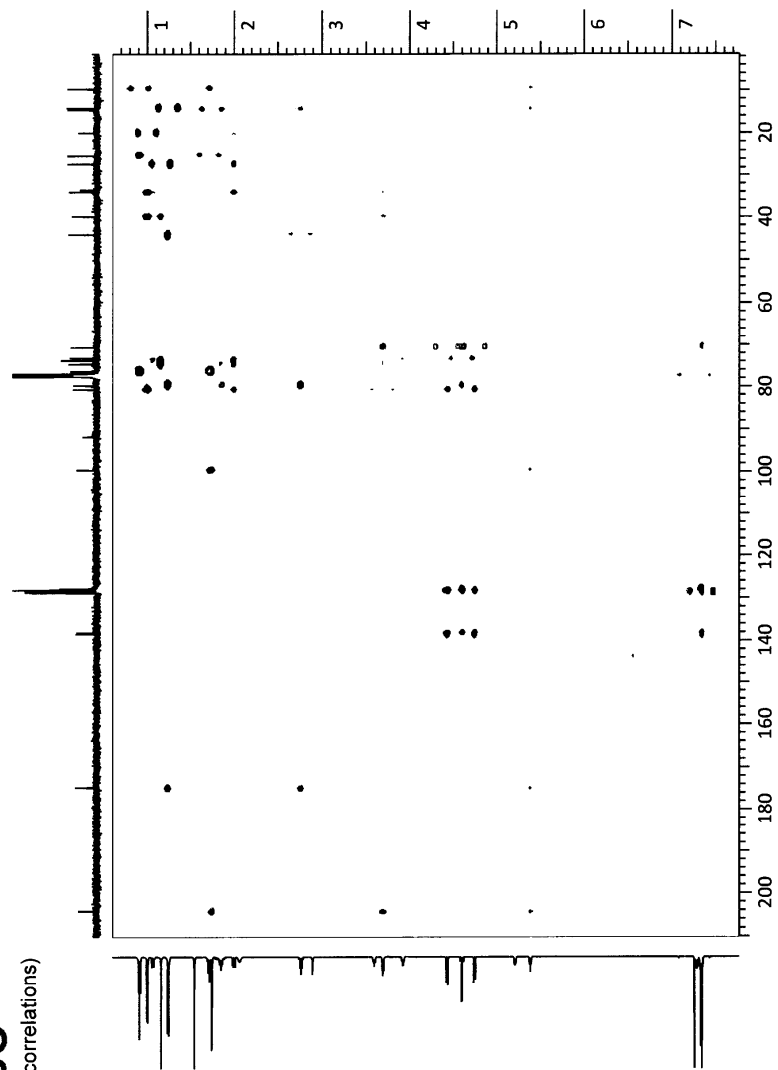
1D TOCSY spectra

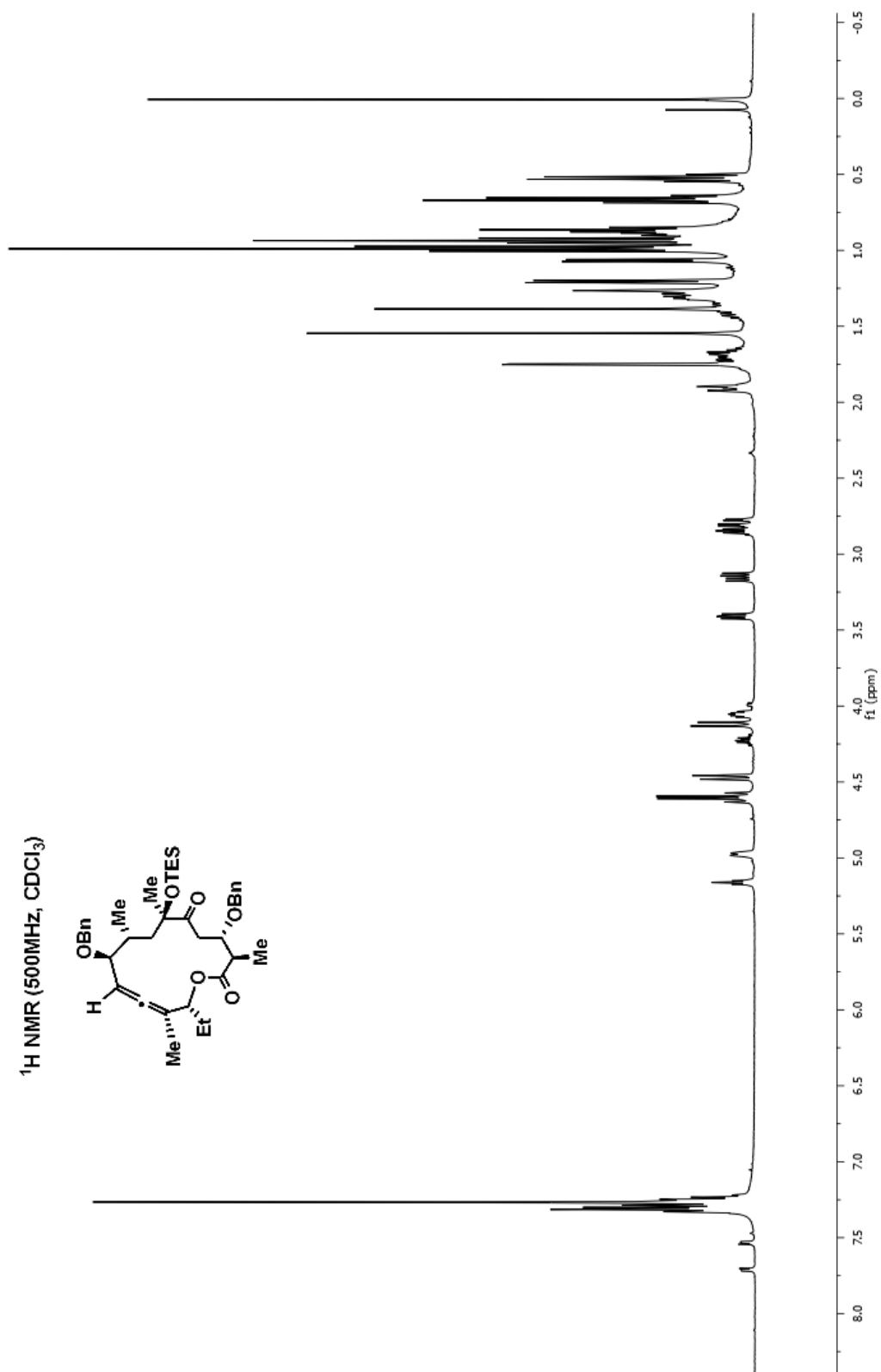


NOESY

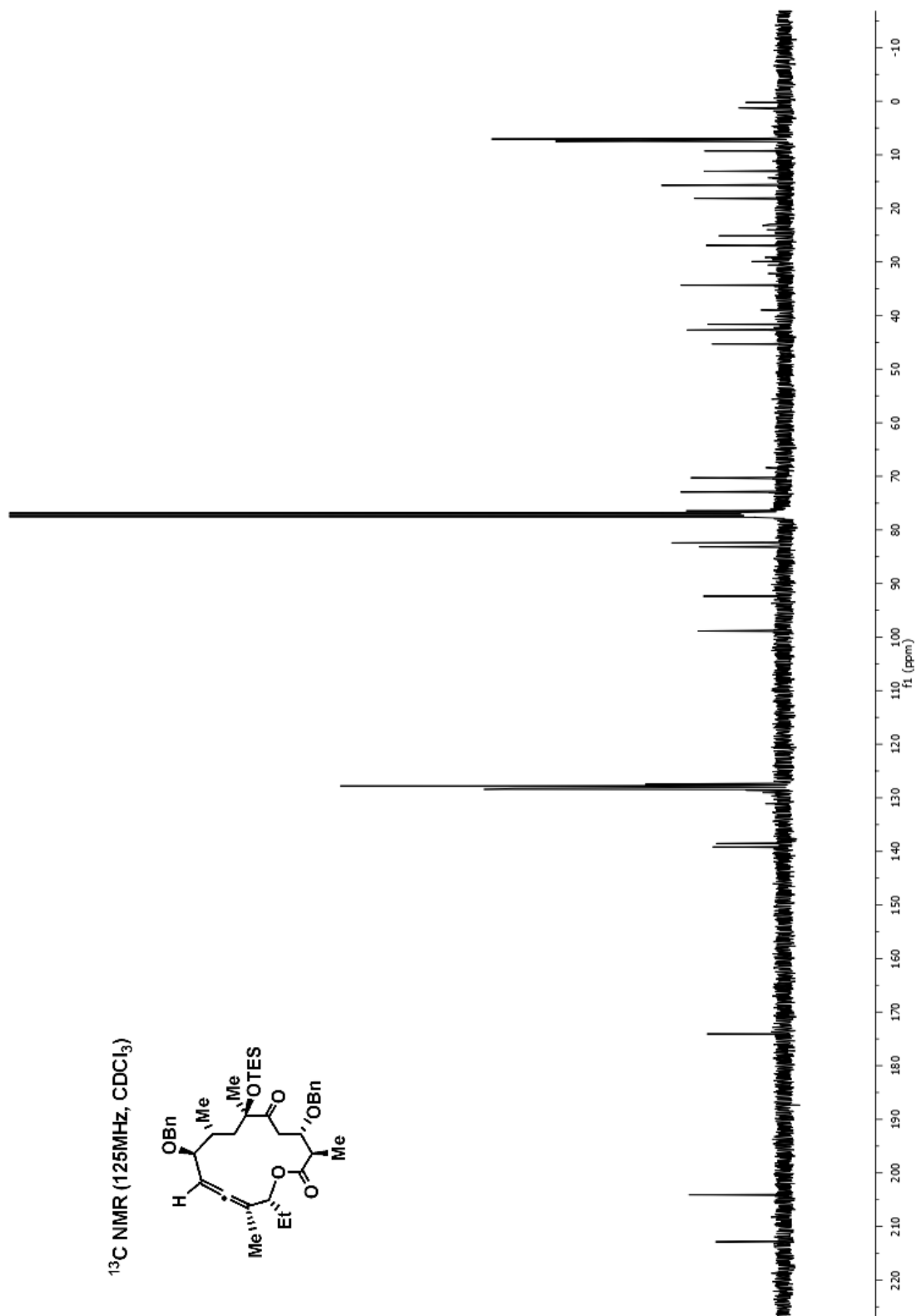
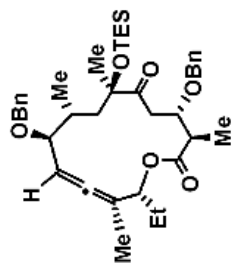


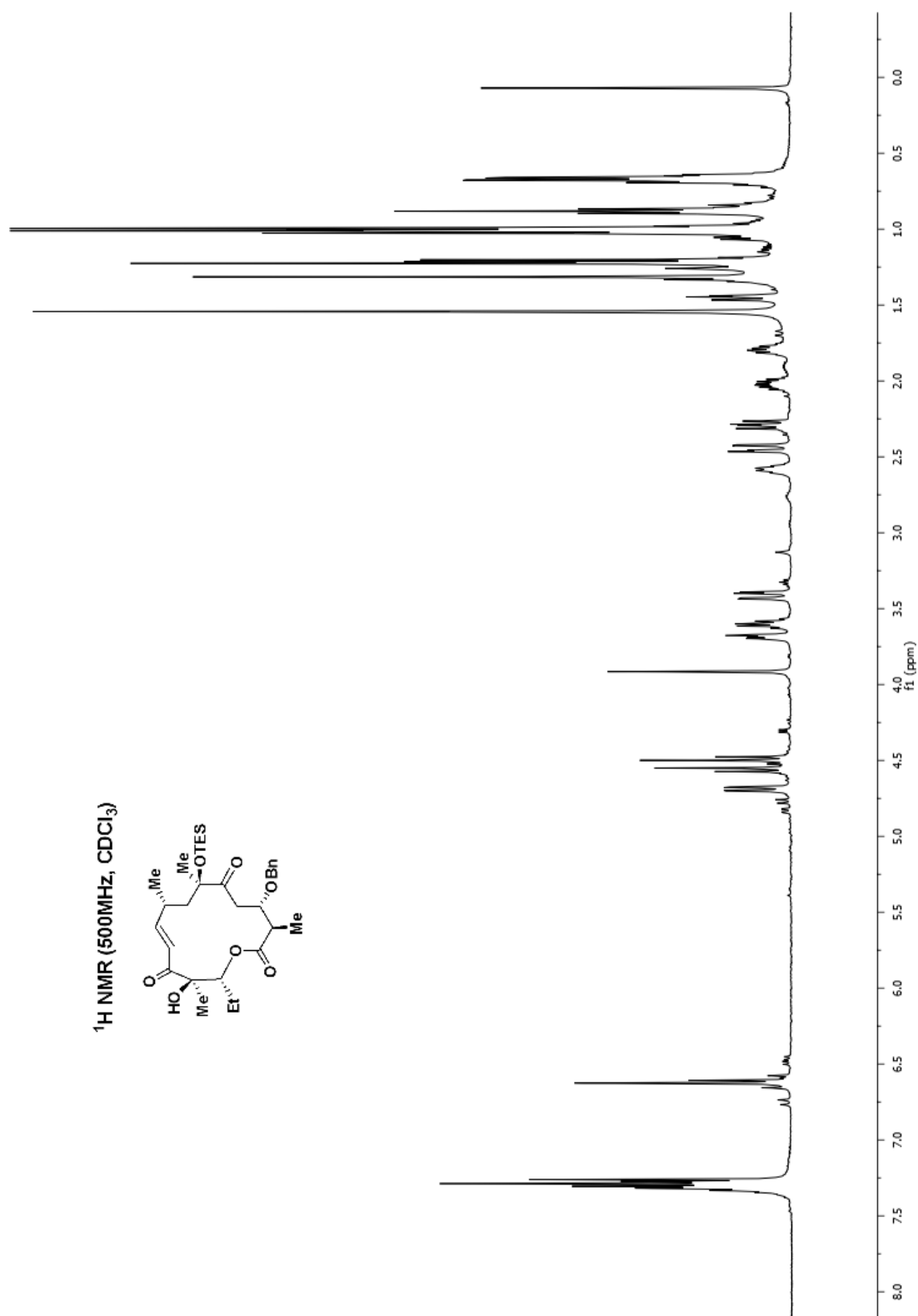
gHMBC
(long-range correlations)



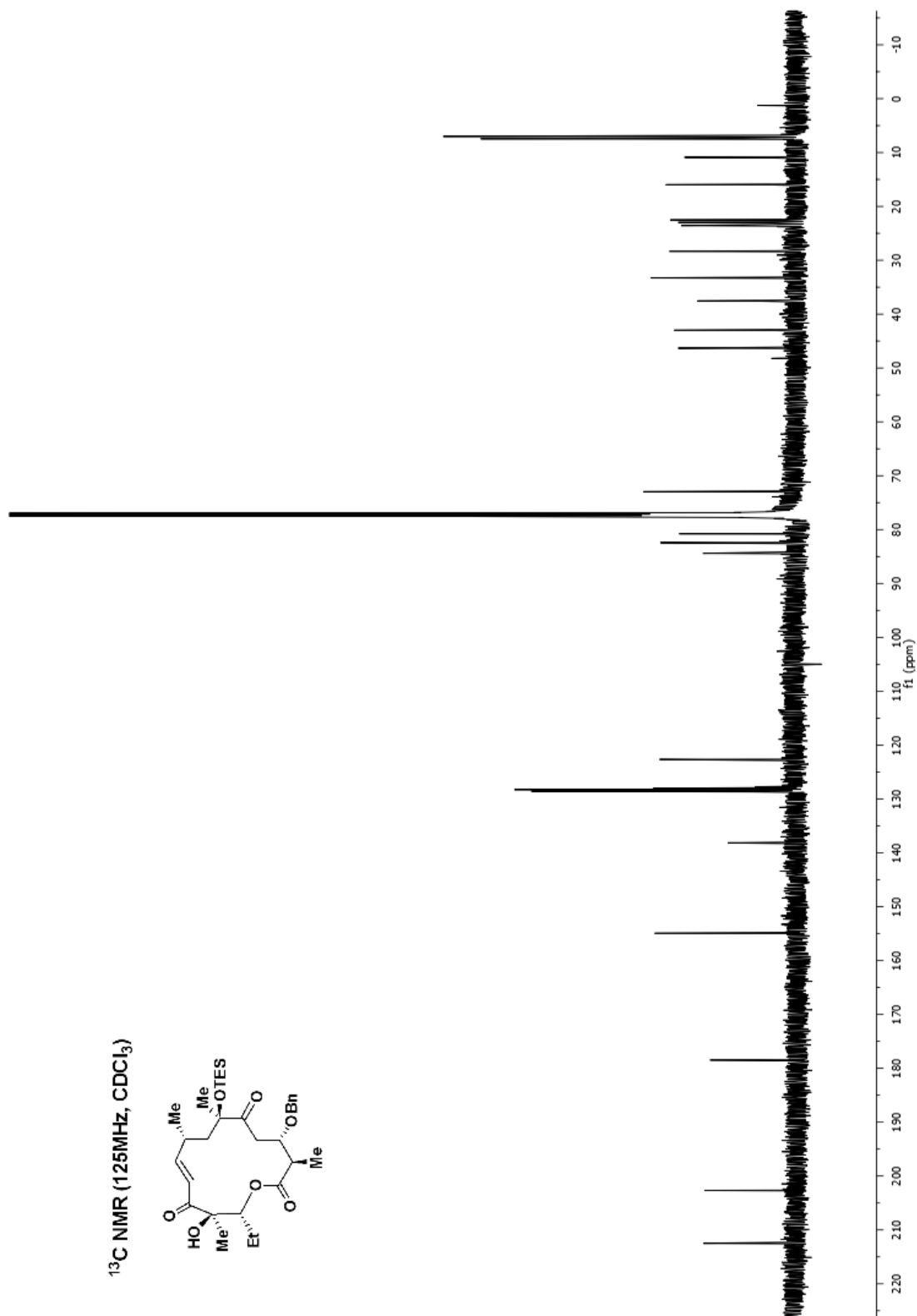
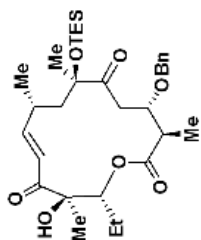


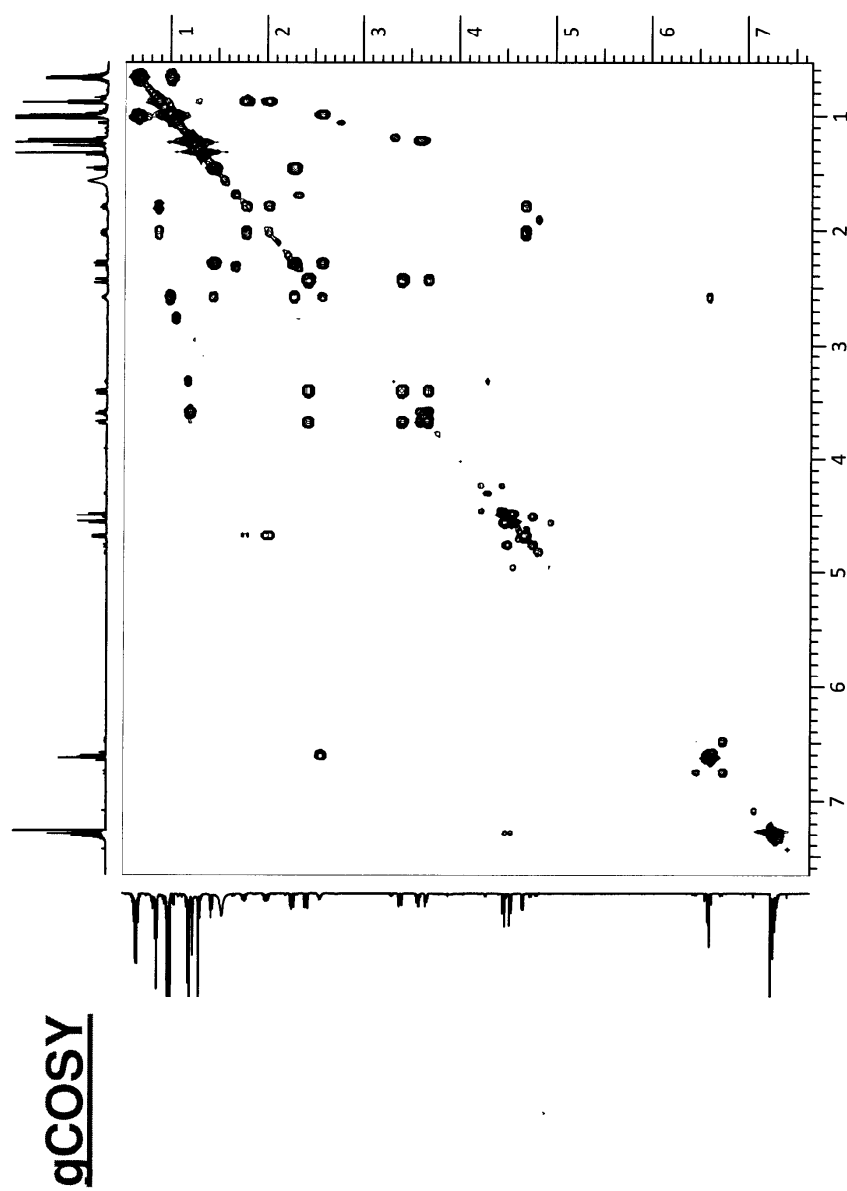
^{13}C NMR (125MHz, CDCl_3)

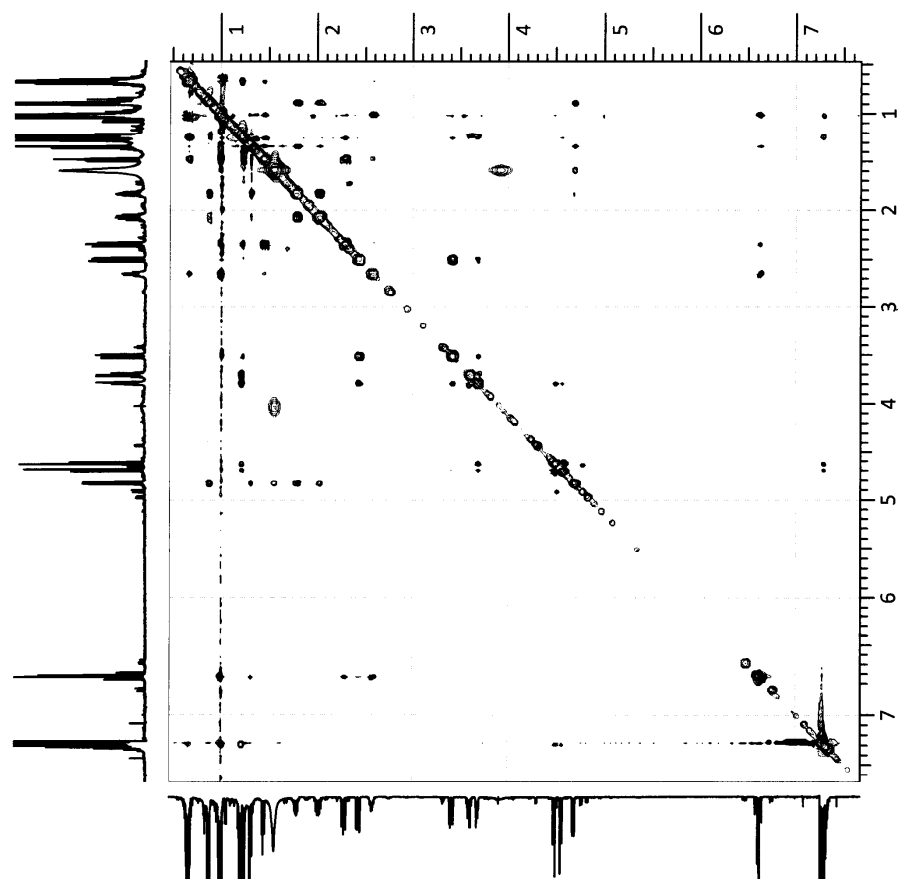




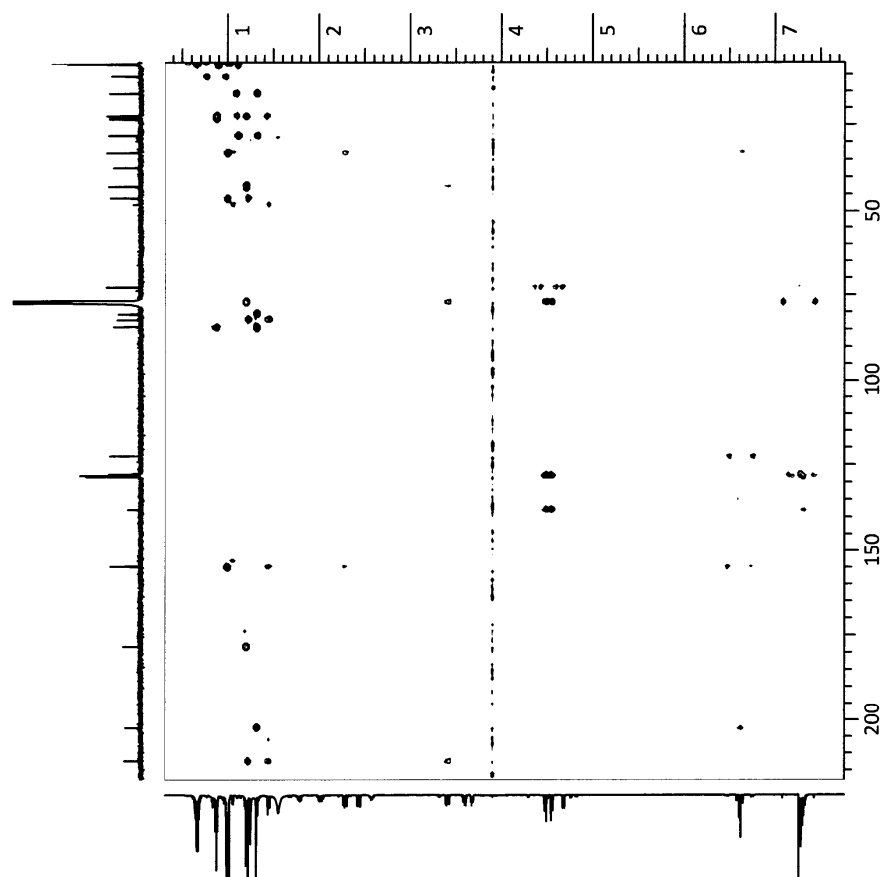
^{13}C NMR (125MHz, CDCl_3)

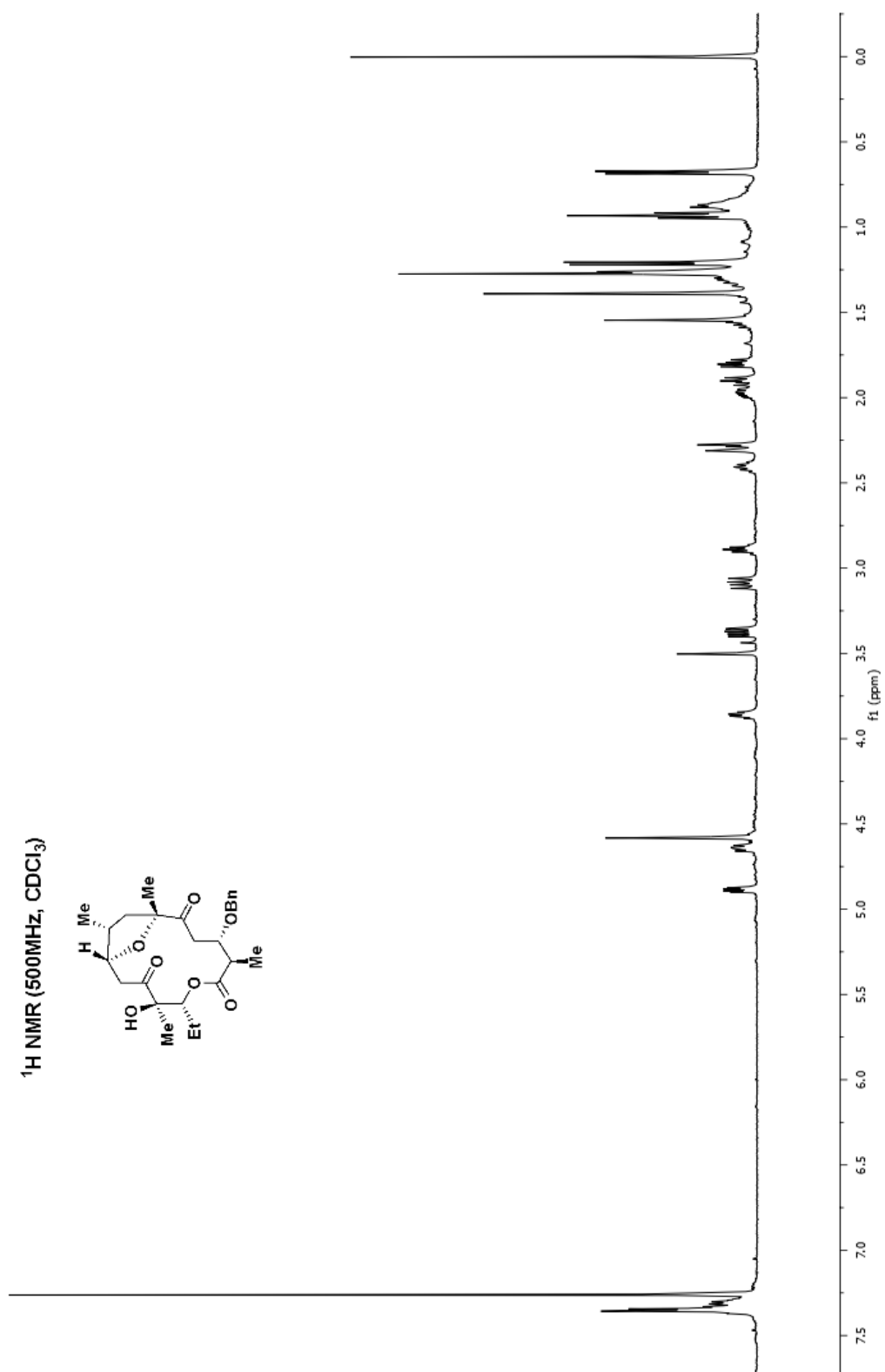


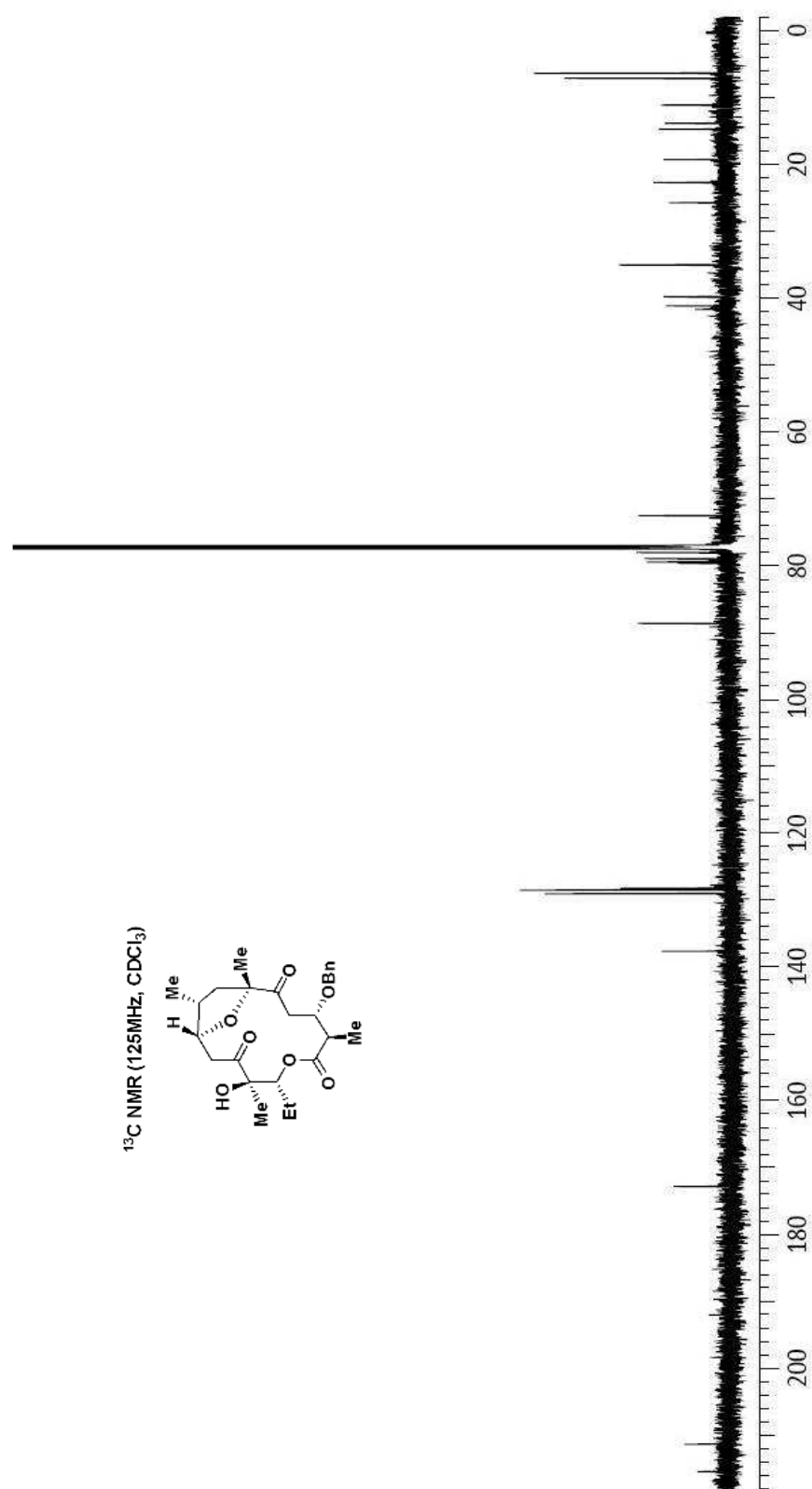




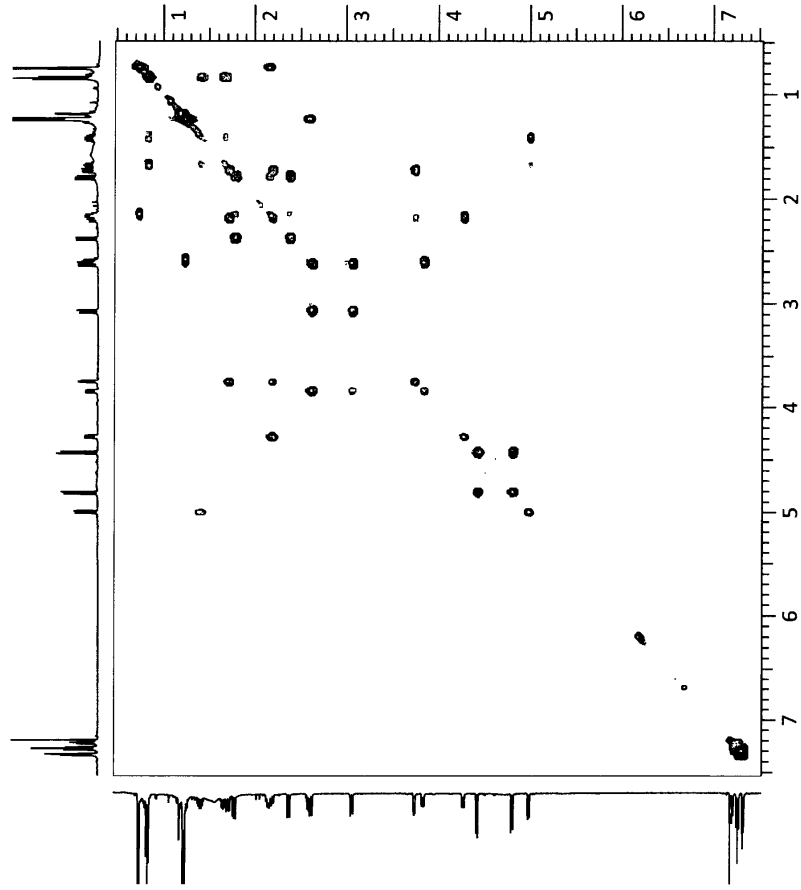
gHMBC



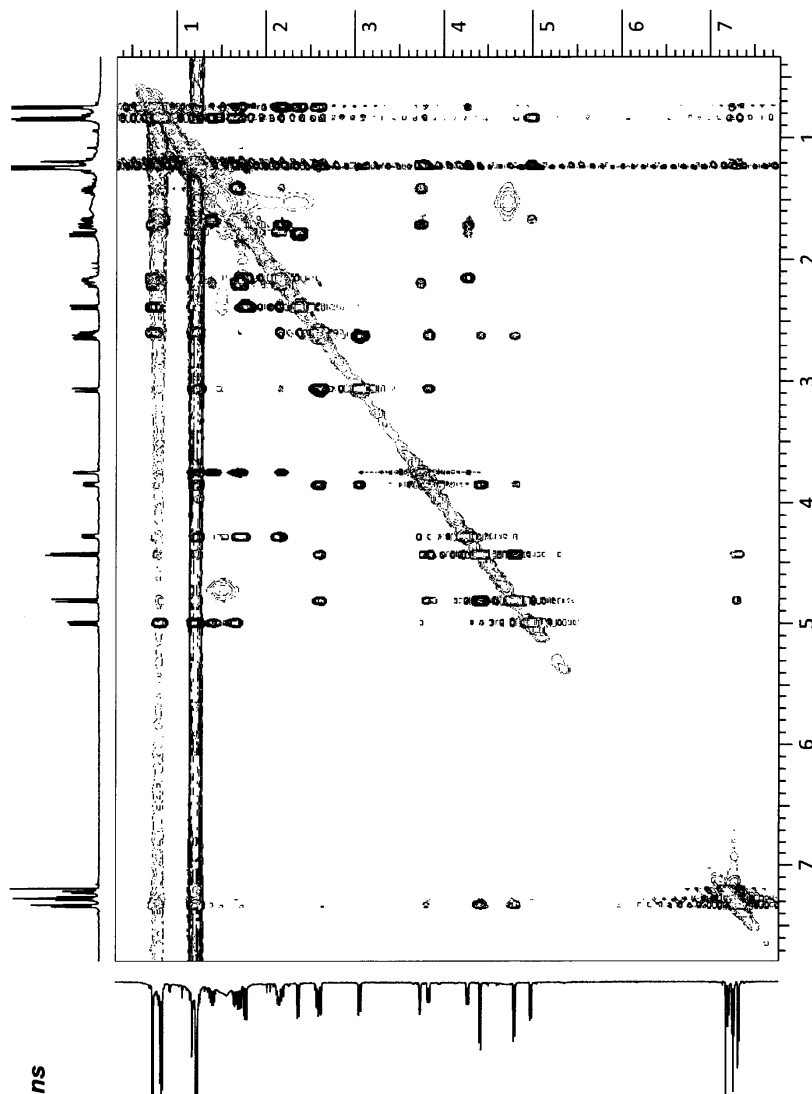




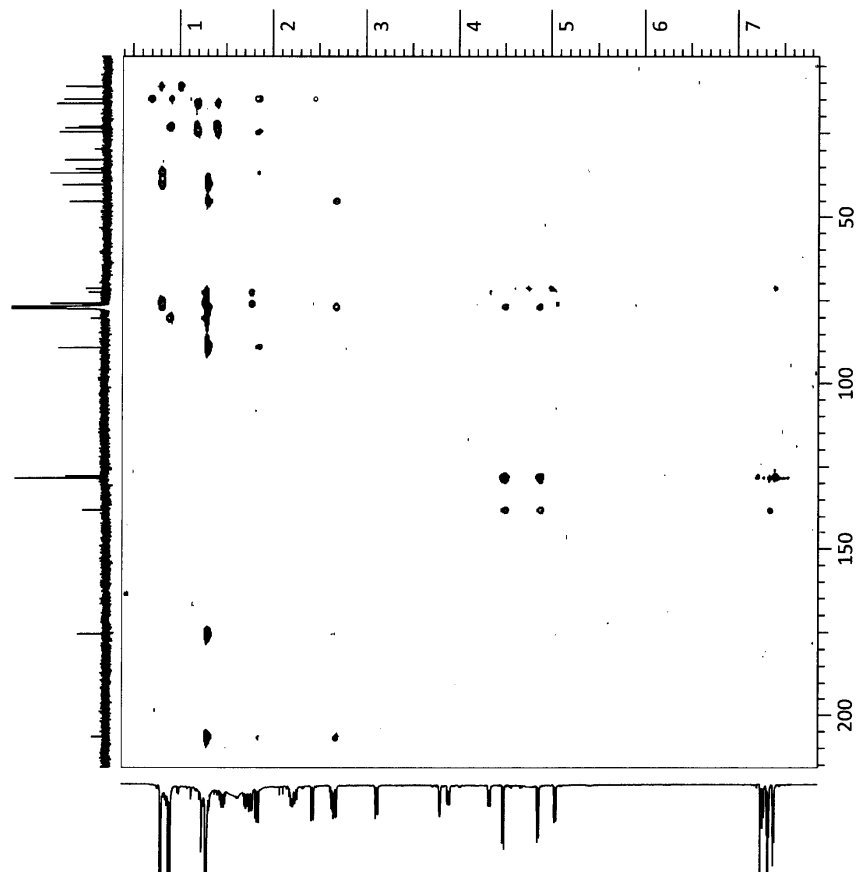
gCOSY

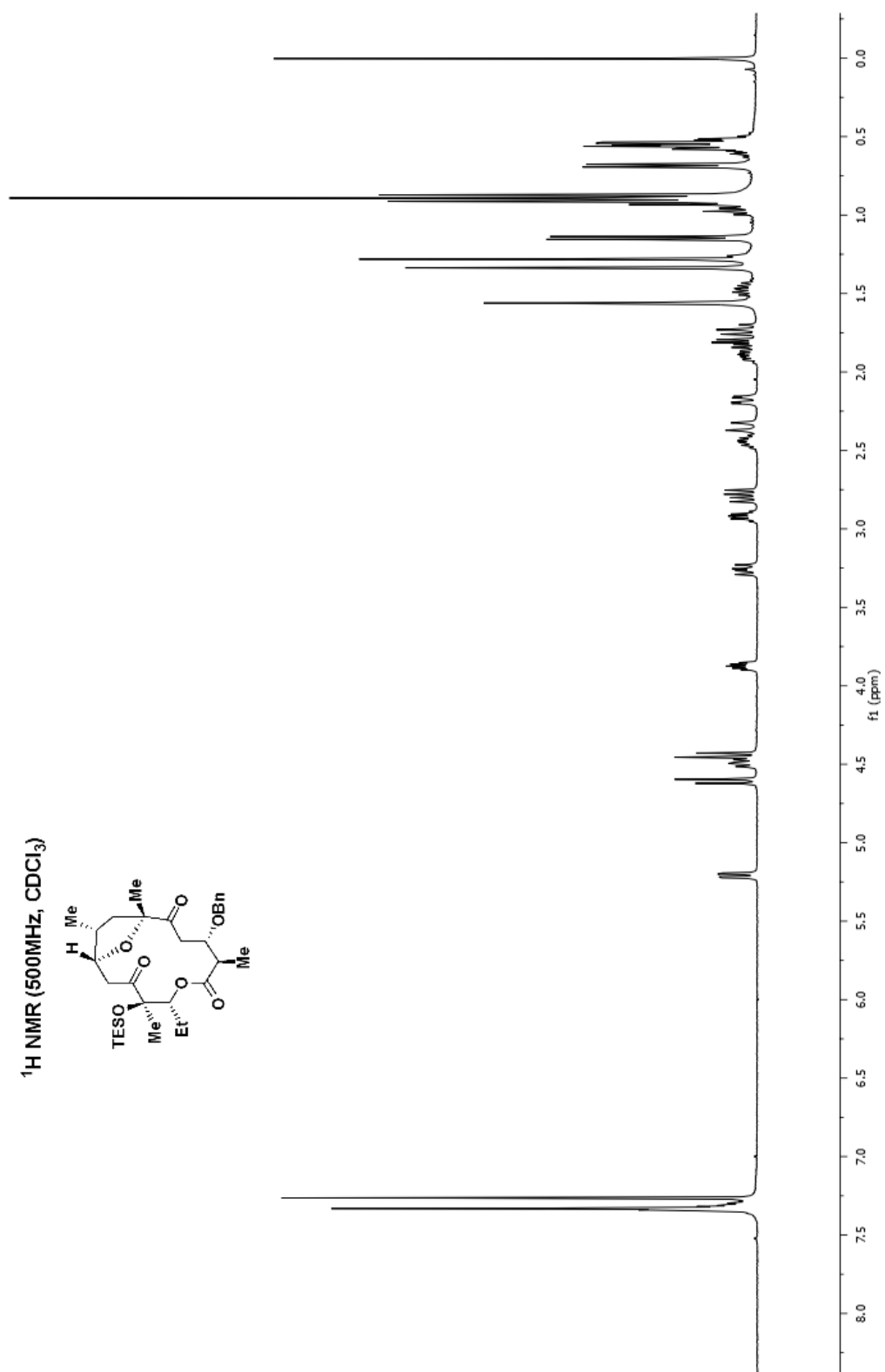


NOESY
correlations

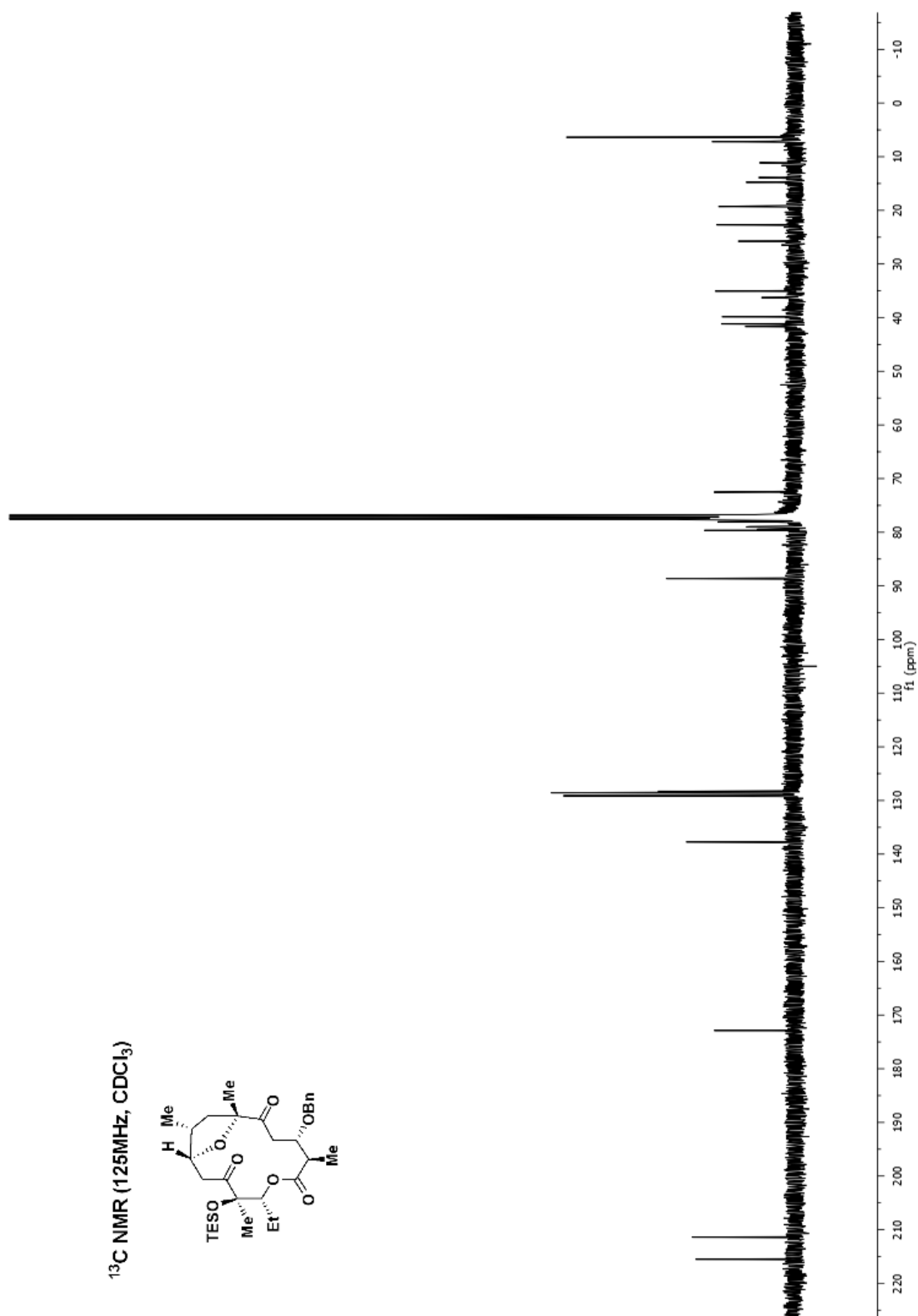
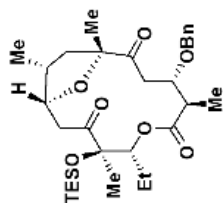


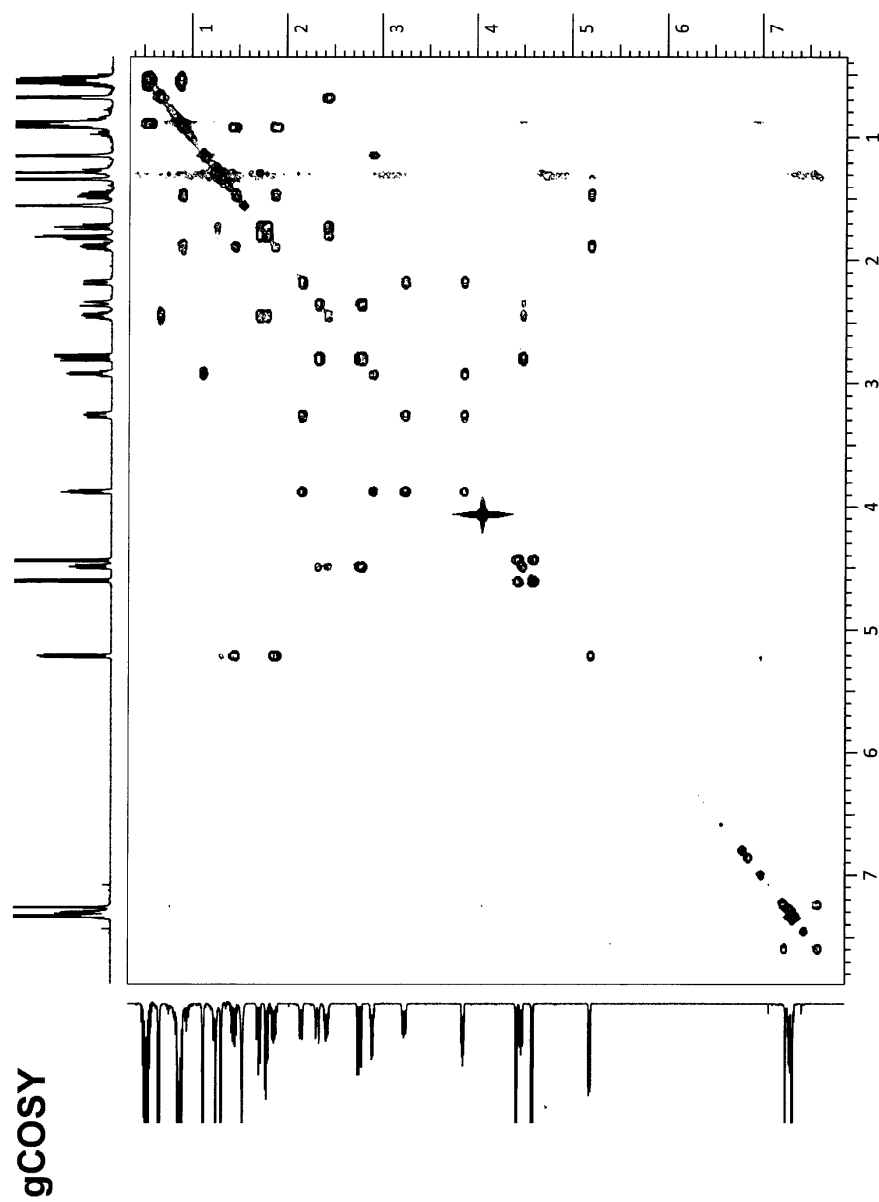
gHMBC
correlations



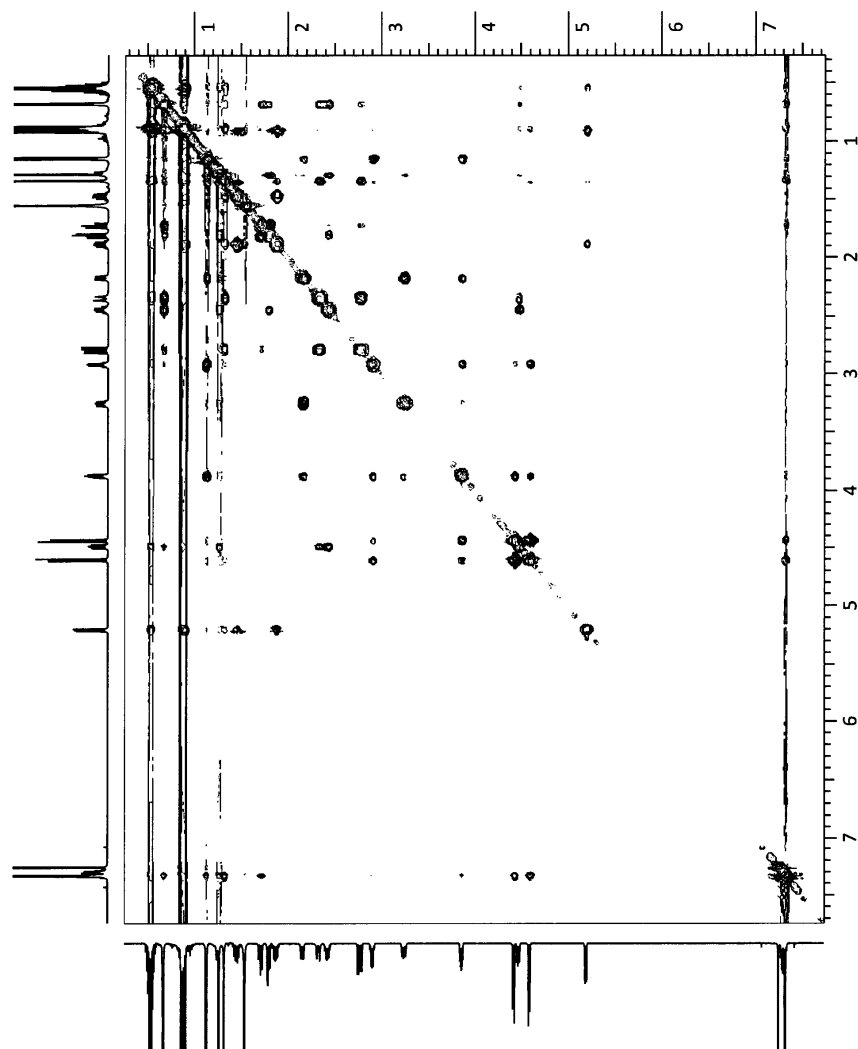


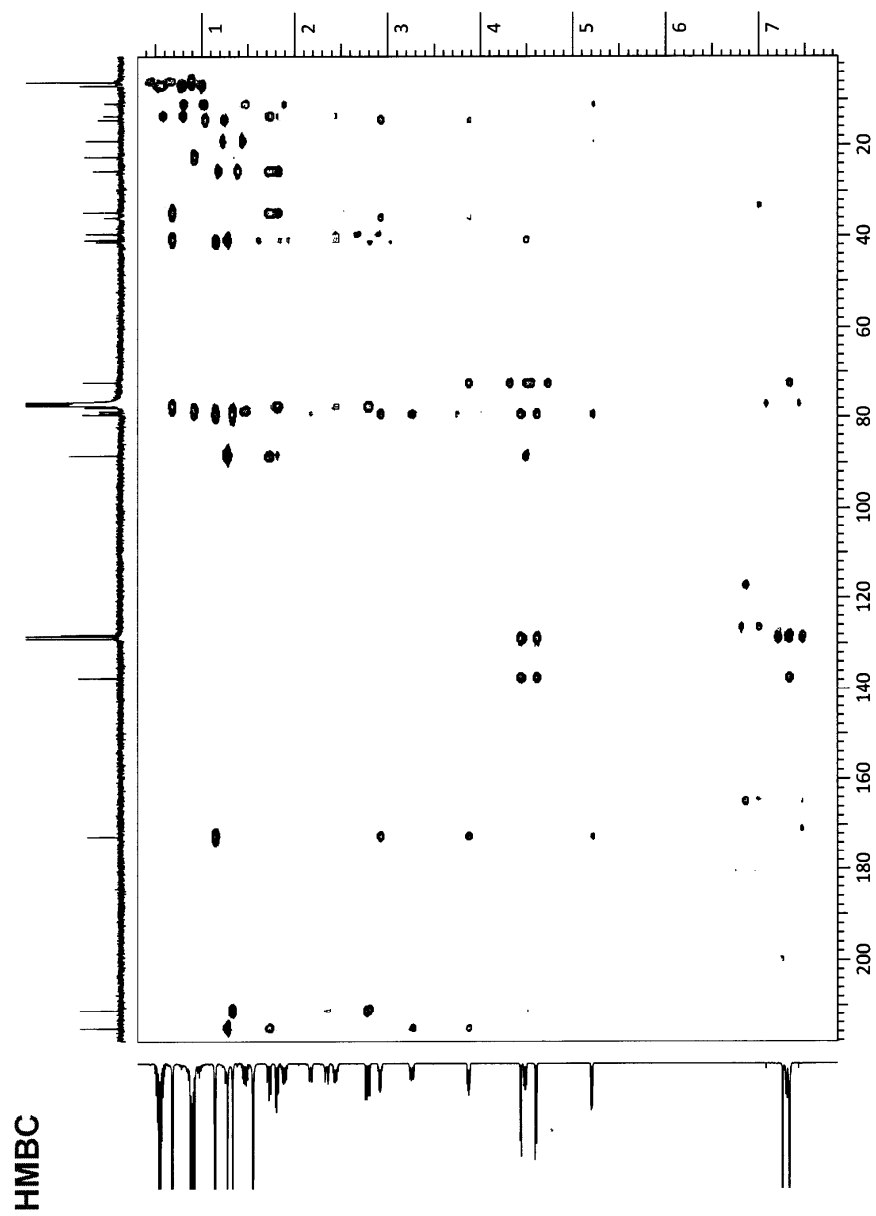
^{13}C NMR (125MHz, CDCl_3)



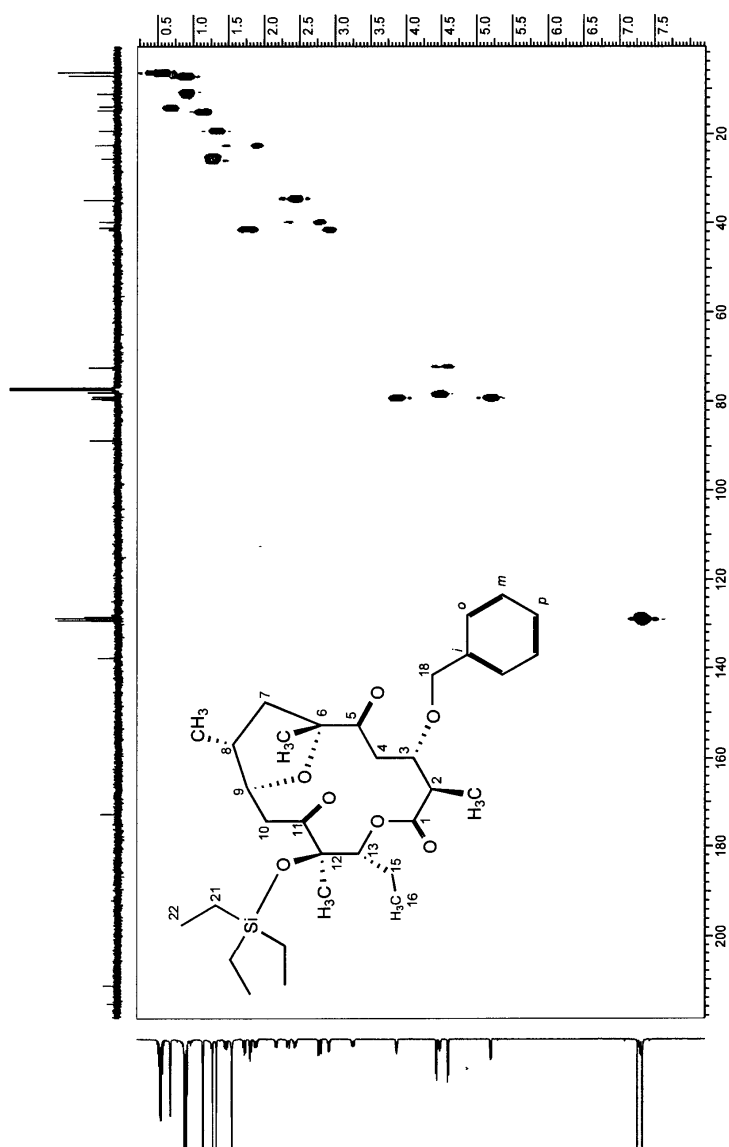


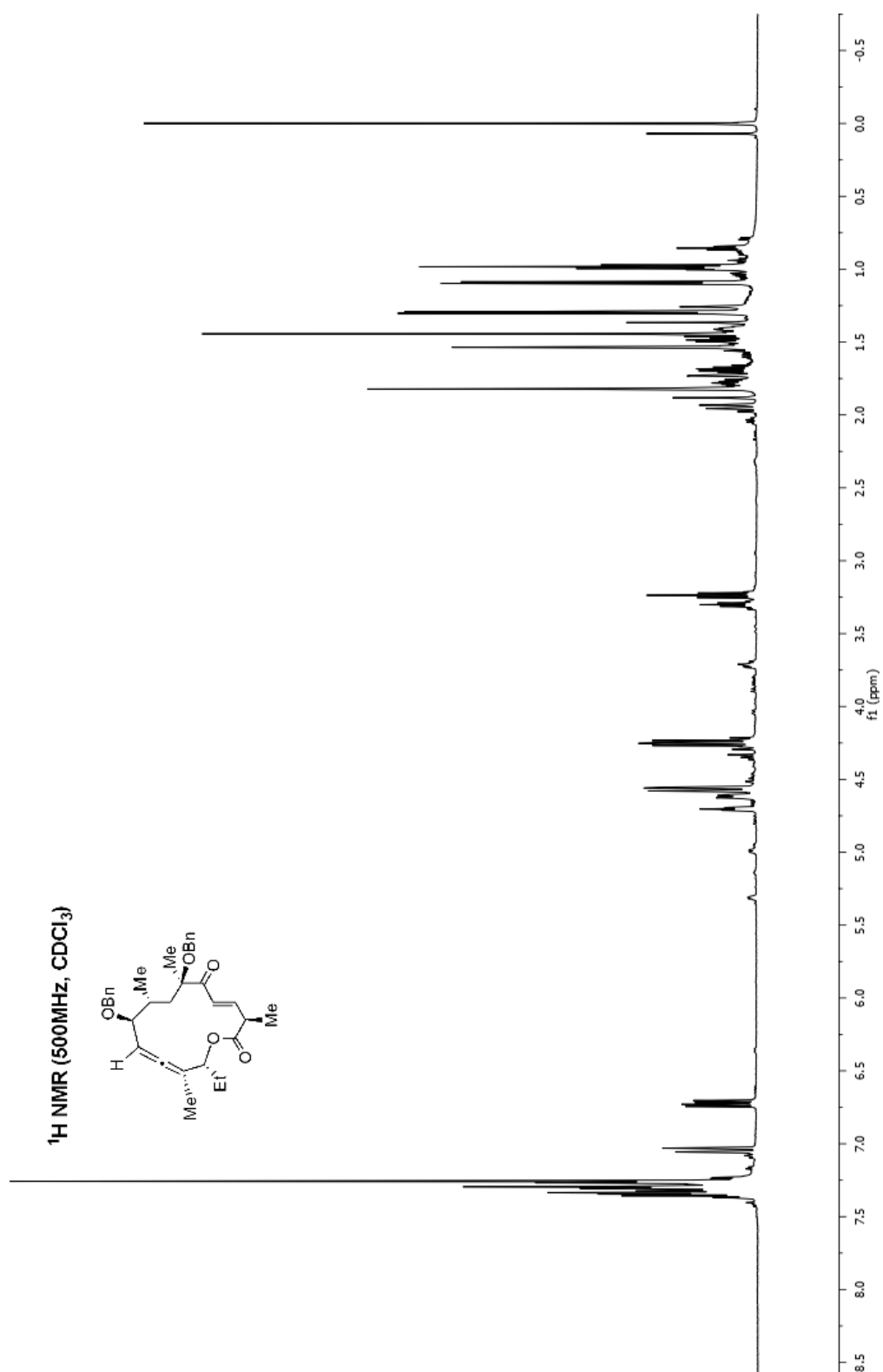
NOESY



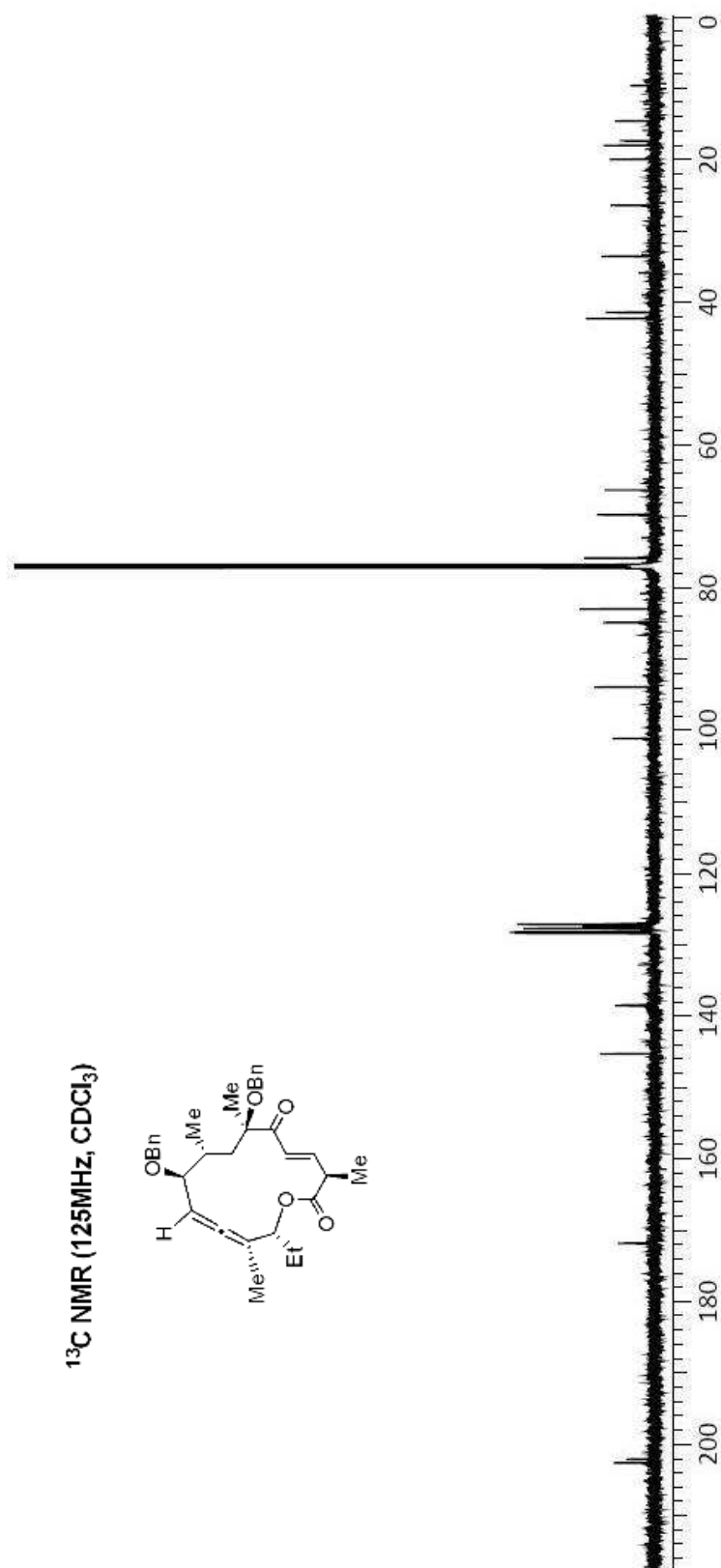
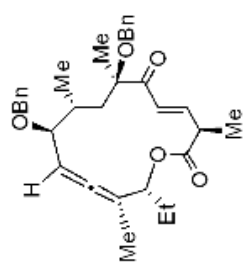


One-bond heterocorrelation (HETCOR) spectrum

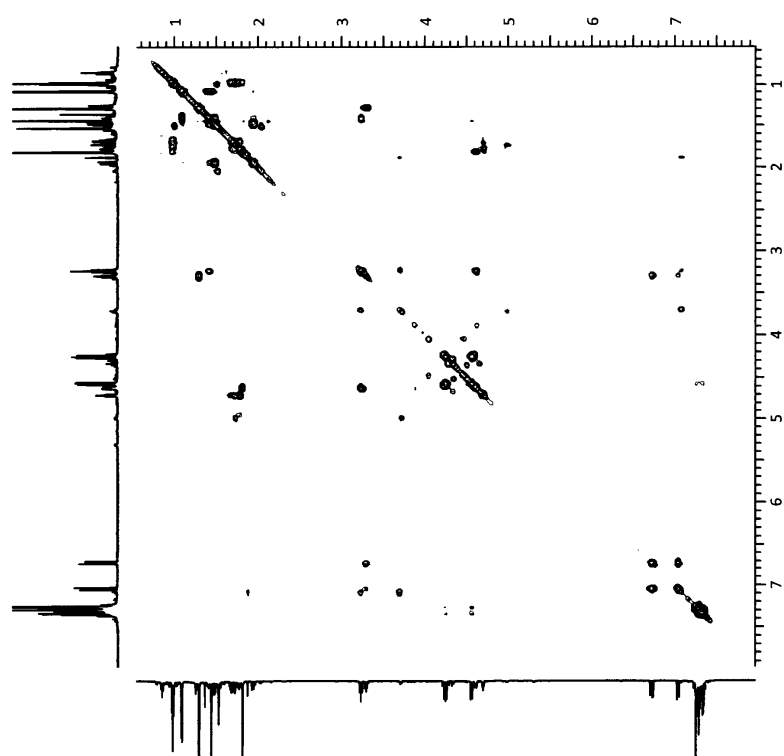


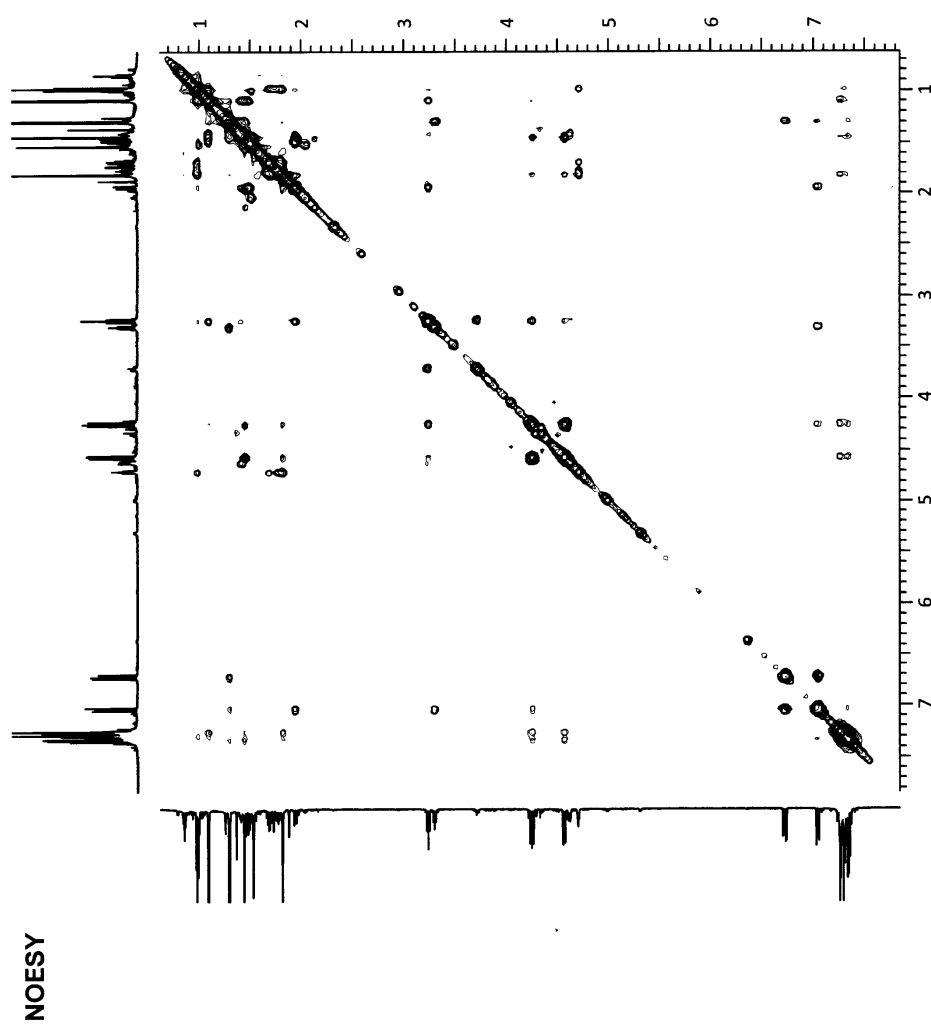


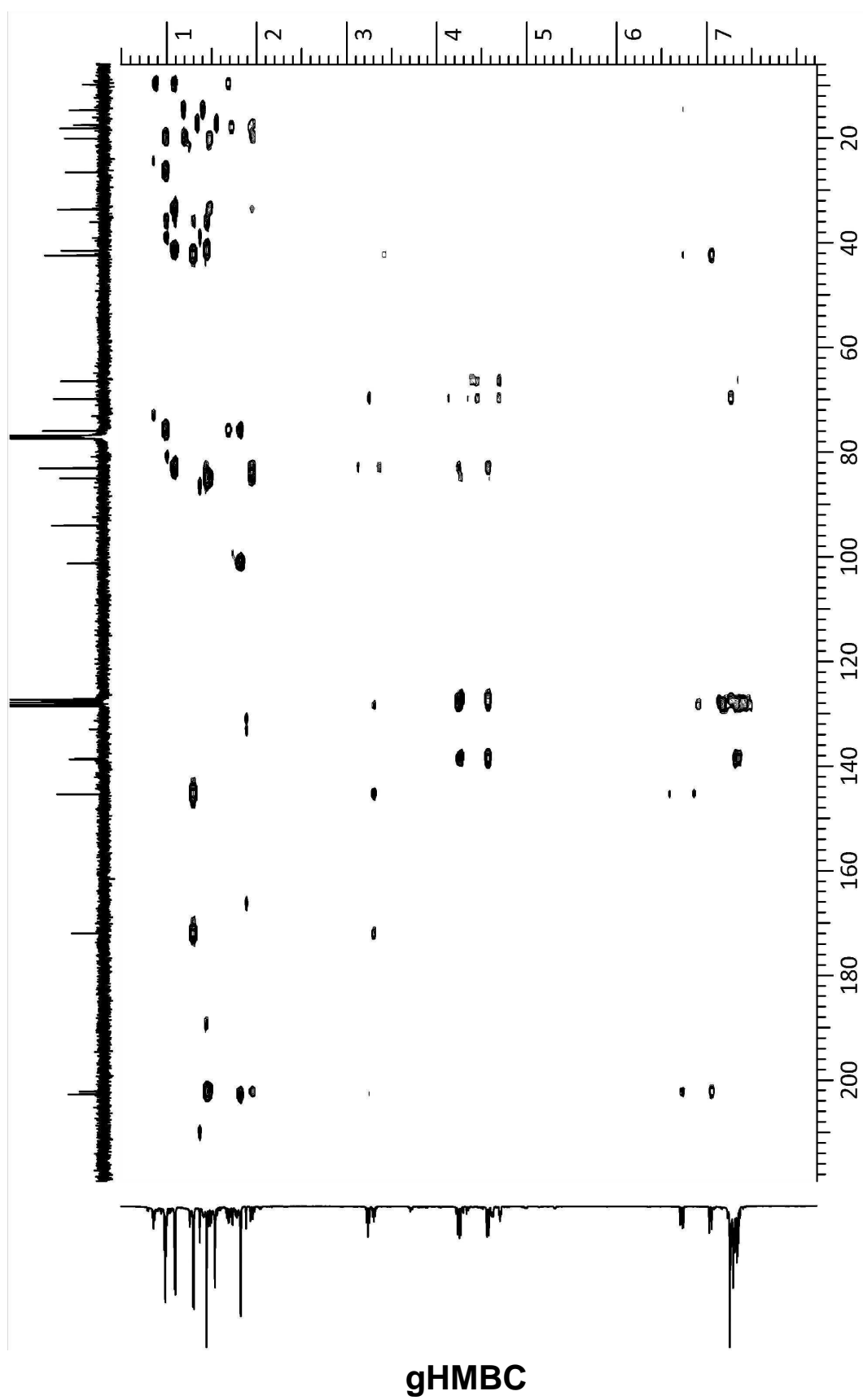
^{13}C NMR (125MHz, CDCl_3)

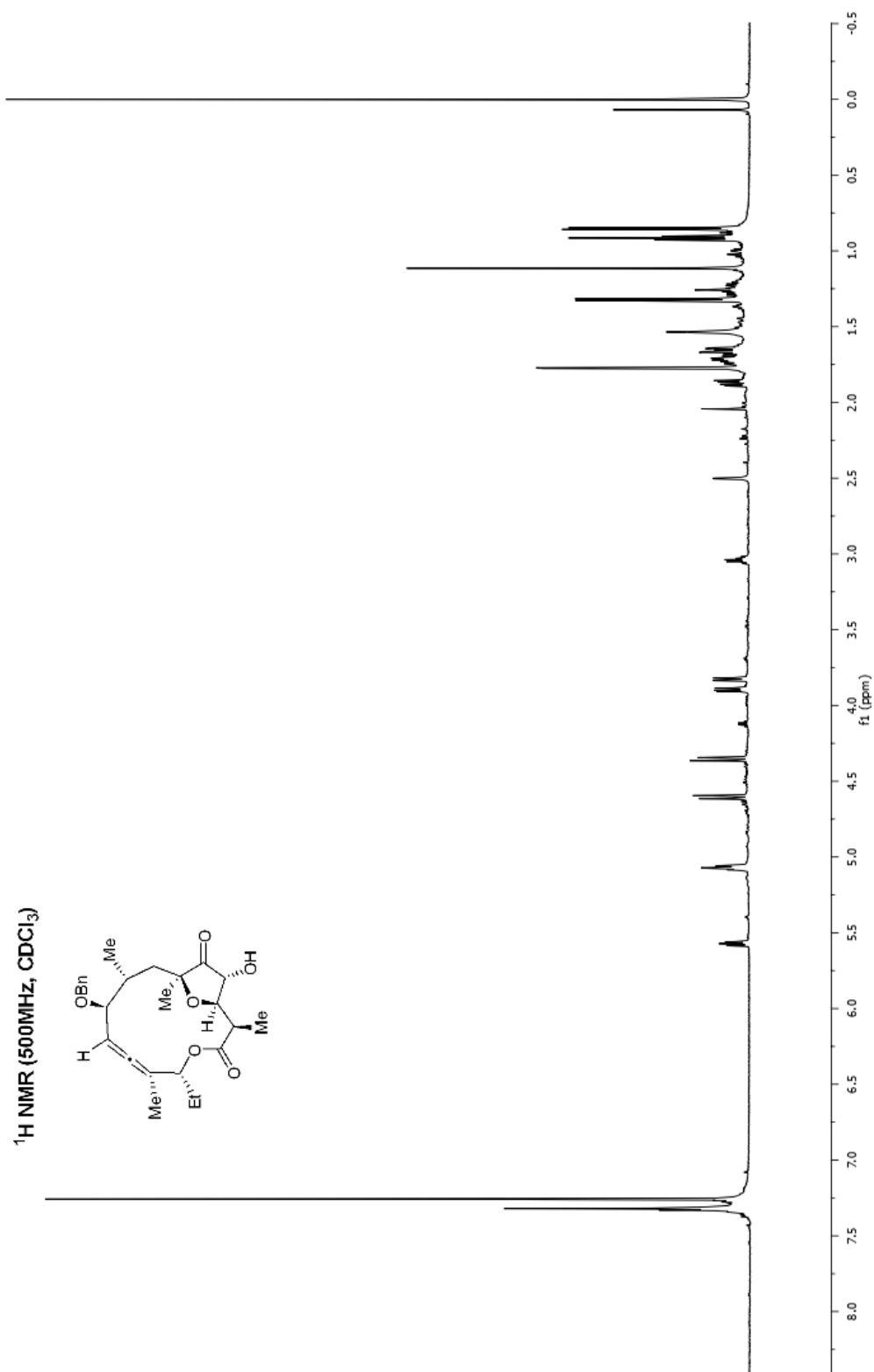


gCOSY

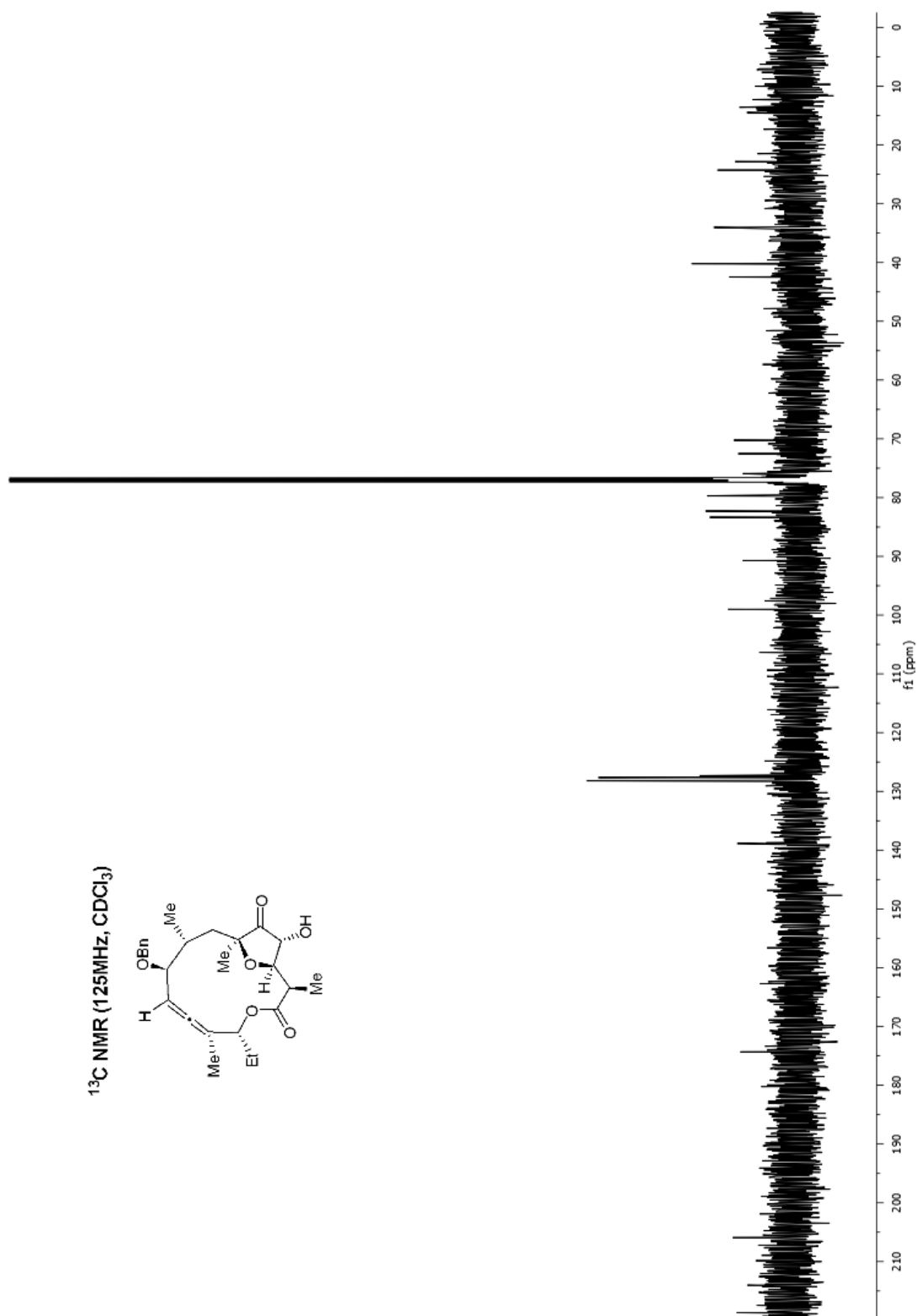
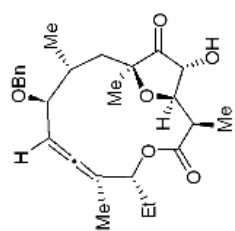


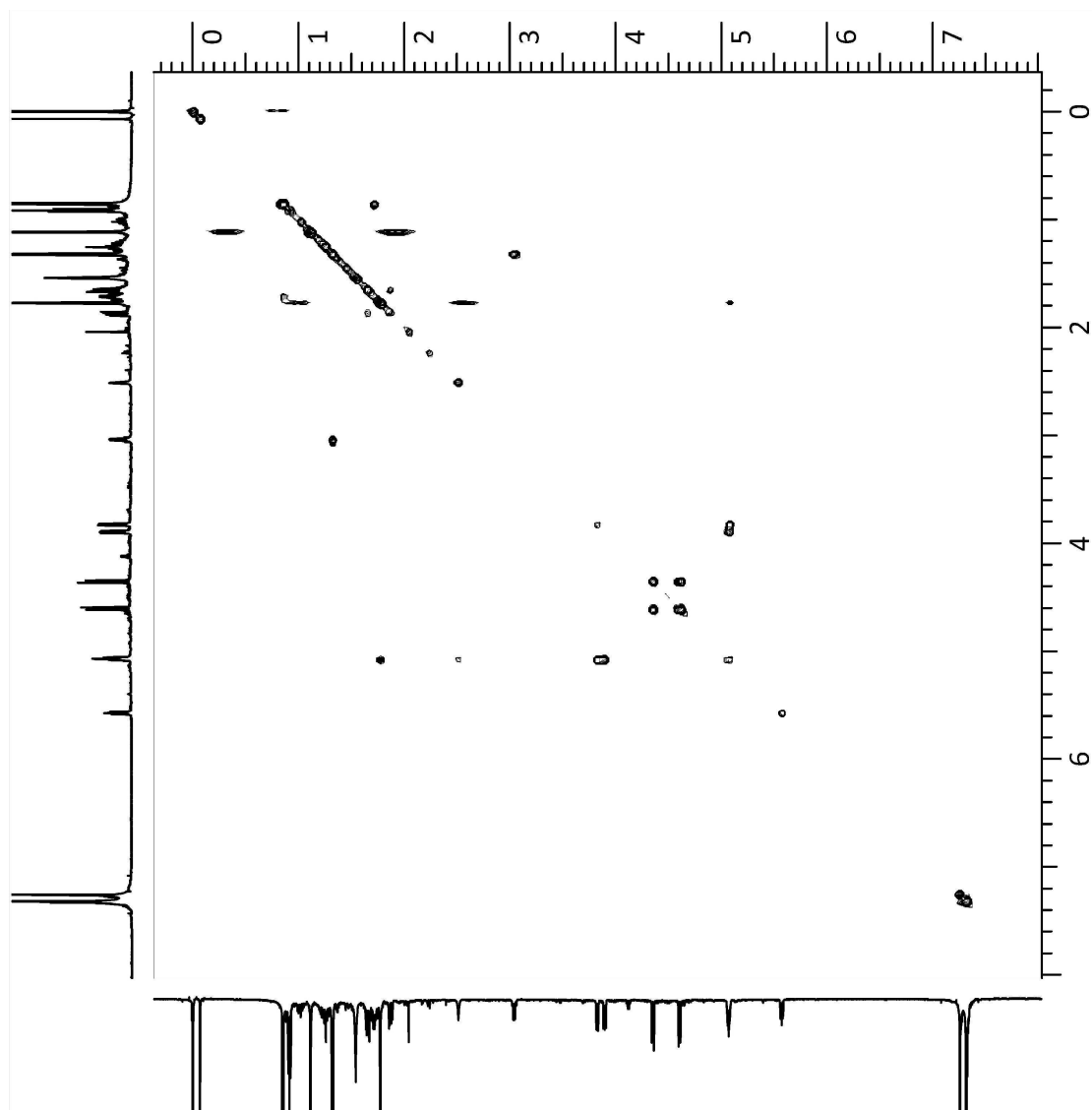




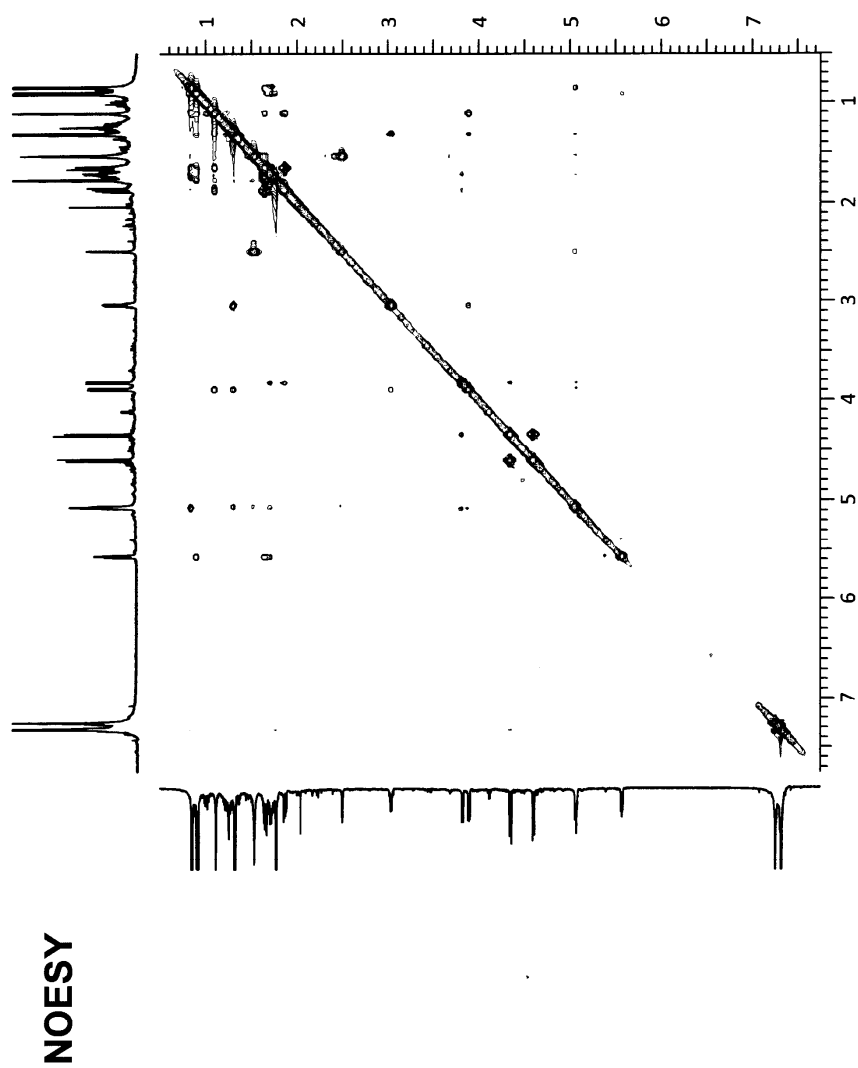


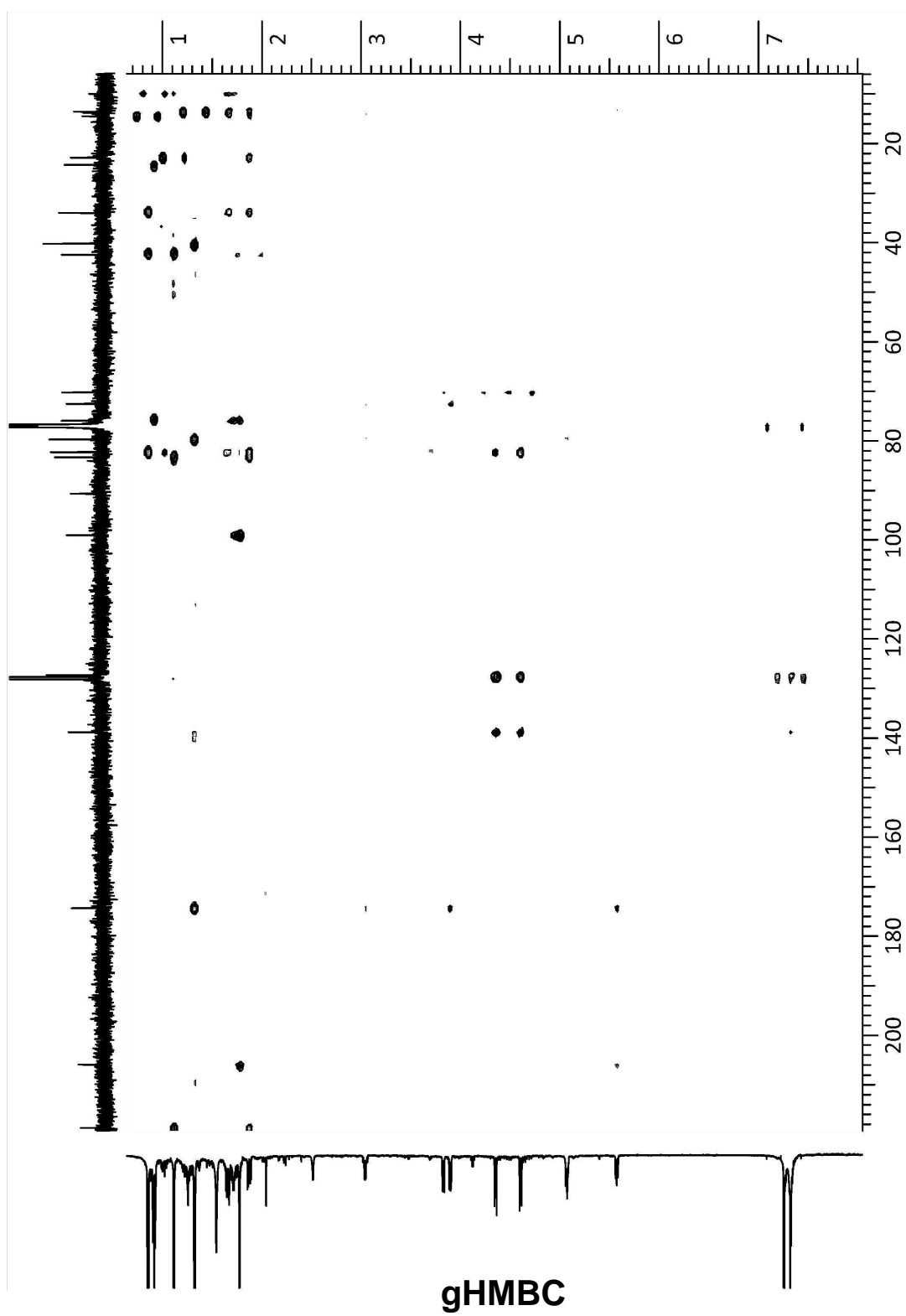
^{13}C NMR (125MHz, CDCl_3)

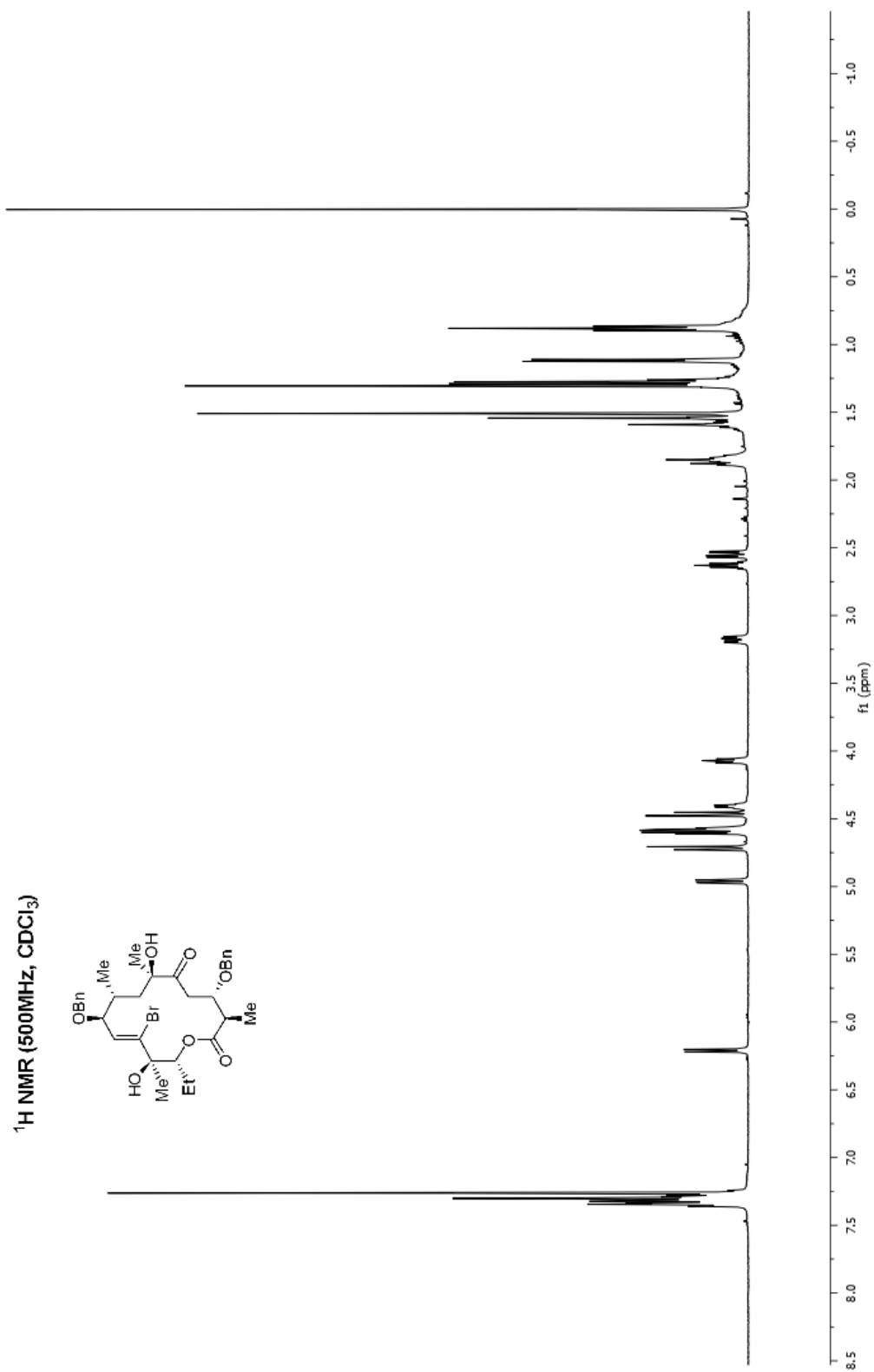


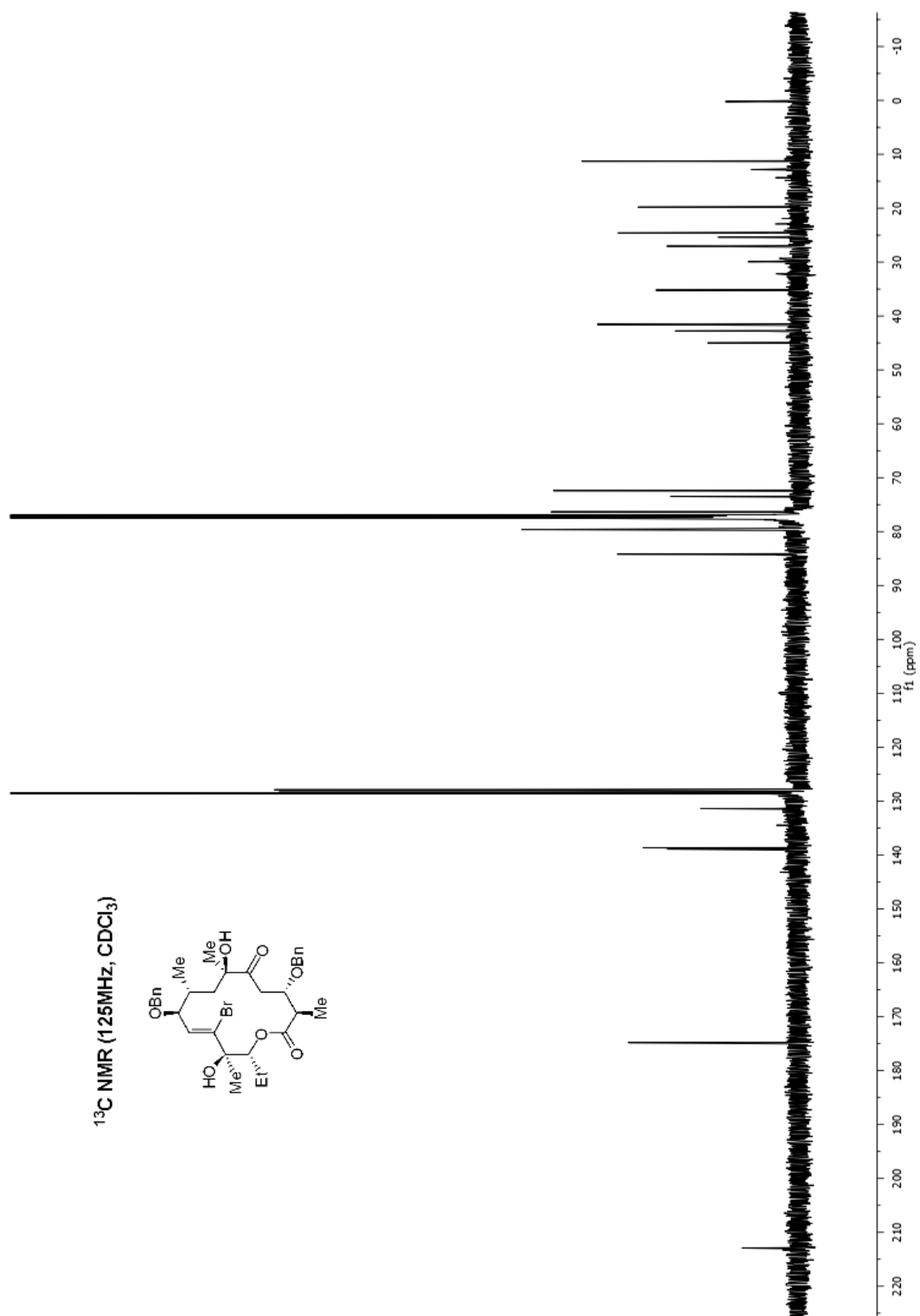


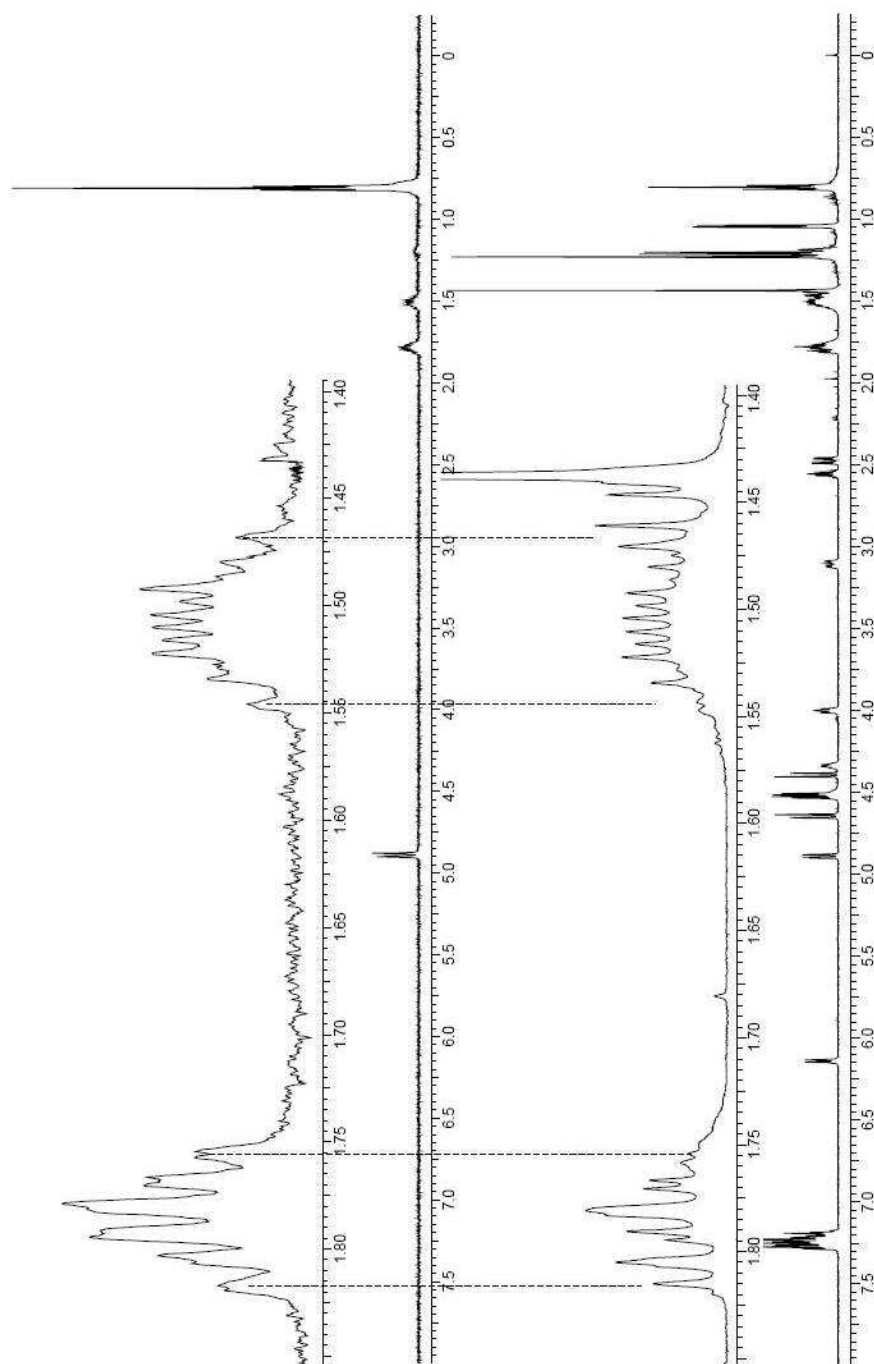
gCOSY

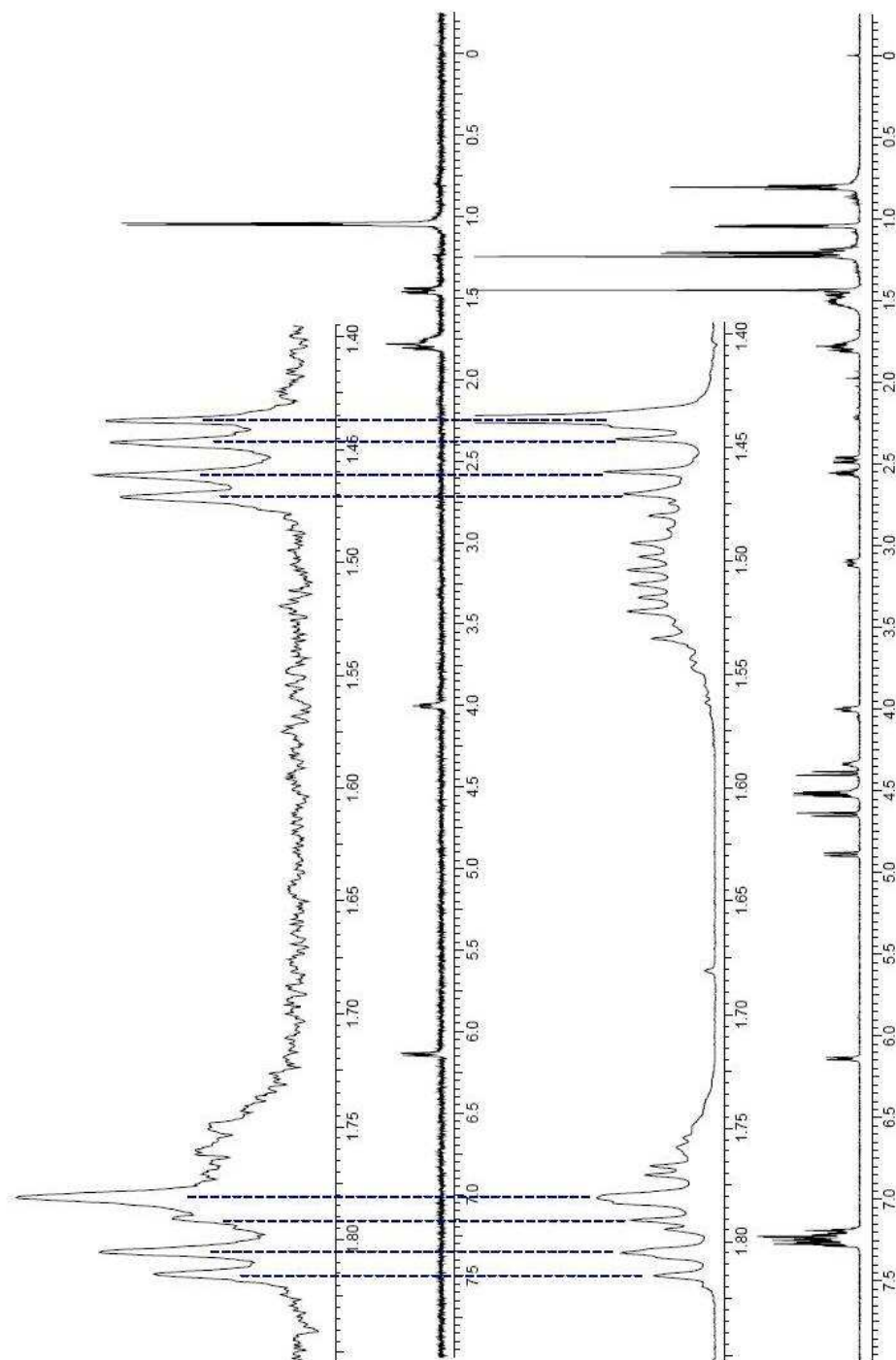


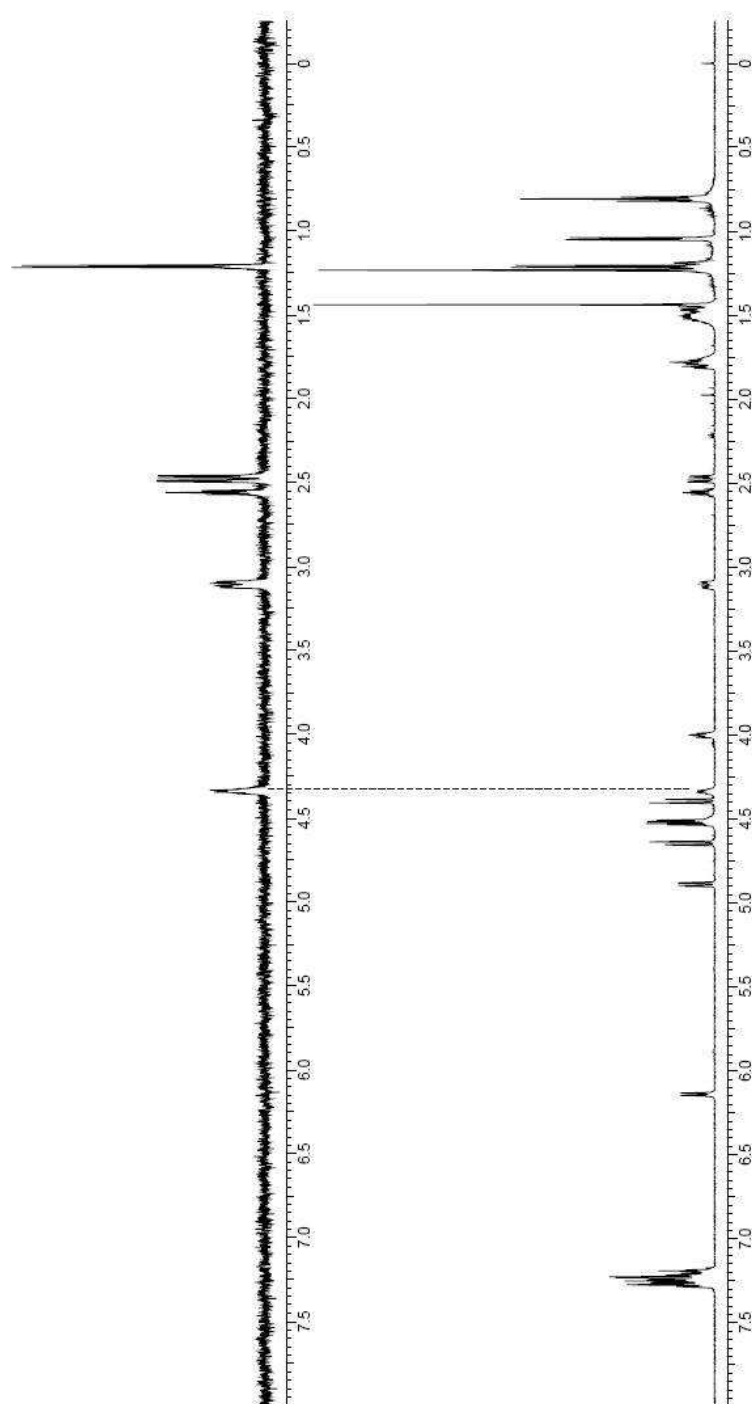


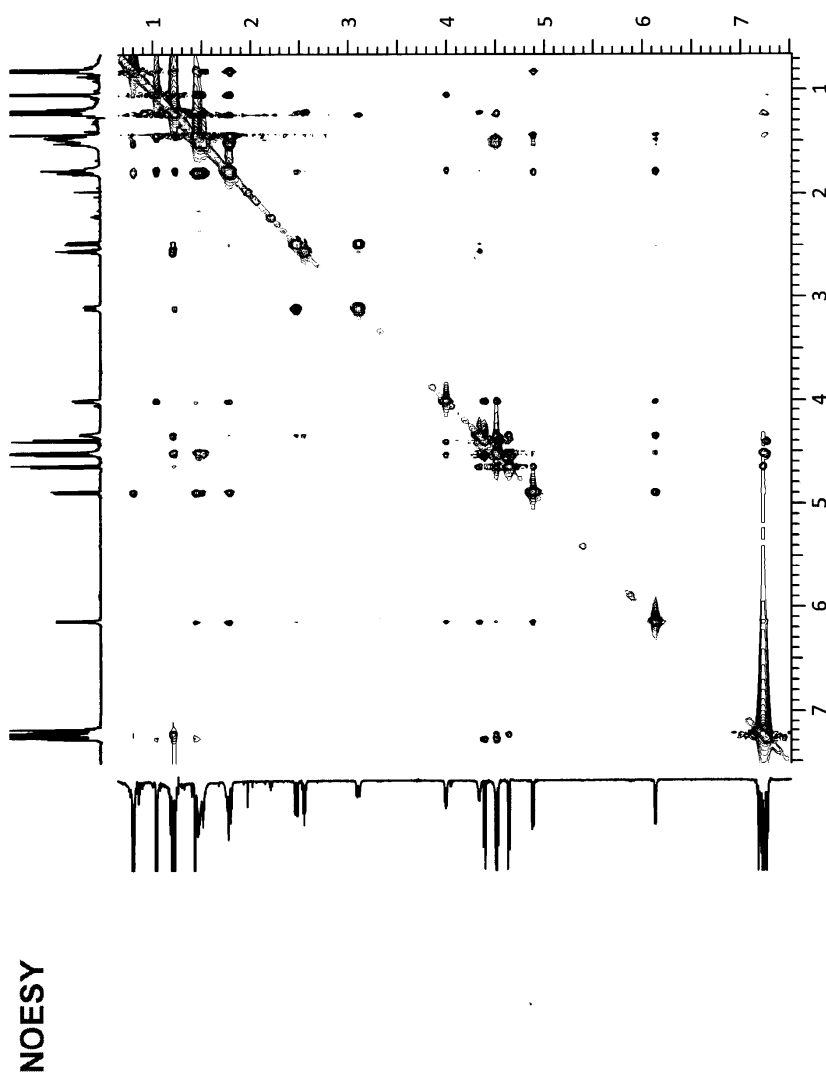


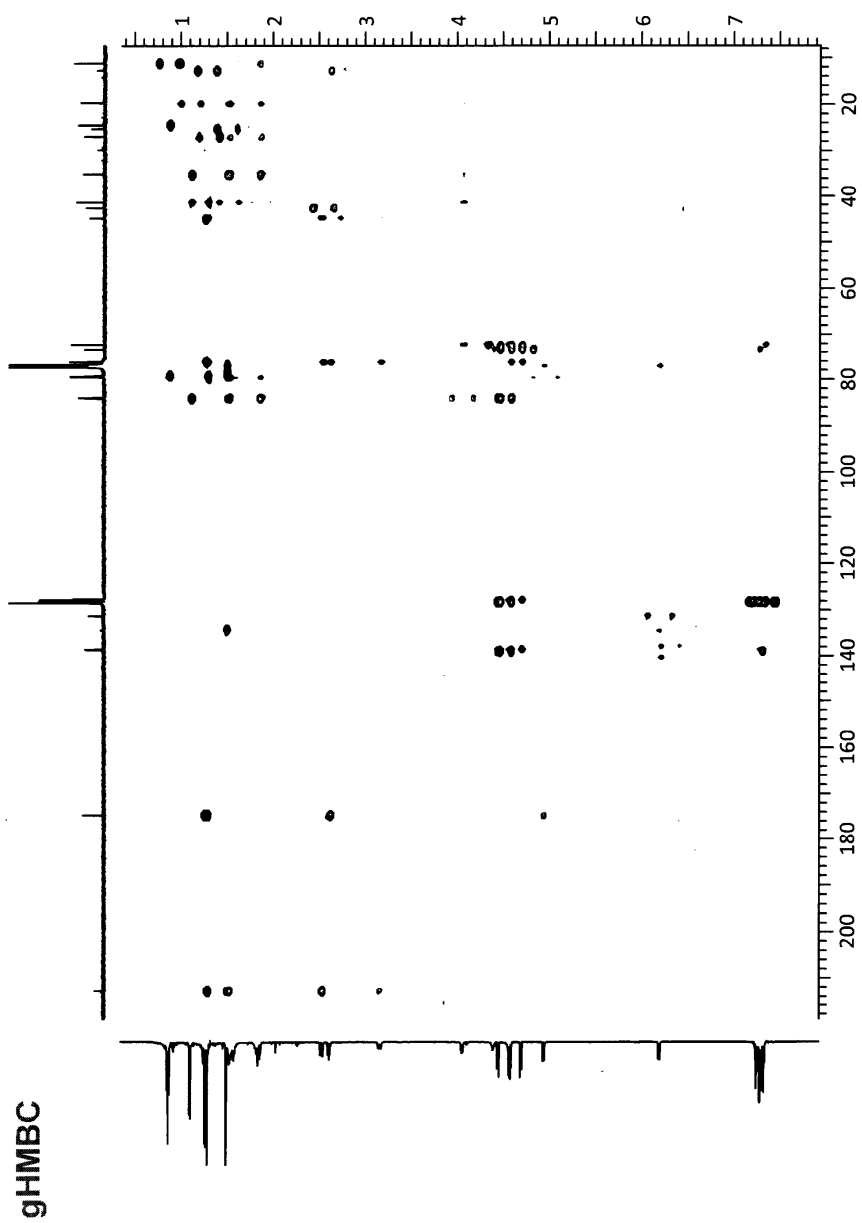


1D TOCSY

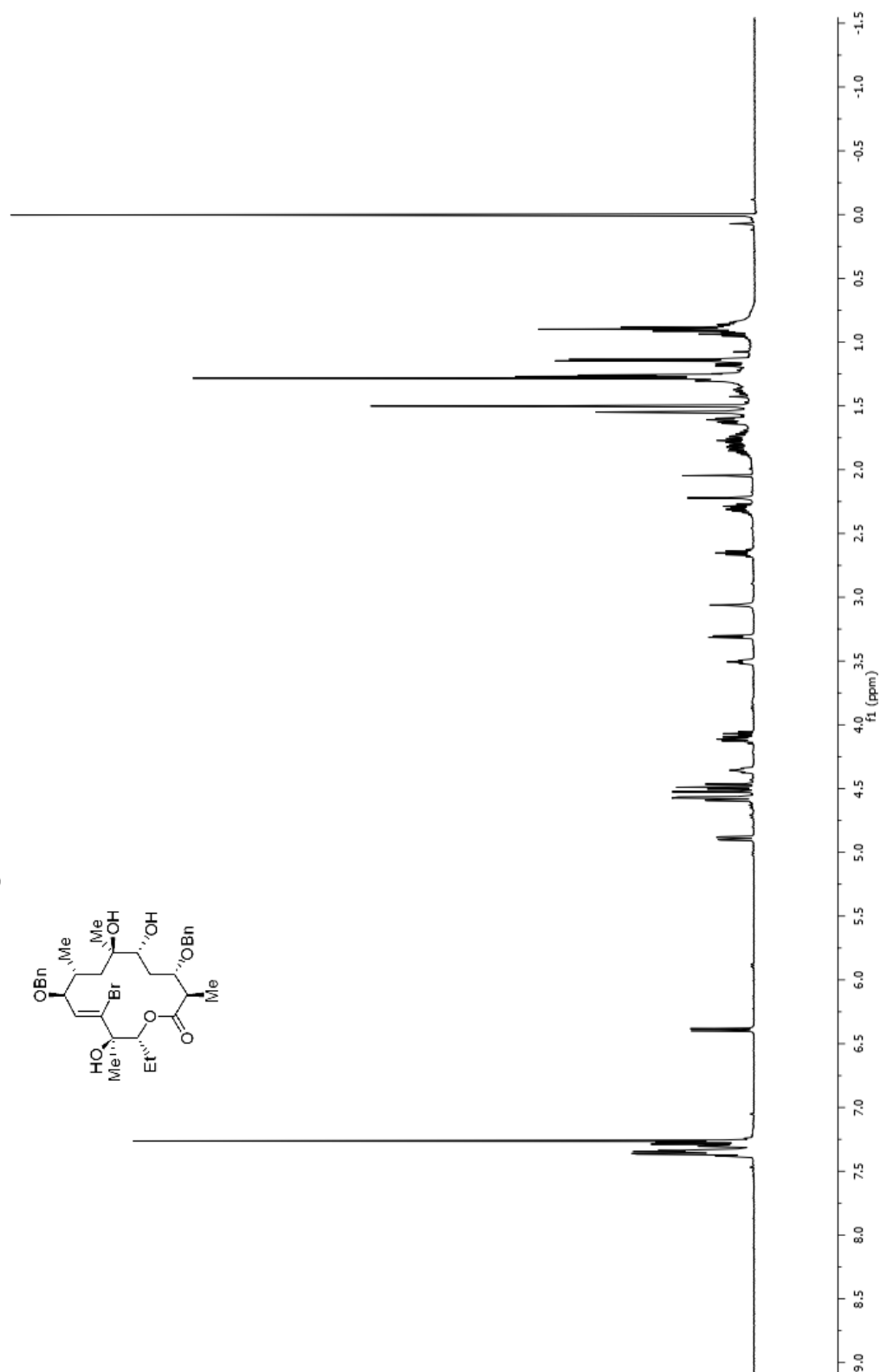
1D TOCSY

1D TOCSY

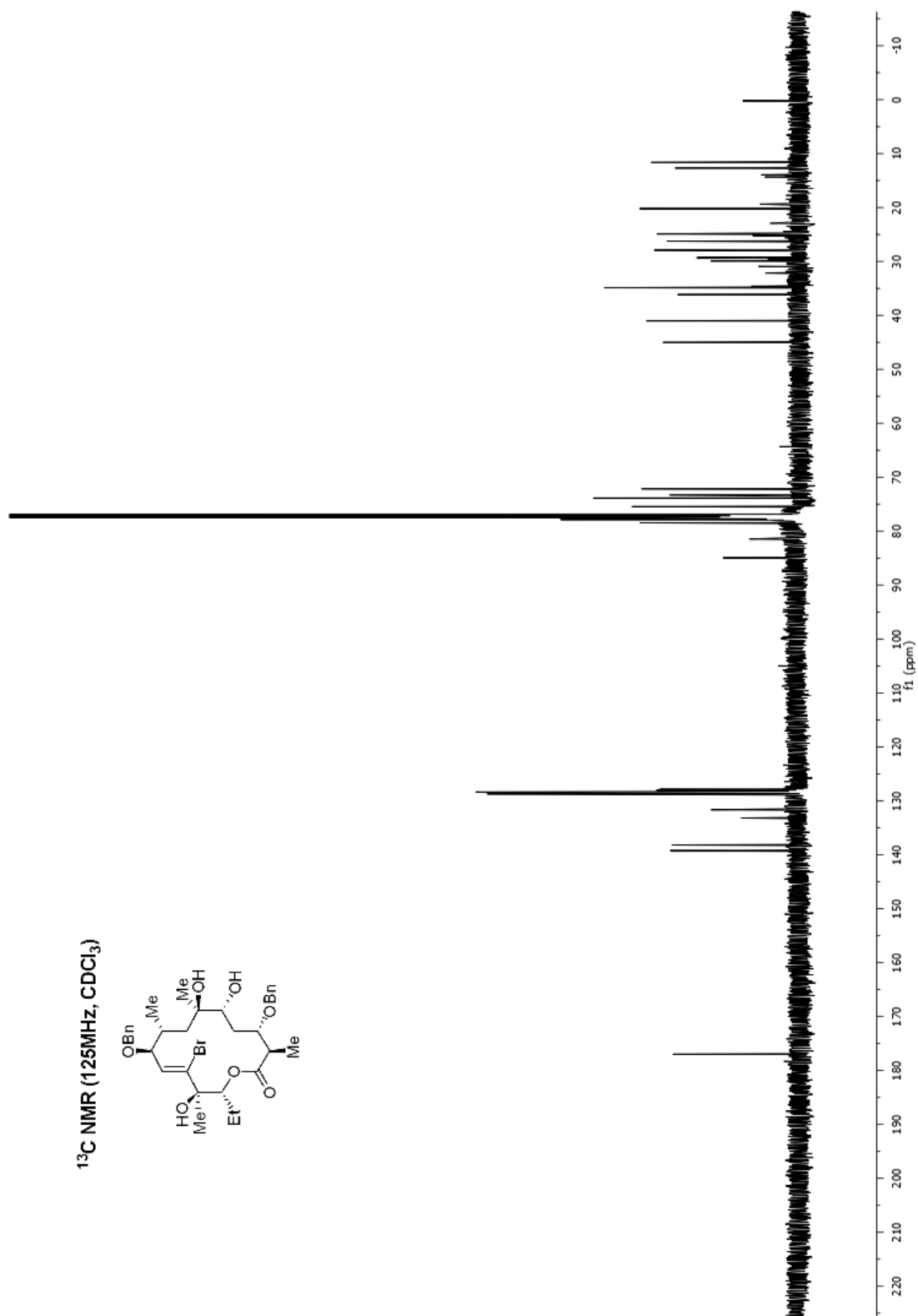
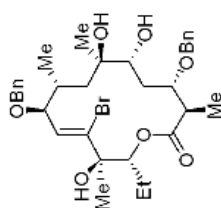


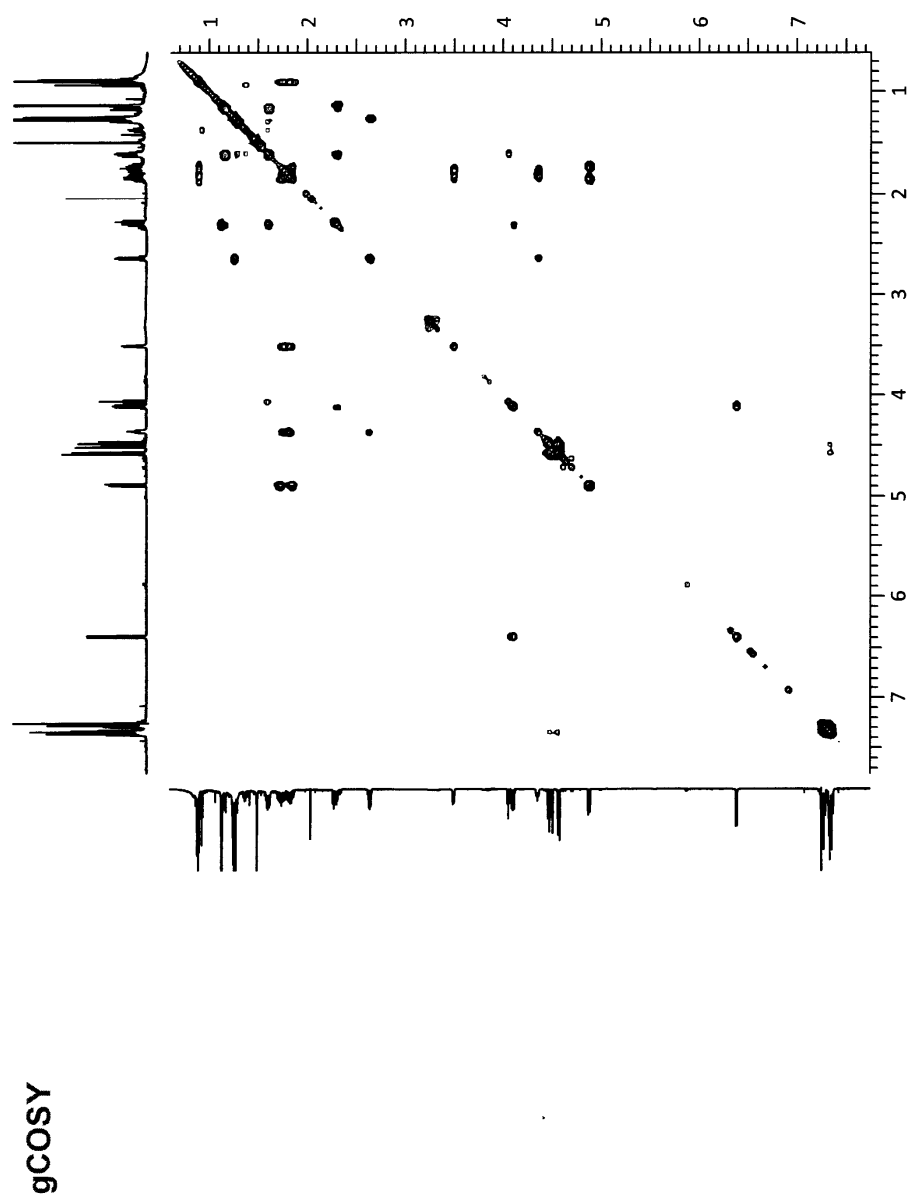


¹H NMR (500MHz, CDCl₃)

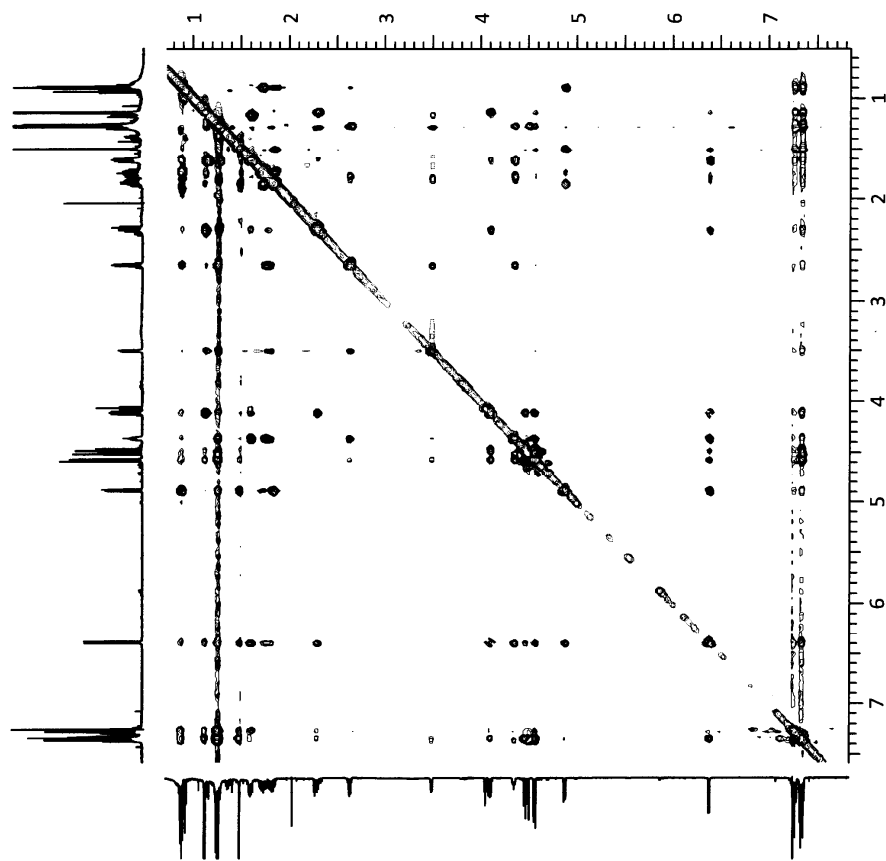


^{13}C NMR (125MHz, CDCl_3)

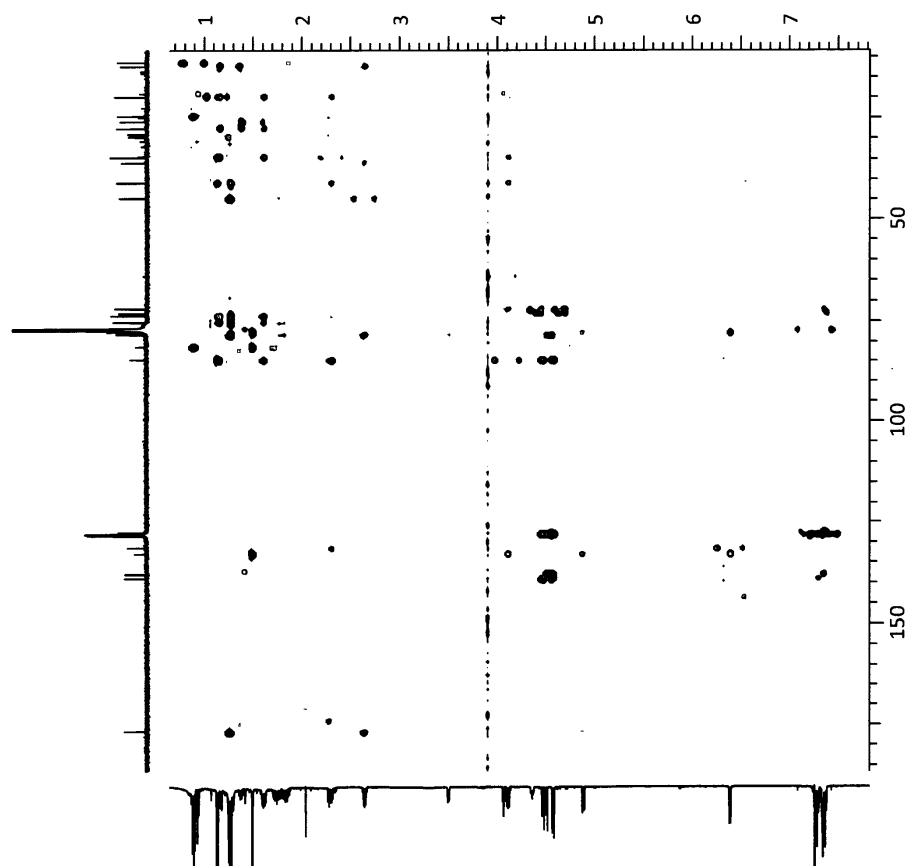


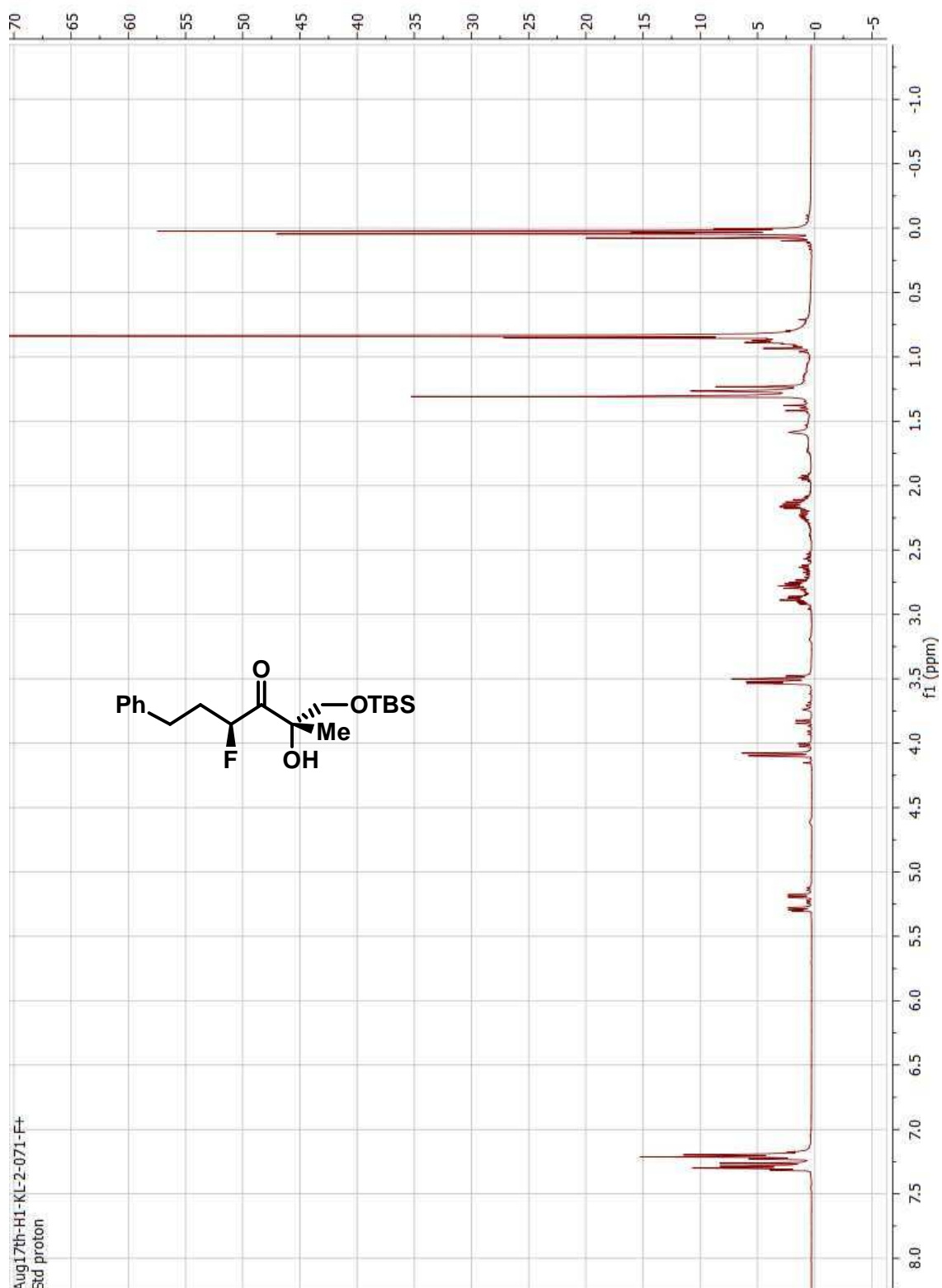


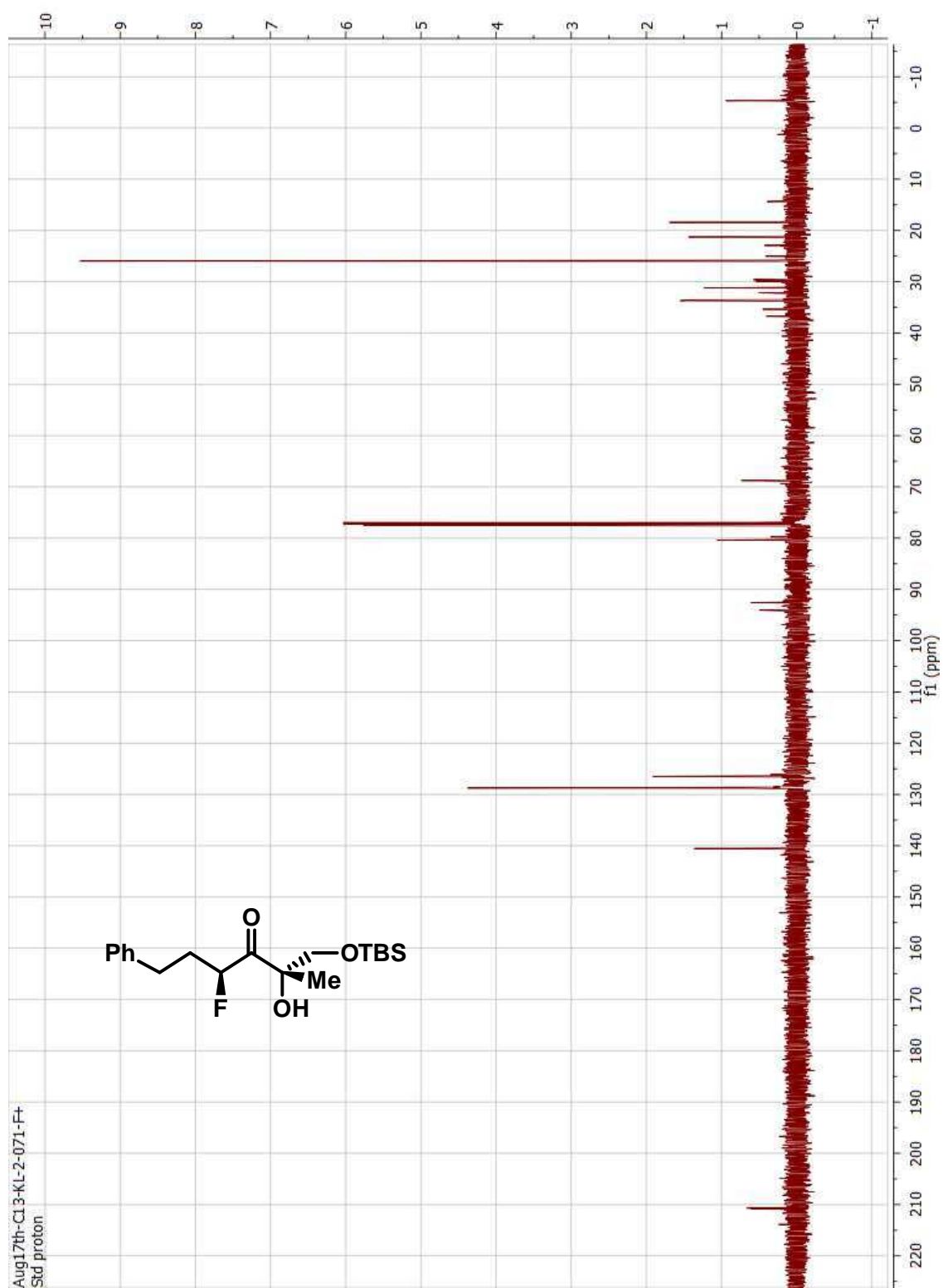
NOESY

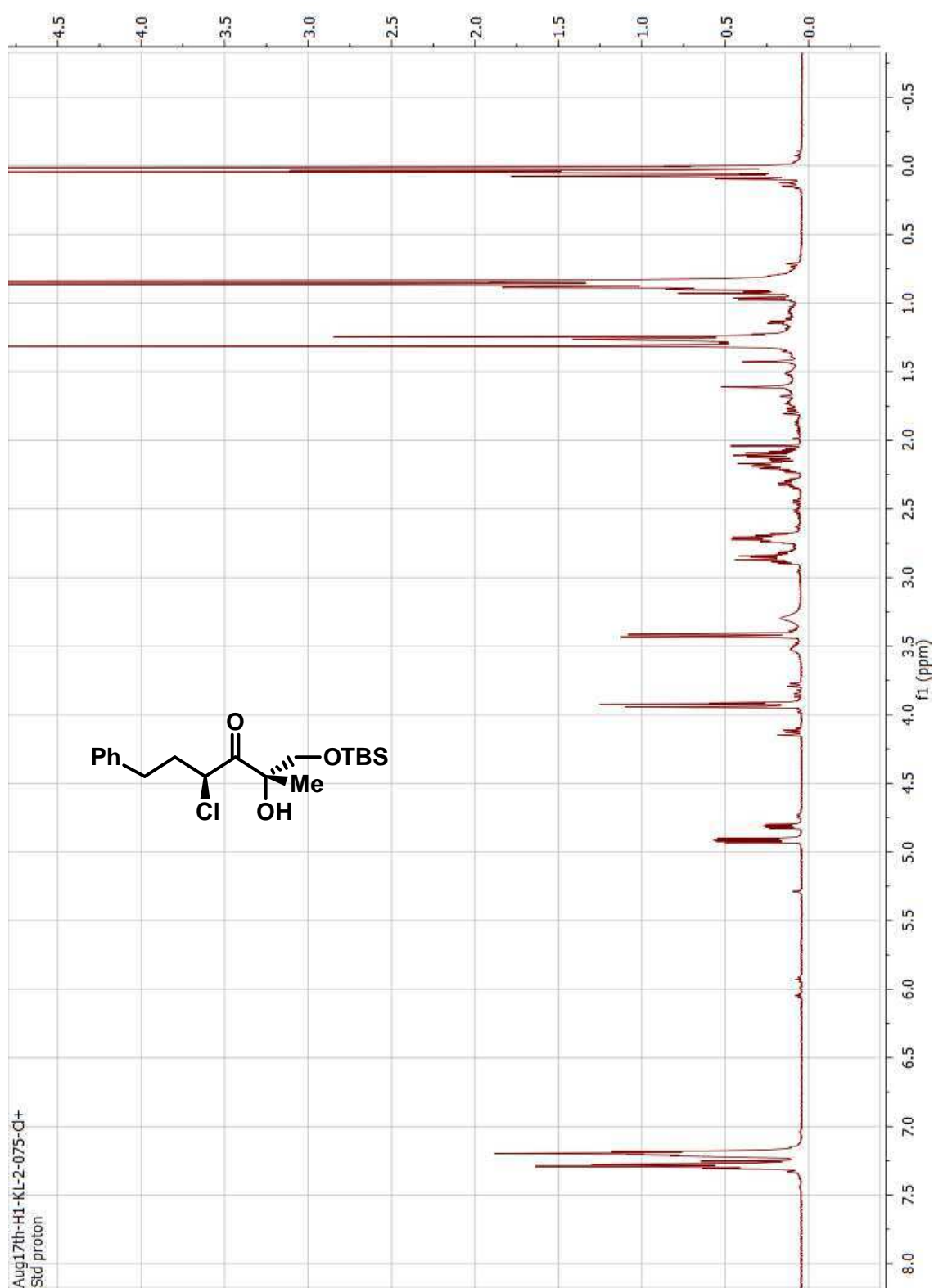


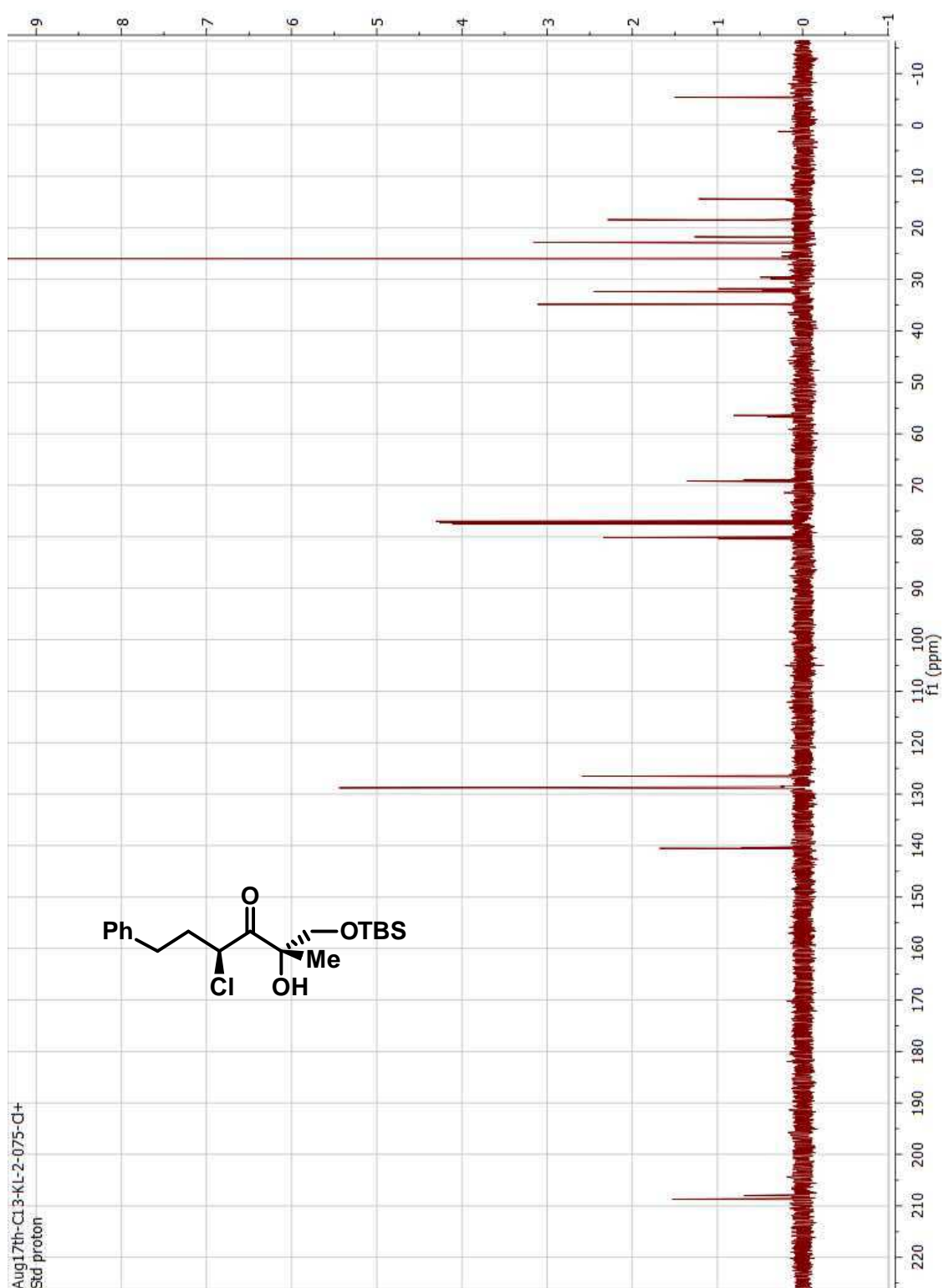
gHMBC

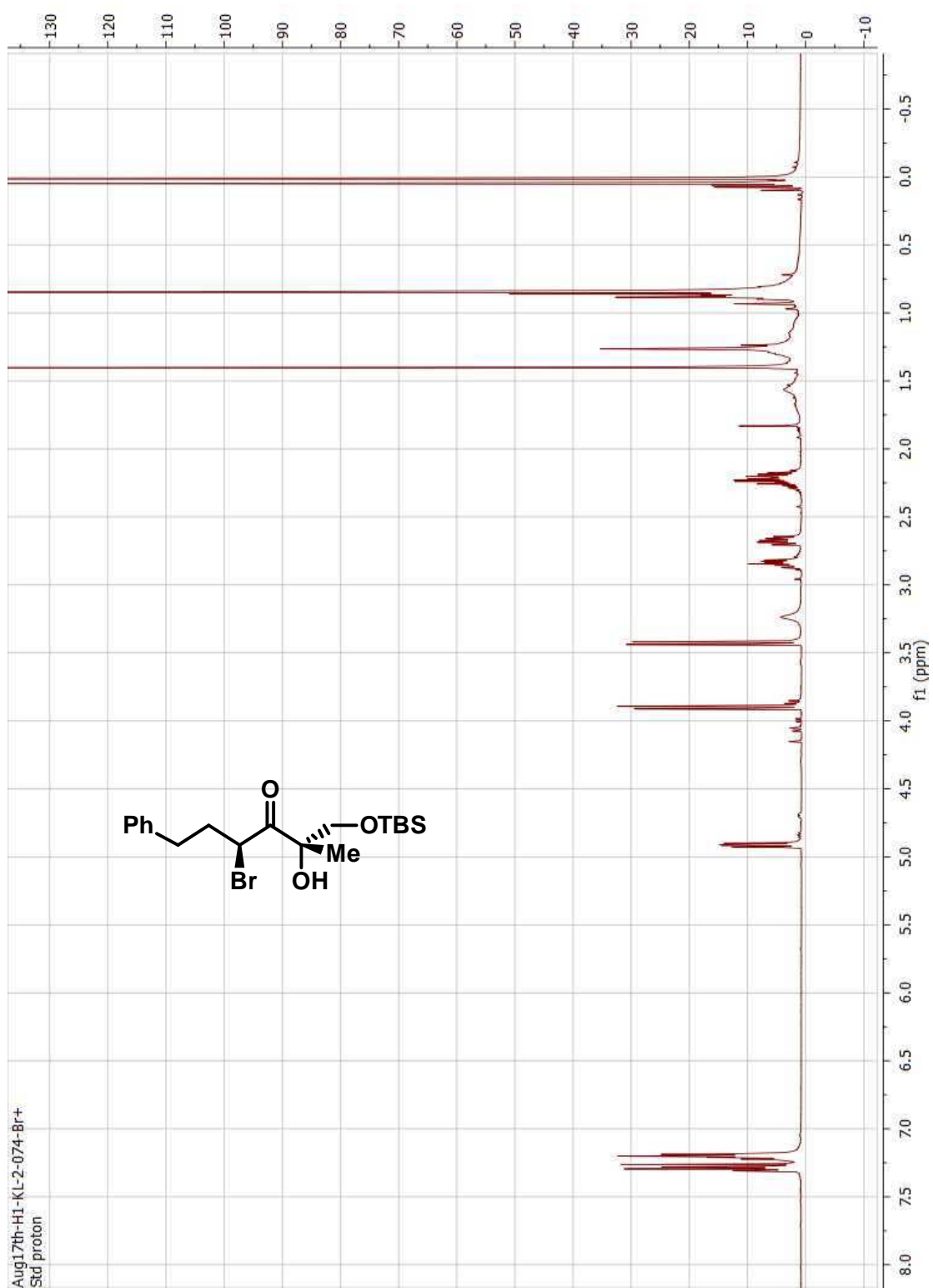


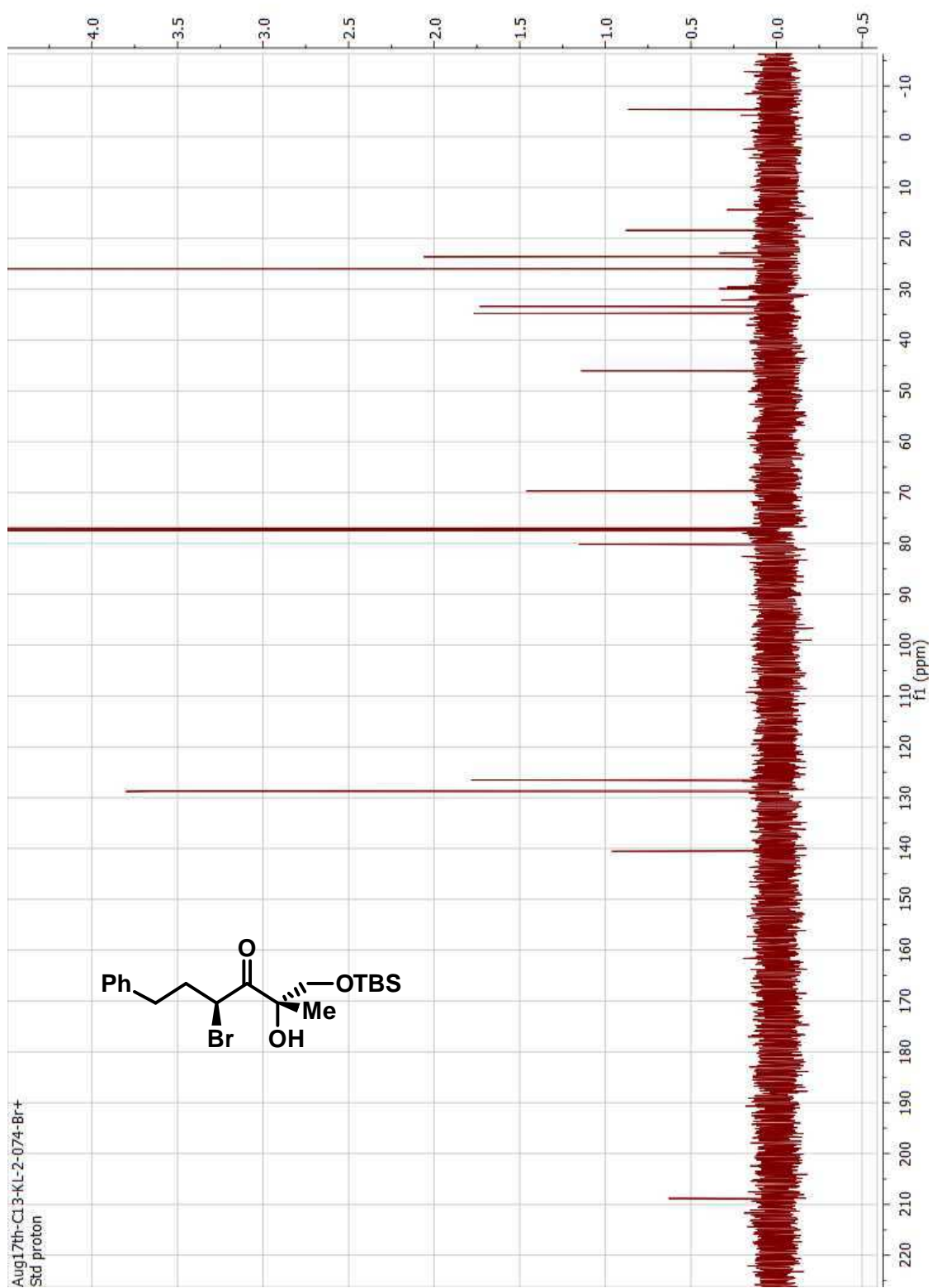


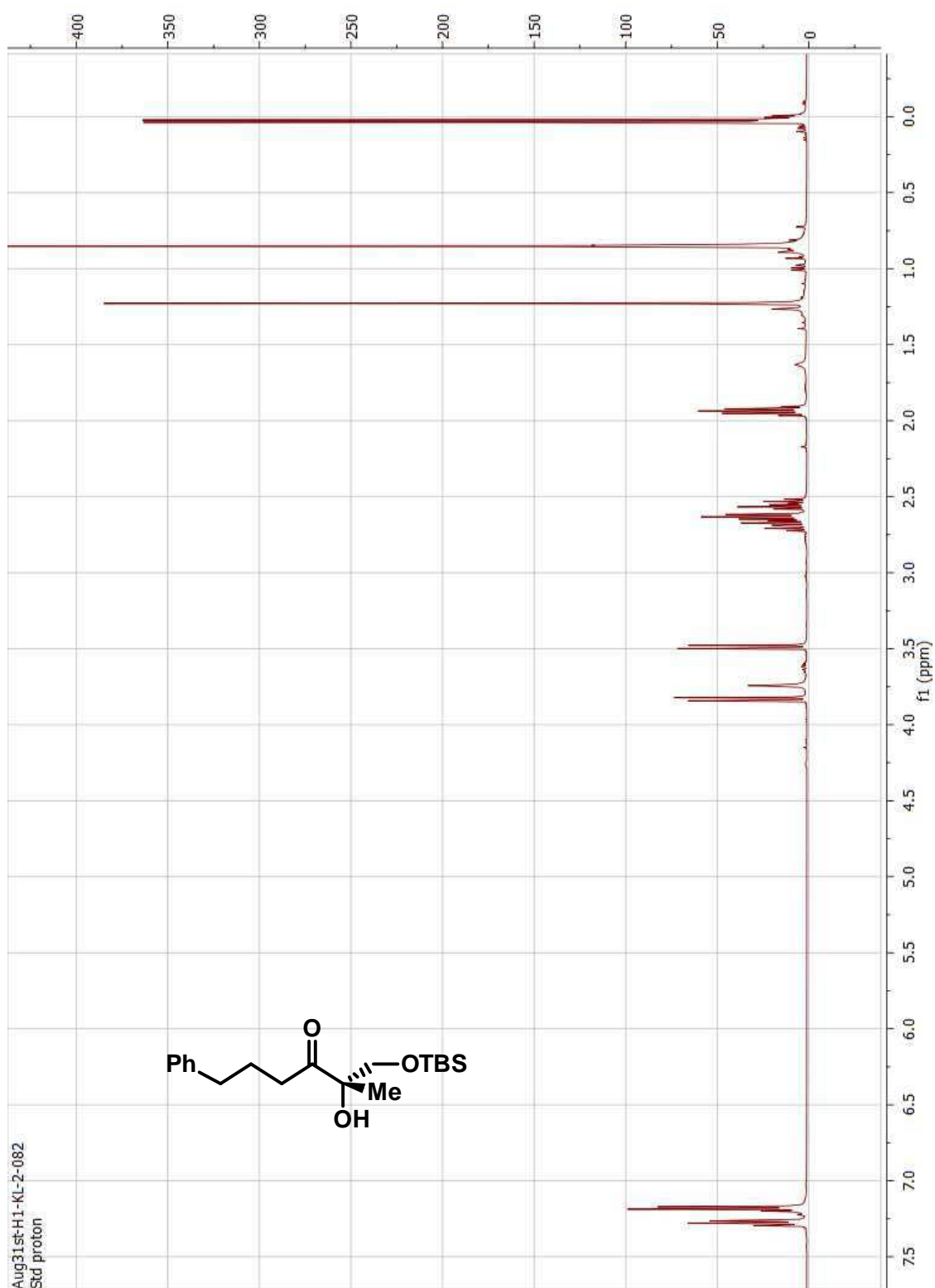


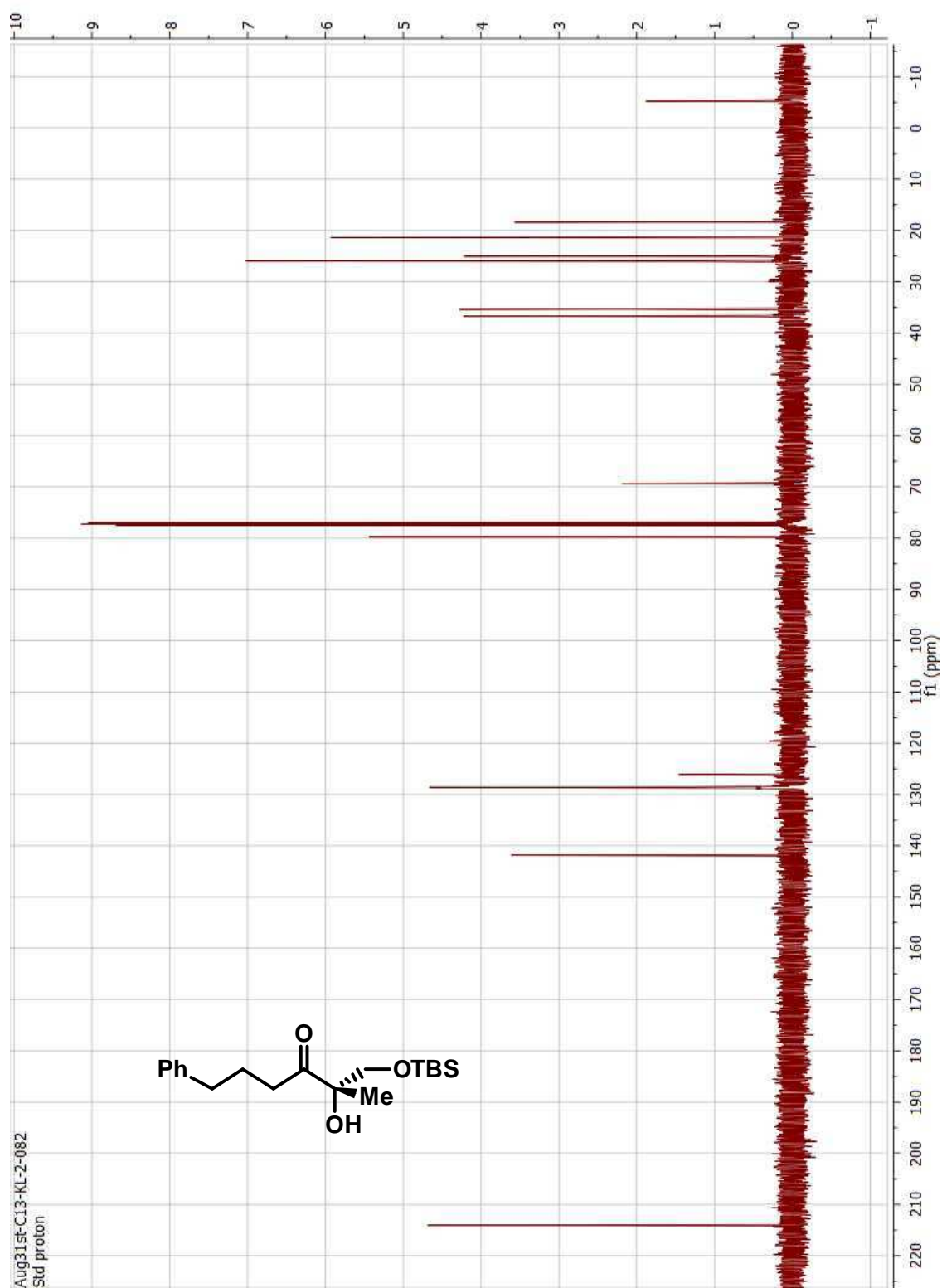


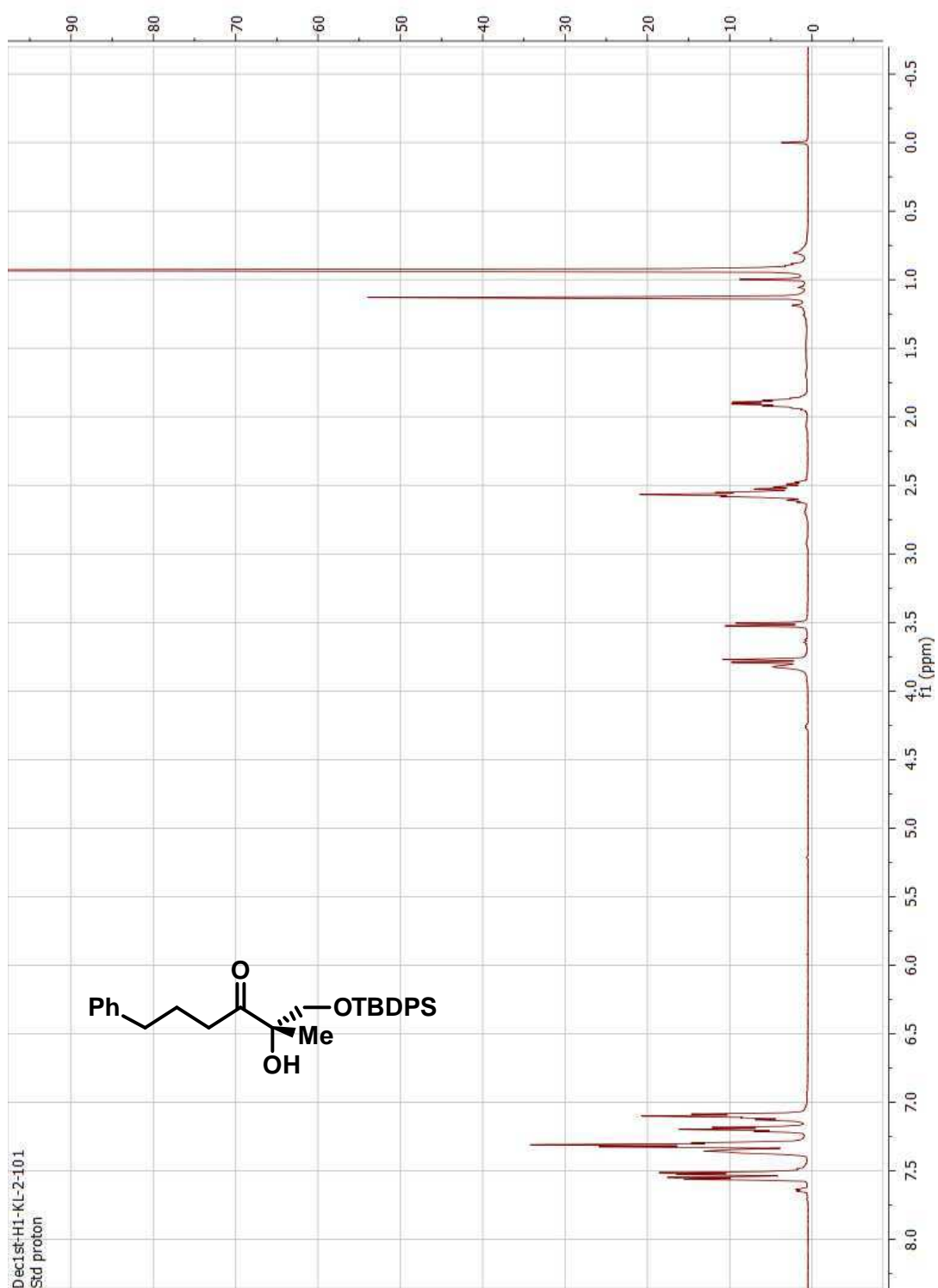


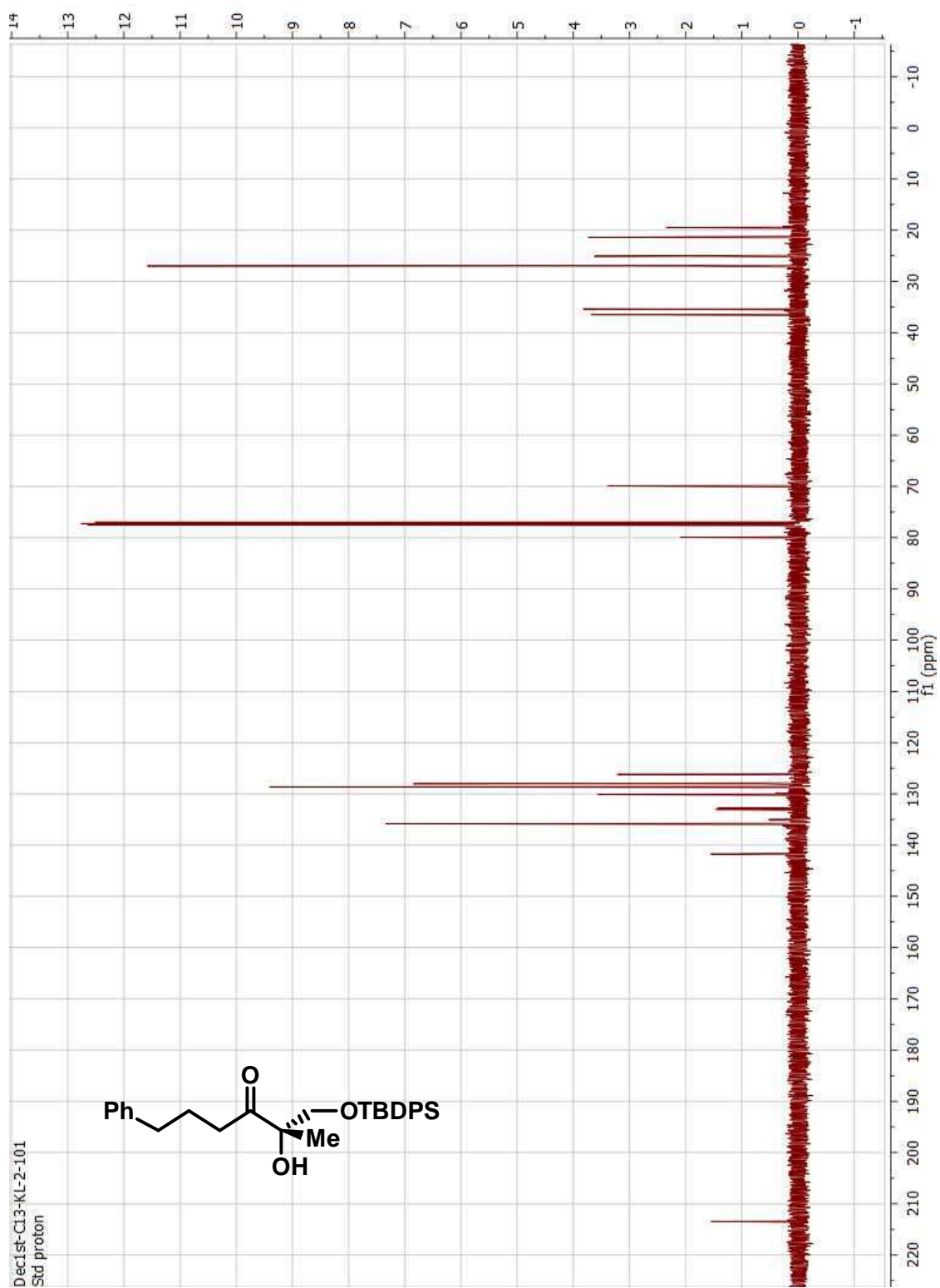


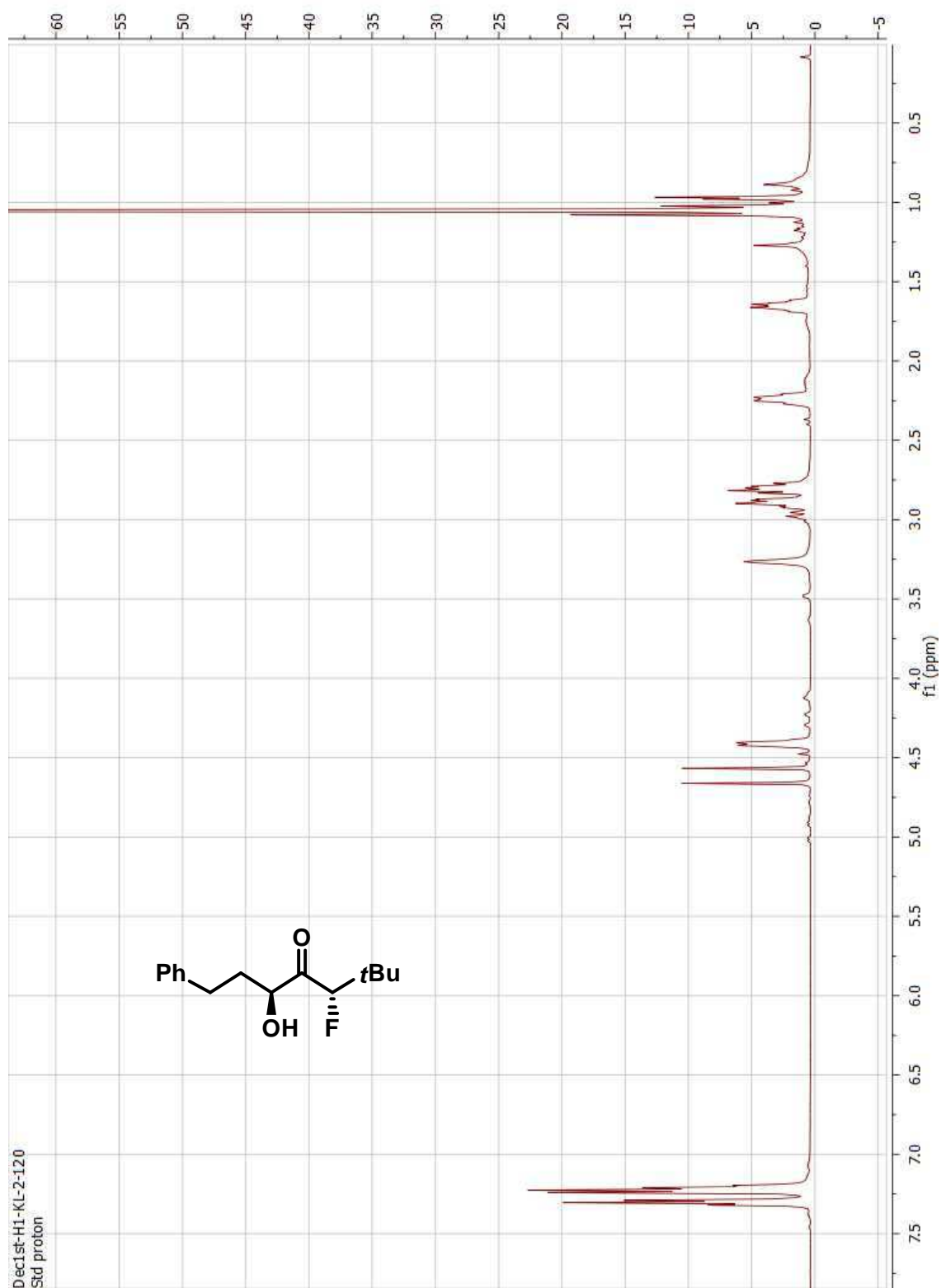


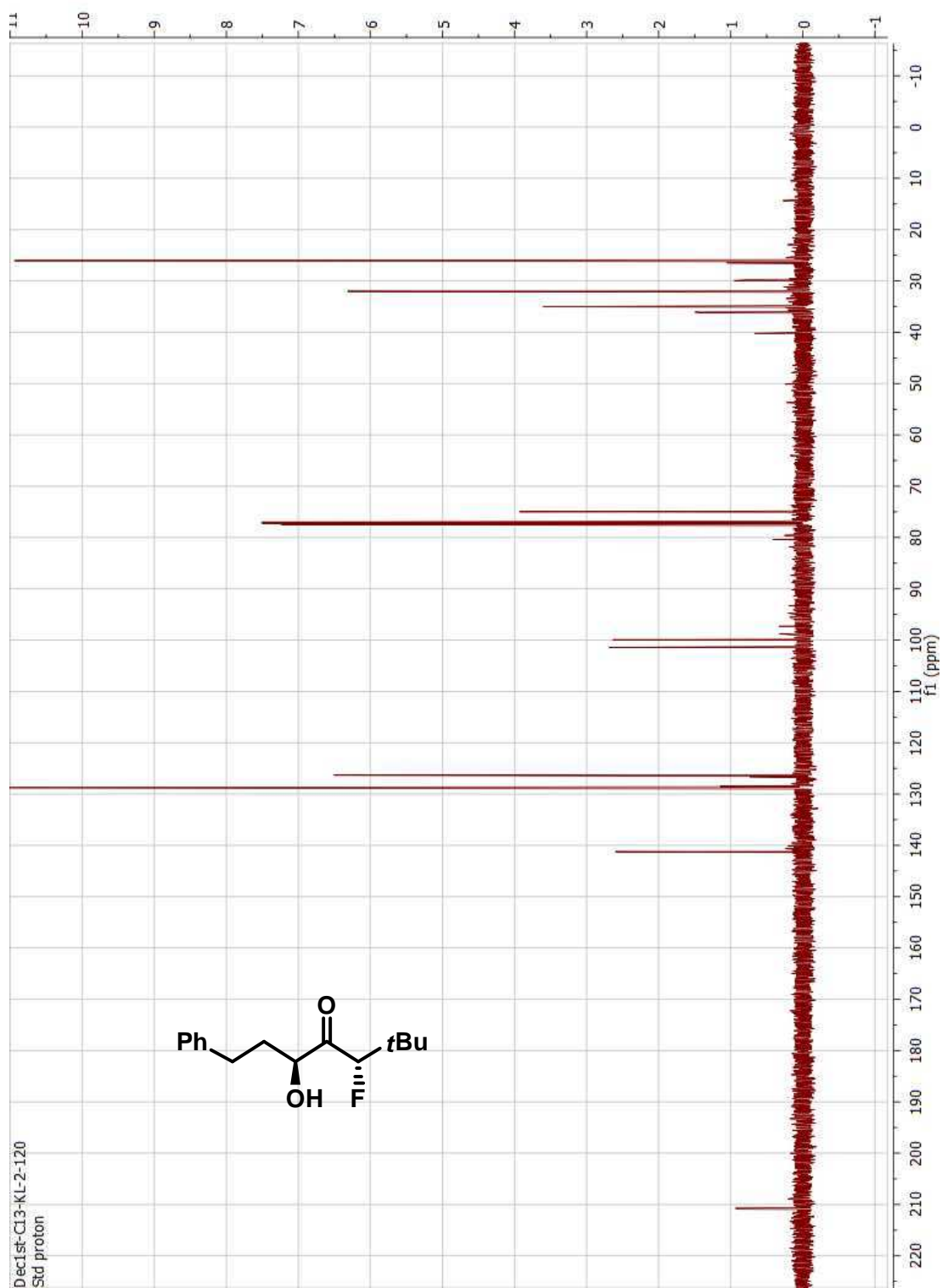


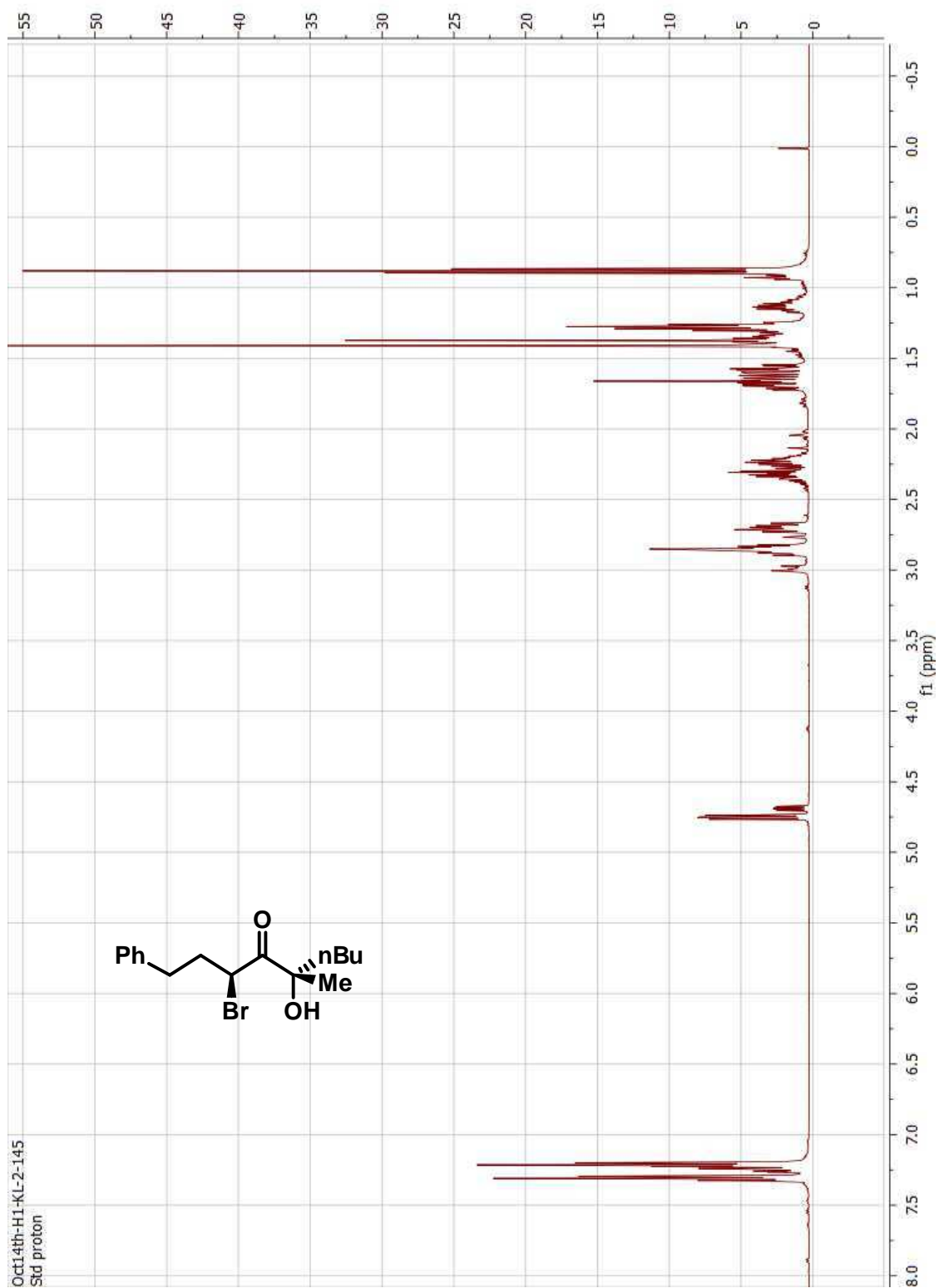


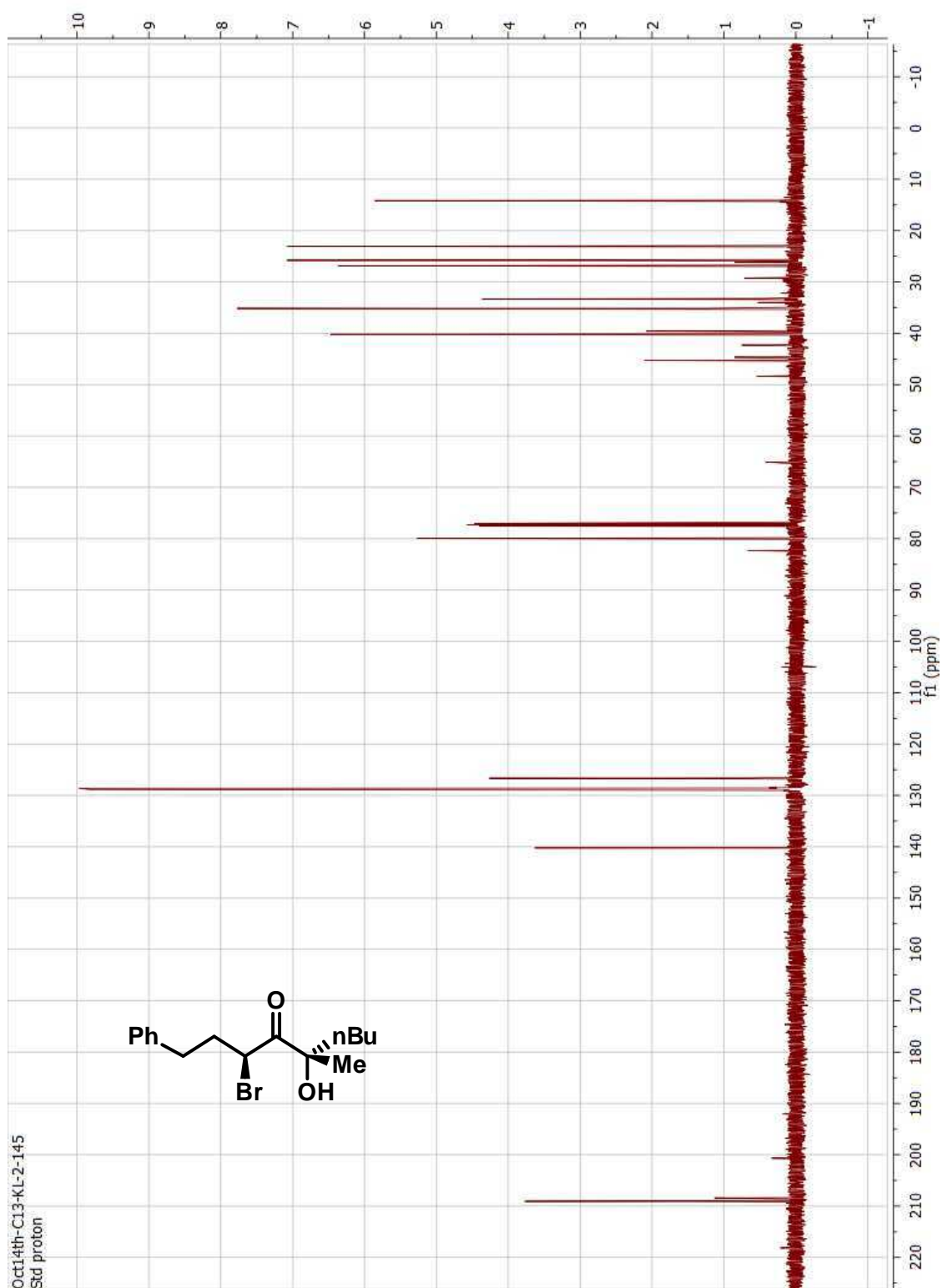


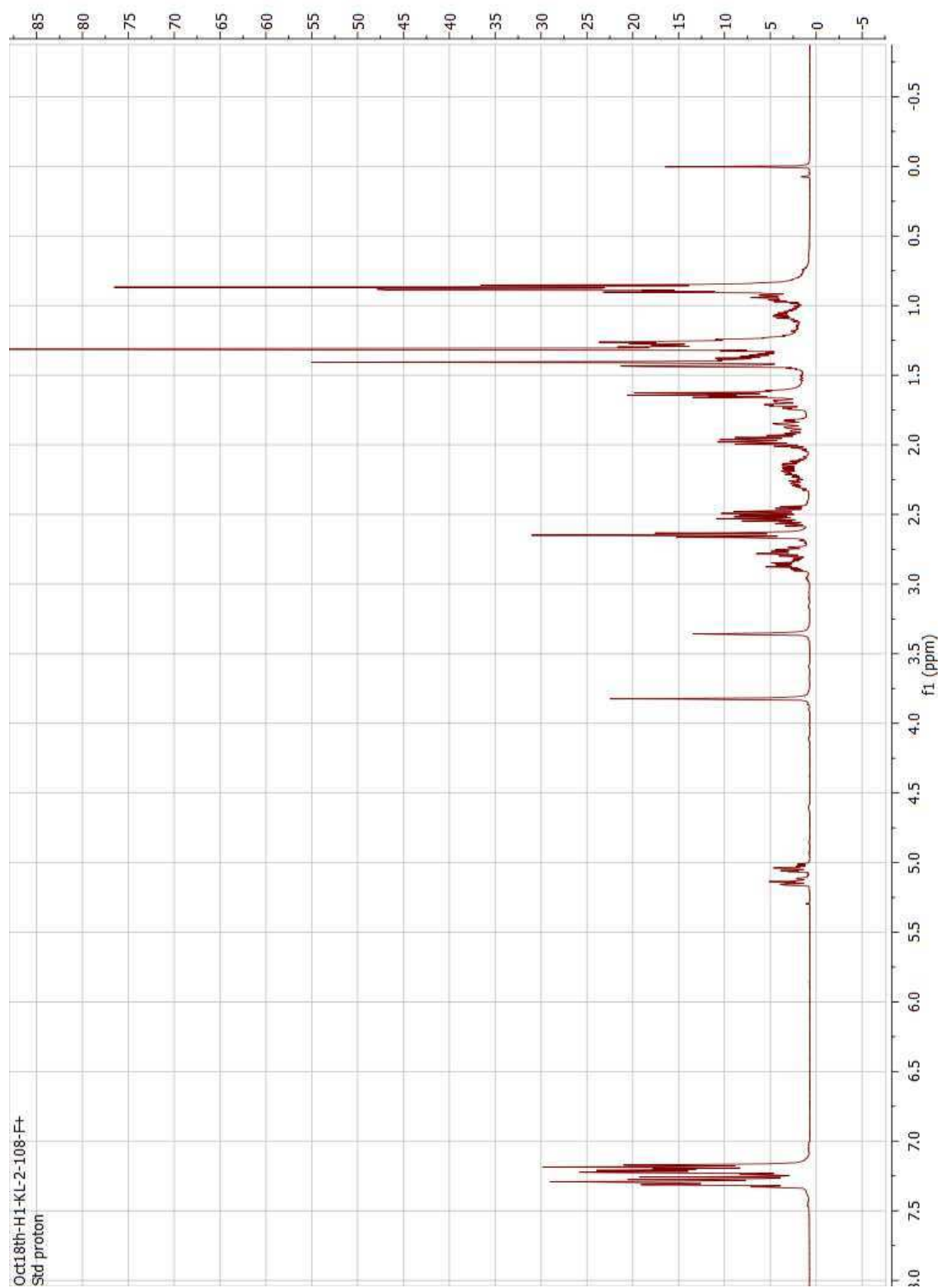


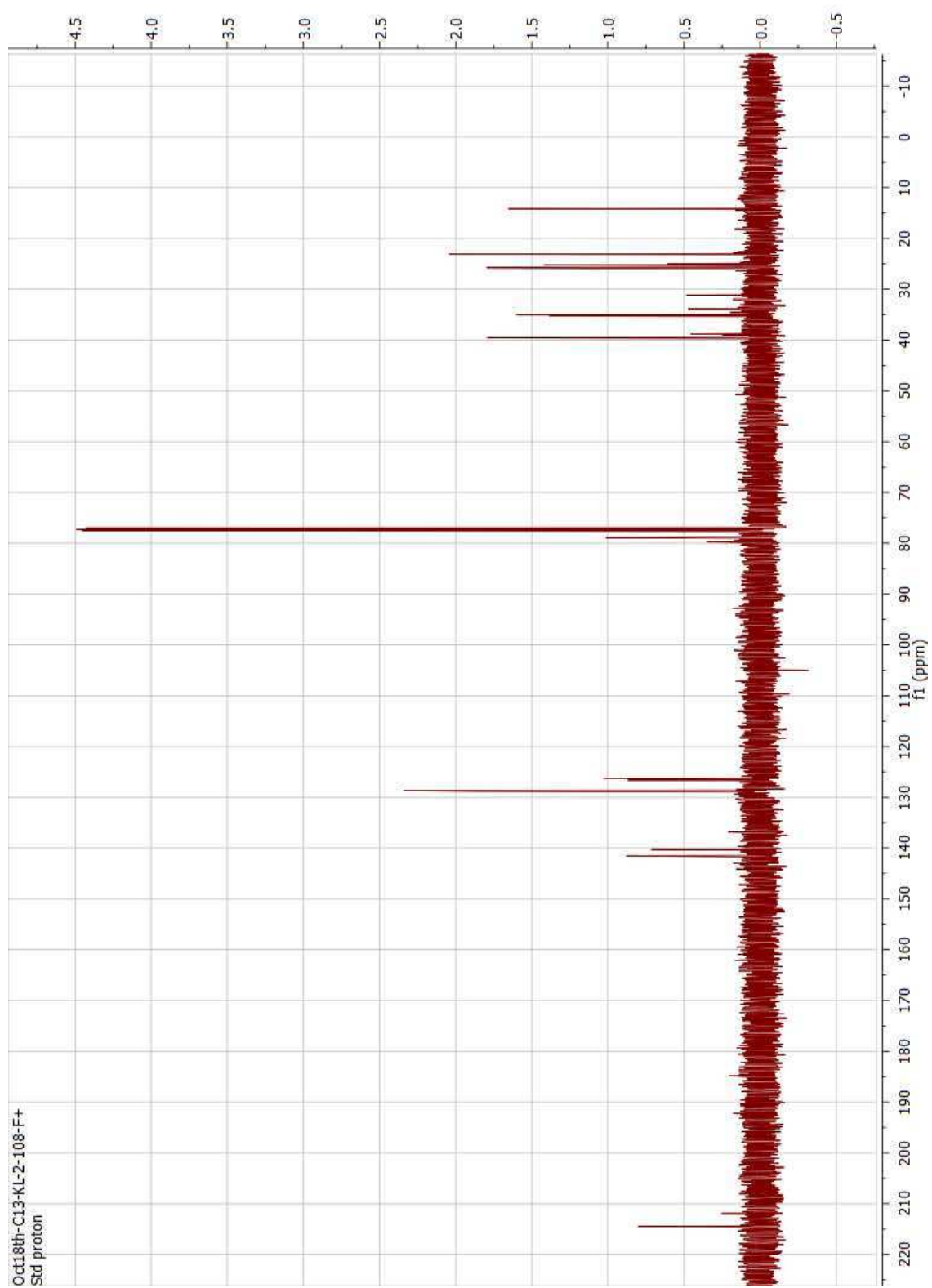


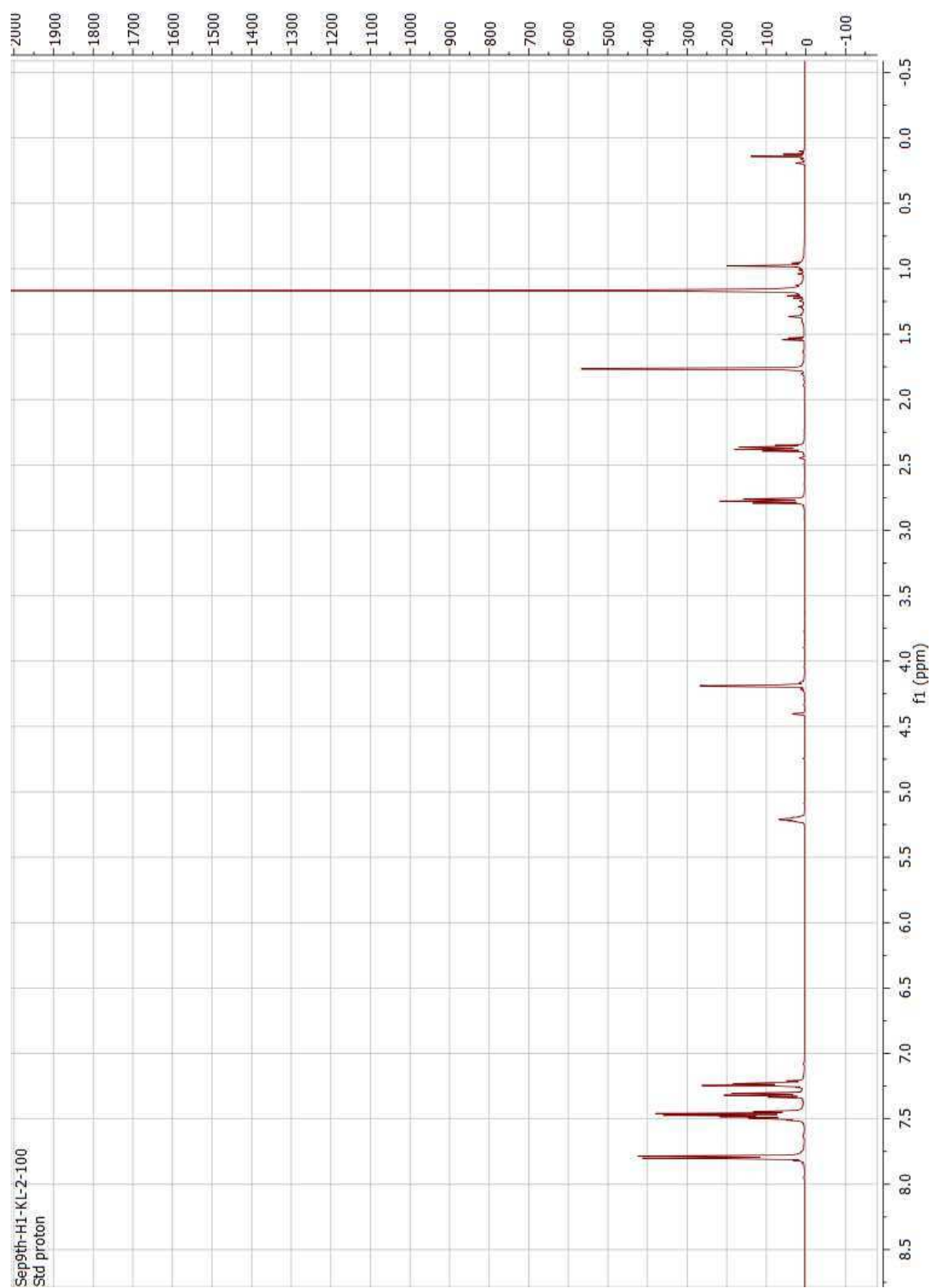


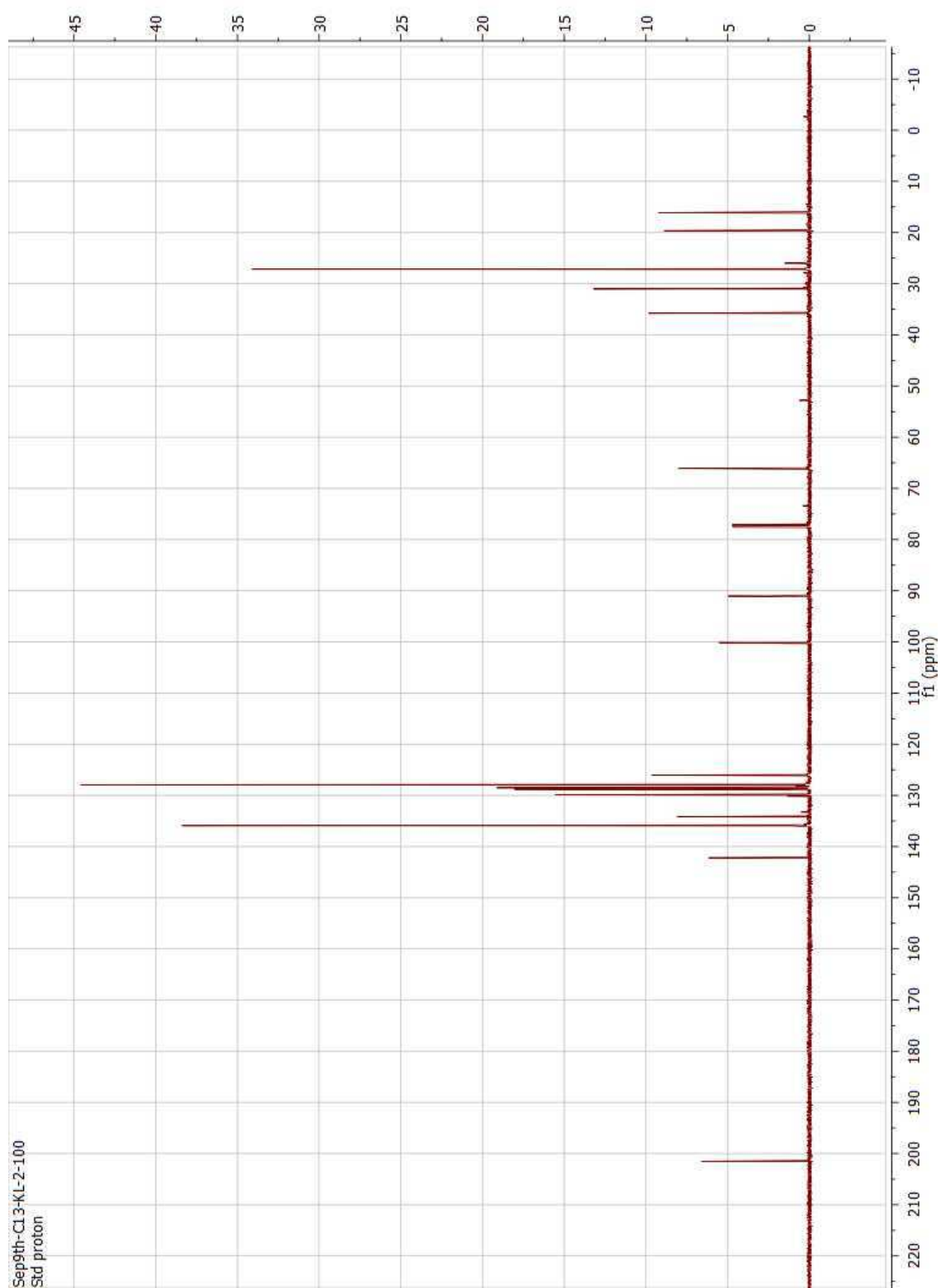


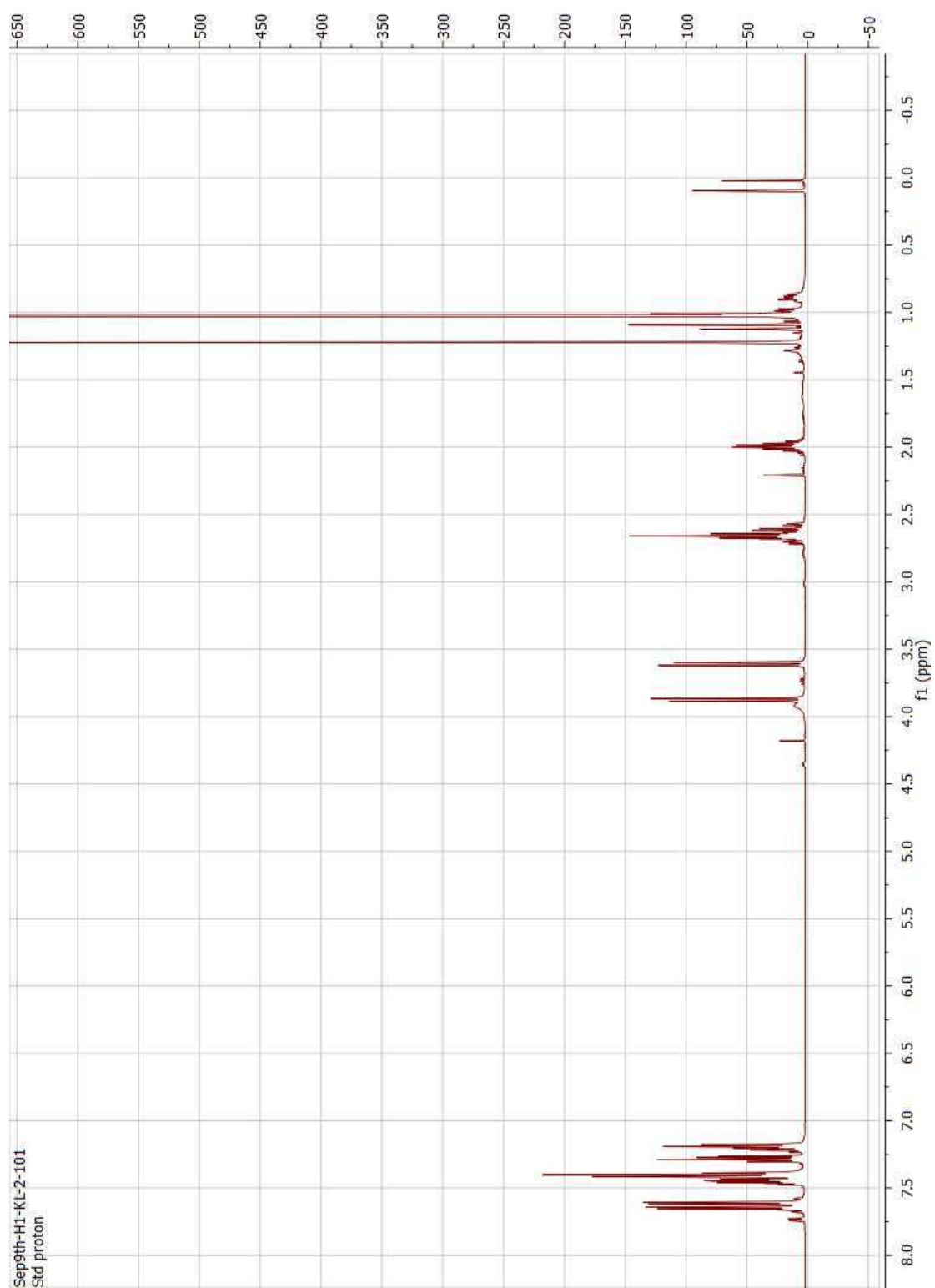


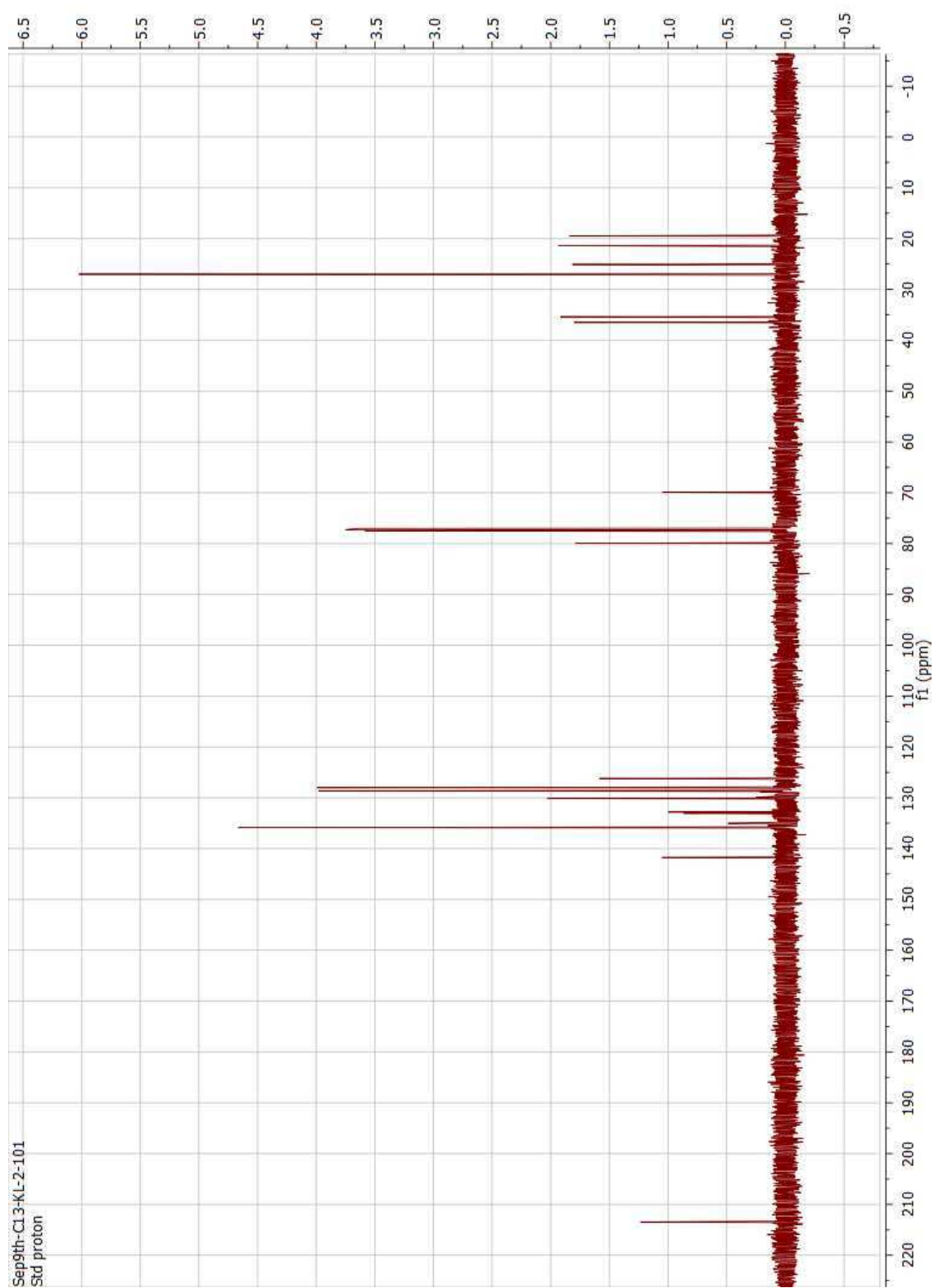


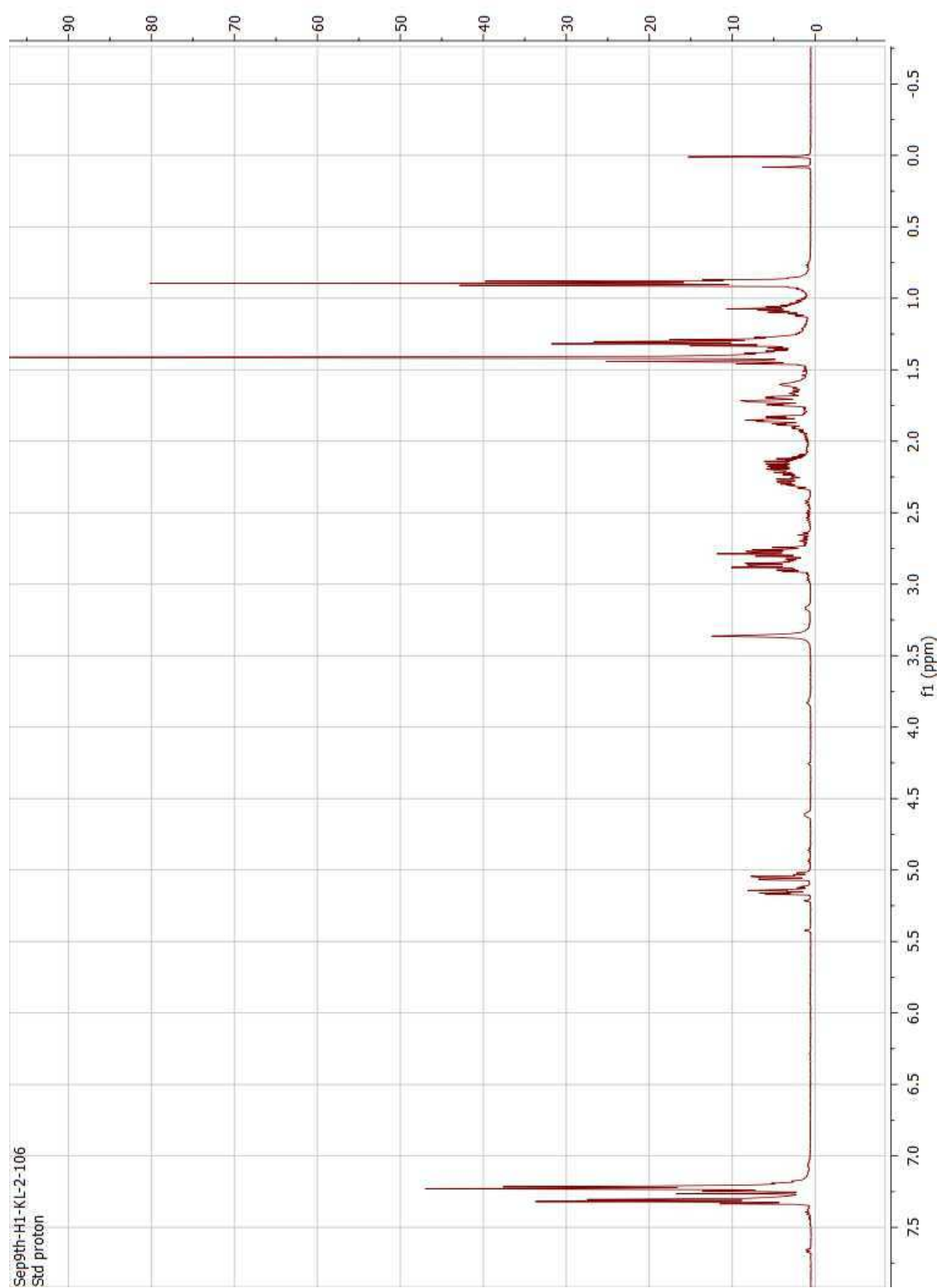


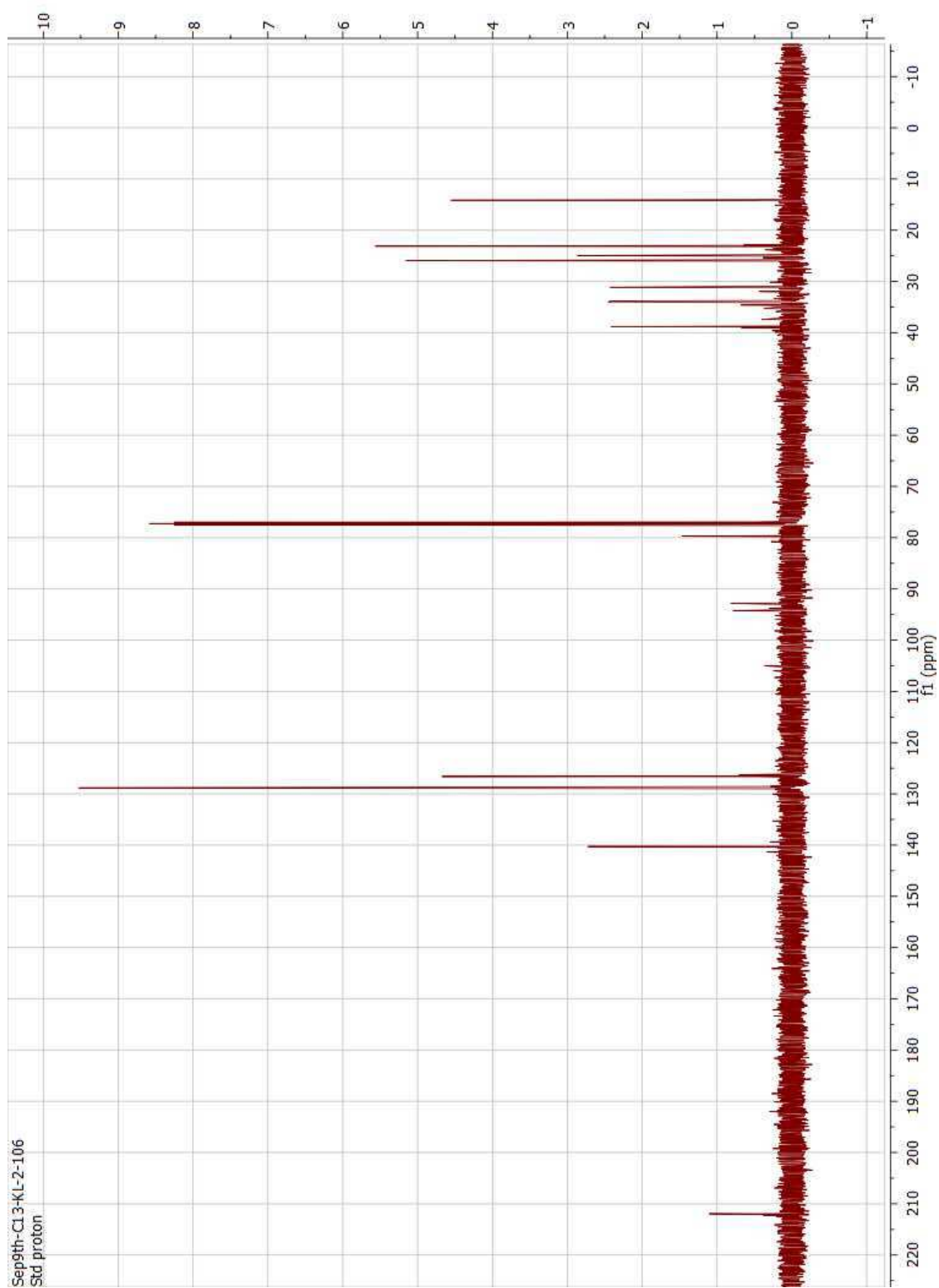


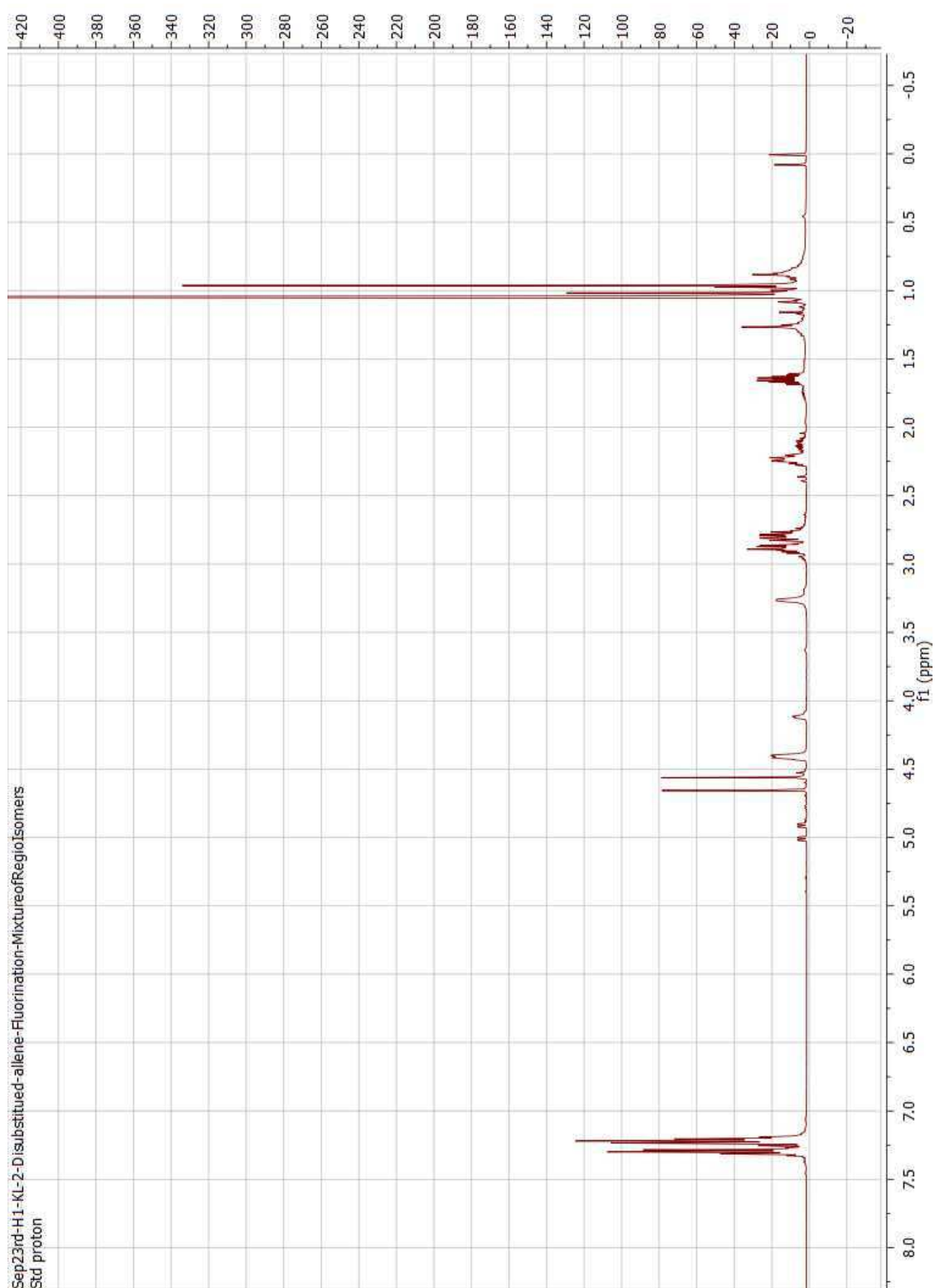


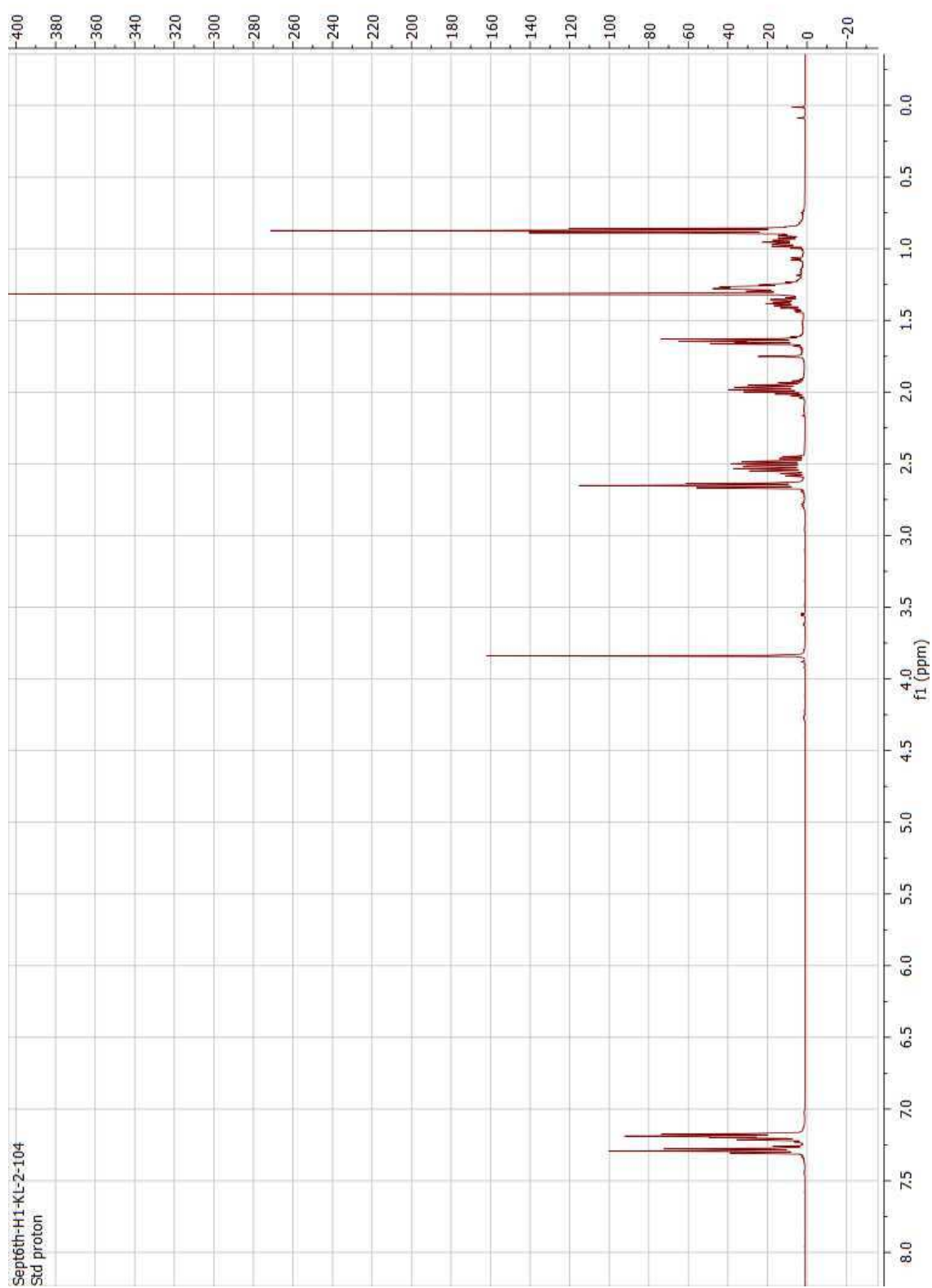


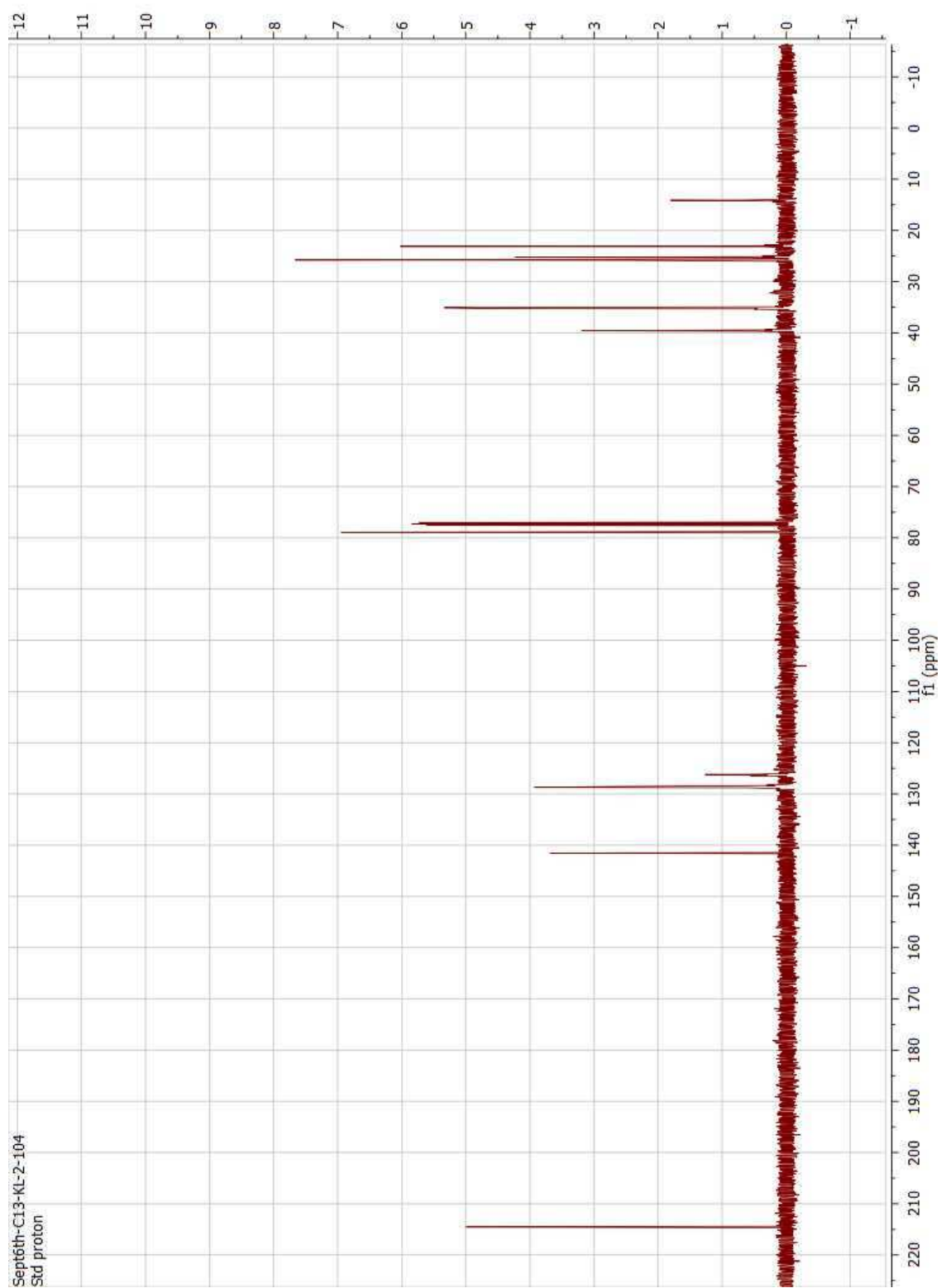


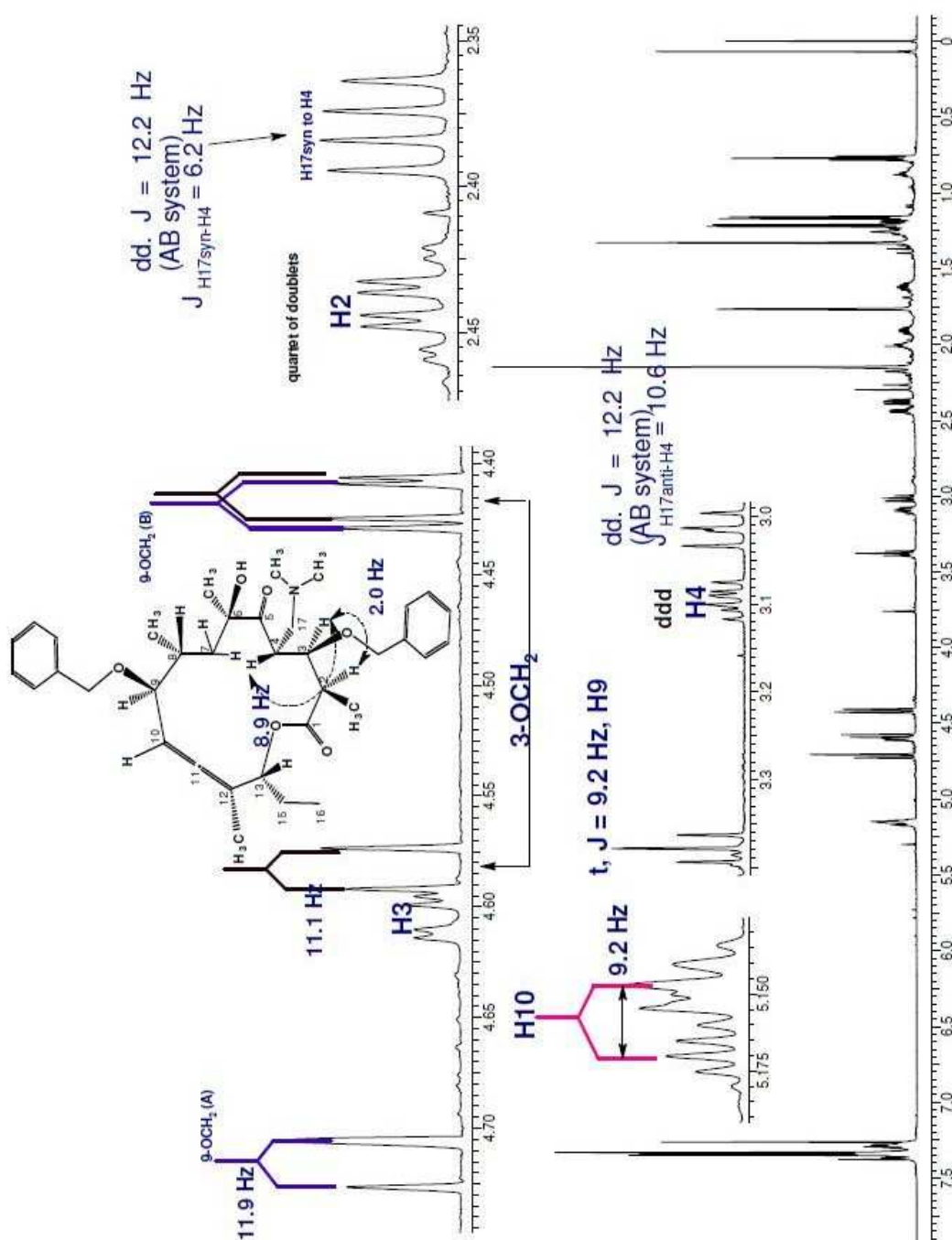




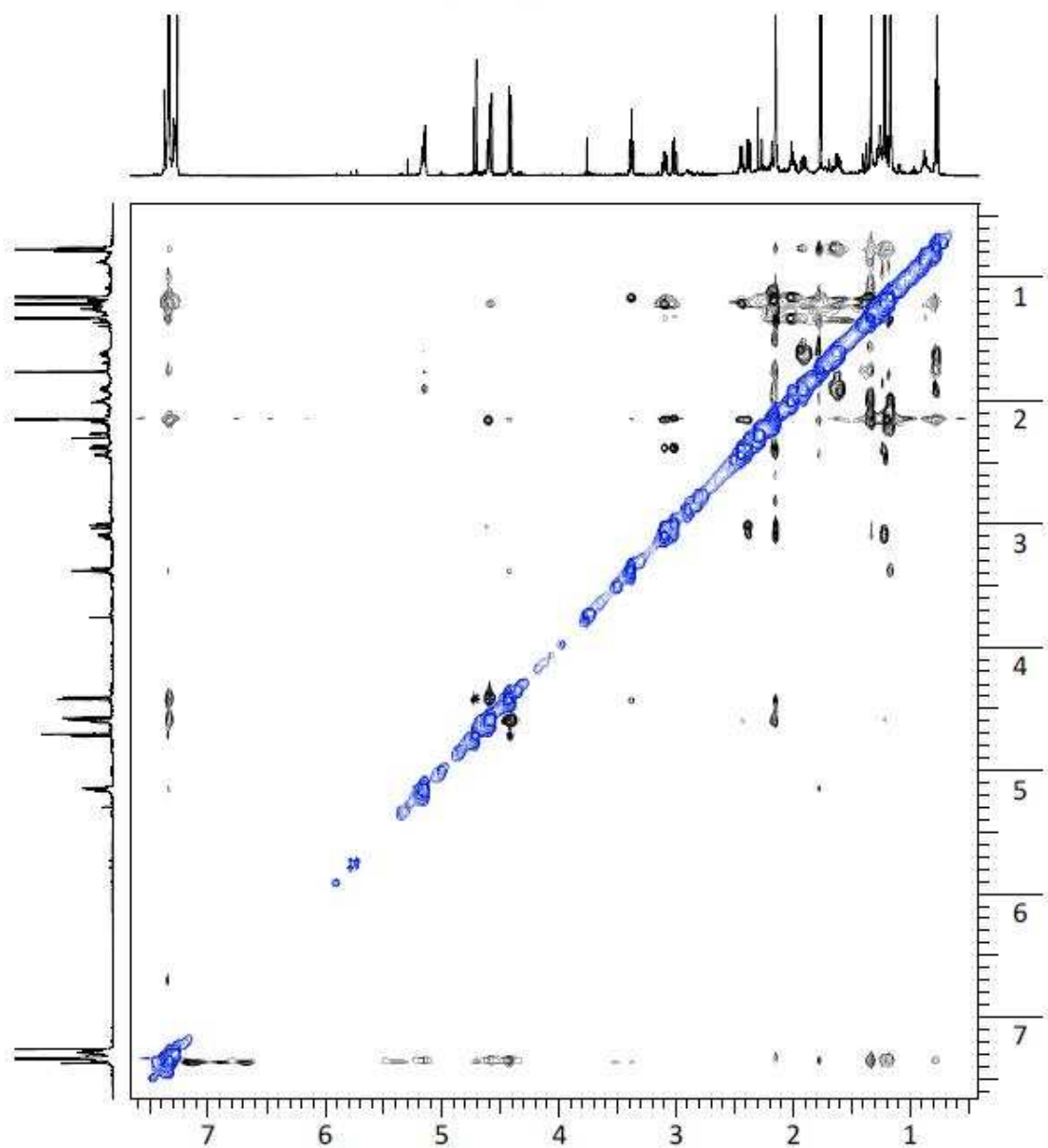


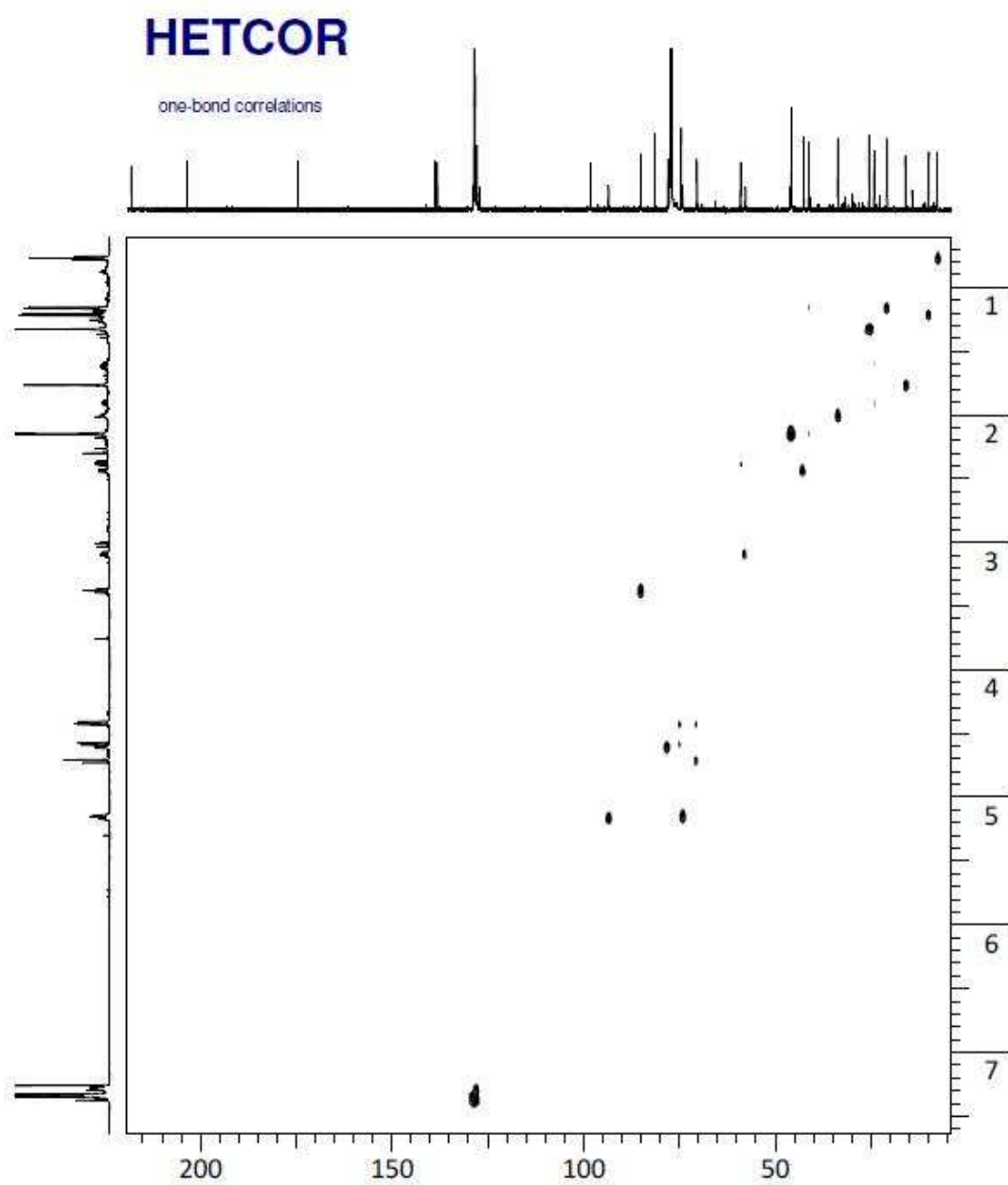






NOESY





CURRICULUM VITAE

Kai Liu

EDUCATION

Ph.D. in Chemistry
2012

Rutgers University –New Brunswick
Advisor: Prof. Lawrence. J. Williams

B.S. in Chemistry and Chemical Biology
2007

Tsinghua University

PUBLICATIONS & PATENTS

Kai Liu, Hiyun Kim, Partha Ghosh, Novruz G. Akhmedov and Lawrence J. Williams, "Direct Entry to Erythronolides via a Cyclic Bis[Allene]" *J. Am. Chem. Soc.* **2011**, *133*, 14968.

Gaojie Hu, Kai Liu, Lawrence J. Williams, "The Brosimum Allene: A Structural Revision" *Org. Lett.*, **2008**, *10*, 5493.

Kai Liu, Lawrence J. Williams, Hiyun Kim, Rojita Sharma, "Macrolide Compounds and Methods and Intermediates Useful for Their Preparation" U.S. Patent Application 13/215,986, 2011.

Pei-Yuan Jin, Kai Liu, Sanhao Ji, Yong Ju, Yu-Fen Zhao, "Synthesis of Novel Steroidal Bioconjugates of phospholipid with AZT" *Phosphorus, Sulfur and Silicon and the Related Elements*, **2008**, *183*, 538-542.

Pei-Yuan Jin, Kai Liu, Sanhao Ji, Yong Ju, Yu-Fen Zhao, "Synthesis of Novel Steroidal Bioconjugates with AZT and Phosphorus" *Synthesis*, **2007**, *3*, 407-441.

Kai Liu, Hiyun Kim, Novruz G. Akhmedov and Lawrence J. Williams, "Allene Osmylation: Beneficial Effects of Electrophile on Catalysis" *Manuscript in preparation*.